Analysis of FDS Predicted Sprinkler Activation Times with Experiments

By

Adam Bittern

Supervised by

Michael Spearpoint

Fire Engineering Research Report 04/8

2004

A project submitted in partial fulfilment of the requirements for the degree of Master of Engineering in Fire Engineering

Department of Civil Engineering
University of Canterbury
Private Bag 4800
Christchurch, New Zealand

For a full list of reports please visit http://www.civil.canterbury.ac.nz/fire/fe_resrch_reps.shtml

Abstract

Fire Dynamics Simulator (FDS) is a computational fluid dynamics model used to calculate fire phenomena. The use of computer models such as FDS is becoming more widespread within the fire engineering community.

Fire engineers are using computer models to demonstrate compliance with building codes. The computer models are continuously being developed as fire science and computing technology advances. It is essential that these models are validated to the point were the fire engineering community can have confidence in there use.

This research report analyses FDS predicted sprinkler activation times with actual sprinkler activation times from a series of chair fires in a 8 x 4 x 2.4 meter gypsum wallboard compartment.

The experiments consisted of a series of chair fires where the mass loss rate and sprinkler activation times were recorded, as well as temperature data. The fire data, compartment details and sprinkler head details were then modelled in FDS.

The research shows that the c-factor values used by the sprinkler activation model in FDS has a significant influence. The c-factor value influenced the sprinkler activation times by as much as 50 %.

FDS predicted sprinkler activation times with varying degrees of success. The success depended on the sprinkler head type modelled and position of the fire. The grid size used for the simulation affected the sensitivity of the comparison.

Acknowledgements

I thank the following people and organisations for their assistance and support during the project:

- Jonathan Shelley for his assistance, and companionship during the long hard days.
- My supervisor Mike Spearpoint for all his assistance and support.
- Graeme Weck for locating the test facility and making available the resources of the Patumahoe Volunteer Fire Brigade.
- Grant Weck for supplying discounted construction materials.
- A special thanks to Patumahoe Volunteer Fire Brigade.
- Greg Mitchell on behalf of the Patumahoe Junior Boys Rugby Football Club for providing us with the test facility.
- Cliff Mears for his support.
- Dr Paula Beever for financial assistance from Engineering Information Research Strategic Analysis, New Zealand Fire Service (NZFS).
- Simon Davis for accommodating the extra workload.
- Chris Mak on behalf of Wormald Fire Protection for supplying the sprinkler heads.
- Jim Roskvist for the installation of the sprinkler system.
- Aquatherm for supplying the piping and fittings for the sprinkler system.
- The New Zealand Fire Service Commission for their support of the Fire Engineering programme at the University of Canterbury.
- Carl Voss for testing the foam specimens in the cone calorimeter.
- And finally but by no means least my partner Emma Witt who has shown an incredible amount of patience and support.

Without their help the project would never have been completed.

Table of Contents

Appendices

List of Figures

List of Tables

1 Introduction

1.1. Overview

Fire engineering is a relatively new discipline in comparison with the established engineering disciplines. With the introduction of performance based fire engineering design around the world as a rational means of providing efficient and effective fire safety in buildings [1], fire engineering has been forced to evolve at a accelerated rate in comparison with the established disciplines such as civil engineering. The complexity, size, construction, use and uniqueness of buildings being built today require the use of complex fire engineering solutions.

The use of computer models in recent years has increased, this can be put down to several factors that include, increased complexity of building design, emergence of performance based design, the increased understanding of the fire phenomena, and the advances made in computer processing power [2].

Computer models form an important part of the engineering solution. These models are used to predict events relating to tenability, fire and smoke spread etc. Computer models vary considerably in complexity from the simple single zone models to the highly sophisticated computational fluid dynamic models.

To determine the accuracy of the computer models it is necessary to validate the models. It is necessary to identify the limits and parameters in which the model will produce meaningful information for the purposes of fire engineering design.

This research report is centered around investigating the validation of a computer model known as Fire Dynamic Simulator 3 (FDS3) produced by National Institute of Science and Technology, USA [3].

1.2. Impetus for research

Computer models have become central to performance based fire engineering design in New Zealand. Zone models including BRANZFIRE [4] and CFAST [5] are used to calculate smoke layer depths and temperatures, optical densities, smoke extraction rates, toxic effects and many other parameters. The models listed above are mainly being used for the purposes of calculating available safe egress time (ASET).

Currently Fire Dynamics Simulator (FDS), is not widely used in New Zealand outside the fire research field. However with the availability of affordable computer technology and the requirement for more detailed engineering analysis, the usage of computational fluid dynamic (CFD) computer models is likely to increase.

It is essential that the fire engineering community can have faith in the use of models such as FDS. There is limited research published investigating the validity of the sprinkler activation times predicted by FDS at the time of the research being undertaken. Several studies have looked at the temperature validations of FDS, this is discussed later. This study will investigate the validity of FDS predicted sprinkler activation times. The research will also build upon previous temperature validation work.

1.3. Research objectives

The objective of the report is to determine the accuracy of FDS in predicting sprinkler activation times. The report will also investigate FDS's ability to accurately predict temperature profiles of pre-flashover compartment fires. To achieve the objectives the following work was undertaken:

1. Twenty two realistic fires were conducted in a medium sized drywall compartment. The mass loss rates, sprinkler activation times and temperature profiles for the experiments were measured.
2. The heat release rates (HHR) of the fires were calculated from the mass loss rate and heat of combustion data.

3. The fire compartment details were used to set up a model in FDS. Simulations were run using the HRR's from the individual fires and sprinkler head properties.
4. The sprinkler activation times and temperature profiles predicted by FDS were compared with the measured values from the experiments.

1.4. Limitations of the Research

Below highlights the known limitations of the experiment phase of this research. The limitations are discussed in more detail later in the report.

- Thermocouple (TC) readings could of been affected by thermal radiation.
- Mass loss rate of the fire is approximised due to load cell increments.
- Fire compartment properties were not 'fresh/new' for each experiment.
- Two types of thermocouples were used.
- Relative humidity and moisture content were not measured.
- Gas velocities in the compartment were not measured.
- Premature fire suppression.

Below highlights the known limitations for the data interpretation:

- The heat release rate of the fire is an approximation.
- TC temperatures lag behind actual gas temperatures.
- Limited data on the physical properties of the compartment materials.
- Sprinkler head, thermocouple and model geometry approximation had to be used.
- The heat release rate modeled by FDS differed at times to the approximated HRR.
- Fuel geometry in FDS differed slightly from experimental fuel geometry.
- Fire spread model in FDS was not used to predict HRR.
- Limited quantity of temperatures measurements.
- No measurements of gas velocities in the compartment.
- Thermal characteristics of sheathed thermocouple.

- Design fires used may skew the sprinkler activation data.

2 Literature Review

This chapter reports briefly on the history of computer models used to calculate and predict fire events, mainly CFD models. Validation work relating to FDS is reviewed, relating to sprinkler activation times.

2.1. Fire models

Fire models have been used to predict fire phenomena in compartments for over 40 years [6]. These models laid the foundations for zone models [7]. Quintiere [2] gives an excellent description of the physical and mathematical assumptions behind the zone modeling concept. Zone models which predict fire development are based on solutions to mathematical equations that describe the physical and chemical behavior of fire.

2.1.1. Zone Models

Zone models divide compartments into volumes called zones. The upper zone which is known as the upper layer contains the hot gases produced by the fire and a lower zone contains the cooler gases. The upper layer receives both energy and mass from the fire and looses energy to the surfaces in contact with the upper layer by conduction and radiation. The principles and equations for zone models are well developed and reasonably approximate reality [2]. These models would include:

- CFAST [5]
- BRANZFIRE [4]
- Plus numerous others.

The computer resources needed to drive these simpler models is minimal in comparison with the computer power available. Zone models have limited room for improvement due to their very nature [8].

2.1.2. CFD Models

The 1970s and 1980s saw the introduction of many general purpose CFD codes that had been developed for industry [6]. CFD models divide the space being modeled into cells. The CFD modeling technique is used in a wide range of engineering disciplines and is based on a complete, time dependent, three dimensional solution of the fundamental conservation laws [2]. The basic laws of mass, momentum and energy conservation are applied in each cell and balanced with all adjacent cells. The governing equations are the Navier-Stokes equations. Sub-models are used to calculate the fire parameters such as combustion, flame spread and turbulence etc [9]. CFD have long been established in the United Kingdom [9]. CFD models have been developed for types of industrial applications including turbine design [10] and over the last 30 years have become a useful tool within the engineering community [11]. The usefulness of this tool has been closely tied to the advent of the personal computer and increasing processor speed [11].

This section gives a brief overview of selected CFD models. It is not the intention of the section to detail the selected models, however there are several pieces of work that describe CFD models in more detail, these include ‘Literature Review on the Modeling of Fire Growth and Smoke Movement’ by Bounagui, A., Benichou, N [12].

SOFIE - simulation of fires in enclosures – is a CFD model that contains a multitude of sub models developed for fire applications. SOFIE uses a type of turbulence model called the k-ε turbulence model with a sophisticated eddy break up model for combustion [12].

SMARTFIRE is a CFD model developed by the Fire Safety Engineering group at the University of Greenwich with U.K. Home Office collaboration. SMARTFIRE uses an automated grid generation component. The system is capable of meshing multi-compartment enclosures. It uses rule based technology to produce a reasonable grid based on the geometrical and scenario data input by the user [13]. SMARTFIRE uses the k-ε turbulence model.

JASMINE which stands for Analysis of Smoke Movement in Enclosures was developed especially for fire applications by the Fire Research Station based in the United Kingdom in the early 1980s [14]. It evolved from the 2-dimensional steady state CFD code called MOSIE. Processes of convection, diffusion and entrainment are simulated by the Navier-Stokes equations [14].

CFX is a commercial model that was developed by AEA Technology. It can be used for assessing fire dynamics, fire structure issues and fire suppression [12]. The CFX model has several options to deal with turbulent flows arising from fire.

2.2. Model Validation

This section gives a brief description of validation work undertaken for CFD models for domestic enclosure sized fires. For validation work undertaken the most commonly used experimental data sets were those established by Stecker, Quintiere and Rinkenin [7][15]. These are referred to as the 'Steckler et al' experiments [6]. The experiments involved measuring temperature and velocity profiles in a domestic compartment which was subjected to heating from a methane burner with a variable HRR.

The Steckler experiments have been used to validate models such as Phoenics by Mawhinney [7], FLOW3D by Kerrison [16], JASMINE by Markatos and Cox [14]. Generally the models had problems dealing with boundary conditions however the prediction data compared well with the test data [6].

Petterson [6] provides a greater insight into the validation of CFD models for domestic-sized enclosures and large scale enclosure fires. Other validation work has been carried out by Nielsen [17] for SMARTFIRE. This work was done at the University of Canterbury, New Zealand.

2.2.1. Validation Work Done for FDS

This section reports on several pieces of validation work that has been carried out for FDS. In particular work that validates temperature and sprinkler activation performance.

Combustion Science and Engineering undertook a comparison of FDS with experimental data [11]. The following scenarios were compared:

1. Room test with a convective flow.
2. Calibration of a burning couch.
3. Smoke detector activation.

The convective flow comparison did not involve a fire but instead used a heating element to introduce heat into the 1.2 m long x 1.2 m wide x 1.8 m high compartment. Instrumentation recorded the temperature, velocity and heat flux profiles of the compartment. A model was set up in FDS to mimic the compartment closely as possible.

Overall the comparisons between the actual and experimental results indicated that FDS model predictions agreed well with the room test data for both mean temperature and velocity, with one exception near the boundary surface located at the ceiling. This study also noted that the temperatures predicted by FDS were dependent upon the grid size.

An HRR curve for a couch was compared with the predicted HRR curve from FDS using the couch dimensions and material properties to produce the input data. The couch was allowed to burn solely based upon its prescribed material properties.
A HRR comparison was conducted between the actual data and the predicted values. After several iterations of redefining the physical dimensions of the modeled couch, the model mimicked the burning history of the actual burn.

The study also made a comparison between actual and predicted smoke detector activation times. Test data from Underwriters Laboratories (UL) test room experiments where compared with FDS predicted data using the geometry and fire sizes etc. The results from these comparisons where favorable.

Petterson [6] carried out validation work using data from the McLean's Island tests - undertaken by the Civil Engineering Department, University of Canterbury, NZ. The test compartment consisted of two International Standards Organisation (ISO) rooms,

2.4 m long x 3.6 m wide x 2.4 m high joined together by a centrally placed 2.0 m x 0.8 m doorway [18]. The non-fire room had the end wall removed (open). This was to provide ventilation and allow the smoke and gases to flow freely out into the natural draft exhaust hood above.

An LPG burner was used to provide fires ranging from 55 kW to 165 kW. Nine thermocouple trees were used in the experiments to measure the compartment temperatures. Other measurements were taken such as species concentrations and layer heights. Petterson reported that FDS generally gave temperature prediction within 15 % of the experimental values. It was reported that most of the gas temperatures predicted were slightly low.

Another validation study is 'Comparison of FDS Model Predictions with FM/SNL Fire Test Data' done for NIST by Friday and Mowrer [19]. FDS simulations were compared with data taken from experiments known as Factory Mutual/ Sandia National Laboratory tests. These tests were sponsored by the U.S. Nuclear Regulatory Commission.

The test enclosure was 18.3 m long by 12.2 m wide by 6.1 m high. The compartment was fitted with a series of instruments that included aspirated and non-aspirated thermocouples, velocity probes and gas analysers.

Steady and unsteady state fires were used for the experiments. Peak fire intensities ranged from 500 kW to 2 MW. Normal ventilation rates varied from 1 – 10 air changes per hour. In general the simulations predicted higher temperatures than the experimental temperatures. The unsteady state fire simulations resulted in comparable results to the actual experimental results.

A study by Olenick, Klassen and Roby titled 'Validation Study of FDS for a High-rack storage Fire Involving Pool Chemicals'[20] investigated the activation times of sprinkler heads. Full-scale experiments on the effectiveness of sprinklers in combating high rack storage fires involving swimming pool chemicals such as calcium hypochlorite were conducted on Jan 26 –27 2000 at the Southwest Research Institute in San Antonio, Texas, USA (SWRI). The calcium hypochlorite was stored on pallets

placed under the wooden slats of the storage rack. Empty boxes and pails were placed around the commodity to simulate typical storage conditions. The fire was ignited between the pailed and boxed commodities.

Sprinkler Identification	SWRI Activation Time (s)	Predicted Activation Time (s)
7	90	95.5
6	95	94.7
Deluge system activated	96	
1	100	118
2	100	116.1
8	100	115.6
10	100	115.4
11	100	117.1
5	105	116.2
9	105	120.0
12	105	120.8
3	115	119.9
4	115	122.9

Table 2-1 Sprinkler activation times - SWRI

The predicted activation times for sprinklers 7 and 6 (see Table 2-1) were approximately that of the actual times. It was reported that after the activation of the first two sprinklers, making comparison between the simulated and experimental data was more difficult and subject to increased error due to changes to the geometry caused by the over-pressurisation of the test room, the activation of the deluge system and the use of the first aid fire fighting equipment. It was reported that these events changed the HRR and flow patterns inside the test chamber, which had an effect on the activation times of the sprinklers.

The authors concluded that the model still managed to predict the activation times of the subsequent sprinklers fairly accurately, and was particularly successful in

continuing to predict the order of sprinkler activation despite over-predicting the time to activate.

Wood and Tubbs published a paper ‘Comparing Fire Dynamics Simulator with Compartment Fire Test Data’ [21]. Experimental data which included sprinkler activation times was taken from experiments conducted by Vettori [22] at NIST. A series of fires were held in a 9.2 m long by 5.6 m wide by 2.4 m high compartment to compare sprinkler activation times for smooth flat ceilings and ceiling with beams.

The authors concluded that once differences in the fire parameters had been accounted for, the predicted activation times were within 20 % of the actual.

2.3. Summary

- FDS is shown from the validation work given in this chapter to generally over predict temperatures, but be within 20 % of the actual temperatures.
- FDS predicts sprinkler activation times reasonably well, being within 20 % of the actual times. The times tend to be conservative.

3 Methodology and Experiments

3.1. Methodology

The methodology that is employed to investigate the validity of sprinkler activation times predicted by FDS is given below:

- Set up compartment and telemetry.
- Conduct a series of furniture burns in which the mass loss rate, temperature profiles and sprinkler activation times are measured.
- Analyse the experimental data.
- Establish HRR curves from the mass loss rate of the fuel package and heat of combustion data for the foam.
- Set up FDS with compartment characteristics and design fires for experiments.
- Run FDS simulations for experiments calculating the predicted HRR curve, temperature profiles and sprinkler activation times.
- Prepare predicted data into a form that can be compared with actual experimental data.
- Compare the data sets.
- Conclude on findings from the comparison.

3.2. Equipment and Assembly

The section will describe the equipment and apparatus, how it was used and how data was collected and recorded. The mass loss rate of the fire was obtained by using the following equipment:

- Load cell with 5-gram increment.
- Load cell protection system (see Figure 3.1).
- Computer.

Visual observations were collected by:

- Video camera.
- Digital still camera.

The fuel assembly consisted of:

- A horizontal and vertical fabric covered foam slab (see Figure 3.2).
- Metal frame (see Figure 3.3).
- Spill plate.

The compartment was constructed to UL1626 Standard for Safety for Residential Sprinklers for Fire Protection Service for residential heads [23]. The compartment consisted of:

- UL1626 drywall compartment.
- Two headed sprinkler system.
- Various sprinkler heads.

Given below is a list of equipment and apparatus used for the experiments. To measure the temperature profile of the compartment the following equipment was used:

- Junction box.
- Data logger.
- 8 thermocouples with extension cable (see Figure 3.4 and Figure 3.6).
- Computer.

Fire Source

- Solid petroleum firelighters (see Figure 3.5).
- Propane plumbers gas torch.

First Aid Fire Fighting Equipment

- Rega Napsack pump pack.
- Dry powder fire extinguisher

Figure 3.1 Protection system

Figure 3.2 Fuel package

Figure 3.3 Chair frame

Figure 3.4 Sprinkler and thermocouple

Figure 3.5 Firelighter

Figure 3.6 Thermocouple tree

3.2.1. Temperature Measurement

Type K thermocouples [24] were used to measure gas temperatures. 6 x 500 mm stainless steel sheathed mineral insulated probes were used for 2 vertical wall thermocouple trees. Two bare wire type K mineral insulated probes were placed adjacently to the sprinklers. For installation configurations see Figure 3.7 and Figure 3.8

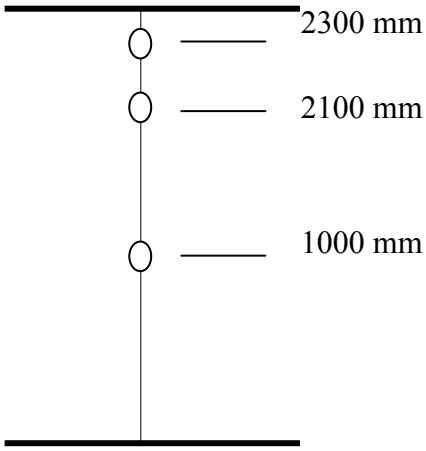

Figure 3.7 TC heights

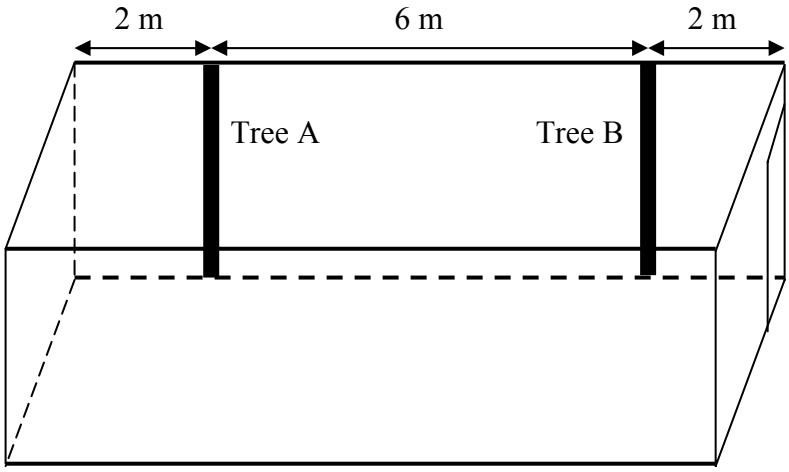

Figure 3.8 Thermocouple tree location

A TC-08 thermocouple data logger [25] manufactured by Pico Technology limited collect and converted the thermocouple voltage outputs into temperatures. A laptop computer with Pico data logging software was used to record temperature data.

3.2.2. Load Cell

The load cell used for the measurement of the mass loss rate measured in increments of 5 grams. The output signal from the load cell was then converted into kilograms by the display unit (refer to Mettler Toledo guide [26]). The data was logged by Windows Hyper Terminal using a serial link. The mass loss data was then transferred to Microsoft Excel were it was manipulated into a mass loss rate.

3.2.3. Load Cell Protection

In order to protect the load cell from the effects of fire, a protection system was installed. Three metal trays that fitted within each other formed a protective barrier. The trays cocooned the load cell limiting exposure to fire products. The intention was to fill the bottom tray with water to form a water seal with the top tray, with the load cell being housed within the middle tray. It was found that the gas temperature and fire product concentration at the level of the load cell was minimal. Therefore water was not used in the protective assembly. Plasterboard strips were used to cover the cabling. Plasterboard sheets were used to (1000 mm x 800 mm) protected the scales from thermal radiation and debris from the fire.

3.2.4. Visual Recording

A video camera recorded footage of the experiments. This gave a visual record of fire development and sprinkler activation times. A digital camera was used to take photos of the experiments, rig and equipment.

3.2.5. Compartment Assembly

The compartment was specifically made for the purposes of the experimental work. The compartment was constructed with timber-framed walls and ceiling, lined with 10 mm thick gypsum plasterboard. A layer of acrylic paint was applied to the inside surface of the plasterboard. The compartment had internal dimensions of 8 m long by 4 m wide by 2.4 m high (see Figure 3.9)

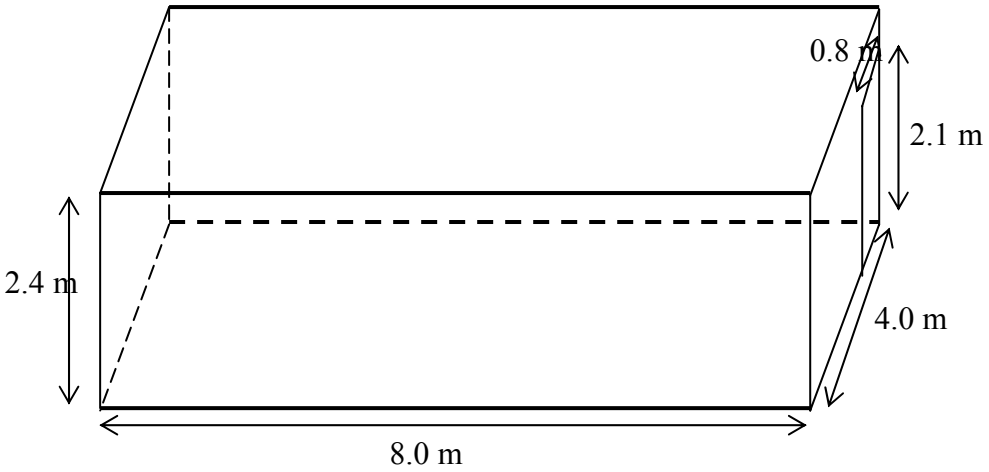

Figure 3.9 Assembly layout

The walls were made from modules that varied in width from 0.4 m to 1.2 m. The modules were bolted together to form the outer walls. The ceiling was constructed with the beams running perpendicular to the length of compartment. The purling was screwed to the underside of the beams, with plasterboard being screwed to the purling. Sealant and masking tape completed the seal between the plasterboard sheets. The compartment was laid on a concrete floor.

For the purposes of accommodating observers windows were included. The windows were 910 mm x 460 mm in size, two were positioned at ground level and two position no higher than 1200 mm. The total surface area that windows occupied was less than 2 % of total interior surface.

The door set comprised of a wooden frame with a plywood door leaf. The door leaf had dimensions of 2100 mm high and 800 mm wide.

3.2.6. Fuel Assembly

Fabric covered foam blocks formed the fuel load for the experiments. They were constructed to mimic foam-covered seats, and thus produce fires that would be representative of foam covered seat fires. The foam blocks were 500 mm x 400 mm x 100 mm in size, approximately 0.56 kg in mass. Plasterboard (400 mm x 500 mm) formed the backing for the fabric covered foam blocks. The backing prevented the foam from falling off the assembly during the burns.

- Acrylic fabric was used to cover the foam packages. The fabric weighted 10 grams per meter squared.
- 28 kg/m^3 cushion grade non-fire retarded polyurethane foam was used as the fuel. Typical of NZ domestic foam.
- 10 mm plasterboard was used for foam block backing.
- General purpose glue and staples used to fix fuel package together.

The following details (see Figure 3.10) the method used to manufacture the fabric covered fuel packages:

1. Foam blocks were cut to size.
2. Plasterboard sheets are cut to size- 500 mm x 400 mm.
3. The foam blocks and plasterboard sheets are glued together.
4. Dead weights are placed on top of the foam blocks while the glue dries.
5. The fabric is then cut to size – 700 mm x 800 mm.
6. The foam blocks are then centered on the fabric.
7. One edge of the fabric is glued and stapled to the plasterboard.
8. The opposite edge of the fabric is glued and stapled to the plasterboard.
9. This is repeated for the two remaining fabric edges.

3.2.7. Ignition Source

Solid petroleum firelighters were used to start the fire. The firelighters dimensions: 20 mm x 20 mm x 10 mm. A propane gas torch was used to ignite the firelighter. The fire products given by the burning firelighter was negligible in comparison with the fire products given by the burning fuel package. This method of fire setting was chosen because of its repeatability, and its ease of application.

It is assumed for the purposes of the experiments that there is minimal water loss (evaporation) from the plasterboard during the fire. The effect on the mass loss rate is assumed to be negligible. It was impossible to distinguish between the mass loss rate

of fabric and foam. This has a negligible effect on the simulations as there was a limited amount of fabric mass compared with fuel mass.

Plasterboard backing

Foam slab

Foam slab- side view

Cover photo 1

Cover photo 2

Cover photo 3

Seat slab

End view

Figure 3.10 Cushion assembly

3.2.8. Fire Fighting Equipment

To extinguish the fire a Rega Napsack pump was used. This was used due to:

1. Its availability.
2. Effectiveness.
3. Low usage of water - less contamination in the compartment.
4. Ease of use.

3.3. Sprinkler system

A sprinkler system was installed with a sprinkler head spacing of 4 m – this meets the spacing requirements of UL1626 Standard for Safety for Residential Sprinklers for Fire Protection Service for residential heads [23], NZS 4515 [27], NZS 4517 [28] and NZS 4541 [29]. Figure 3.11 shows the sprinkler system schematic. The domestic mains provided the water supply. The main isolation valve was positioned between the main sprinkler feed and the domestic mains. The sprinkler main split in to two sprinkler branches at the T-junction. The branch piping was fixed to the topside of the ceiling beams.

The sprinkler system was charged but not connected to a continuous water supply. This was to provide a thermal mass in the piping closest to the sprinkler head. This was achieved by installing isolation valves, just upstream of the sprinkler heads. Pressure gauges were installed to indicate sprinkler activation.

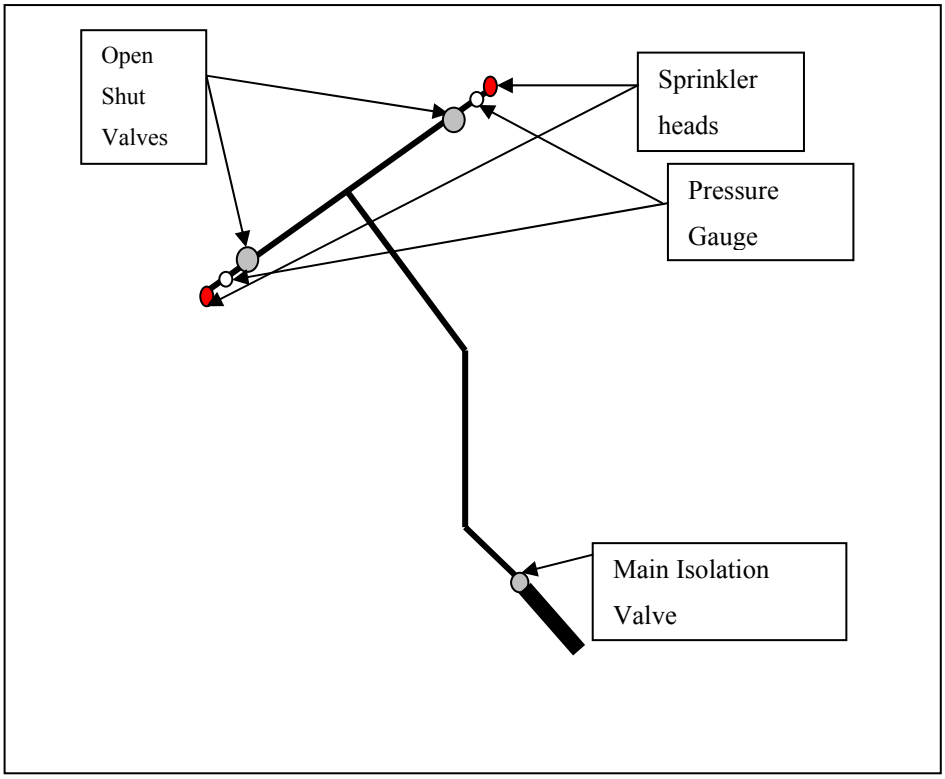

Figure 3.11 Sprinkler schematic

3.3.1. Sprinkler Heads

Four types of sprinkler heads were used for the experiments. The sprinkler heads were not selected for technical requirements, but were typical of what is available on the New Zealand market. They were donated by a fire protection company. The sprinkler heads used provided a variation in response time index and activation temperature. From Figure 3.12 - Figure 3.15 it may appear as the sprinkler heads were recessed. The photos are misleading. The top of the glass bulb was level with the ceiling.
The following sprinkler heads were used for the experiments:

1. Residential type A 68 ^{o}C– TYCO F680, Pendant.
2. Residential type B 68 ^{o}C - TYCO TY2234, Pendent.
3. Standard Response, Standard Coverage 68 ^{o}C – TYCO 3251, Pendent.
4. Standard Response, Standard Coverage 93 ^{o}C – TYCO 3251, Pendent.

3.3.2. Residential Type A Sprinkler Head

Detailed specifications could not be obtained for sprinkler head type (Figure 3.12) F680. The details given below were obtained from Gem residential fire protection product catalogue [30].

- Intended for use in one and two family dwellings and mobile homes as per NFPA 13D [31], residential occupancies up to four stories in height per NFPA 13R [32], and the residential portion of any occupancy per NFPA 13[33].
- 68°C activation temperature.
- Finishes: Standard - chrome plated and white polyester.
- Response time index (RTI) = 36 $m^{1/2}s^{1/2}$
- c-factor = 0.65 $(m/s)^{1/2}$ (estimate)
- 3 mm glass bulb.

3.3.3. Residential Type B Sprinkler Head

The following information was taken from Tyco/ Fire and Building Products technical data sheet TFP400 [34]. See Figure 3.13 for TY 2234 photo.

Technical Information

- RTI = 36 $m^{1/2}s^{1/2}$
- c-factor = 0.65 $(m/s)^{1/2}$ (estimate)
- 3 mm glass bulb.

3.3.4. Standard Response, Standard Coverage 68 ^{o}C and 93 ^{o}C

The following information was taken from Tyco/ Fire and Building Products technical data sheet TFP151[35] (Figure 3.14 and Figure 3.15).

Technical Data

- RTI = 95 $m^{1/2}s^{1/2}$, (estimate)
- c-factor = 0.65 $(m/s)^{1/2}$ (estimate)
- 5 mm glass bulb.

Figure 3.12 Residential A

Figure 3.13 Residential B

Figure 3.14 Standard response 68°C

Figure 3.15 Standard response 93°C

3.4. Sprinkler Head Factors

This section discusses factors that effect the activation of sprinkler heads.

3.4.1. Sprinkler operation

This section briefly describes the operation of sprinklers, for a more detailed account literature such as the Fire Engineering Design Guide [1], NFPA Fire Protection Handbook [36], SFPE Handbook of Fire protection [37] provide greater detail on the subject.

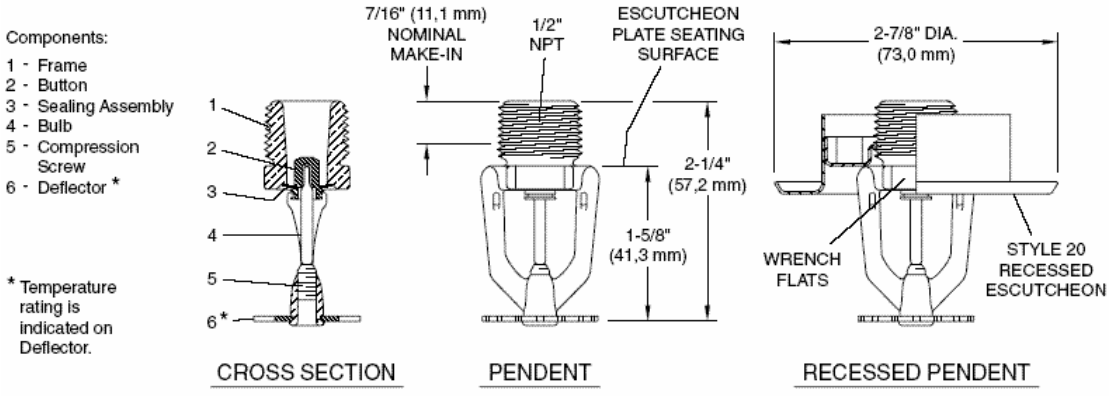

Figure 3.16 Sprinkler head schematic

The sprinklers used for the experiments were of the glass bulb variety (Figure 3.12 - Figure 3.16[34]). The frangible bulb is a sealed glass bulb that contains a liquid which nearly fills the bulb. As a result of either convection or radiative heat transfer the liquid heats up and expands. If the bulb is heated enough the internal pressure due to the expansion will cause the bulb to break allowing the valve to leave the orifice. This allows water to flow from the sprinkler. The glass bulbs are designed so they break when they reach a predetermined temperature [1].

3.4.2. Factors Effecting Operation

The operation of a sprinkler depends on several factors other than the given activation temperature, Nash and Young [38] describe the factors as:

A. Actual operating temperature of sprinkler.
B. Thermal capacity of those parts of the sprinkler which affect operation (Quantified by RTI/c-factor).
C. Ease of transfer of heat from the air to the affected parts of the sprinkler (RTI/c-factor).
D. Rate of growth of the fire in terms of its convective heat output.
E. Height of the ceiling below which the sprinkler is mounted.
F. 'Shape' of the ceiling below which the sprinkler is mounted.
G. Thermal qualities of the ceiling assembly.
H. Distance between sprinkler and ceiling.
I. Horizontal distance of sprinkler from fire.
J. Extraneous factors affecting the pattern of flow of the gases from the fire to the sprinkler.
K. Rate of rise of air temperature surrounding the sprinkler.

For the experiments factors E,F,G,H and I do not vary. Factors B,C and D vary with the fire and sprinkler head. Factor A varies with the individual sprinkler head and is explained below. J varies as the flow patterns may be affected by the door configuration. Factor K varies with experiment due to differences in fire characteristics.

The glass bulbs are filled with liquid, in the case of the sprinklers used in the experiments it is an alcohol water mixture, this varies with manufacturer [38]. Other parameters also vary with manufacturer, such as the quantity of liquid in the bulbs and the type and condition of the glass used [38]. This variation in construction does lead to difference in the given nominal activation temperature and the actual activation temperature. Figure 3.17 [38]highlights the variation in actual sprinkler temperatures to nominal activation temperatures.

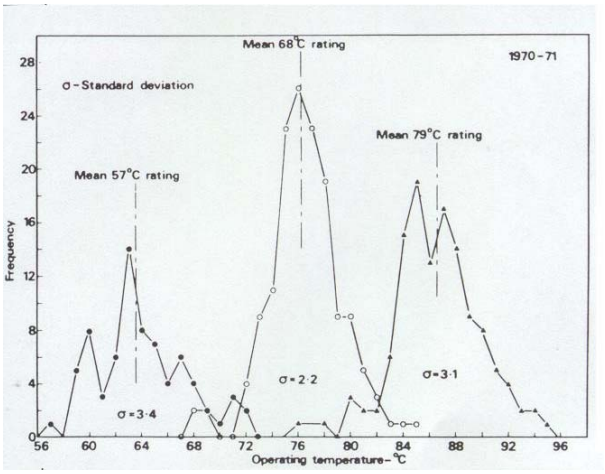

Figure 3.17 Sprinkler activation distribution

The Comité Européan des Assurances [38] proposed a standard for the approval of sprinklers for insurance purposes. By setting maximum variations in temperatures from the nominal activation temperatures for the glass bulbs, some degree of accuracy can be obtained. The proposed standard gives the following requirements: 'The operating temperatures of a sample of 50 glass bulbs shall be such that they indicate a population having the following characteristics:

- A population standard deviation not greater than 5°C.
- None of the 50 glass bulb sprinklers, or glass bulbs, shall operate at a temperature of less than nominal minus 3°C.
- The population mean shall not exceed the nominal temperature by more than 6°C (for 57°C or 68°C ratings) or 8°C (for 79°C, 93°C , 141°C , 182°C and 204 °C - 260°C ratings)'.

The sprinklers used in the experiments have been verified to meet the standard used by Factory Mutual, 'Approval standard for Automatic Sprinklers for Fire Protection'. This places conditions on the variation of actual sprinkler activation temperatures. The standard stipulates the operating temperature for all samples shall be with ± 3.5 percent of the marked nominal temperature rating [39].

It is clear that the actual sprinkler activation temperatures may vary from the nominal sprinkler temperatures for the experiments. The variation in actual activation temperatures may result in meaningful differences between the FDS predicted activation times and the experimental activation times.

3.4.3. Sprinkler Sensitivity

The sensitivity of a sprinkler head depends on the RTI and conduction factor. Basically the more sensitive the sprinkler head, the quicker it will activate per given fire. Figure 3.18 represents the sensitivity parameters for the Factory Mutual standard. Sprinkler heads that have Factory Mutual approval must comply with the RTI and c-factor parameters given by Figure 3.18.

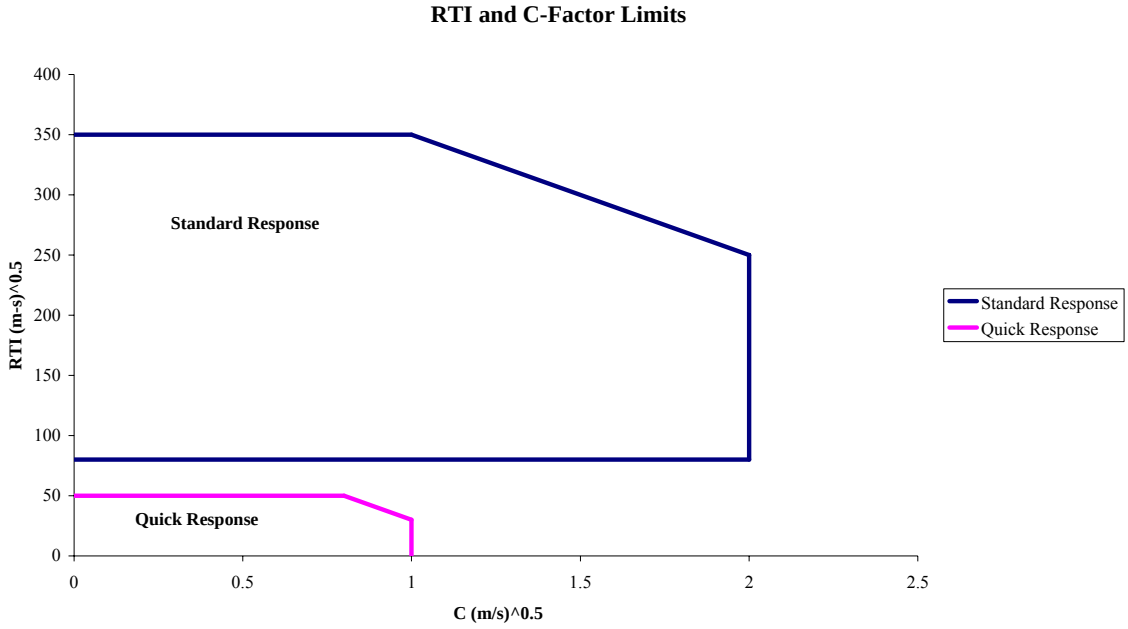

Figure 3.18 RTI and c–factor limits for best case orientation

3.4.4. Response Time Index

The RTI is a measure of pure thermal sensitivity, which indicates how fast the sprinkler can absorb heat from its surroundings sufficient to cause activation. A sprinkler head with a large RTI will take longer to activate than a sprinkler with a low RTI (see Figure 3.19) [1][40]. The RTI is a calculated figure taking account of the

actual function time of a glass bulb mounted in a sprinkler or other devices in given standard conditions and is an indication of the thermal function of the glass bulb. To measure sensitivity Factory Mutual Global Research have developed firstly the concept of 'tau' factor then later the RTI.

The time factor tau is a representation of either:

- Where the temperature of the environment is continuously increasing, the time constant is the amount of time by which the body lags behind its environment after some initial period of time equal to approximately 4 times the time constant.
- Under the plunge test condition where the temperature of the environment is constant, the time constant is effectively the amount of time necessary for the body to move 62.8 % of the way to the temperature of its heated environment.

$$\tau = \frac{mc}{h_c A} \qquad \text{Equation (1)}$$

where,

m = mass of body (kg)

c = specific heat of the body (J/kg K)

h_c = convective heat transfer co-efficient (kW/m.K)

A = area of the body exposed to gas flow (m^2)

The Plunge Test was firstly developed for use with sprinklers in 1976, using the plunge test apparatus. This apparatus consists of a circulating air oven with a known air temperature and velocity. The air temperature is set well above the nominal operating temperature of the sprinkler. At time t = 0, a sprinkler is "plunged" into the heated air. The amount of time it takes the sprinkler to operate is recorded. This time is assumed to be the time necessary for the sprinkler operating mechanism to move from room temperature to nominal operating temperature. The use of the plunge test permits the determination of the time constant.

The RTI gives a more meaningful measure of thermal sensitivity because it is independent to velocity [41]. The RTI is the product of the thermal time constant of the heat-responsive element and the square root of the associated gas velocity [41]. RTI is given by :

$$RTI = \tau u^{1/2} \qquad \text{Equation (2)}$$

where

u = velocity (m/s)

In order to take in to account the conduction of heat away from the sprinkler bulb, Factory Mutual modified equation (2) to take into account a term known as the conduction factor.

$$RTI_v = \frac{RTI}{\left(1 + \frac{c}{\sqrt{u}}\right)} \qquad \text{Equation (3)}$$

RTI_v = Virtual RTI c = conductivity factor $(m/s)^{1/2}$

The virtual RTI can be successful whenever the gas velocity is fairly constant, or does not change rapidly with time [41].

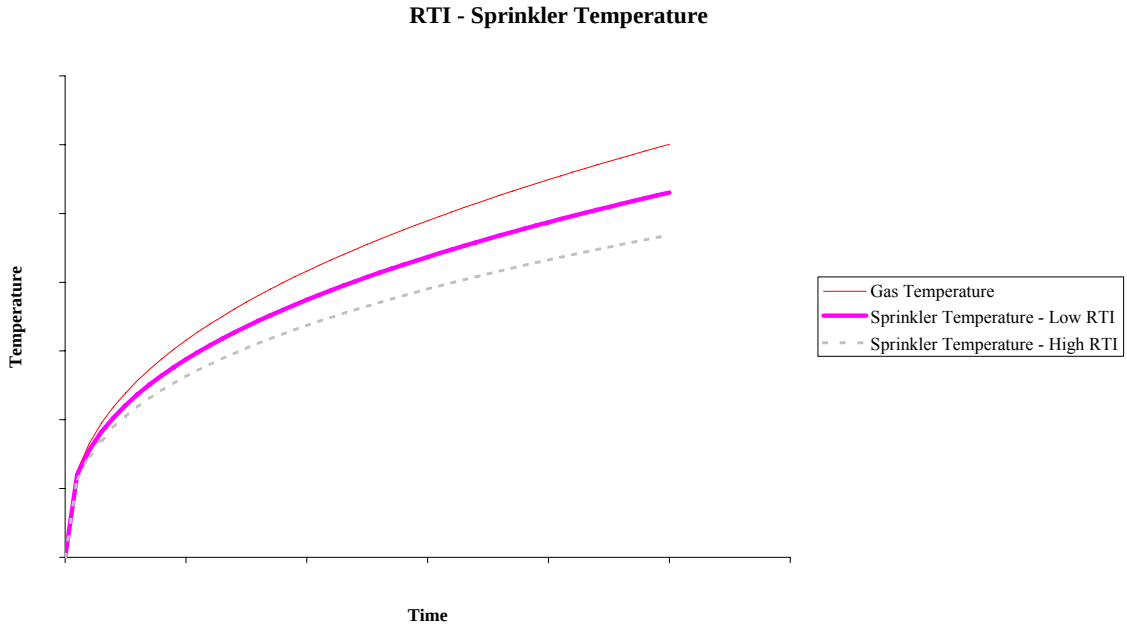

Figure 3.19 RTI temperature time relationship

The need to add a conductivity term to the model of sprinkler response was recognized in 1986 [42]. The conductivity factor is a measure of how much of the heat picked up from the surrounding gas is conducted into the sprinkler housing from the glass bulb [43]. These losses can become critical under low velocity conditions. Heskestad [42] reported that c–factors have a critical role to play and the effects of c–factor becomes increasingly important as RTI decreases and fire growth becomes slower.

For the simulations different values for c-factors were used, this demonstrated the effect that c-factors had on sprinkler activation times. See section 3.3.1 and 3.4 for more detail.

3.5. Experiments

This section describes the experiments and the method/process used for undertaking the experiments.

3.5.1. Experiment Introduction

The experimental process was relatively short, from start to finish it took no longer than 10 minutes from lighting of the fire to the extinguishing of the fire. However the ventilation and ‘cool down’ time was considerably longer. To reduce this a positive pressure ventilation fan was used to clear the smoke and flush the compartment with cooler air. The use of the fan reduced the commissioning time.
The ambient temperature of the compartment increased as a result of the residual heat from the experiments. The changing ambient temperature was accounted for in FDS by programming the prior ambient temperature given by the sprinkler thermocouple for each experiment.

3.5.2. Experiment Procedure

The experimental procedure was:

1. Sprinkler head placement.
2. Fuel placement.
3. Start the telemetry.
4. Door configured.
5. Light Fire.
6. Set door configuration
7. Fire development.
8. Sprinkler Activation.
9. Fire extinguishment.
10. Decommissioning.

3.5.3. Sprinkler Head Placement

Branch isolation valves were used to isolate the water supply prior to the change over from the used sprinkler heads to new sprinkler heads. Once the sprinkler heads were in place the isolation valve were opened, to allow water in, then shut.

3.5.4. Placement of Fuel

The material covered foam slabs were positioned on the metal chair frame. The backing slab was then mechanically attached to the metal frame with a screw and nail connection. This prevented the package falling during the experiments. The load cell was zeroed before the fuel package was placed on the assembly. See Figure 3.20.

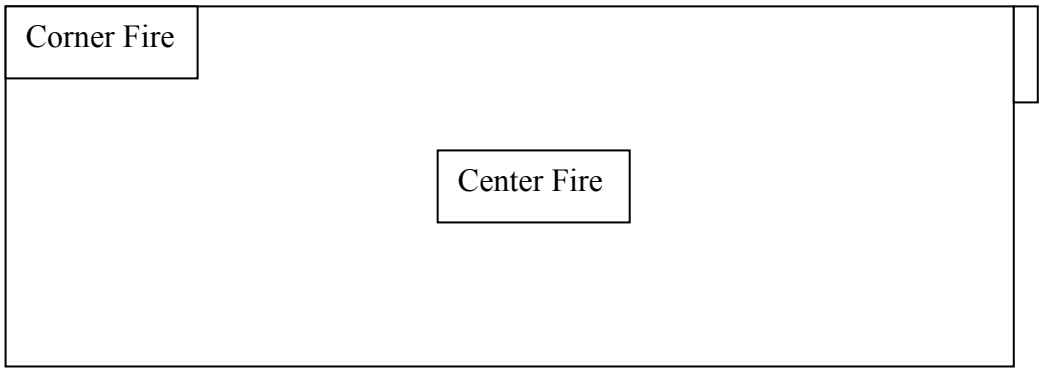

Figure 3.20 Fire Position

Experiment	Fire Position
1 - 15	Center
16 - 22	Corner

Table 3-1 Fire position

3.5.5. Start Data Recording of Ambient Conditions

The next step was to start recording the ambient conditions. The thermocouple and mass loss data logging started 60 seconds before the ignition of the firelighter. The video camera was started. The telemetry was installed/checked at the beginning of each set of experiments. Data files for the thermocouple data and mass loss data were opened in the computers.

3.5.6. Fire Commencement

A firelighter was placed on the rear middle of the bottom foam slab. A propane torch was used to ignite the firelighter, after approximately 60 seconds of ambient data had been recorded. The stopwatch was started at this point. The door was either left open or shut. Table 3-2 details the door position for the experiments.

Experiment	Door Position
1 – 10	Open
11 – 22	Shut

Table 3-2 Door position

3.5.7. Fire Development

The fire was left to develop until both sprinklers had activated.

3.5.8. Sprinkler Activation

Sprinkler activation times were established visually by seeing the activation through the window or by observing the pressure gauge. Sprinkler activation were also identified by the noise of the bulb breaking. At this stage the data logging and videoing stopped.

3.5.9. Fire Extinguishment

A Rega Napsack fire pump was used to extinguish the fire. This method proved very effective in extinguishment of the fire without contaminating the compartment with excess water. Water damage to the experimental rig and assembly did not occur as a result of this process.

3.5.10. Decommissioning

A positive pressure fan was used to clear the smoke and cool the compartment. The fan was positioned at the entrance of the compartment. This fan was run for a minimum of 10 minutes.

3.5.11. Ambient Temperature

The ambient temperature within the compartment varied. The increase in ambient temperature was high as $10^{o}C$. FDS accommodated the variation in ambient temperature by programming the measured ambient temperatures into the individual FDS input files.

3.5.12. Summary

The equipment and procedure outline above was used for the 22 experiments detailed in this report. For some of the experiments, there were problems with the measurement of the compartment temperatures due to TC failure for TC position 1 and 2 for experiments 1 through10, or data recording difficulties for experiments 11 through 15. If the experiments were to be repeated it would be recommended that the fires are burned until the fuel is completely exhausted. This would give a more complete HRR curve.

4 Heat of Combustion

This section contains information on how the heat of combustion (HoC) for the foam was obtained. The section does not detail the process, analysis and calculations used to establish the HoC. Section three, chapters 2 and 3 of the SFPE Handbook of Fire Protection Engineering 3rd edition [44] gives details on the process, analysis and calculations used.

4.1. Calculation

In order to calculate HRR curve for the simulations it was necessary to establish a HoC for the foam. The foam was tested in a cone calorimeter [44], instead of assuming a HoC from available literature. It was felt that by obtaining the actual HoC, there would be less uncertainty with the FDS calculations.

For the experiments two different batches of foam were used. For each batch 3 samples were taken to be tested in the cone calorimeter. By using the oxygen depletion method the HRR data was produced for the samples. Figure 4.1 and Figure 4.2 show the heat release rate curves for the samples.

The total energy released was divided by the total mass consumed to give the effective heat of combustion. The 3 samples for both batches showed good replication. As per the standard an average was taken for each batch [44]. For foam 1 an effective heat of combustion of 21 MJ/kg was used to calculate the HRR, and 20.4 MJ/kg for foam 2.

Sample	Foam 1 (MJ/kg)	Foam 2 (MJ/kg)
1	22.3	20.3
2	20.3	20.8
3	20.5	20
Average	21	20.4

Table 4-1 HoC foam

HRR (MW) = HoC (MJ/kg) x Mass Loss Rate (kg/s) Equation (4)

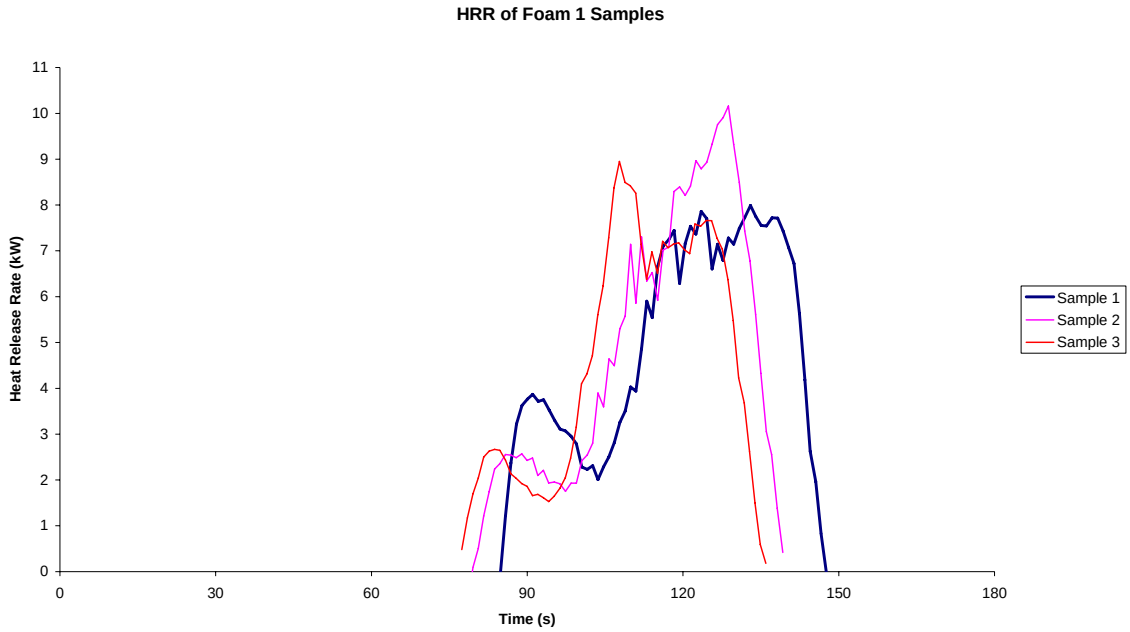

Figure 4.1 HRR of foam 1 samples

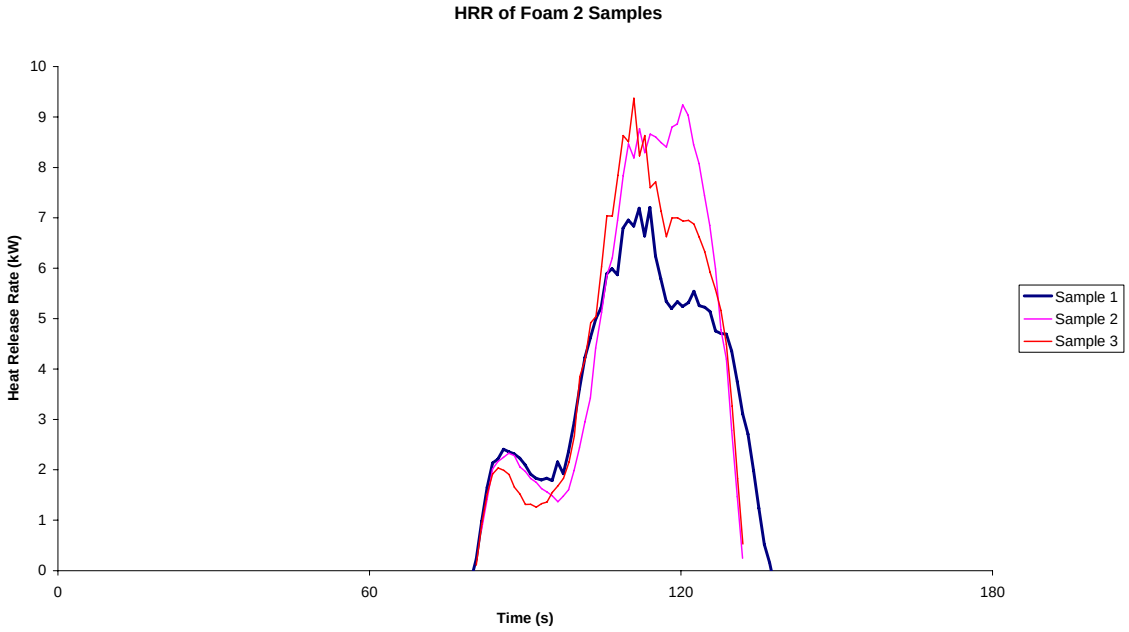

Figure 4.2 HRR of foam 2 samples

Experiment	Batch
1 – 10	Foam 1
11 – 22	Foam 2

Table 4-2 Foam batch used for experiments

Table 4-2 details what batch of foam was used for the experiments.

5 Experimental Results

5.1. Observations

This section gives a qualitative account of what was observed from the experiments.

- Fire growth varied with experiment.
- As fire size increased, flame length increased.
- As the fire developed the smoke layer depth increased.
- The type of sprinkler head affected sprinkler activation time.
- As fire size increased, the radiation given off increased. This was felt through the observation window.
- The backing cushions were consumed by the fire.
- The bottom cushions were persevered in comparison with the backing cushion.
- Sprinkler activation times varied with fire position.
- Limited water discharge from sprinkler heads did not have noticeable effects on the fire.
- Fire growth effected sprinkler activation times.
- For the corner fires, the sprinkler closest to the fire always activated first, if the sprinkler heads were of the same type.
- For center room fires with the same sprinkler head type on each side of the fire, the activation times were generally within a few seconds of each other.

Figure 5.1 shows the development of the fire for experiment 21.

Fire start

Fire Start + 20 seconds

Fire Start + 40 seconds

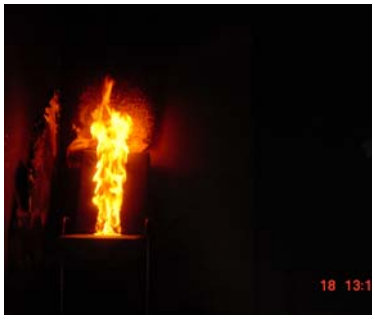

Fire Start + 60 seconds

Fire Start + 80 seconds

Fire Start + 100 seconds

Fire Start + 120 seconds

Fire Start + 140 seconds

Figure 5.1 Observation photos for chair fire in the corner

5.2. Experimental Results and Discussion

The following sections presents the experimental results for sprinkler activation times, heat release rate curves and temperature measurements.

5.3. Data Presentation and Analysis

In this section the method in which the raw data was converted is described and discussed. As with any experimental data it is necessary to reduce it into a usable form.

5.3.1. Load cell

Due to technical constraints of the load cell and data logger, a mass loss rate curve could not be given directly from the load cell output. Chapter 4 describes the load cell and data logging method used for the experiments. The output from the load cell was recorded by a laptop computer using Hyper Terminal software. The load cell did not have a facility to record a time function on the output stream. Effectively giving a mass loss but not a mass loss rate.

To investigate the possibility of using the load cell for the experiments, a bench top investigation was undertaken. It was suggested that the frequency of the load cell output was fixed. Therefore a series of experiments was undertaken to firstly establish:

1. The output frequency of the load cell with a static load.
2. The output frequency of the load cell with several different static loads.
3. The output frequency of the load cell with variable load.

The duration of each experiment varied from 2 minutes to 15 minutes. In total 20 experiments were undertaken to establish the frequency output. The Hyper Terminal files were then imported into Microsoft Excel. Each output segment occupied a single cell within Excel, i.e. 200 outputs filled 200 cells. For each experiment the number of cells filled were counted. This total was then divided by the run time for the

experiment. The figure given would translate to the number of data outputs per second.

This figure was initially calculated for runs of 2 – 5 minutes, but it was found that the accuracy varied to 1 decimal place. It was suggested that the variation in accuracy was due to human error in the starting and stopping process. Therefore to minimize these inaccuracies, experiments were undertaken over a 15 minute interval (for 5 runs). This gave 5 results in which the outputs per second were measured within 13.78 – 13.83 range. This gave an average of 13.81 outputs per second. This was the figure used to obtain the mass loss curve.

To obtain the mass loss curve the data was manipulated using Microsoft Excel. The following procedure was used to convert the load cell data in to a mass loss curve:

1. The hyper terminal file were inserted into Microsoft Excel.
2. A time function was inserted into Excel – 13.81 outputs per second.
3. The file was zeroed.
4. A centered moving average of 20 seconds was calculated.
5. The mass loss was then calculated by subtracting the centered 20 second moving average for the previous second from the present centered 20 second moving average.

The above procedure was used to establish the mass loss curves for the experiments. The data for the ambient conditions (pre fire start) was removed in order to marry it up with the temperature data and sprinkler activation data. The ambient data was deleted from the Excel worksheet, and subsequently the column containing the time was adjusted to start at zero.

A centered moving average of 20 seconds was chosen for the following reasons:

1. Using a 10 second moving average gave a spiking unstable curve.
2. Using a 30 second moving average reduced the responsiveness and accuracy of the curve by too much.
3. Using a moving average of 20 seconds it was felt that the curve would be responsive and stable.

The rate of change was numerically calculated. This was done by subtracting the previous moving average from the new moving average. A difference of 1 second between the two moving averages was chosen. It was felt that a decrease in the time intervals would not cause an increase in accuracy, and an increase in interval time would reduce the resolution of the curves.

5.4. Thermocouple Temperatures

The data logger used to log the thermocouple temperatures allows the transportation of the data into Microsoft Excel. The data file records the measured temperatures against time.

Due to equipment constraints only 8 thermocouple were available for measuring compartment temperatures. Table 5-1 gives the numbering and locations of the thermocouples.

Thermocouple	Tree	Location
TC 1	Sprinkler 1	Adjacent to sprinkler 1
TC 2	Sprinkler 2	Adjacent to sprinkler 2
TC 3	Tree 1	2.3 m above floor level
TC 4	Tree 1	2.1 m above floor level
TC 5	Tree 1	1.0 m above floor level
TC 6	Tree 2	2.3 m above floor level
TC 7	Tree 2	2.1 m above floor level
TC 8	Tree 2	1.0 m above floor level

Table 5-1 Thermocouple numbering and location

5.5. Sprinkler activation times

The sprinkler activation times are expressed in seconds and are referenced as per the diagram below.

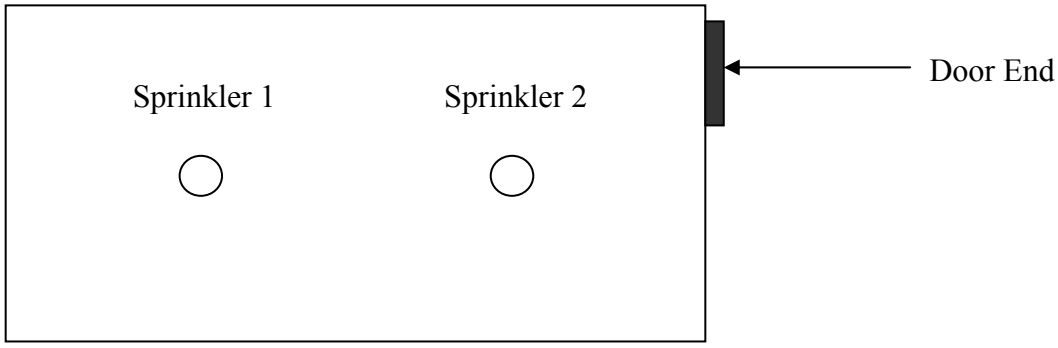

Figure 5.2 Sprinkler location schematic

Figure 5.2 shows the sprinkler location.

5.6. Data Presentation

This section gives the results for experiments 1,10 and 17, these experiments were typical of a center fire with the door open, a center fire with the door shut and a corner fire. Appendix A contains all the experimental results. The following information is given per experiment:

- Fire position.
- Door configuration.
- Sprinkler head type.
- Sprinkler head activation times.
- Thermocouple temperatures.
- Heat release rate curves.

5.6.1. Experiment 1

- Fire position: Center of room
- Door configuration: Open

	Head 1	Head 2
Sprinkler Head Type	Residential A	Residential A
Sprinkler Head Activation Times (secs)	210	250

Table 5-2 Activation times experiment 1

Figure 5.3 is representative of the temperature profile for experiments 1 – 10. From the start of the fire to around 50 seconds there is little change in temperatures. As the fire develops (60 –70 seconds) TC 1 starts to register a change in temperature. TC 3 and 4 measures an increase in temperature at about 80 seconds. TC 1,3,4,6,7 rapidly increases in temperature from about 150 seconds onwards. At this point TC 5 and 8 start to register a change.

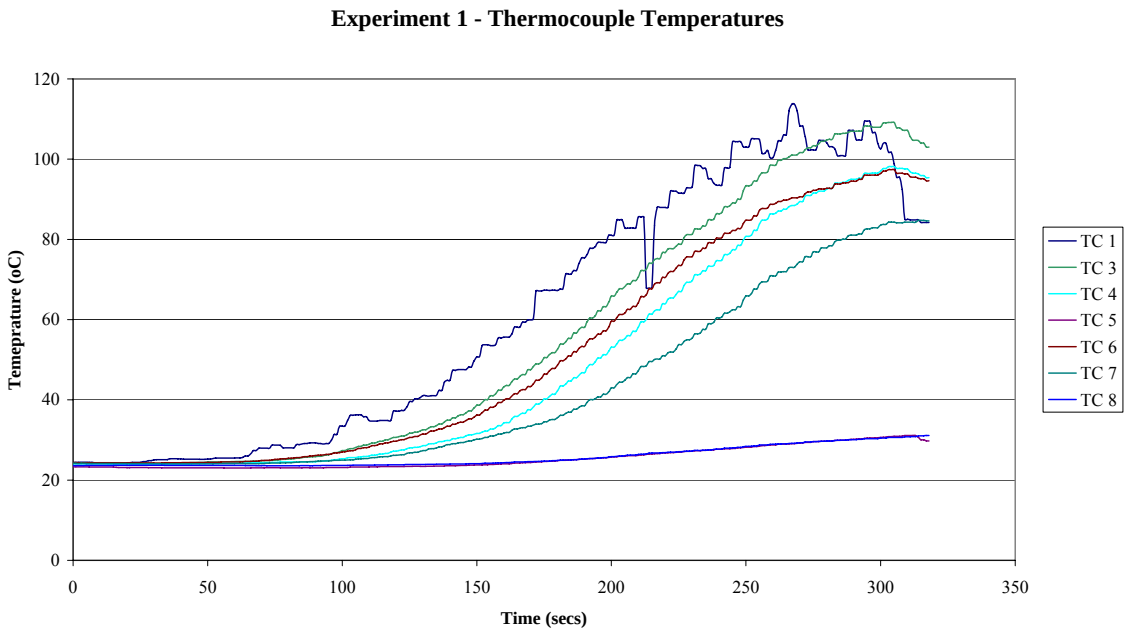

Figure 5.3 Experiment 1 - thermocouple temperatures

The temperature profile is what would be expected for a compartmental fire in the early stages of development. The blip in the line of TC 1 at 210 seconds results from the water discharge from the sprinkler activation.

From the TC measurements it can be seen that the TC's that are closer to the door measure lower temperatures. This would be expected as the open door would introduce colder air to the compartment.

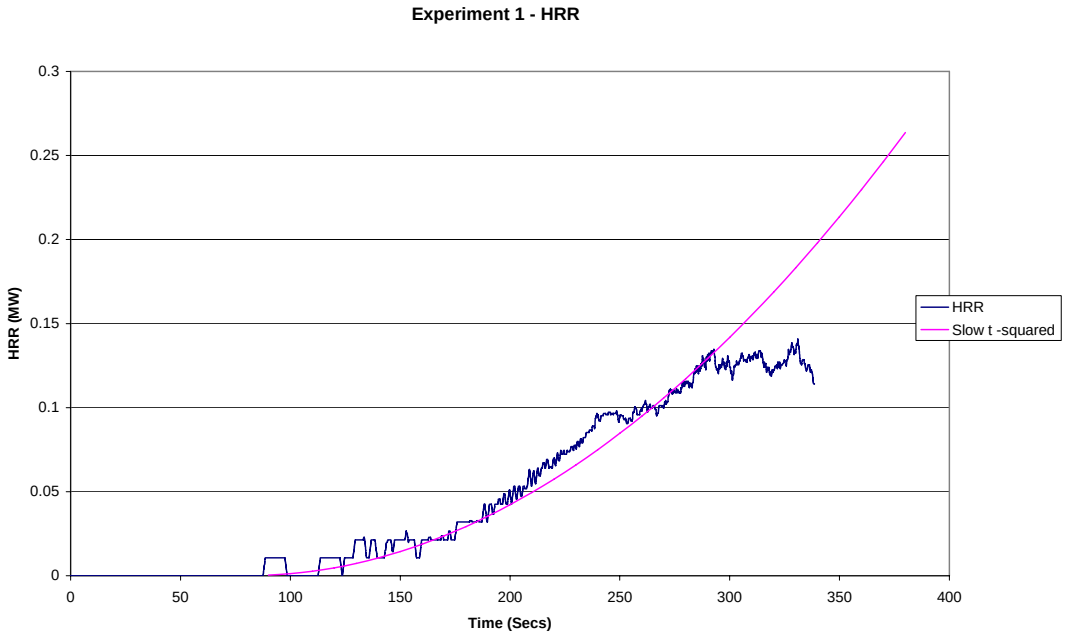

Figure 5.4 Experiment 1 – HRR

Figure 5.4 details the HRR curve for experiment 1. The mass loss data for the experiment is multiplied with the heat of combustion of the foam. The mass loss is measured in 5 gram increments. The fire can burn 5 grams of fuel over a prolonged period, but the load cell will only register it at a single point. This is a problem when there is a low mass loss rate, as per the first 100 seconds of the experiment 1.

Generally the heat release rate of the fire can be described as a slow t-squared fire. Karlsson and Quinterie describe t-squared fires [2]. It took about 150 seconds to reach approximately 130 kW once the fire had established itself.

5.6.2. Experiment 10

- Fire position: Center of room
- Door configuration: Open

	Head 1	Head 2
Sprinkler Head Type	Residential A	Residential B
Sprinkler Head Activation Times (secs)	183	184

Table 5-3 Sprinkler activation times experiment 1

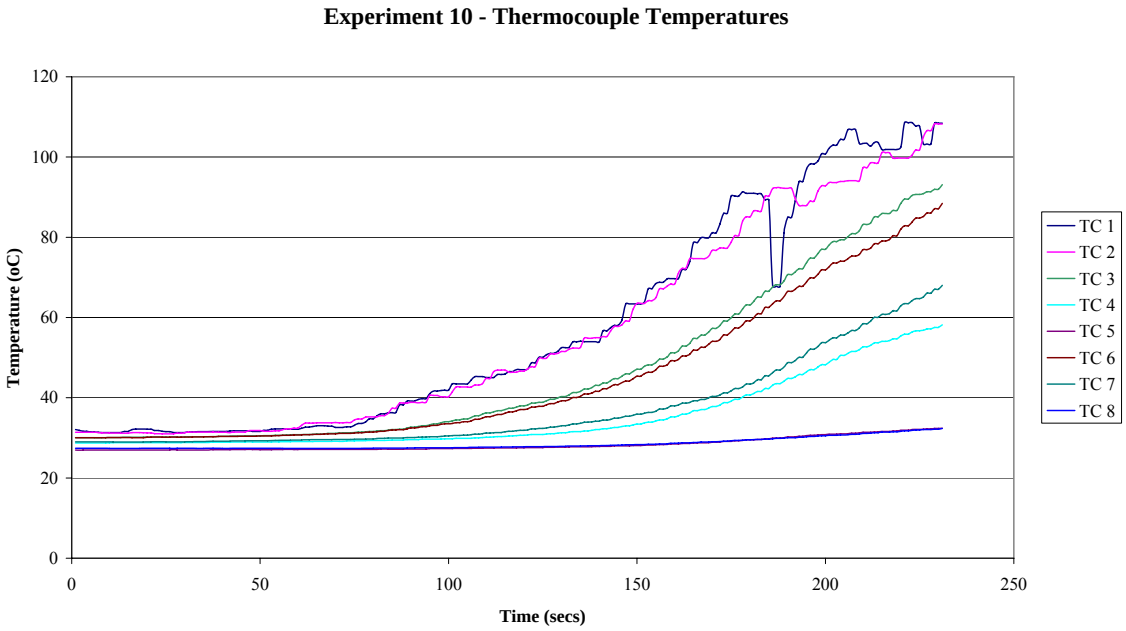

Figure 5.5 Experiment 10 - thermocouple temperatures

Experiment 10 (Figure 5.5) is similar to experiment 1. It is interesting that TC 1 increases in temperature more quickly than TC 2, after 150 seconds of fire development.

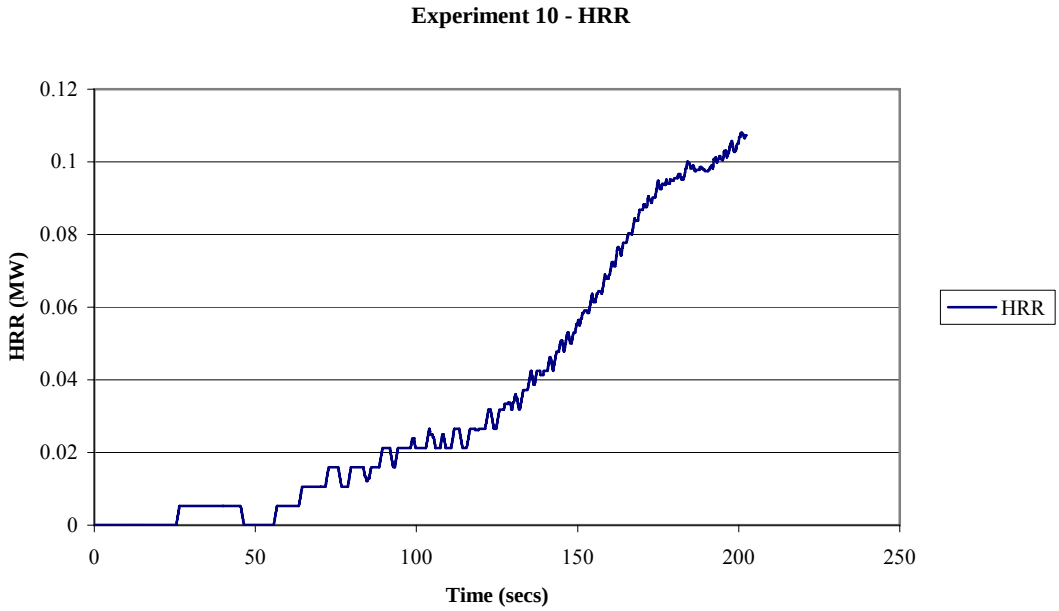

Figure 5.6 Experiment 10 – HRR

The HRR curve for experiment 10 (Figure 5.6) follows the same pattern as the HRR curve for experiment 1.

5.6.3. Experiment 17

- Fire position: Corner of room
- Door configuration: Shut

	Head 1	Head 2
Sprinkler Head Type	Residential B	Residential A
Sprinkler Head Activation Times (secs)	181	228

Table 5-4 Sprinkler activation times experiment 17

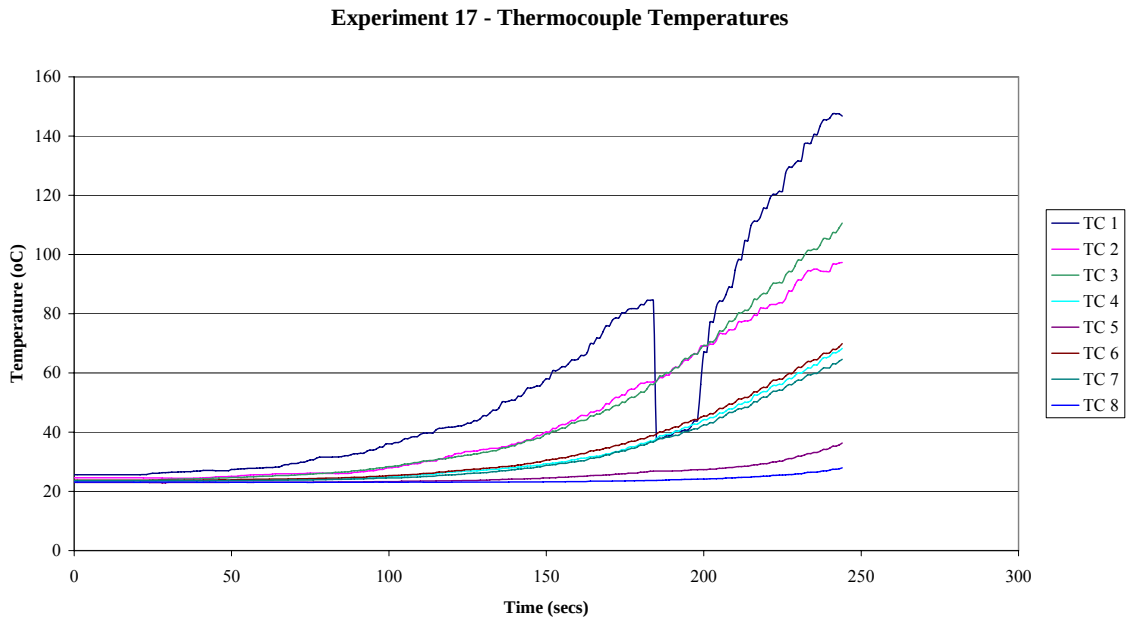

Figure 5.7 Experiment 17 - thermocouple temperatures

Figure 5.7 shows a typical temperature profile for experiments 17 – 20. It can be seen that the fire position changes the temperature profile significantly from the temperature profile for a centrally positioned fire such as for experiment 1 or 10. TC's 1,3,4 and 5 measure a change in temperature more quickly than the more distant TC's (2,6,7 and 8). This would be expected as the hot gases pass by the closer TC's, before they are subjected to more cooling on the way to passing the more distant TC's.

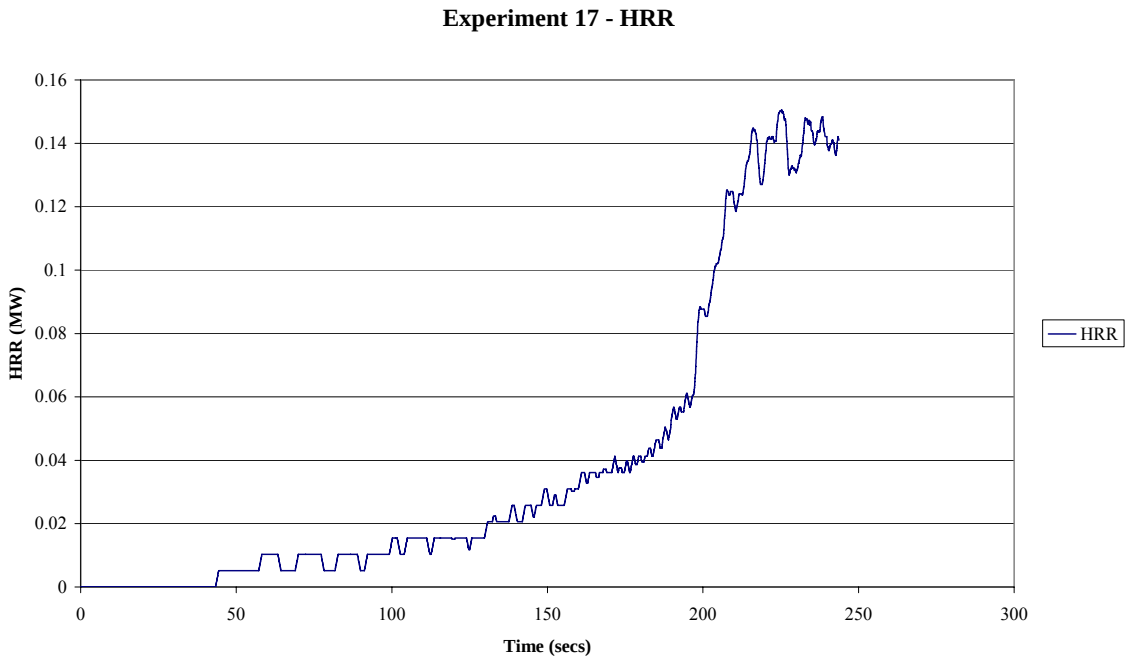

Figure 5.8 Experiment 17 – HRR

Figure 5.8 gives the HRR for experiment 17. From about 50 seconds to 200 seconds a slow t squared curve would approximately represent the fire. At around 190 seconds the growth of the fire accelerates- a fast t squared fire would represent this increase. This may be a result of the chair being placed in the corner, thus being subjected to increased levels of radiation feed back, which is also known as the corner effect.

5.7. Sprinkler Activation Times

This section discusses the sprinkler activation times. Factors such as sprinkler head type, fire position and heat release rate are taken into account to identify patterns or relationship involving the activation times of the sprinkler heads.

5.7.1. Sprinkler Activation Bins

The sprinkler activations are placed into bins based on (or combinations of):

1. Sprinkler head type.
2. RTI.
3. Fire position.
4. Door configuration.
5. Heat release rate parameters.
6. Sprinkler thermocouple temperature.
7. Activation temperatures.

5.7.2. Center Fire, Door Open, 68^{o}C

Centre fire, door open, activation temperature					
Experiment	Head 1	Time (secs)	Head 2	Time (secs)	Difference
1	Residential A	210	Residential A	250	40
2	Residential A	225	Residential A	211	14
7	Residential A	182	Residential A	186	4
3	Residential B	192	Residential B	192	0
8	Residential B	182	Residential B	187	5
9	Residential B	233	Residential B	230	3
4	SS 68	226	SS 68	226	0
5	SS 68	266	SS 68	272	6
6	SS 68	216	SS 68	211	5
10	Residential A	183	Residential B	184	1

Table 5-5 Center fire door open and activation temperature

It took 182 seconds for the quickest sprinkler activation (Experiment 8, head 1, residential B), and 272 seconds for the slowest activation (Exp 5, head 2, SS). The

difference between sprinkler head activations for the individual experiments ranges from 0 to 40 seconds with an average of 7.8 seconds.

5.7.3. Center Fire, Door Shut, Activation Temperature

Centre fire, door shut, activation temperature					
Experiment	Head 1	Time (secs)	Head 2	Time (secs)	Difference
11	SS 68	199	Residential B	175	24
12	SS 68	246	Residential B	228	18
13	SS 68	204	Residential B	194	10
14	SS 68	203	Residential B	187	19
15	SS 68	270	Residential B	253	17

Table 5-6 Center fire door shut and activation temperature

It took 175 seconds for the quickest sprinkler activation (Exp 11, head 2, residential B), and 270 seconds for the slowest activation (Exp 15, head 1, SS). The average sprinkler activation time for a sprinkler at position head 1(non door end) is 224.4 seconds and for head 2 (door end) is 207.4 seconds. The difference between the two averages is 17 seconds. The difference between sprinkler head activations for the individual experiments ranges from 10 to 24 seconds with an average of 17.6 seconds.

5.7.4. Corner Fire, Door Shut

Sprinkler type corner fire, door shut					
Experiment	Head 1	Time (secs)	Head 2	Time (secs)	Difference
16	Residential B	178	Residential A	244	66
17	Residential B	181	Residential A	228	47
18	SS 68	187	Residential A	221	34
19	SS 68	189	Residential A	223	34
20	SS 68	205	Residential A	-	-
21	SS 93	216	SS 93	330	114
22	SS 93	205	SS 93	263	58

Table 5-7 Corner fire door shut

- denotes no activation occurred

It took 178 seconds for the quickest sprinkler activation (Exp 16, head 1), and 330 seconds for the slowest activation (Exp 21, head 2).

5.8. Heat Release Rate Curve Influence

It is intuitive to expect that sprinkler activations times will be shorter for fires that develop faster and are of a greater magnitude. This section looks at the experimental results to investigate if there is a relationship between the HRR and sprinkler activation times.

The figure of 40 kW was chosen as it is representative of the value where the HRR of the test fires, start to develop at a increased rate. 40 kW also encompassed all the data sets, the HRR for some of the experiments is low as 41 kW at the time of sprinkler activation.

Experiment	Head 1	Activation Time (secs)	HRR @ Time of Sprinkler Activation	Head 2	Activation Time (secs)	HRR @ Time of Sprinkler Activation	Difference	Time to 40 kW (secs)
1	Res A	210	0.051	Res A	250	0.095	40	141
2	Res A	225	0.09	Res A	211	0.084	14	147
7	Res A	182	0.105	Res A	186	0.108	4	130
3	Res B	192	0.103	Res B	192	0.103	0	140
8	Res B	182	0.088	Res B	187	0.0905	5	150
9	Res B	233	0.0841	Res B	230	0.0811	3	190
4	SS 68	226	0.125	SS 68	226	0.125	0	139
5	SS 68	266	0.116	SS 68	272	0.125	6	193
6	SS 68	216	0.129	SS 68	211	0.126	5	133
10	Res A	183	0.098	Res B	184	0.098	1	135
12	SS 68	246	0.111	Res B	228	0.107	18	171
13	SS 68	204	0.106	Res B	194	0.102	10	130
14	SS 68	203	0.093	Res B	187	0.072	19	152
15	SS 68	270	0.1248	Res B	253	0.0946	17	201

Table 5-8 Table HRR center fire

The time it takes the heat release rate to reach 40 kW (see Table 5-8) ranges from 130 to 201 seconds, with the majority being within the range of 130 - 150 seconds with an average of 153.7 seconds. The lowest HRR at the time of sprinkler activation is 51 kW (Exp 1, res A, head 1) and 125 kW for the highest HRR at time of sprinkler activation.

Experiment	Head 1	Time (secs)	HRR @ Time of Sprinkler Activation	Head 2	Time (secs)	HRR @ Time of Sprinkler Activation	Difference	Time to 40 kW (secs)
16	Res B	178	0.0158	Res A	244	0.0331	66	264
17	Res B	181	0.041	Res A	228	0.136	47	172
18	SS 68	187	0.105	Res A	221	0.14	34	154
19	SS 68	189	0.072	Res A	223	0.086	34	148
20	SS 68	205	0.05	Res A	-	-	-	167
21	SS 93	216	0.092	SS 93	330	0.012	114	157
22	SS 93	205	0.11	SS 93	263	0.075	58	151

Table 5-9 HRR corner fire

- denotes no activation occurred

The time it takes the heat release rate to reach 40 kW ranges from 148 to 264 seconds (see Table 5-9), the majority of the times range from 150 - 170 seconds with an average of 173.2 seconds. The lowest HRR at the time of sprinkler activation is 41

kW (Exp 17, res B, head 1) and 136 kW for the highest HRR at time of sprinkler activation.

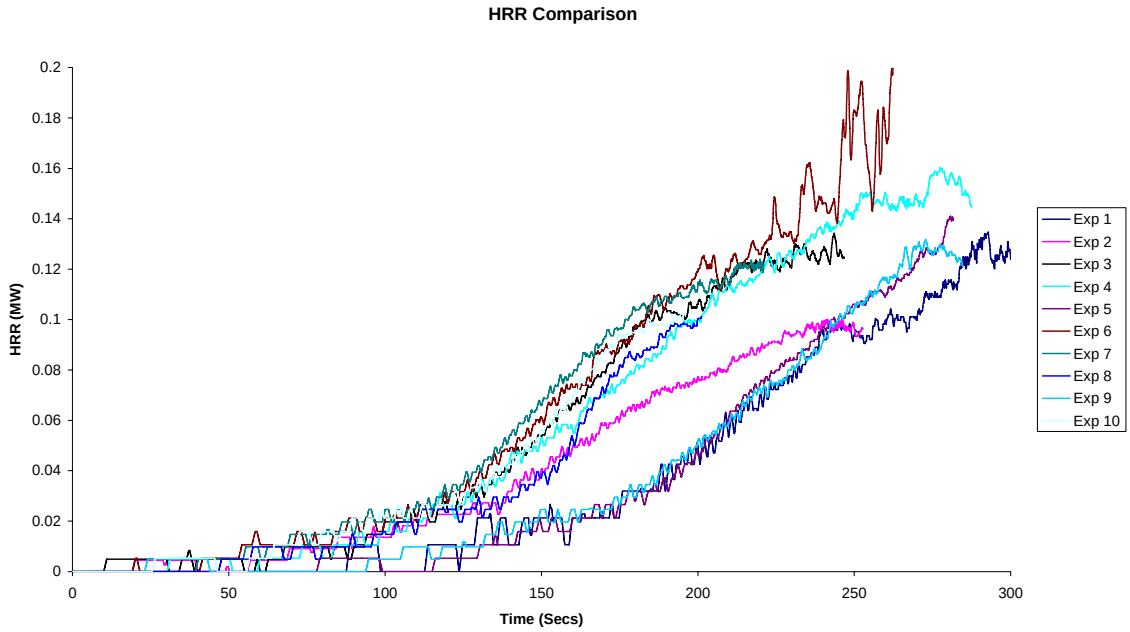

Figure 5.9 HRR Comparison for center fires

Table 5-8, Table 5-9 and Figure 5.9 show that there is a strong influence from the fire development on the sprinkler activation times. The HRR curve for experiment 7 develops more quickly than the HRR curve for experiment 1, this is reflected in the activation times as the residential sprinkler heads for experiment 1 lag considerably in comparison with the residential sprinkler head activations times for experiment 7. This observation is also true for experiments 5 and 6 which involved standard response heads. By comparing the HRR curves with sprinkler activation times it is seen that the quicker the HRR curve increases (quicker fire development), the sooner the sprinklers activate.

5.9. Temperature of Gas at Activation

This section details the temperature of the adjacent gas to the sprinkler heads.

Experiment	Head 1	Time (secs)	Gas temp at sprinkler head (oC)	Head 2	Time (secs)	Gas temp at sprinkler head (oC)
1	Res A	210	86	Res A	250	-
2	Res A	225	89	Res A	211	-
7	Res A	182	-	Res A	186	96
3	Res B	192	93	Res B	192	-
8	Res B	182	-	Res B	187	90
9	Res B	233	93	Res B	230	87
4	SS 68	226	106	SS 68	226	-
5	SS 68	266	97	SS 68	272	-
6	SS 68	216	100	SS 68	211	-
10	Res A	183	90	Res B	184	89
11	SS 68	199	98	Res B	175	86
12	SS 68	246	-	Res B	228	-
13	SS 68	204	-	Res B	194	-
14	SS 68	203	-	Res B	187	-
15	SS 68	270	-	Res B	253	-
16	Res B	178	87	Res A	244	82
17	Res B	181	85	Res A	228	88
18	SS 68	187	105	Res A	221	85
19	SS 68	189	100	Res A	223	82
20	SS 68	205	101	Res A		-
21	SS 93	216	123	SS 93	330	-
22	SS 93	205	119	SS 93	263	110

Table 5-10 Table Sprinkler thermocouple temperature at time of sprinkler activation

- denotes no temperature data was collected

From Table 5-10 it can be seen that for sprinkler heads with an activation temperature of 68^{o}C the minimum temperature of a sprinkler thermocouple at the time of activation was 82^{o}C and the maximum temperature was 106^{o}C. The average temperature was 92^{o}C. For the residential type sprinkler heads the TC temperatures generally ranged from 80 – 95^{o}C at the time of sprinkler activation and 100 – 105^{o}C for standard response 63^{o}C. For standard response 93^{o}C the range was 110 – 123^{o}C.

The measured TC temperatures represent the gas temperature in and around the sprinkler heads. It cannot be assumed that the actual gas temperatures are being measured:

- Due to the thermal characteristics of the thermocouples there is a lag between actual gas temperature and TC temperature,
- The thermocouple is a point measurement, therefore does not represent the entire space around the sprinkler heads. It is possible that there is a variation in gas temperature around the sprinkler heads, a single probe can not measure this. The gas velocity and temperature both vary in space around the sprinkler head.

The difference in sprinkler activation temperature and measure temperature ranges from 14 – 25^{o}C for residential heads and 29 - 38^{o}C for SS 68^{o}C heads and 17 – 30^{o}C for SS 93^{o}C.

5.9.1. Summary of Sprinkler Activations

The nominal activation temperatures of the sprinkler heads influenced the sprinkler activation times. This has been reported by Isman [43]. From the experimental data it can be deduced that the sprinkler heads will activate in this order for the same fire based on the temperature ratings:

1. Residential A or B
2. SS 68^{o}C
3. SS 93^{o}C

It was found that the RTI of the sprinkler heads affected the sprinkler activation times. Fleming [40] reports that the smaller the RTI, the quicker the sprinkler activation. The residential sprinklers and SS 68^{o}C have the same nominal activation temperature, but for the same fire conditions would have different sprinkler activation times. The residential heads had an RTI of 36 m $^{1/2}$s $^{1/2}$ and the standard response heads had a RTI of 95 m $^{1/2}$ s $^{1/2}$. Generally the difference in activation times was in the range of 10 – 25 seconds between an residential and SS 68^{o}C head for a given fire.

From the experimental data it can be deduced that the sprinkler heads will activate in this order for the same fire based on the RTI (if all other parameters are the same):

1. 36 $m^{1/2}$ $s^{1/2}$
2. 95 $m^{1/2}$ $s^{1/2}$

The fire position in relation to the sprinkler head significantly affected the sprinkler activation times. When the fire was placed centrally, the sprinkler activation times for locations sprinkler 1 and 2 were within seconds of each other for identical sprinkler heads per experiment. For the corner fire the sprinkler activation times varied by 34 seconds for residential heads and 114 seconds for SS 93^{o}C.

From the limited experimental data it is difficult to clearly define if the door configuration had an effect on sprinkler activation times. There may be a decrease (quicker activation) in activation times for sprinkler location 2 (door end) when the door is shut, but this is not significant and difficult to assign to the door being shut.

With the door open combustion products would leave the compartment, but there is a 400 mm high reservoir that would trap the hot gases surrounding the sprinkler head which is continuously being charged with hotter products. The cooler gas would leave by the door opening with the hotter gases heating the sprinkler head. Therefore the door open position should have a minimal effect on the sprinkler activation times for the fire type and size used in the experiment.

As it would be expected fires that release large amounts of heat into the compartment sooner will raise the temperature of the compartment more quickly, this was evident in the experiments.

The TC temperatures that were measured around the sprinkler head at time of sprinkler activation varied considerably. The TC temperatures were higher for sprinklers with high RTI's in comparison with sprinklers with lower RTI's.

5.9.2. Results Summary

- Residential sprinklers activate before standard response head (if all else is the same).
- Gas activation temperatures are highest for standard response heads.
- More aggressive HRR curves result in quicker activations.
- Sprinkler activation times are dependent on ‘distance from fire’.
- Activation times are dependent on nominal temperature rating of bulbs.
- The difference in activation times for the residential and standard response heads 68^{o}C was not greater than 10 %.

6 FDS Model

This section of the report gives a brief account of the scientific and mathematical principles used by Fire Dynamics Simulator 3. It is not the intention of this section to discuss the model in great detail. There are several pieces of work that discuss the fundamentals of the model, such as the technical guide given for the program [3] and research projects by Petterson [6] and Hume [45]. These projects were chosen as they were both written by students attending at the University of Canterbury. This section is based on work done by Petterson and technical manual.

6.1. FDS Background

The rapid growth of computing power and the maturing of CFD, has led to the use of these models for fire applications [3]. The majority of this work is based on the conceptual framework provided by the Reynolds - average form of the governing equations, in particular the κ-ε turbulence model pioneered by Patankar and Spalding [46]. However due to the limitations of the κ-ε turbulence model FDS uses the 'Large Eddy Simulation' techniques to model turbulence. The basic idea behind the LES technique is that the eddies that account for most of the mixing (turbulence) are large enough to be modeled with reasonable accuracy by using the equations of fluid dynamics [3]. The small scale mixing is modeled by sub-models or discounted.

6.1.1. Hydrodynamic model

The general equations of fluid dynamics describe a rich variety of physical processes, such as aerodynamics, water flow etc. These equations that describe the mass, momentum and energy of a fluid have been simplified by Rehm and Baun [3]. The simplified equations use an approximate form of the Navier – Stokes equations for flow in a thermally expandable multi-component fluid. The original Navier-Stokes equations, as well as derivations from first principles, are given by Hinze [47].

The simplified equations are known as the 'low mach number' combustion equations [3]. They describe the low speed motion of a gas driven by chemical heat release and buoyancy forces.

Four equations of conservation are central to the simplified form of the Navier-stokes equations. These equations cover conservation of mass, momentum, energy and species. In order to numerically solve the equations in FDS they are discretised in space using a 2nd order central difference method and in time using a 2nd order predictor- corrector scheme [3].

6.1.2. Conservation of Mass

$$\frac{\partial \rho}{\partial t} + \nabla . \rho u = 0 \qquad \text{Equation (5)}$$

where

u = vector describing the velocity in the u,v and w directions.

Practically the conservation of mass equation can be described as (if the density is constant) what flows in to a control volume must flow out [14]. The conservation of mass states that the rate of mass storage, due to density changes within a control volume is balanced by the net rate of inflow of mass by convection [12].

6.1.3. Conservation of Momentum

By applying Newton's second law of motion the conservation of momentum equation is derived. Simply this states that the rate of change of momentum of a fluid element is equal to the sum of the forces acting on it [14].

$$\rho\left(\frac{\partial u}{\partial t} + (u.\nabla)u\right) + \nabla \rho = \rho g + f + \nabla . \tau \qquad \text{Equation (6)}$$

The left hand side of this equation expresses the rate of change of momentum of a volume of fluid, the right hand side reflects the forces acting on it. The forces include gravity (g), an external force vector (f) and a measure of the viscous stress (τ) acting on the fluid within the control volume. Gravity is important as it represents the influence of buoyancy on the flow.

The viscous stress is given by the product of viscosity and a measure of velocities that the fluid volume is subjected to. A deformation tensor is used to account for the velocity term. For Large Eddy Simulations the sub grid analysis was developed by Smagorinsky is used to model the viscosity [3]. This uses the deformation factor to arrive at a value for the local turbulent viscosity based on the fluid density, an empirical constant and a characteristic length which is in the order of the grid size used in the model. The turbulent viscosity is then used to calculate thermal conductivity and diffusivity for the model [3].

The equations for the conservation of momentum is simplified to obtain an expression that can be solved quickly and directly in the model calculations using fast Fourier transforms.

6.1.4. Conservation of Energy

The energy equation accounts for the energy accumulation due to internal heat and kinetic energy, as well as the energy fluxes associated with convection, conduction, radiation, the inter diffusion of species and the work done on the gases by viscous stresses and body forces [14]. In general it describes the balance of energy within the control volume. The FDS model uses:

$$\frac{\partial}{\partial t}(\rho h) + \nabla.\rho h u - \frac{\partial \rho}{\partial t} + u.\nabla\rho = q''' - \nabla.q_r + \nabla.k\nabla T + \nabla.\sum_1 h_1(\rho D)_1 \nabla Y_1 \quad \text{Equation (7)}$$

The left side describes the net rate of accumulation, the right side is comprised of the various energy gain or loss terms that contribute to this accumulation.

6.1.5. Conservation of Species

The following equation is used to preserve the conservation of species:

$$\frac{\partial}{\partial t}(\rho Y_1) + \nabla.\rho Y_1 u = \nabla.(\rho D)_1 \nabla Y_1 + W_1''' \quad \text{Equation (8)}$$

Petterson [6] describes equation 8 as, “The first term on the left side represents the accumulation of species due to a change in density, the second term is the inflow and outflow of species. The right side gives the inflow or outflow of species from the control volume due to diffusion and the production rate of the particular species.”

6.2. Combustion Model

For LES, FDS uses a mixture fraction model. LES assumes turbulent mixing of combustion gases with the surrounding atmosphere [3]. It is assumed that the mixing controls combustion and species of interest can be represented by a variable known as the mixture fraction (Z). The mixture fraction model is based on the assumption that large-scale convective and radiative transport phenomena can be simulated directly, but physical processes occurring at small length and time scales must be represented in an approximate manner [6].

The mixture fraction is a conserved quality representing the fraction of material at a given point that originated as fuel [3], and is defined as:

$$Z = \frac{sY_f - (Y_0 - Y_0^{\infty})}{sY_f^I + Y_0^{\inf}} \quad ; \; s = \frac{\nu_0 M_0}{\nu_f M_f} \qquad \text{Equation (9)}$$

Z varies from 1 in the region containing only fuel, to zero where the oxygen where the oxygen mass fraction equals its ambient value, $Y_0^{\inf}$.

The combustion model approximates the combustion process in both space and time so that the fire can be simulated more efficiency [48], and assumes that large scale convection and radiative transport can be modeled directly while small scale mixing can be ignored. Since the combustion processes are on a much shorter time scale than the convection processes, a infinite reaction rate is assumed. The fuel and oxygen can not co-exist [3]. Subsequently, at a point both species instantaneously vanish, their mass fractions dropping to zero.

This leads to the simplification of equation (9) to obtain the flame mixture fraction (Z_f) equation:

$$Z_f = \frac{Y_0^{\inf}}{sY_f^{Ii} + Y_0^{\inf}} \qquad \text{Equation (10)}$$

The point Z_f defines the flame in the computational domain [48]. This point is referred to as the flame sheet.

The assumption that fuel and oxidizer cannot co-exist leads to the 'state relation' between the oxygen mass fraction Y_o and Z [3]

$$Y_0(Z) = Y_0^{\inf}\left(1 - Z/Z_f\right) \qquad <Z_f \qquad \text{Equation (11)}$$

$$0 \qquad Z>Z_f$$

The mass fraction of all other species of interest can be described by individual state relations based on the mixture fraction. This explained in greater detail in Floyd et al [48]. Figure 6.1[3] represents the relations between the mixture fraction and the mass fraction of various species for propane.

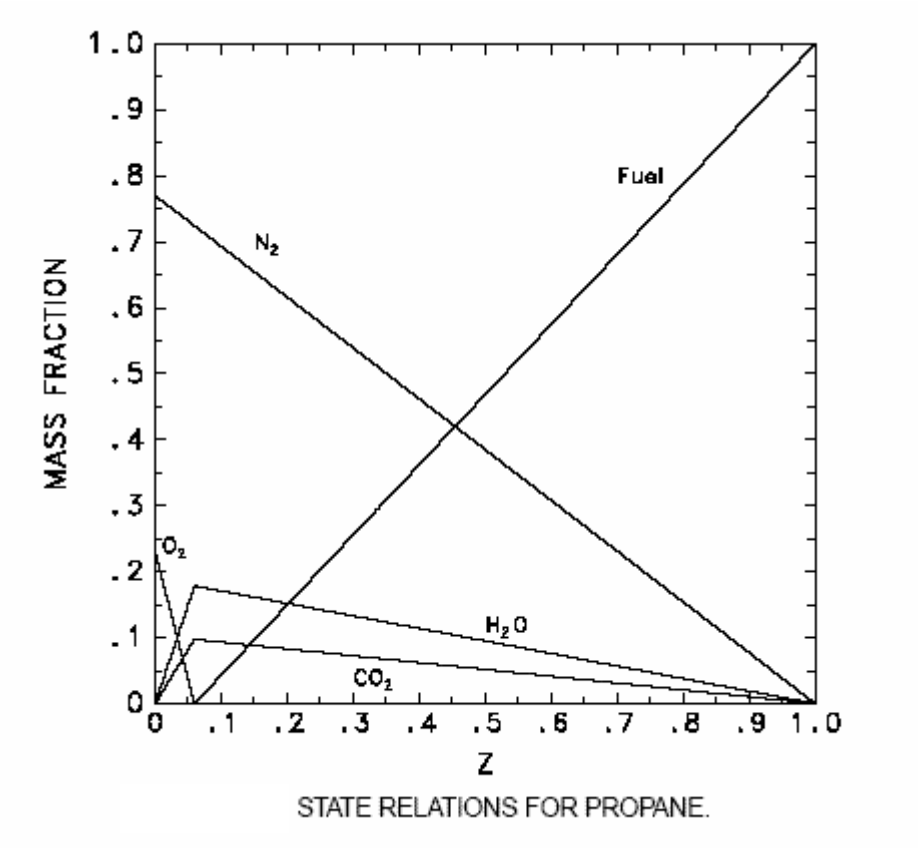

Figure 6.1 State relations for propane

The local oxygen mass fraction can be used to determine the oxygen consumption rate (m_o'''). This is then used to calculate the local HRR by multiplying it with the HRR per unit mass of oxygen (ΔH_o) [3].

The mixture fraction model has several limitations, both numerical and physical. The numerical limitations are related to the resolution of the underlying numerical grid. One problem that occurs due to the local HRR calculation procedure i.e. that if the fire is not adequately resolved the flame surface defined by the mixture fraction $Z = Z_f$ will tend to underestimate the observed flame height. A measure of how well the fire is resolved is given by the non-dimensional expression $D^*/\delta x$, where D* is the characteristic fire diameter

$$D^* = \left(\frac{\dot{Q}}{\rho_\infty C_p T_\infty \sqrt{g}} \right)^{\frac{2}{5}}$$ Equation (12)

A better estimate of the flame height can be provided by using a different value for the mixture fraction (Z). The effective mixture fraction ($Z_{f,eff}$) is:

$$\frac{Z_{f,eff}}{Z_f} = \min\left(1, C\frac{D^*}{\delta x}\right)$$ Equation(13)

Where C is an empirical constant [3].

6.3. Thermal Radiation Model

A modified finite volume method is used to calculate the radiative fluxes within FDS. The method is derived from the Radiative Transport Equation (RTE) for non-Scattering grey gas [45]. The method relates radiation intensity to wavelength. A method similar to the finite volume method used in fluid flow is then used to solve this initial equation.

FDS assigns the temperature generated from the flame sheet to the adjacent cells, this causes lower temperatures as the temperature in the cell is an average as compared to a point in the diffusion flame. Because radiation is dependent on the forth power of the temperature, this method of temperature assigning can have a significant impact on the calculated radiation. Elsewhere the temperature is calculated with greater confidence so the source term can assume its ideal value [3]. The radiation relations become:

$\kappa I_b = \kappa\sigma T^4/\pi$ Outside flame zone Equation (14)

$\chi_r q'''/4\pi$ Inside flame zone

Where q''' is the HRR per unit volume and χ_r is the local fraction of that HRR emitted as thermal radiation. K is the local absorption coefficient and is dependent on the mixture fraction and temperature. σ is the Stefan-Boltzman constant. Its is determined by a sub-model implemented in FDS called RADCAL [3].

6.4. **Sprinkler Activation Model**

The sprinkler activation model is based on the differential equation put forward in Quantification of Thermal Responsiveness of Automatic Sprinklers Including Conduction Effects by Heskestad and Bill [42] reports McGratten [3]. Terms are added to account for radiative heating and cooling by water droplets in the gas from previously activated sprinklers. The water supply was turned off for the purposes of the FDS simulations.

$$\frac{dT_I}{d_t} = \frac{\sqrt{|u|}}{RTI}(T_g - T_I) - \frac{c}{RTI}(T_I - T_m) - \frac{C_2}{RTI}\beta|u| \qquad \text{Equation (15)}$$

Where

T_I = link temperature

Tg = gas temperature in the neighborhood of the link

Tm = temperature of the sprinkler mount

β = the volume fraction of (liquid) water in the gas stream

$|u|$ = the velocity of the air streaming by the sprinkler

RTI = response time index ($m^{1/2}s^{1/2}$)

c = c-factor $(m/s)^{1/2}$

C_2 is a constant that has been empirically determined by DiMarzo [49] to be 6 x 10^6 $K/(m/s)^{0.5}$.

The inclusion of the far right term in Eq.(15) is important in considering how small droplets introduced into the ceiling jet by activated sprinklers can delay or inhibit second or third row sprinklers from activating. However there is minimal water usage by the sprinklers during the experiments.

For this research we are only interested in the sprinkler activation model. The technical guide contains more information about the modeling of sprinklers in FDS.

6.5. Heat Detectors Activation Model

The equation given for the change in temperature of a heat detector is :

$$\frac{dT_l}{dt} = \frac{\sqrt{|u|}}{RTI}(T_g - T_l) \qquad \text{Equation (16)}$$

Where $|u|$ is the velocity of the air streaming by the heat detector, Tg is the gas temperature in the neighborhood of the element, T_l is the temperature of the element and RTI of the heat detector.

6.6. Model Input Specification

This section reports on the development of the input file used for FDS simulations. There are differences in the individual input files. The differences involve location of the fire, the HRR curve of the design fire, the configuration of the door, and the type of sprinkler heads modelled.

6.6.1. Input File

The first line of the input files names the output file, which in this case is ‘experiment 1’. The title section does not perform a part of the simulation, but is intended to give a short description of the input file.

```
&HEAD CHID=’EXPERIMENT 1’, TITLE=’INPUT FILE FOR EXP 1’/
```

The next line describes the quantity of cells to be used in the computational domain. For the input file for experiment 1there are 90 cells in the X direction, 45 in the Y direction and 25 in the Z direction.

```
&GRID IBAR=90,JBAR=45,KBAR=25/
```

The next line describes the physical size of the domain. The domain is 9 m long, 4.5 m wide and 2.5 m high. An example grid size of 100 mm x 100 mm x 100 mm was used for the simulation file detailed here.

```
&PDIM XBAR0=-0.8,XBAR=8.20,YBAR0=-0.30,YBAR=4.20,ZBAR=2.5/
```

The next input line defined the maximum time in that the simulation would be run for. In the case of this simulation the maximum time was 450 seconds.

```
&TIME TWFIN= 450. /
```

This set of input lines relate to the fire. The first line specifies that any surface (SURF) that is tagged with a surface identification of a fire will have a maximum heat release rate per unit area of 3500 kW (equates to the maximum value on the HRR curve for the experiment taking into account the vent area). The fire is to follow the growth and decay specified by the RAMP lines given. The ramp lines represent the HRR curves from the fire for experiment 1. The fire is programmed to have a RAMP number of 0 (lowest HRR) at time 0, and 1 (highest HRR) at 331 seconds. The OBST line details the dimensions of the firebase, and the VENT line specifies the surface area in which pyrolyzed fuel is ejected. The surface identification of the fuel package is inert, as the HRR curve is being prescribed.

```
&SURF ID='FIRE',HRRPUA=3500,RAMP_Q='CHAIR FIRE' /
&VENT XB=3.9,4.3,1.9,2.0,0.65,0.65,SURF_ID='FIRE' /
&OBST XB=3.9,4.3,1.9,2.0,0.0,0.65,BLOCK_COLOR='GREEN',
    SURF_ID='INERT'/
&RAMP ID='CHAIR FIRE',T=0.0,F=0.0/
&RAMP ID='CHAIR FIRE',T=92.0,F=0.071/
&RAMP ID='CHAIR FIRE',T=180.0,F=0.228/
&RAMP ID='CHAIR FIRE',T=240.0,F=0.678/
&RAMP ID='CHAIR FIRE',T=276,F=0.786/
&RAMP ID='CHAIR FIRE',T=292,F=0.95/
&RAMP ID='CHAIR FIRE',T=331,F=1.0/
```

It was decided to use a vent size of 100 mm by 400 mm for the fire at a height of 650 mm. Observation from the experiments showed that the fire spread from the ignition point favored the direction of the vertical lying foam slab. The vertical foam slab became engulfed in fire at an early stage in comparison with the horizontal foam slabs. In all cases after the fire had been extinguished there was no foam left on the vertical slab while depending on the fire about 1/3 – 2/3 of the horizontal foam was left unburned.

It would not be realistic to model the vent in FDS as the total area of the foam, not including the base as the total area of the foam was not involved in the fire. Therefore it was modeled as a vent matching the cross sectional area of the vertical foam slab. The height of the vent was chosen as 650 mm.

It is possible to model various vent sizes that would produce flame heights of different sizes and subsequently effect the heat transport to the upper layer [2]. It is suggested that the parameters chosen give a relatively good comparison to the real fire if we examine the temperature data from the output files.

The MISC line prescribes the reaction to be used, which is polyurethane in our case. The line also contains information that specifies what and where the database is located. The database contains information relating to the properties of the materials, the reaction specifications and sprinkler head descriptions.

```
&MISC REACTION='POLYURETHANE',
DATABASE_DIRECTORY='c:\nist….\database3\'/
```

The positions and dimensions are specified through the OBST lines. The obstructions are constructed by inputting a set of coordinates that describe an rectangular object. These rectangular objects then are used to construct the compartment. For the purposes of Smokeview a color can be specified to a object, gray in our case, this is done by the BLOCK_COLOR='GRAY' prompt. Smokeview is a software tool designed to visualize numerical calculations generated by FDS [50]. The obstruction are specified as being gypsum plasterboard by using the SURF_ID='GYPSUM BOARD' prompt line. The details of the plasterboard is found in the specified

database. The coordinates give a 8 m long x 4 m wide x 2.4 m high plasterboard lined compartment, with an opening for the door. Notice that the observation windows are not included.

```
&OBST XB=0.0, 8.2, 0.0, 0.1, 0.0, 2.4 BLOCK_COLOR='GRAY',
      SURF_ID='GYPSUM BOARD' / WALL  RIGHT
&OBST XB=8.1, 8.2, 0.0, 4.2, 0.0, 2.4 BLOCK_COLOR='GRAY',
      SURF_ID='GYPSUM BOARD' / WALL  BACK
&OBST XB=0.0, 8.2, 4.1, 4.2, 0.0, 2.4 BLOCK_COLOR='GRAY',
      SURF_ID='GYPSUM BOARD' / WALL  LEFT
&OBST XB=0.0, 0.1, 0.0, 0.3, 0.0, 2.4 BLOCK_COLOR='GRAY',
      SURF_ID='GYPSUM BOARD' /  DOOR BLOCK
&OBST XB=0.0, 0.1, 0.3, 1.1, 2.0, 2.4 BLOCK_COLOR='GRAY',
      SURF_ID='GYPSUM BOARD' / DOOR SOFFIT
&OBST XB=0.0, 0.1, 1.0, 4.2, 0.0, 2.4 BLOCK_COLOR='GRAY',
      SURF_ID='GYPSUM BOARD' / WALL FRONT
&OBST XB=0.0, 8.2, 0.0, 4.2, 2.4, 2.5 BLOCK_COLOR='GRAY',
      SURF_ID='GYPSUM BOARD' / CEILING
```

The VENT line specifies that the domain boundary is open.

```
&VENT CB='XBAR' ,SURF_ID='OPEN' /
&VENT CB='XBAR0',SURF_ID='OPEN' /
&VENT CB='YBAR' ,SURF_ID='OPEN' /
&VENT CB='YBAR0',SURF_ID='OPEN' /
&VENT CB='ZBAR' ,SURF_ID='OPEN' /
```

The THCP lines specify where the gas temperatures will be measured. This is done by specify the co-ordinates of where the measurements are to be taken. And using the ‘TEMPERATURE’ prompt. The TC’s are labeled by using the LABEL prompt. This makes the identification of the TC’s easier in the output files. This is done for all 8 TC’s.

```
&THCP XYZ=6.0,2.1,2.380,QUANTITY='TEMPERATURE',LABEL='1' /
&THCP XYZ=2.0,2.1,2.380,QUANTITY='TEMPERATURE',LABEL='2' /
&THCP XYZ=6.0,0.6,2.3,QUANTITY='TEMPERATURE',LABEL='3' /
&THCP XYZ=6.0,0.6,2.1,QUANTITY='TEMPERATURE',LABEL='4' /
&THCP XYZ=6.0,0.6,1.0,QUANTITY='TEMPERATURE',LABEL='5' /
&THCP XYZ=2.0,0.6,2.3,QUANTITY='TEMPERATURE',LABEL='6'/
&THCP XYZ=2.0,0.6,2.1,QUANTITY='TEMPERATURE',LABEL='7' /
&THCP XYZ=2.0,0.6,1.0,QUANTITY='TEMPERATURE',LABEL='8' /
```

The HEAT lines specify information relating to the heat detectors used to measure the temperatures. The XYZ input gives the co-ordinate of the heat detector. The RTI specifies the RTI of the heat detectors, and the ACTIVATION_TEMPERATURE is the activation temperature of the detector. A activation temperature of 160^{o}C has been chosen because it is unlikely that this temperature will be reached in the compartment. The heat detectors are being used to measure temperatures.

```
&HEAT XYZ=6.0,0.6,2.3,RTI=30.,ACTIVATION_TEMPERATURE=160./
LOCATION 3
&HEAT XYZ=6.0,0.6,2.1,RTI=30.,ACTIVATION_TEMPERATURE=160./
LOCATION 4
&HEAT XYZ=6.0,0.6,1.0,RTI=30.,ACTIVATION_TEMPERATURE=160./
LOCATION 5
&HEAT XYZ=2.0,0.6,2.3,RTI=30.,ACTIVATION_TEMPERATURE=160./
LOCATION 6
&HEAT XYZ=2.0,0.6,2.1,RTI=30.,ACTIVATION_TEMPERATURE=160./
LOCATION 7
&HEAT XYZ=2.0,0.6,1.0,RTI=30.,ACTIVATION_TEMPERATURE=160./
LOCATION 8
```

The SPRK lines specifies the sprinkler locations and properties. XYZ gives the coordinates of the sprinkler, and the MAKE prompt specifies the sprinkler type to be used. The sprinkler types are kept in the database specified on the MISC line. The sprinkler heads are virtually modeled therefore it is possible to locate multiple sprinklers at the same point in FDS. Since the sprinkler heads will not introduce any

water in to the compartment, the cooling effect of the sprinkler heads activating can be ignored. The K value and pressure value in the sprinkler data files are changed to 0 to stop water flow. For the simulation 12 sprinkler data files were set up to accommodate the temperature ratings, RTI and c-factors of the various sprinkler heads. The sprinkler head details are kept in the database. The sprinkler head height is set to be 20 mm under the ceiling height, this represent the position of the glass bulb.

```
&SPRK XYZ=2.10000   2.1000   2.380, MAKE='K-25' / sprinkler 1 c=0
&SPRK XYZ=6.10000   2.1000   2.380, MAKE='K-25' / sprinkler 2
&SPRK XYZ=2.10000   2.1000   2.380, MAKE='K-26' / sprinkler 1 c=0.3
&SPRK XYZ=6.10000   2.1000   2.380, MAKE='K-26' / sprinkler 2
&SPRK XYZ=2.10000   2.1000   2.380, MAKE='K-27' / sprinkler 1 c=0.65
&SPRK XYZ=6.10000   2.1000   2.380, MAKE='K-27' / sprinkler 2
&SPRK XYZ=2.10000   2.1000   2.380, MAKE='K-28' / sprinkler 1 c=1
&SPRK XYZ=6.10000   2.1000   2.380, MAKE='K-28' / sprinkler 2
```

Below is an example of a sprinkler data file for a residential sprinkler head with a RTI of 36 and a c-factor of 0.3.

```
MANUFACTURER
TYCO
MODEL
RESIDENTIAL
OPERATING_PRESSURE
0.0
K-FACTOR
0.0
RTI
36.
C-FACTOR
0.30
OFFSET_DISTANCE
0.20
ACTIVATION_TEMPERATURE
```

```
68.
SIZE_DISTRIBUTION
1
1300.,2.43,0.58
VELOCITY
1
30. 90. 10.0
```

The SLCF lines specify the slice files for temperature and gas velocity. A slice file contains data (temperature and velocity) recorded within a rectangular array of grid points at each recorded time steps. Continuously shaded contours are drawn for simulation quantities.

```
&SLCF PBX=4.1 QUANTITY='TEMPERATURE'/
&SLCF PBY=0.4 QUANTITY='TEMPERATURE'/
&SLCF PBY=1.9 QUANTITY='TEMPERATURE'/
&SLCF PBX=0.1 QUANTITY='TEMPERATURE',VECTOR=.TRUE. /
&SLCF PBX=2.1 QUANTITY='TEMPERATURE',VECTOR=.TRUE. /
```

7 Grid Sensitivity Analysis

This section reports on the effect that gird size selection had on simulations undertaken for this research.

The effect that grid size had on the simulations was investigated to determine a optimum grid size that would be adopted for future simulations, as finer grids requires more computational time and power [3]. It is important to determine an appropriate grid size that optimizes solution accuracy and time [12].

7.1. Grid Resolution Analysis

To determine the effect that grid size had on the simulations, experiment 8 was simulated several times using different grid sizes. Experiment 8 was chosen, as it was the only 50 mm simulation that was run to a successful end. Other simulations were run using a 50 mm grid, but these simulations ended prematurely. It would have been beneficially if there was data for TC's 1 and 2 (sprinkler TC's).

Unfortunately no temperature data was recorded for TC 1. The quality of the resolution depends on both the size of the fire and the size of the grid cells [3]. Simulations were run for the grid sizes detailed in Table 7-1. The data output against time taken to run the simulation was compared to ascertain the advantages and disadvantages associated with grid size selection.

Simulations	Grid Sizes (m)	Height /Grid Ratio
1	0.15 x 0.15 x 0.15	16
2	0.10 x 0.10 x 0.10	24
3	0.075 x 0.075 x 0.075	32
4	0.05 x 0.05 x 0.05	48

Table 7-1 Grid sizes for Simulations

7.1.1. Computation Time

Figure 7.1 shows the computation time for the four simulations. This shows that finer grids require more computing time, roughly 16x for a decrease of 50 % in grid size [51]. The given simulation times are approximate.

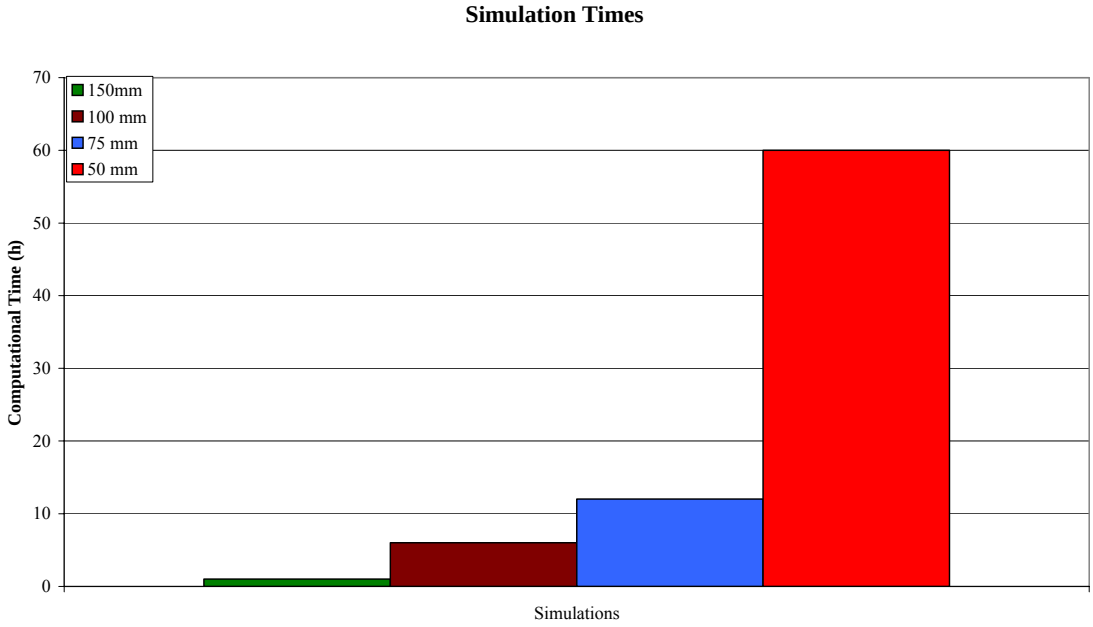

Figure 7.1 Computation time for all cases

7.1.2. Temperature Predictions

Comparing the predicted temperature (See Figure 7.2) with the actual, 75 mm and 100 mm grid gave the best match, as well as being similar. FDS under predicts the temperature for 150 mm grid and over-predicts for 50 mm grid. Figure 7.3 shows the predicted temperatures for TC 2. Unfortunately TC 2 was defective for experiment 8 resulting in no temperature data.

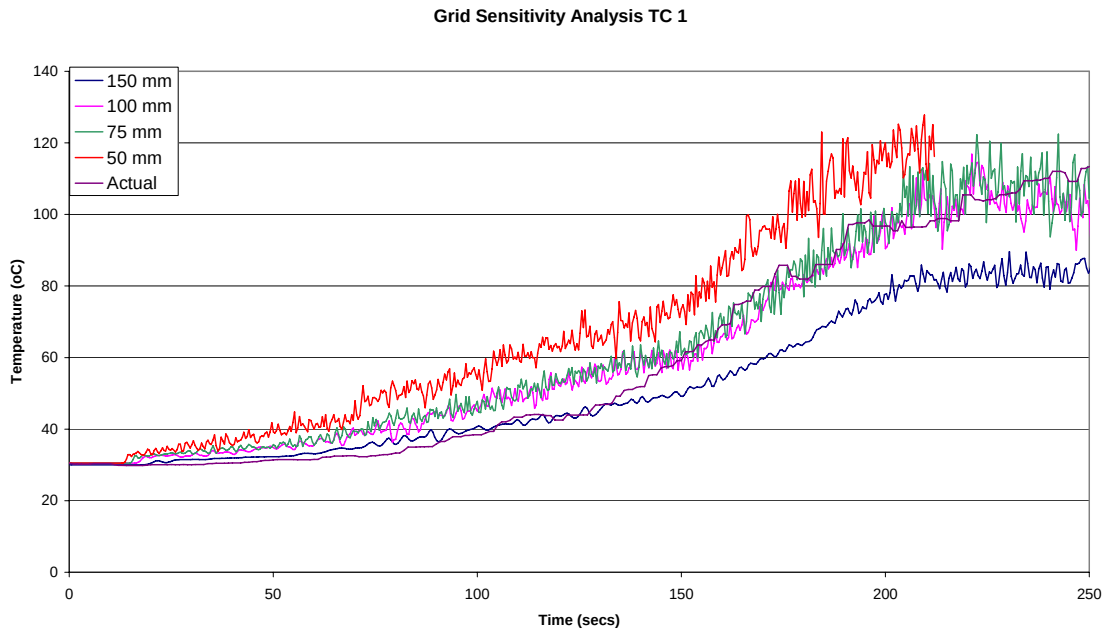

Figure 7.2 Grid sensitivity analysis TC 1

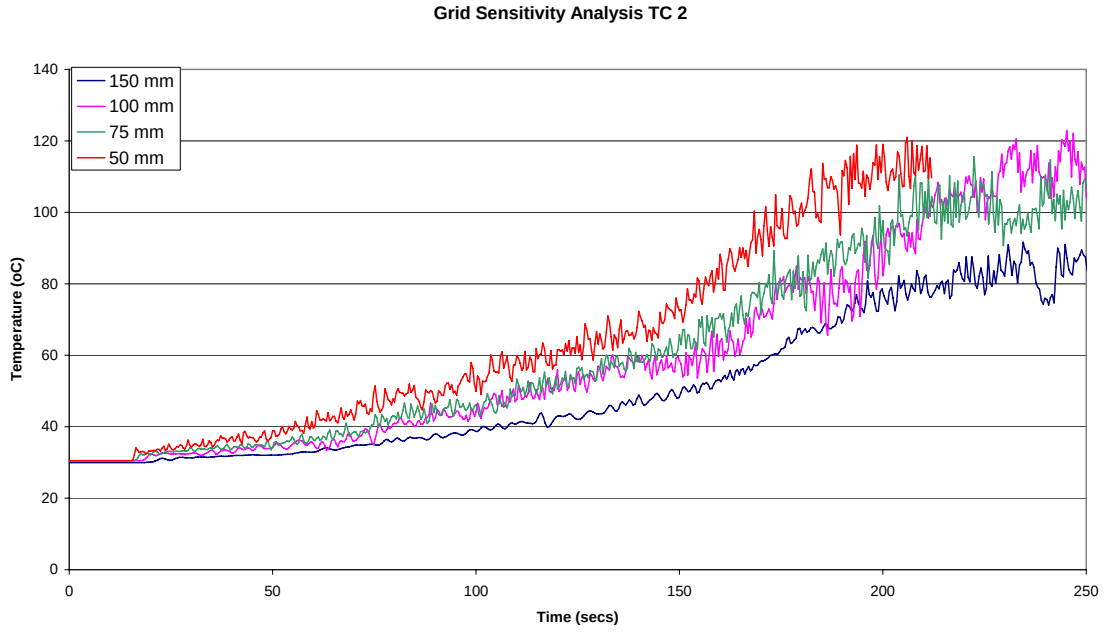

Figure 7.3 Grid sensitivity analysis TC 2

7.1.3. Sprinkler Activation Times

The sprinkler activation times were compared for the different grid sizes. Table 7-2 contains the activation times.

Grid Size (mm)	Sprinkler 1 (secs)	Sprinkler 2 (secs)
50 x 50 x 50	190	193
75 x 75 x 75	214	220
100 x 100 x 100	225	230
150 x 150 x 150	450+	450+
Actual	182	187

Table 7-2 Grid sensitivity

Fifty-millimeter grid size gave (Table 7-2) the closest comparison and the 150 mm grid give the worst comparison. The sprinklers did not activate for 150 mm grid simulation. The difference between the activation times for 75 mm and 100 mm grid was minimal.

7.2. Conclusion

If accuracy and computational time is taken into account, simulations using 100 mm grid give reasonable accuracy and the simulation time was not excessive. 50 mm grid gives the closest comparison for sprinkler activation times, however this is probably a result of higher gas temperatures being predicted. The 150 mm grid did not give good comparisons for either the TC temperatures or sprinkler activation times. The 75 mm grid gives slightly better comparisons for sprinkler activation times than the 100 mm grid with the temperature profiles being similar.

The 150 mm grid simulation did not compare favourably for either temperature or sprinkler activation times, through it took least computing time to run. The 50 mm grid simulation gave the best comparison for the sprinkler activation times, the temperature predictions were significantly higher. The required computational time was greatest for 50 mm grid simulations. The simulations using 75 mm and 100 mm

grid sizes gave similar temperature profiles and sprinkler activation times. The time taken to run the 100 mm grid simulation was substantially less than it was for the 75 mm grid.

It was decided to use 100 mm grid size for future simulations. For experiment 8, 100 mm grid simulation gave sprinkler activation times and TC temperatures which were within 20 % of the actual.

8 FDS Results

This chapter discusses the predicted temperature profiles and sprinkler activation times.

8.1. Experiment 10 – Center Fire

Figure 8.1 illustrates the predicted temperature profile for experiment 10. The TC numbering and positioning for the FDS simulation is the same as for the actual experiments.

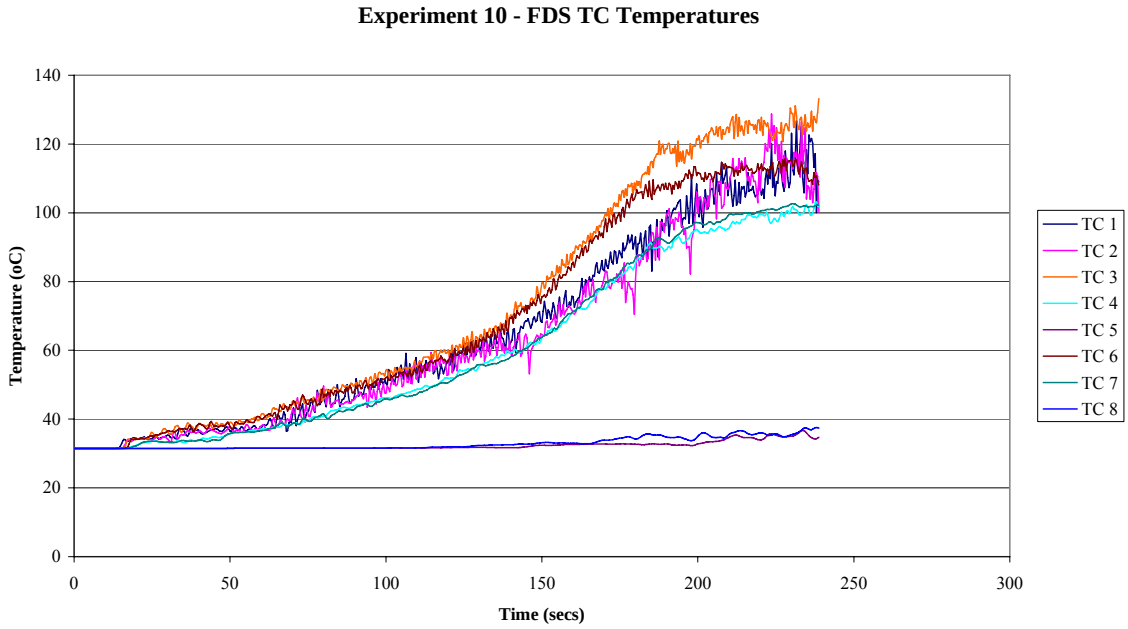

Figure 8.1 FDS predicted temperatures - experiment 10

The temperatures predicted by FDS using the thermocouple function is representative of the gas temperatures in the compartment, it is not equivalent to the temperature being measured by the TC's for the experiments. A thermocouple probe when emerged in hot gas will not instantly measure the actual gas temperature, it will measure the increased temperature of the probe junction. The temperature change of the TC junction will lag behind the raised temperature of the surrounding gas until the probe junction is heated. The speed in which the junction changes temperature is related to the thermal responsiveness of the TC.

The predicted temperature profile for experiment 10 (see Figure 8.1) is typical of experiments 1- 10. TC's 1 – 8 record the ambient temperatures for the first 20 seconds. At roughly 25 seconds TC 1 – 6 register a temperature increase. The rate that which the TC's register an increase in temperature accelerates between 150 – 300 seconds. At about 170 seconds TC 7 and 8 begin to register an increase in temperature. At about 300 seconds the increase in temperatures for all TC's plateau out. The maximum predicted temperatures in the compartment are in the region of 125^{o}C for TC 1 and 2.

TC 1 and 2 are positioned adjacent to the sprinkler heads. It would be expected that the predicted temperatures for TC 1 and 2 (due to there proximity to the fire and elevated level) would be higher than the temperatures for TC 3 and 6. Figure 8.1 shows that FDS predicts that temperatures for TC 3 and 6 are higher than TC 1 and 2. The following reasons are suggested for this:

- TC's 1 and 2 are positioned closely to the plasterboard, this may result in the plasterboard acting as a heat sink reducing the temperature of the adjacent gas.
- The grid size used for the simulations may limit the accuracy of FDS.

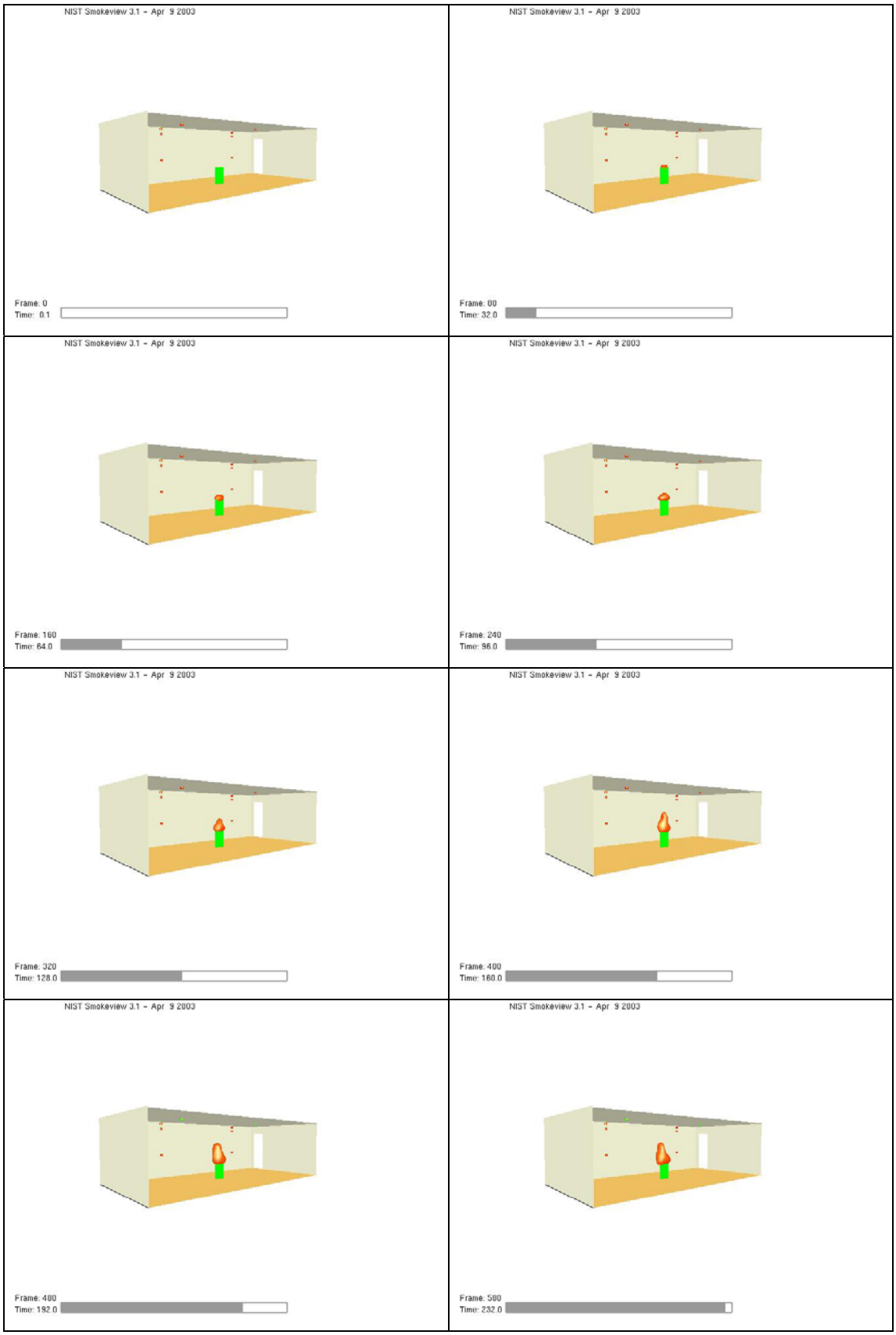

Figure 8.2 Smokeview center fire

Figure 8.2 shows a Smokeview illustration for experiment 10. Figure 8.3 shows the central temperature slice for experiment 10.

The temperatures measured by the thermocouples closest to the open door are generally lower than for the corresponding thermocouples positioned at the non-door end of the compartment. This would be expected because heat would escape out of the open door and incoming air would cool the TC's closest to the door. This was too observed for the actual experiments. The temperature difference was most evident between TC 3 and 6.

8.2. Experiment 17 – Corner Fire

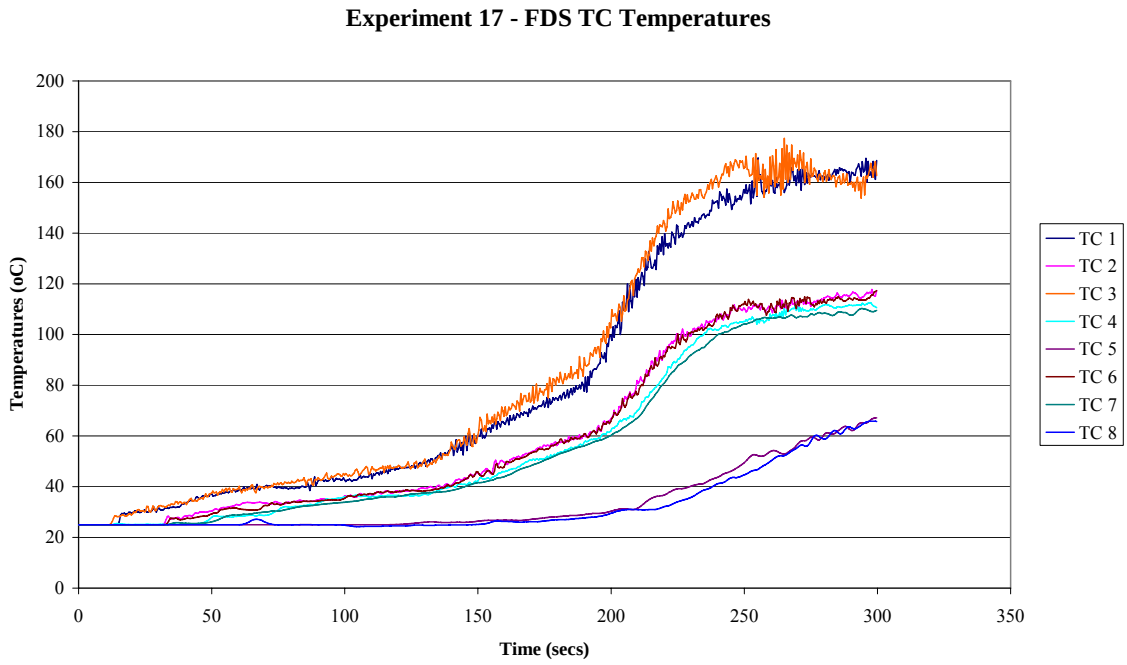

Figure 8.4 FDS Temperatures – experiment 17

Figure 8.4 shows the predicted temperature profile for experiment 17. The temperature profile given for experiment 17 is typical for experiments 16 - 22.

Experiment 17 (as well as 16 – 22) fundamentally differs from experiments 1 – 15 in that the fire is in the corner of the compartment. This alters the temperature distribution of the compartment in comparison with experiments 1 – 15. The TC's that are closest to the fire register a change in temperature more quickly and of a greater

magnitude than the more distant TC's. Also TC 1, 3, 4 and 5 record higher temperatures than TC 2,6,7 and 8. The predicated temperatures for TC 1, 3,4 and 5 are significantly higher than the predicted temperatures of the same TC's for the center fire.

Figure 8.5 shows a Smokeview illustration for experiment 17. Figure 8.6 shows a central temperature slice Smokeview illustration for experiment 17.

Figure 8.2 shows the typical model geometry for experiments 1 – 15.

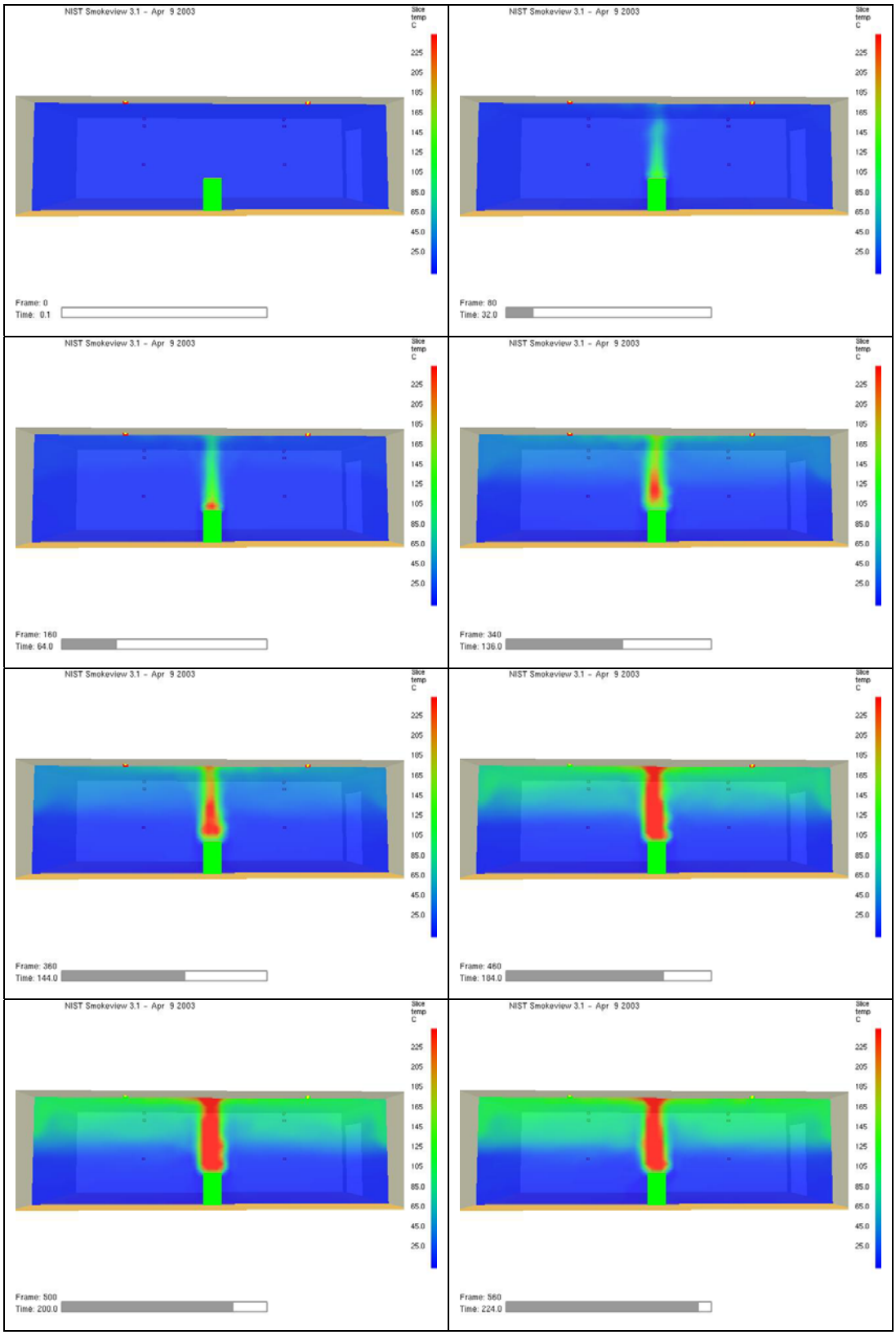

Figure 8.3 Temperature slice file – experiment 10

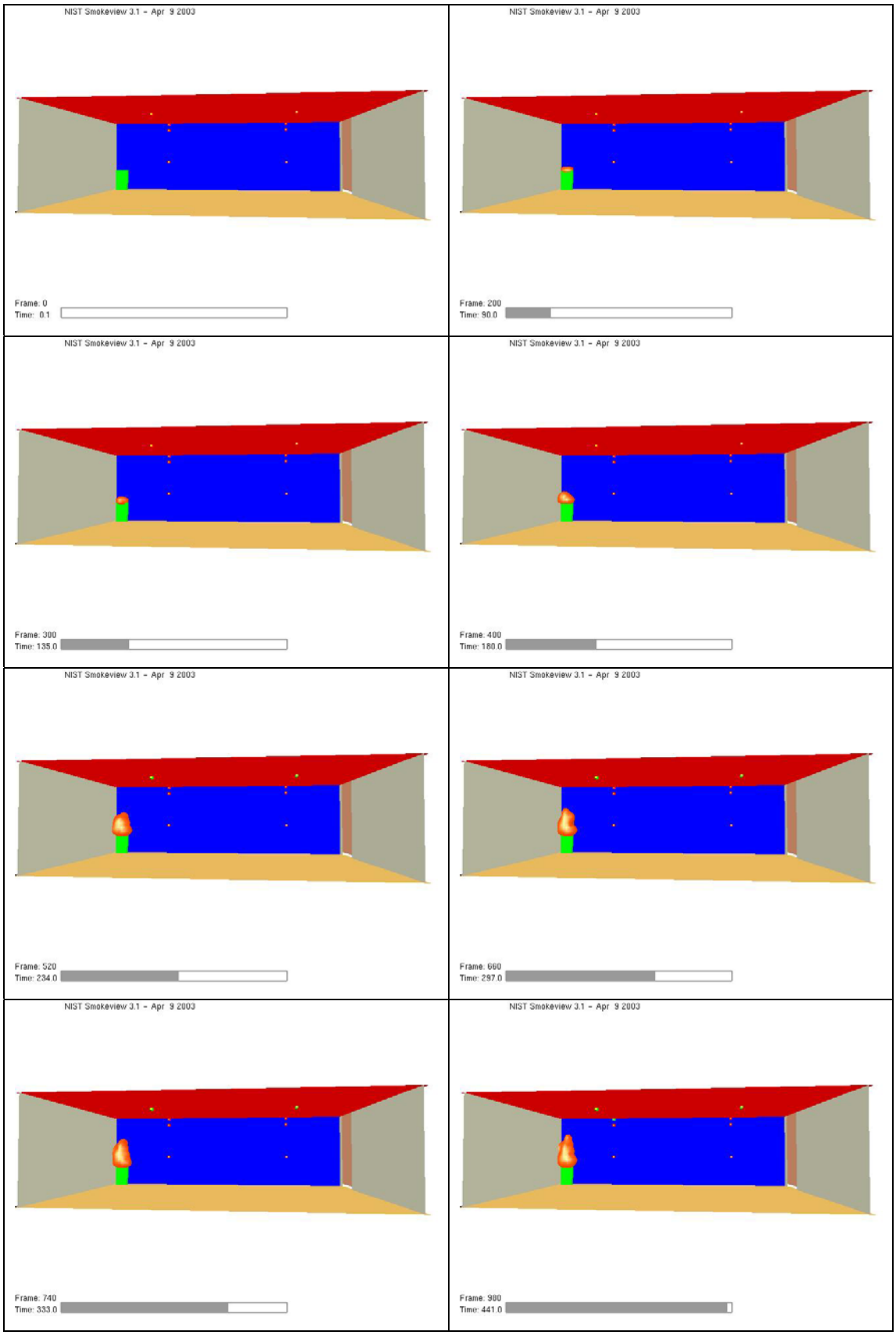

Figure 8.5 Smokeview corner fire – experiment 17

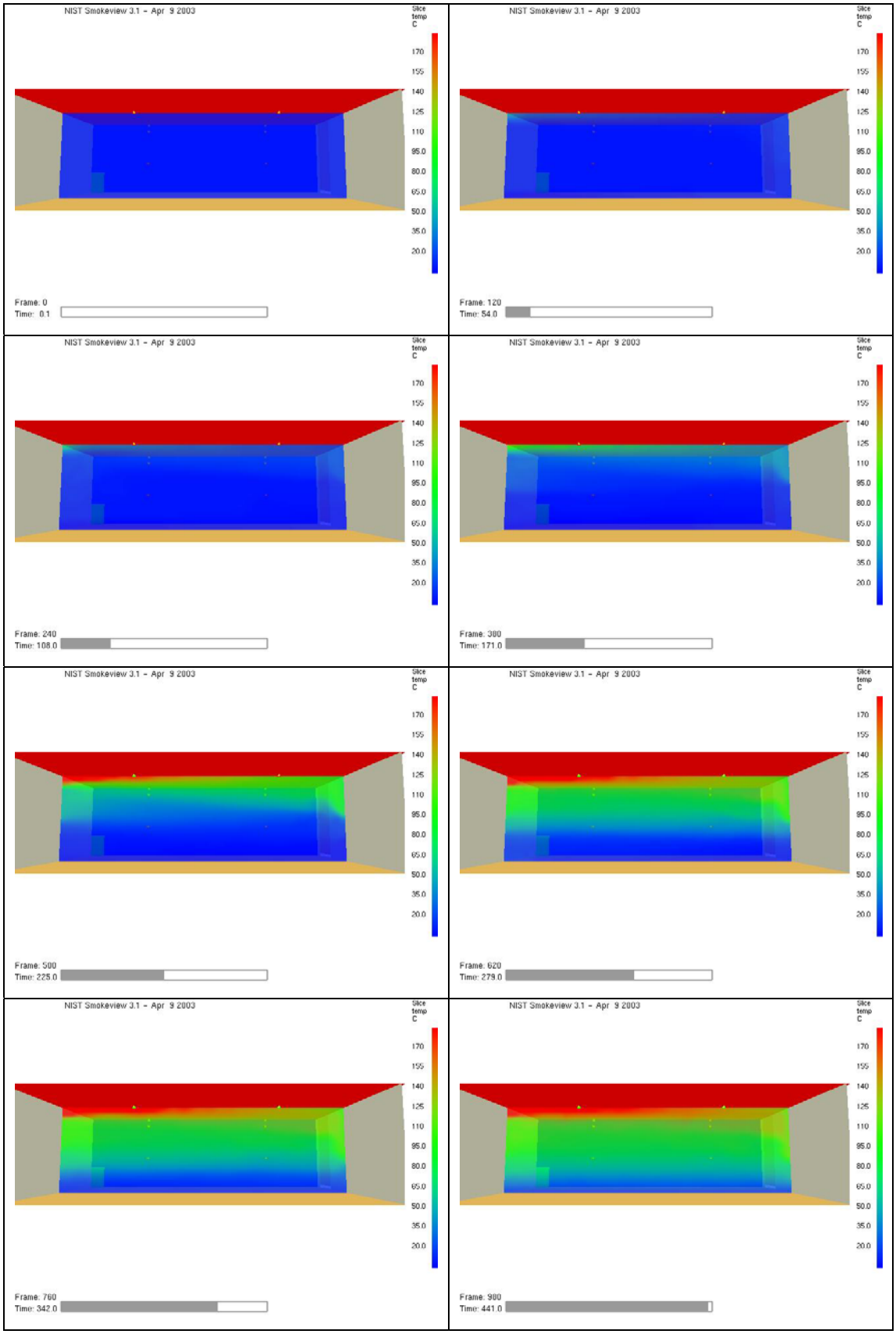

Figure 8.6 Temperature slice file – experiment 17

8.3. Sprinkler Activations

This section reports the predicted sprinkler activation times. The results are presented per sprinkler head type and c-factor. Appendix B contains the numerical data for the sprinkler activation times.

It was not possible to ascertain the exact c-factors for the sprinkler heads at the time when the simulations were being conducted. The sprinkler supplier suggested that a c-factor of 0.65 was suitable, however there was a degree of uncertainty attached to this value. It was decided to use this opportunity to ascertain the effect that varying the c-factors had on the predicted sprinkler activation times. Therefore using information obtained from Figure 3.18 various c-factor values were used for the simulations. These values are given in Table 8-1.

Residential Heads $(m/s)^{½}$	Standard Response Heads $(m/s)^{½}$
0	0.65
0.3	1
0.65	1.5
1	2

Table 8-1 c-factors for sprinklers

8.3.1. Residential Heads

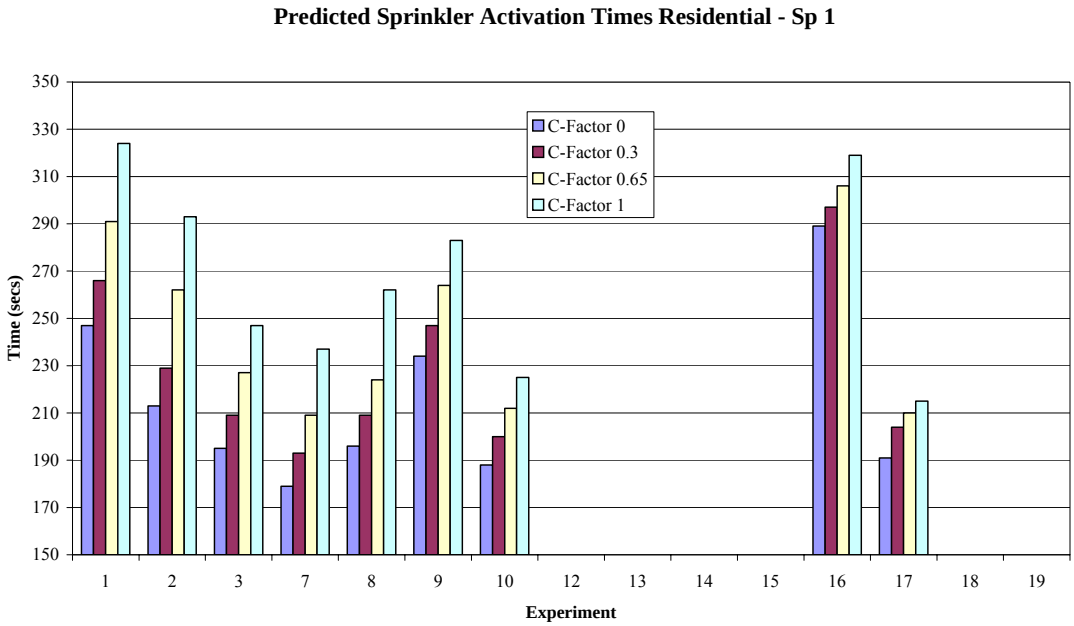

Figure 8.7 Predicted residential sprinkler activation times sp 1

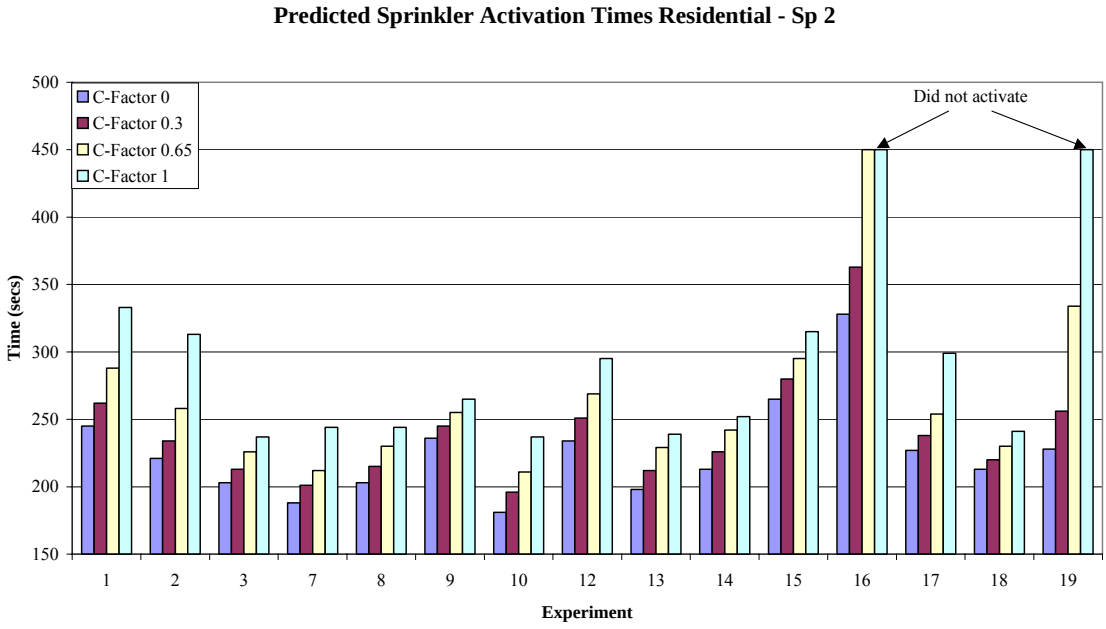

Figure 8.8 Predicted residential sprinkler activation times sp 2

Figure 8.7 and Figure 8.8 illustrates the effect that the c-factor value makes to the predicted activation time. As expected sprinkler response times computed with the value of 0 are shorter (quickest to activate), and when the value of 1 is used, the activation times are longer. The larger the c-factor, the more the heat is conducted away from the glass bulb, thus it requires a higher gas temperature (surrounding the bulb) to allow enough heat to transfer into the bulb, to compensate for the heat being conducted out of the bulb. For experiment 12 head 2 (door end), the difference between the sprinkler activation times for a value of 0 and 1 is 92 seconds or 50 %. The difference between values of 0.3 and 0.65 or 0.65 and 1 can be up to 30 seconds.

8.3.2. Standard Response

The influence of the c-factor is emphasised again by the results given for the SS sprinkler heads. The average difference between the predicted activation times given for c-factor values 0.65 and 2 is 50 %. On several occasions the sprinklers did not activate for the FDS model. For a c-factor of 2, it was more common for the sprinkler not to activate than activate. See Figure 8.9 and Figure 8.10.

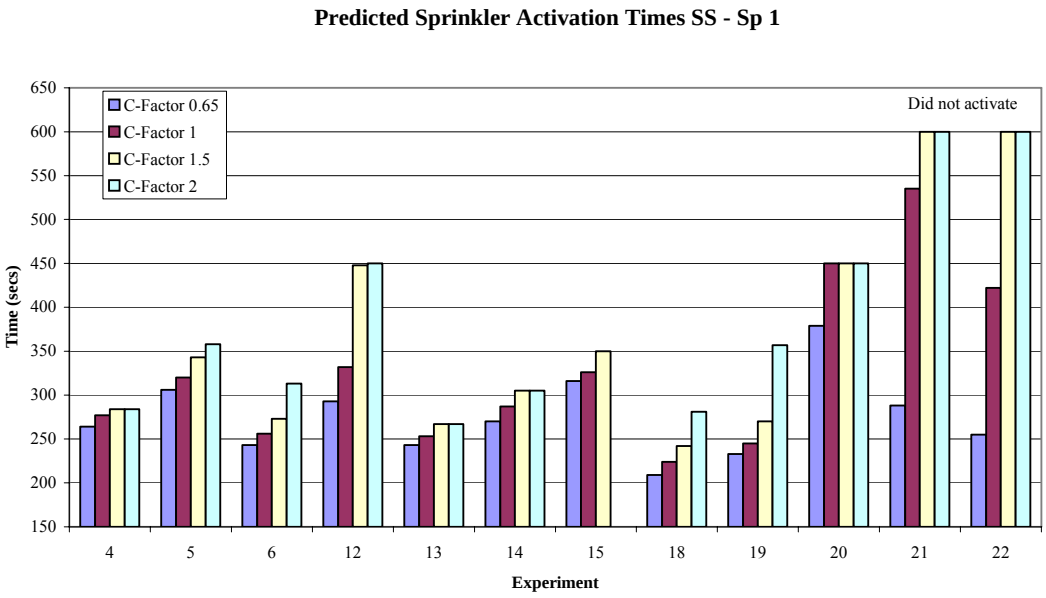

Figure 8.9 Predicted SS sprinkler activation times sp 1

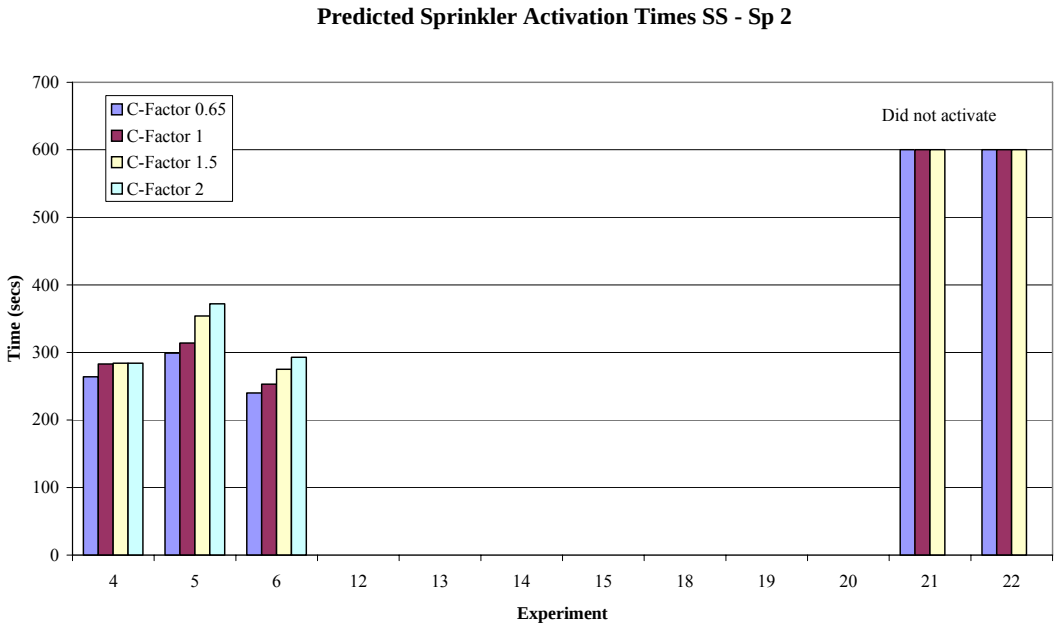

Figure 8.10 Predicted SS sprinkler activation times sp 2

Heskestad [42] discusses the importance of c-factors, and concludes that a large c-factor could result in the non-activation of a sprinkler head if the gas temperatures surrounding the sprinkler head are not high enough, but are over and above the nominal activation temperature.

8.4. Simulation Termination

The simulations were ended when:

1. All sprinklers had activated.
2. 100 seconds had surpassed since the sprinkler had activated in the actual experiment.
3. Or due to PC failure.

8.5. Experiment 16 Data

It is suspected that the mass loss rate data and subsequent HRR data for experiment 16 is defective. Figure 8.11 illustrates a comparison of the mass loss rate for experiment 16 and 17. The actual sprinkler activation times for experiment 17 are longer than for experiment 16. The measured MLR for experiment 16 only reaches 60 % of the magnitude of the mass loss rate for experiment 17, and develops at a slower rate. Therefore caution has to be used when considering the certainty of HRR data for experiment 16.

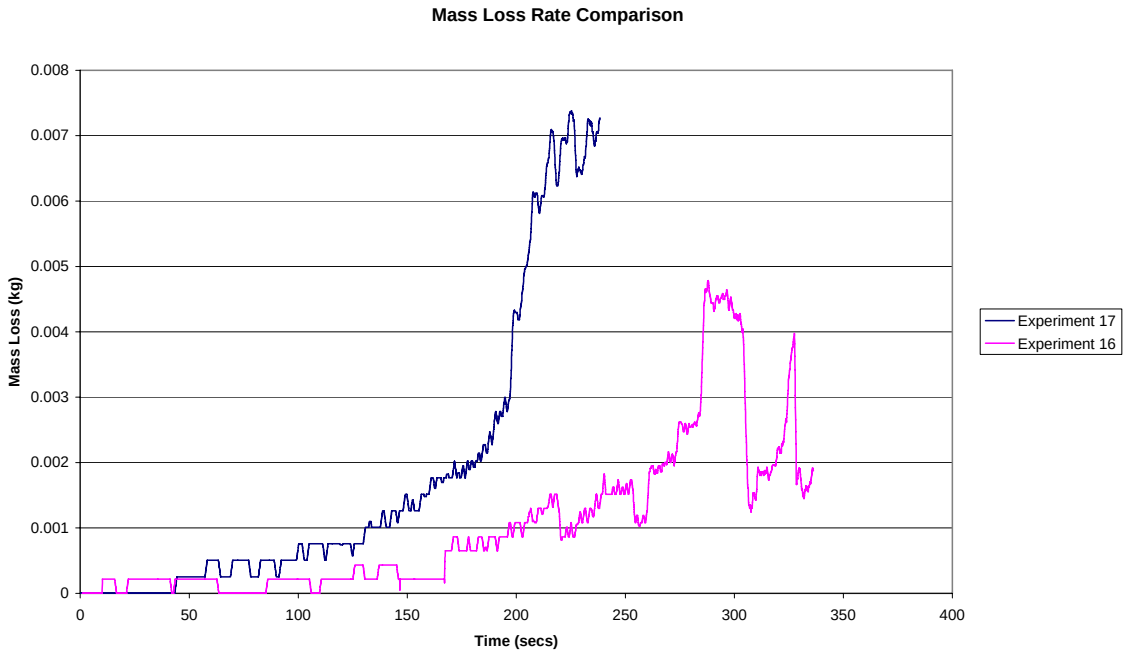

Figure 8.11 Mass loss rate comparison

8.6. Summary

In total over 40 simulations were run using a 100 mm grid size. This eventuated in 21 data sets predicting temperatures and sprinkler activation times. What is apparent is that c-factors as well as RTI, influence the activation times.

9 Comparison

This chapter compares the actual experimental data with the predicted data. Comparisons are made between the temperature profiles, HRR at time of activation, adjacent gas temperatures at time of activation and sprinkler activation times. This section compares the actual temperatures with the predicted temperatures for simulations with a grid size of 100 mm.

9.1.1. Temperature Comparison - Experiment 8

This section compares the actual and predicted TC temperatures for experiment 8.

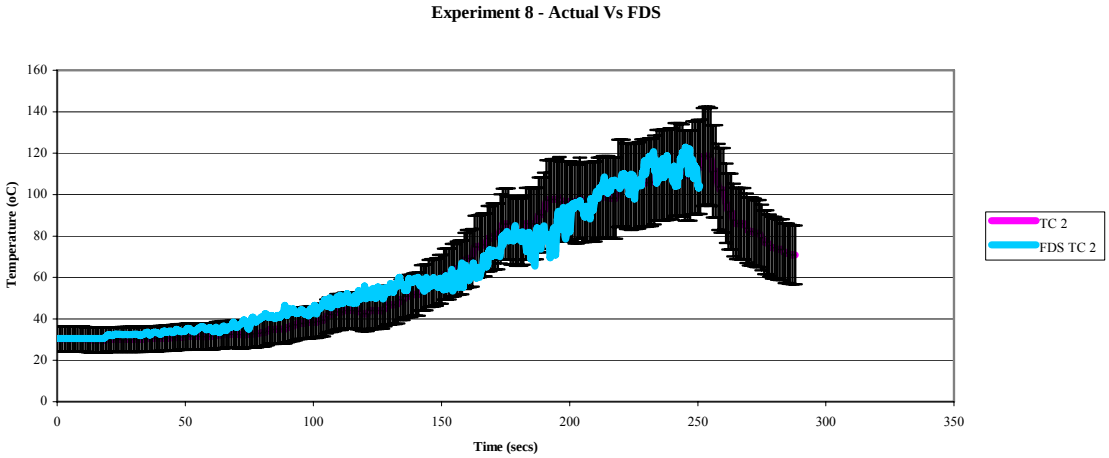

Figure 9.1 Temperature comparison exp 8 TC 2

The FDS predicted temperatures for TC 2 were within 20 % of the actual measured temperatures- see Figure 9.2.

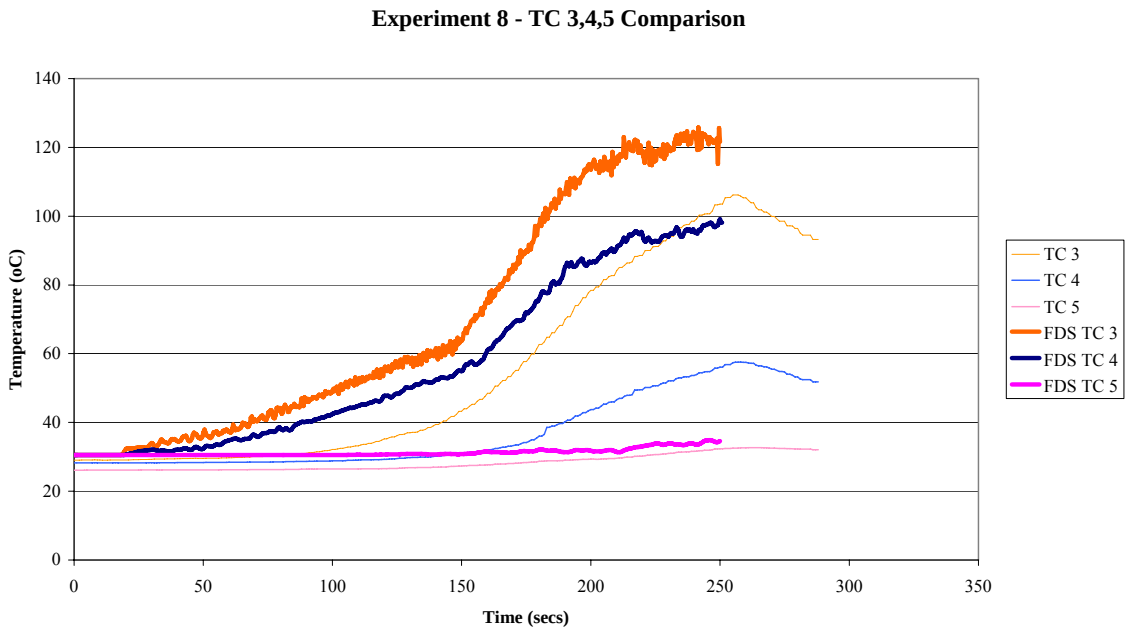

Figure 9.2 Temperature comparison exp 8 TC 3,4,5

For TC 3 (see Figure 9.2) the actual and predicted temperatures are significantly different, with the predicted temperatures being overestimated by 30 – 40 %. The actual temperatures lag behind the predicted temperatures increasing at a similar rate once the lag has been accounted for. Predicted gas temperatures for TC 4 are 50 – 80 % higher than the actual TC temperature. The actual and predicted temperatures for TC 5 are similar, being within 20 %.

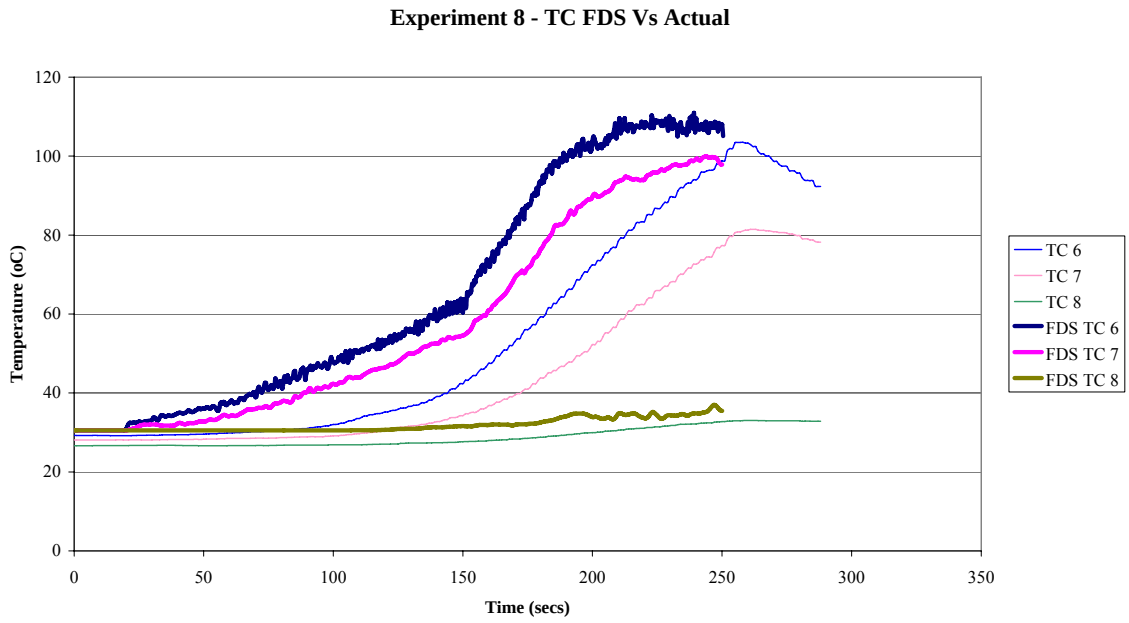

Figure 9.3 Temperature comparison exp 8 TC 6,7,8

From Figure 9.3 it can be seen that temperature comparisons for TC 6,7 and 8 are similar to that of the comparisons for TC 3, 4 and 5. The predicted gas temperatures are higher than the actual TC measured temperatures.

9.1.2. Temperature Comparison - Experiment 17

Experiment 17 differs from experiment 8 in that the fire is located in the corner of the room, on the same side of the compartment as the thermocouple trees. The door to the compartment was shut. The thermocouples positions are exactly the same as per experiment 8 (the TC positions are the same for all experiments).

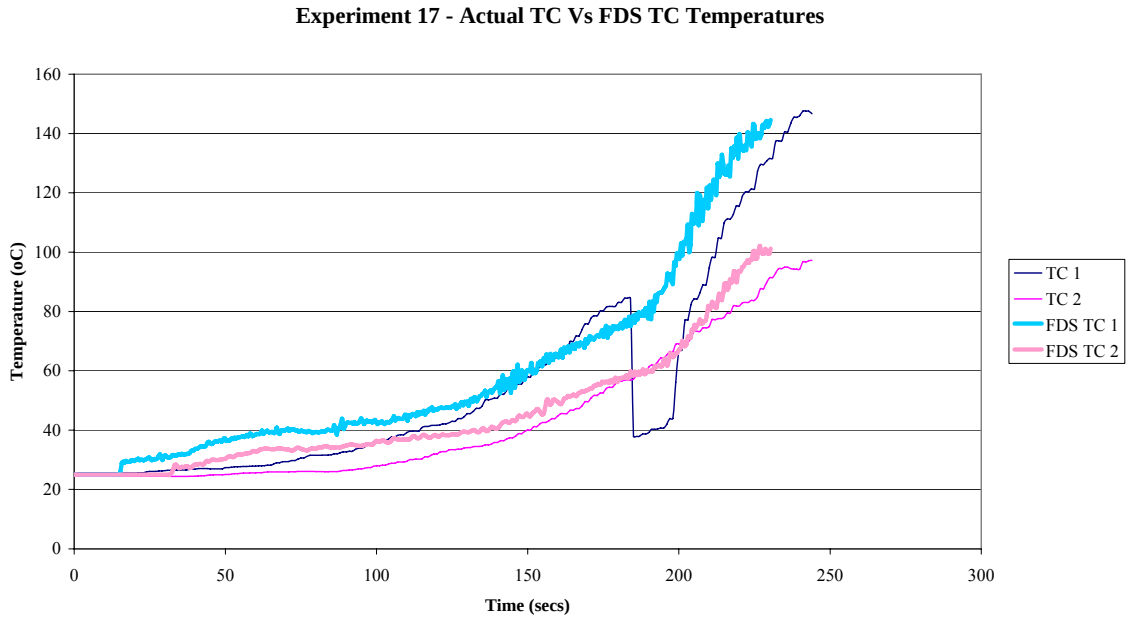

Figure 9.4 Temperature comparison exp 17 TC 1 and 2

The predicted temperature for TC 1 and 2 are similar to that of the actual temperature. For the majority of the time the predicted temperature is within 20 % of that of the actual measured temperature.

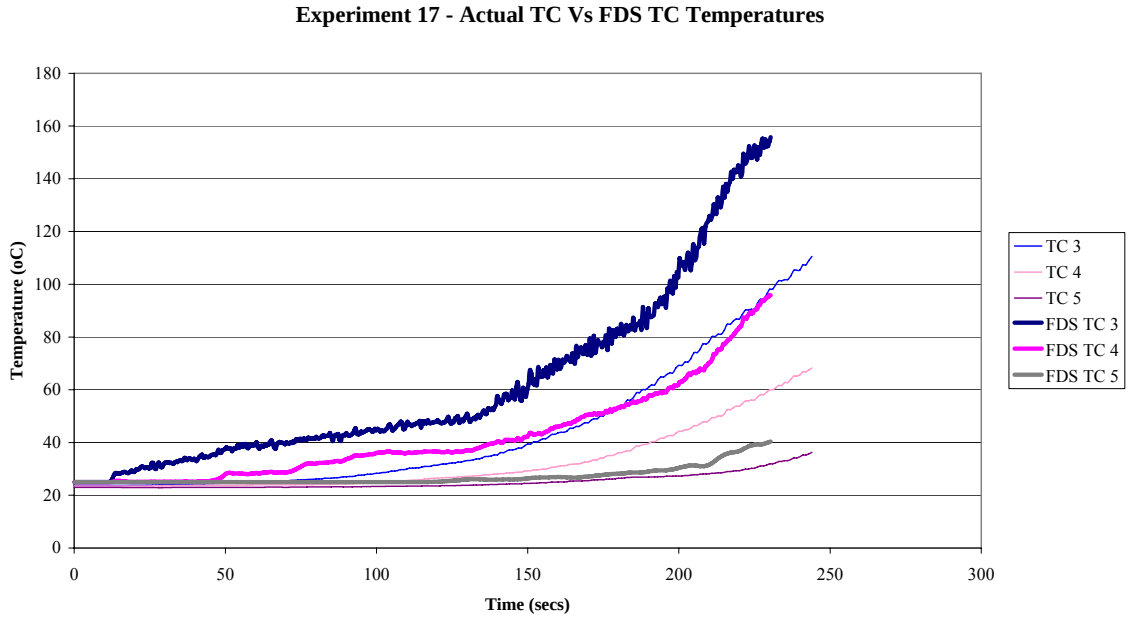

Figure 9.5 Temperature comparison exp 17 TC 3,4,5

The predicted temperatures for experiment 17 (Figure 9.5) TC 3 and 4 are about 30 – 40 % higher than the actual measured TC temperatures. For the majority of the time the predicted temperature for TC 5 is within 20 % of the actual temperature. The predicted temperatures are generally higher than the actual temperatures.

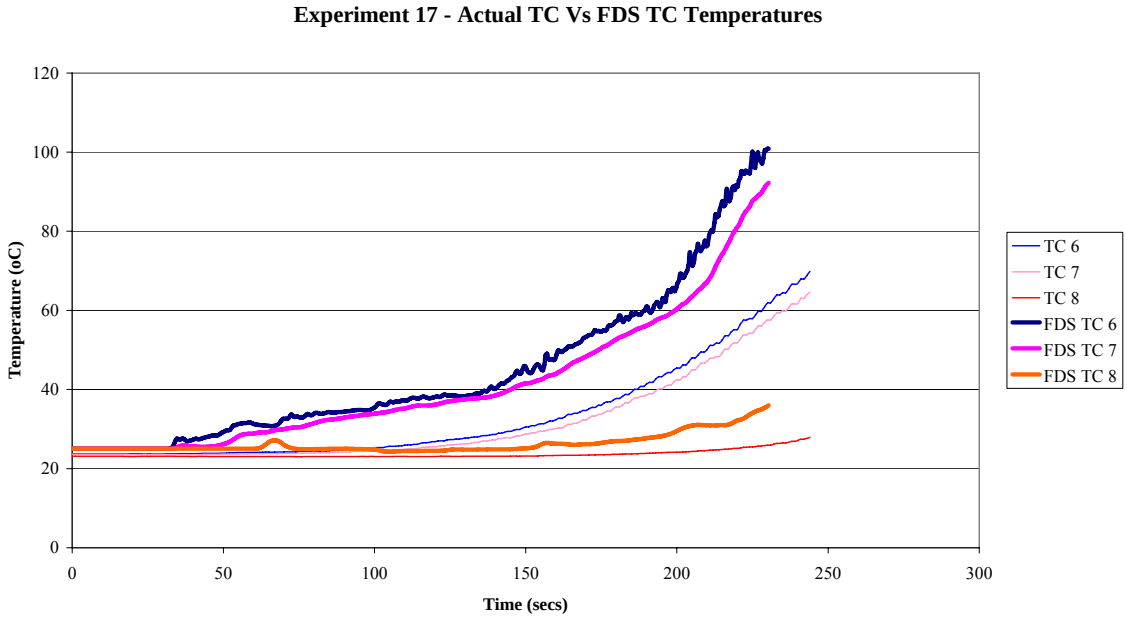

Figure 9.6 Temperature comparison exp 17 TC 6,7,8

For TC 6 and 7 (Figure 9.6) the actual and predicted temperatures differ, generally being overestimated by 30 – 40 %. The actual temperatures lag behind the predicted temperatures but increase at a similar rate once the lag has been accounted for. The predicted temperatures are higher than the actual temperatures.

9.1.3. Comparison Temperature Discussion

Generally the predicted temperatures for TC 1 and 2 (for all experiments) are within 20 % of the actual TC temperatures, however the predicted temperatures for TC's 3,4,6 and 7 can be up to 30 % higher than the actual temperatures. The predicted temperatures for TC 5 and 8 are generally within 20 % of the actual temperatures.

It is reasonable to assume that the predicted temperatures are reasonably accurate for TC positions 1,2 ,7 and 8, but there are considerable differences for TC 3,4,5 and 6. This matter was further investigated for the following reasons:

- The TC construction for TC 1 and 2 varied from TC 3,4,5,6,7,8.
- For TC 7 and 8 minimal temperature change was recorded during the actual experiments.

The TC's used for positions 1and 2 were bare wire TC's, the TC used for positions 3 – 8 were housed in a metal sheath. As the TC temperatures given in FDS represent the gas temperature not a virtual TC temperature, it was thought that the difference (a proportion) between the predicted FDS temperatures for TC 3 – 6 and actual measured TC could be due to the thermal responsiveness of the metal sheaths. This was supported by the closeness of the actual and predicted temperatures for TC positions 1 and 2 - no sheath - and the relative match for TC positions 7 and 8 – relatively little change for both the experiments and simulation.

9.1.4. Alternative Temperature Prediction

A literature review suggested that there can be a considerable lag between the actual gas temperatures and the measured temperatures, and the difference was related to the thickness of the probe sheath. SKUTT [52] who produce ceramic products have reported that TC points that are housed in sheaths that have a high mass will respond more slowly than TC points that are housed in sheaths with a lower mass. They go on to report that TC that are not responsive will lag behind the actual temperature of the kiln when it is being fired up. Bolles reports on the inaccuracies of TC's, in that the measurements can be out by up to 100oF. He too identifies the effect that the thermal mass contributes to the error in measuring actual gas temperatures [53].

To account for the difference in actual and predicted temperatures it was decided to model TC 3 – 8 as heat detectors. The heat detectors were set to activate at 160^{o}C, this figure was chosen because it would be unlikely they would activate as it was unlikely that compartment temperatures would reach this temperature.

For experiment 8 TC's were modeled as heat detectors using RTI values given in Table 9-1. Generally it was found that RTI values of under 20 $m^{0.5}s^{0.5}$ gave temperatures prediction that were significantly higher than the actual experimental data. It was also found that RTI values of over 40 $m^{0.5}s^{0.5}$ predicated temperatures that were significantly lower than the actual.

The heat detectors that were assigned with a response time index of 30 $m^{0.5}s^{0.5}$ proved to give the best match between the actual and predicted times. In general the predicted temperatures were within 20 % of the actual temperatures and also ran parallel to the actual temperatures. Until more research is undertaken, and this method of predicting temperatures proven (or not) to be reliable, caution must be shown if the heat detector temperatures are to be used instead of the TC temperatures.

Assigned RTI ($m^{0.5}s^{0.5}$)	TC's
5	3 – 8
10	3 – 8
15	3 – 8
20	3 – 8
30	3 – 8
40	3 – 8
50	3 – 8

Table 9-1 Heat detector RTI values

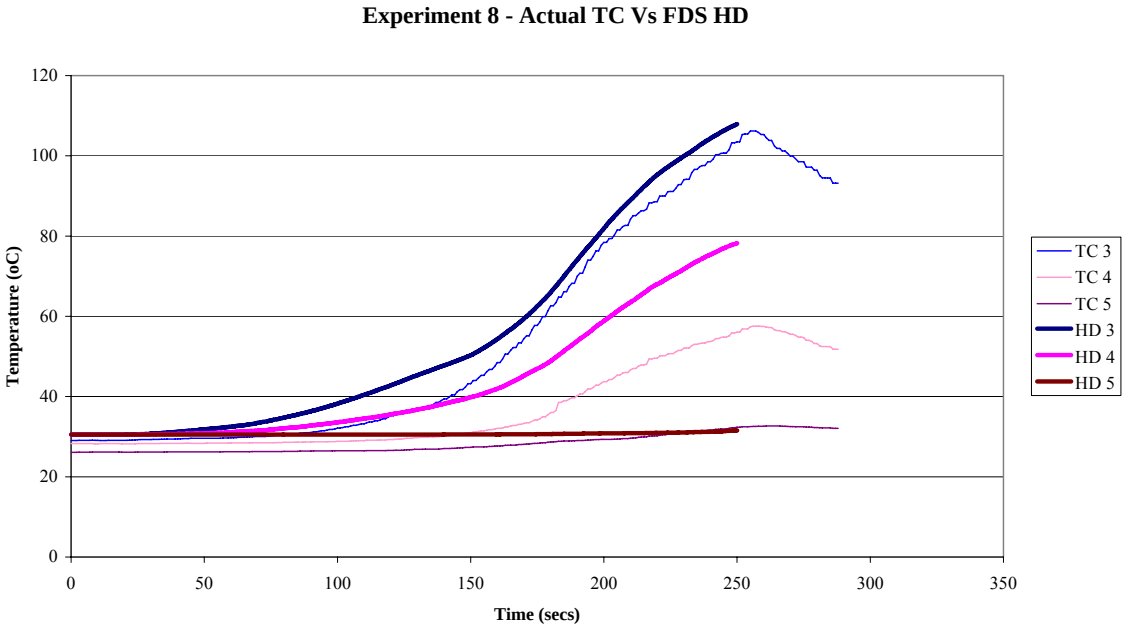

Figure 9.7 Experiment 8 – actual TC Vs FDS HD temperature for TC 3,4 and 5

For experiment 8 (see Figure 9.7) substituting heat detectors (RTI of 30 $m^{0.5}s^{0.5}$) for thermocouples FDS predicted temperatures within 20 % of the actual temperature for TC positions 3 and 5. For TC 4 the difference is over 20 %.

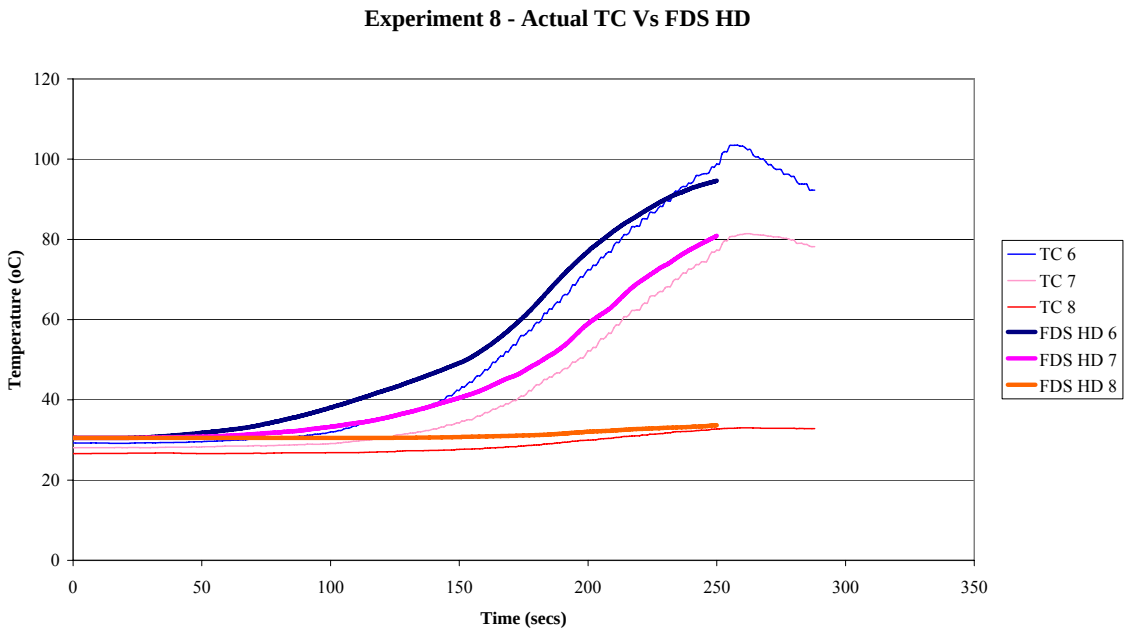

Figure 9.8 Experiment 8 – actual TC Vs FDS HD temperatures for TC 6,7 and 8

The comparison of predicted HD (RTI of 30 $m^{0.5}s^{0.5}$) temperatures for experiment 8 (see Figure 9.9) with actual TC temperatures for TC positions 6,7, 8 is close, the predicted temperatures are within 20 % of the actual measured temperatures.

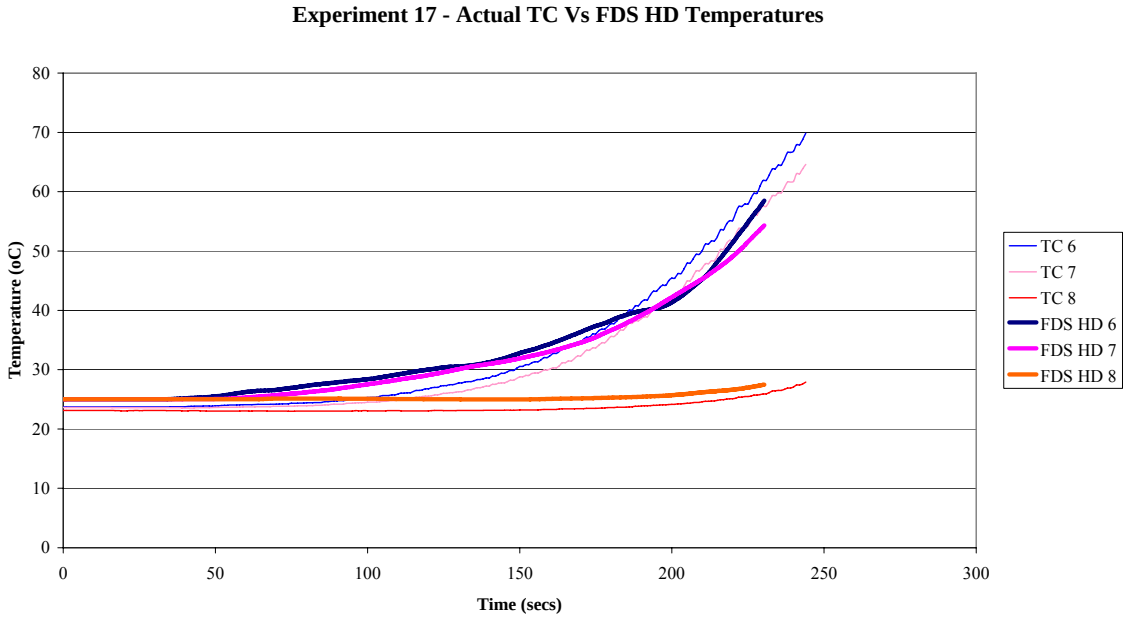

Figure 9.9 Experiment 17 – actual TC Vs FDS HD temperatures for TC 6,7 and 8

The HD's (RTI of 30 $m^{0.5}s^{0.5}$) predicted temperatures within 20 % of the actual measured temperatures for experiment 17 TC 6,7 and 8. See Figure 9.9.

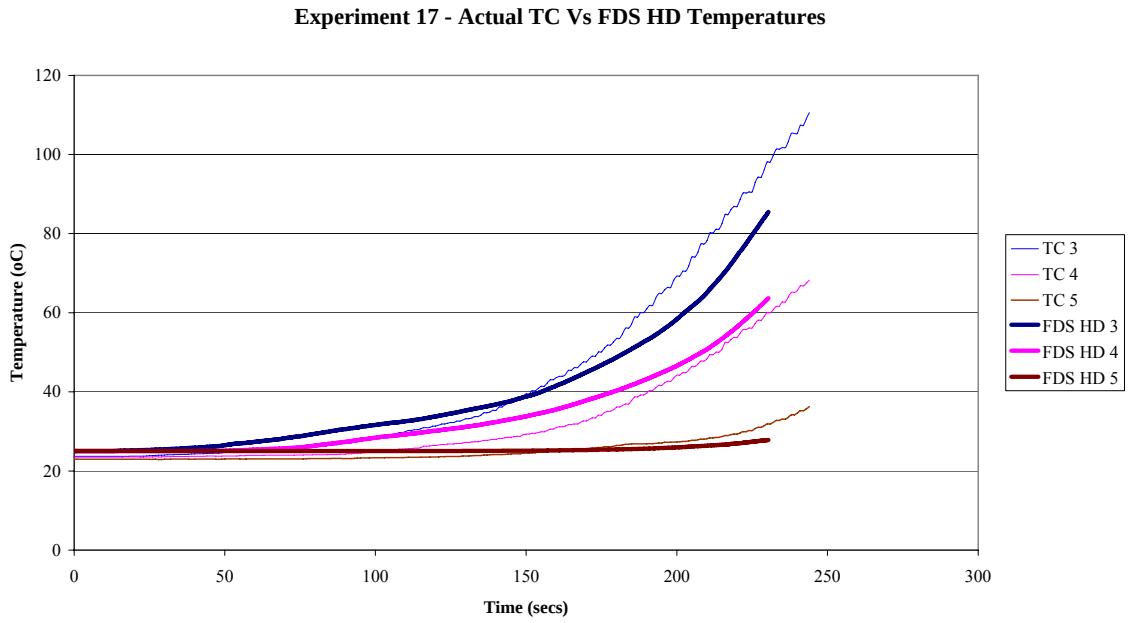

Figure 9.10 Experiment 17 – actual TC Vs FDS HD temperatures for TC 3,4,5

The predicted HD (RTI of 30 $m^{0.5}s^{0.5}$) temperatures for experiment 17 TC 3,4 and 5 (see Figure 9.10) are within 20 % of the actual measured temperatures.

9.1.5. Summary

By simulating TC's as heat detectors the actual measured temperatures and predicted temperatures are comparable. Caution must be taken in using this approach as more research is needed to validate this method. When comparing the bare wire TC (TC 1 and 2) temperatures with the predicted temperatures, and the temperatures for the sheath TC's with the predicted HD temperatures, a comparison that does not generally deviate by more than 20 % is achieved.

For sprinkler activation times, the temperatures measured at the sprinkler head locations are of interest. The actual and predicted temperatures are comparable, but there can be a lag of 5 – 10 seconds between the actual gas temperature and the bare TC temperature, Holman has reported this type of occurrence in a series of experiments he undertook with different types of thermocouples [54].

9.2. Sprinkler Activation Comparison

This Section reports on the comparison of actual and predicted sprinkler activation times. The following comparisons are made:

- General c-factor comparison.
- Residential sprinkler c-factor comparison.
- Standard response sprinkler c-factor comparison.
- Fire position comparison.
- Adjusted HRR comparison.
- Gas temperature at activation comparison.
- HRR at activation comparison.

9.2.1. General c-factor Comparison

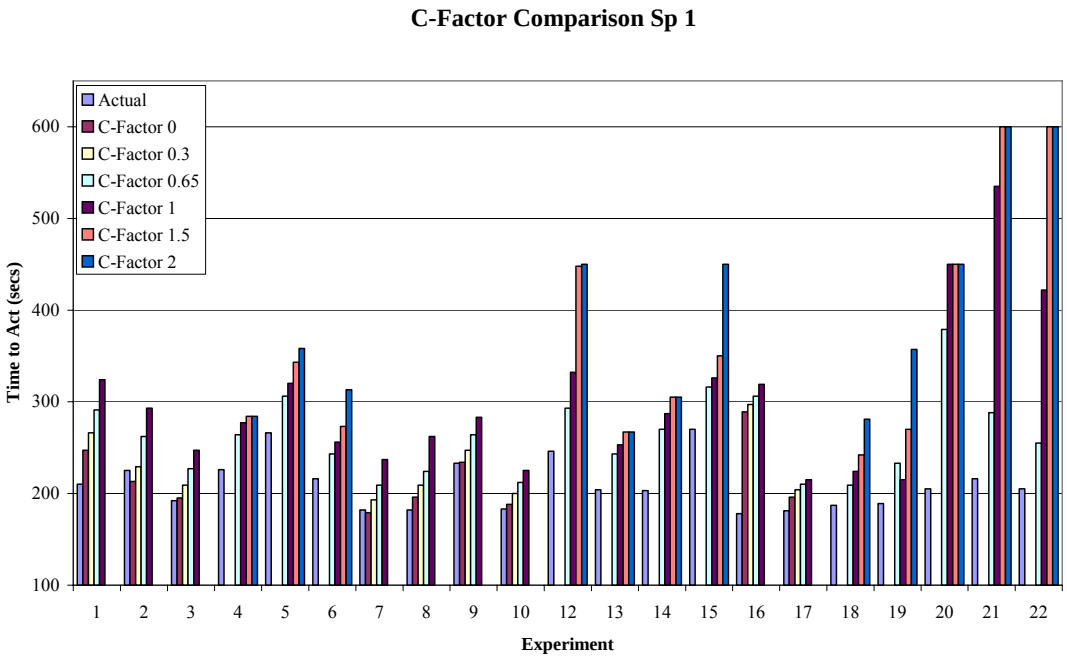

Figure 9.11 c-factor comparison sp 1

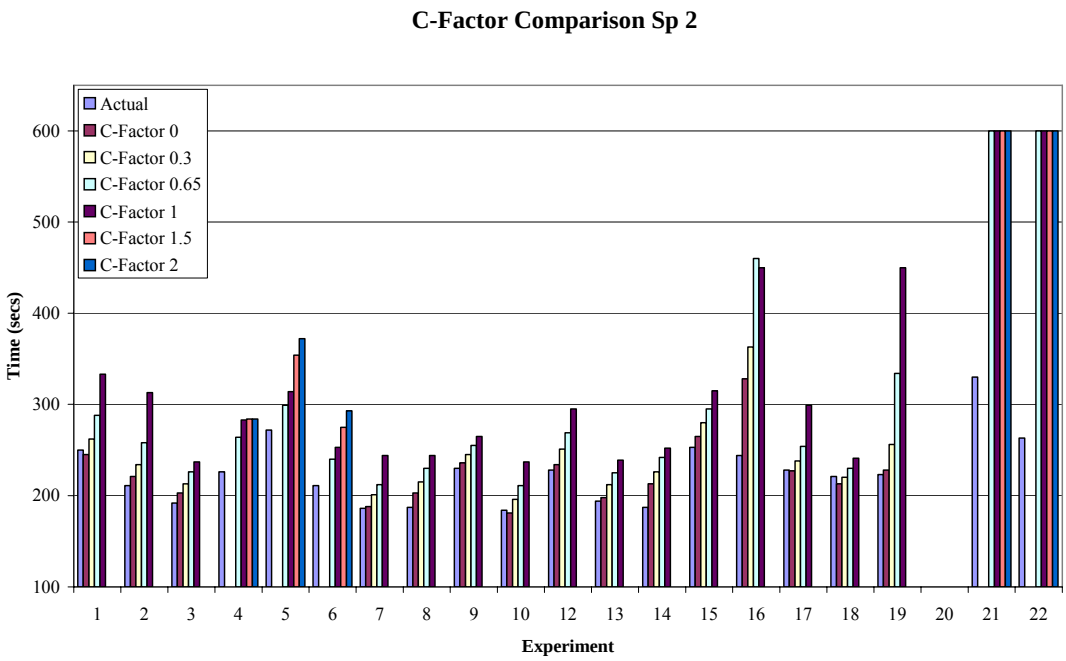

Figure 9.12 c-factor comparison sp 2

Figure 9.11 and Figure 9.12 illustrates the actual and predicted sprinkler activation times for all actual and simulated activations.

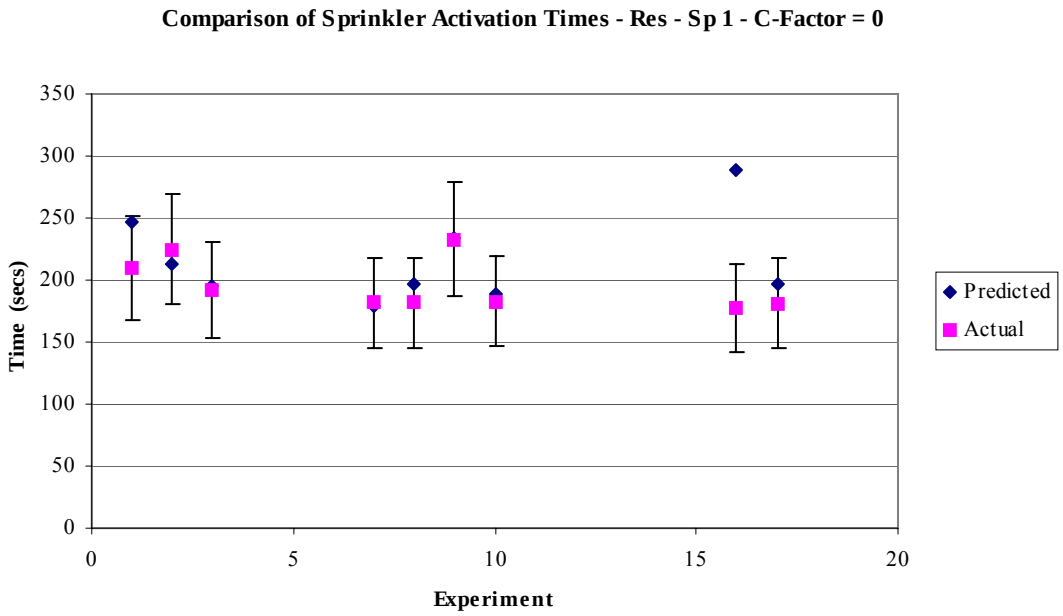

Figure 9.13 Comparison of sprinkler activation times, residential, sp 1 c = 0

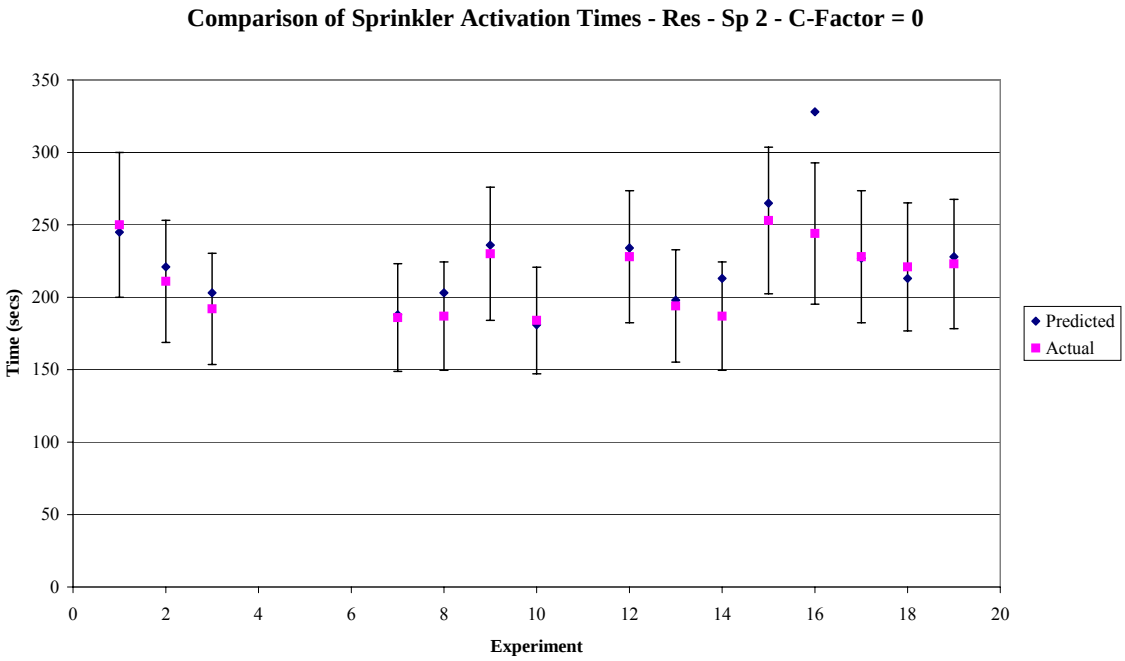

Figure 9.14 Comparison of sprinkler activation times, residential, sp 2 c = 0

Sprinkler Position	< 20 %	< 25 %	< 30 %
1	8/9	8/9	8/9
2	14/15	14/15	14/15
Combined (%)	92	92	92

Table 9-2 Sprinkler comparison residential, c = 0

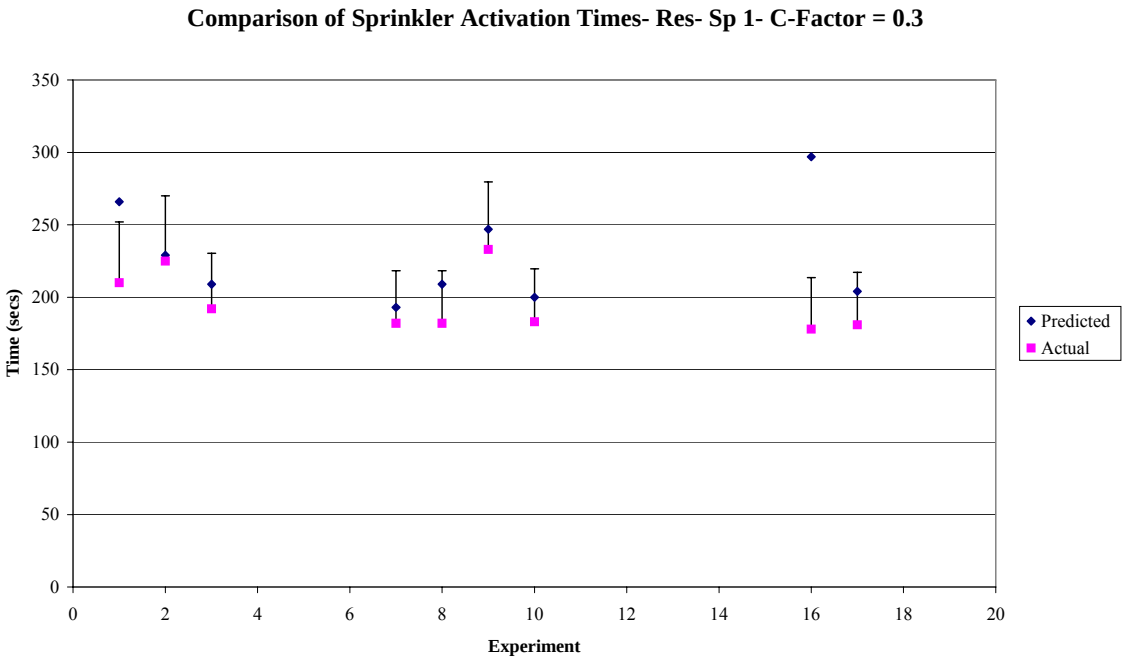

Figure 9.15 Comparison of sprinkler activation times, residential, sp 1 c = 0.3

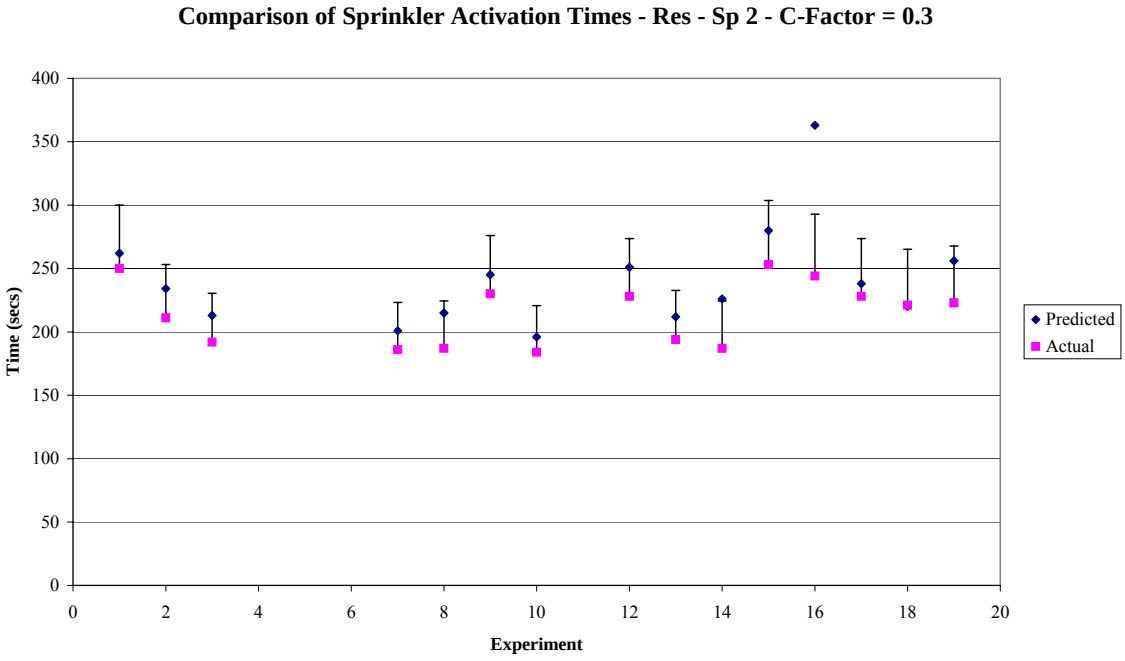

Figure 9.16 Comparison of sprinkler activation times, residential, sp 2 c = 0.3

Sprinkler Position	< 20 %	< 25 %	< 30 %
1	7/9	7/9	8/9
2	14/15	14/15	14/15
Combined (%)	86	86	92

Table 9-3 Sprinkler comparison residential, c = 0.3

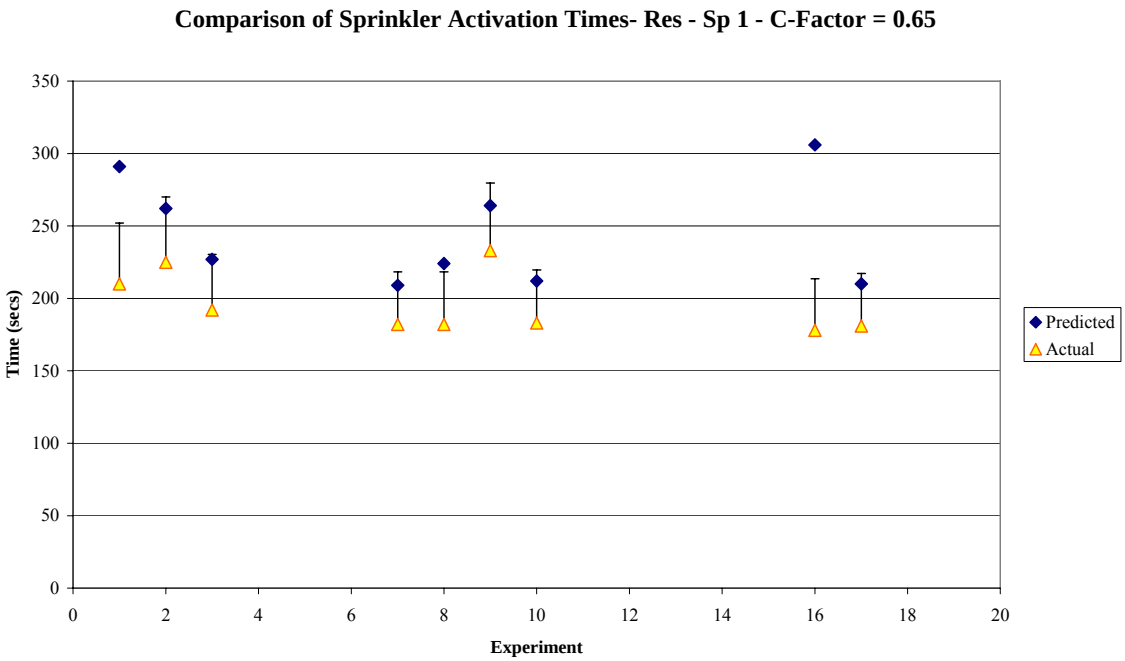

Figure 9.17 Comparison of sprinkler activation times, residential, sp 1 c = 0.65

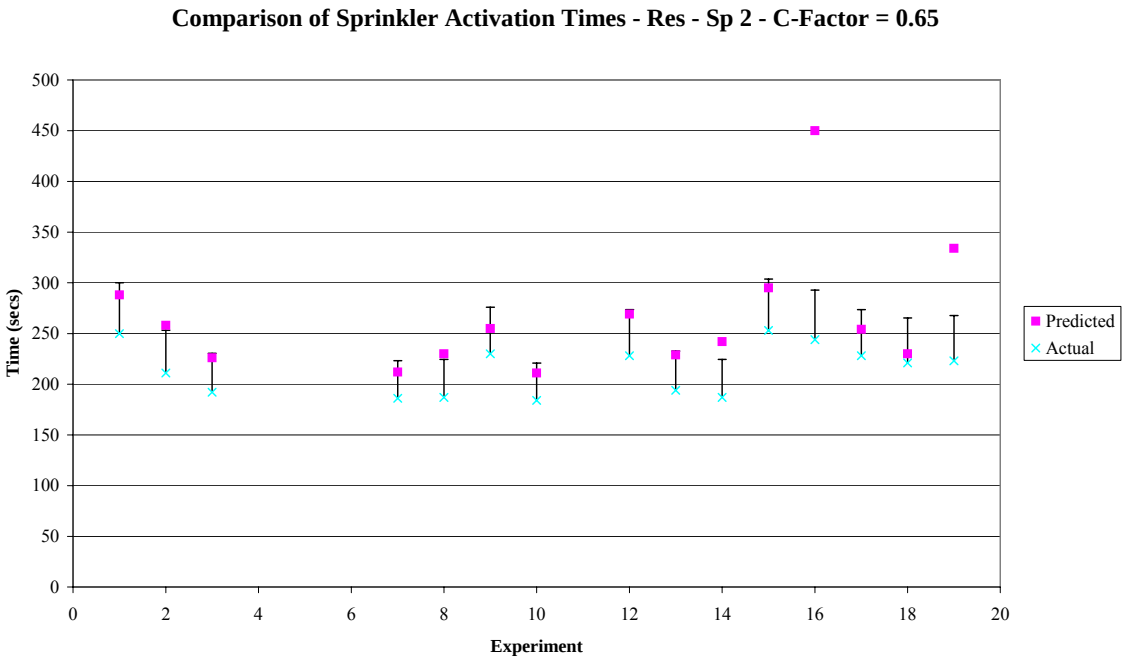

Figure 9.18 Comparison of sprinkler activation times, residential, sp 2 c = 0.65

Sprinkler Position	< 20 %	< 25 %	< 30 %
1	6/9	7/9	7/9
2	10/15	12/15	13/15
Combined (%)	67	79	83

Table 9-4 Sprinkler comparison residential, c = 0.65

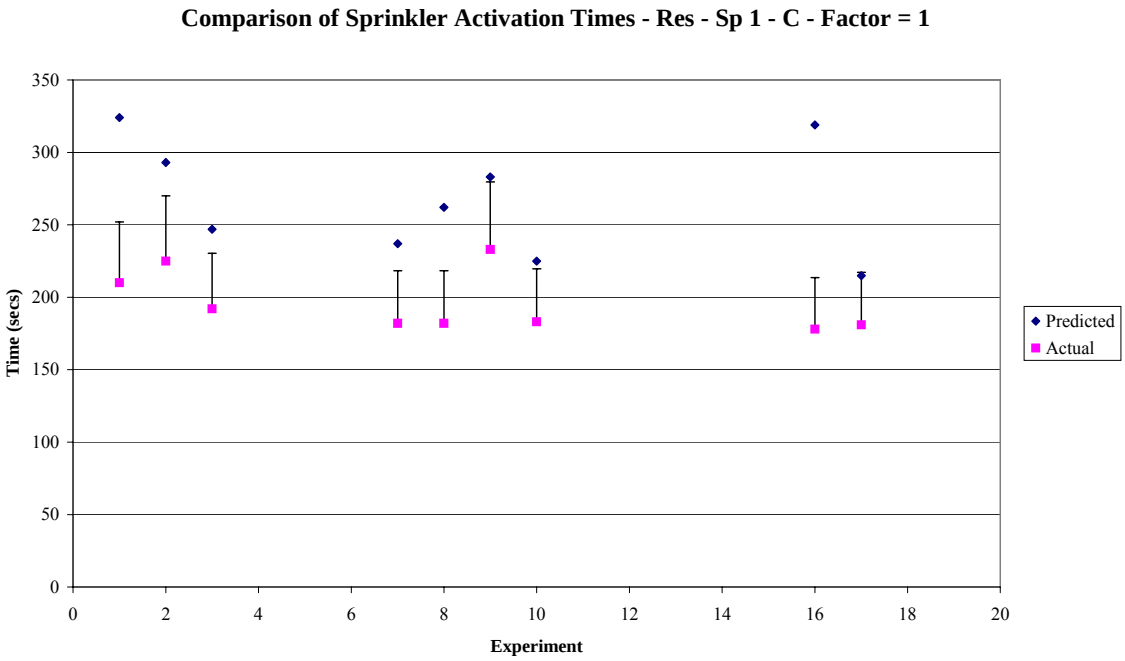

Figure 9.19 Comparison of sprinkler activation times, residential, sp 1 c = 1

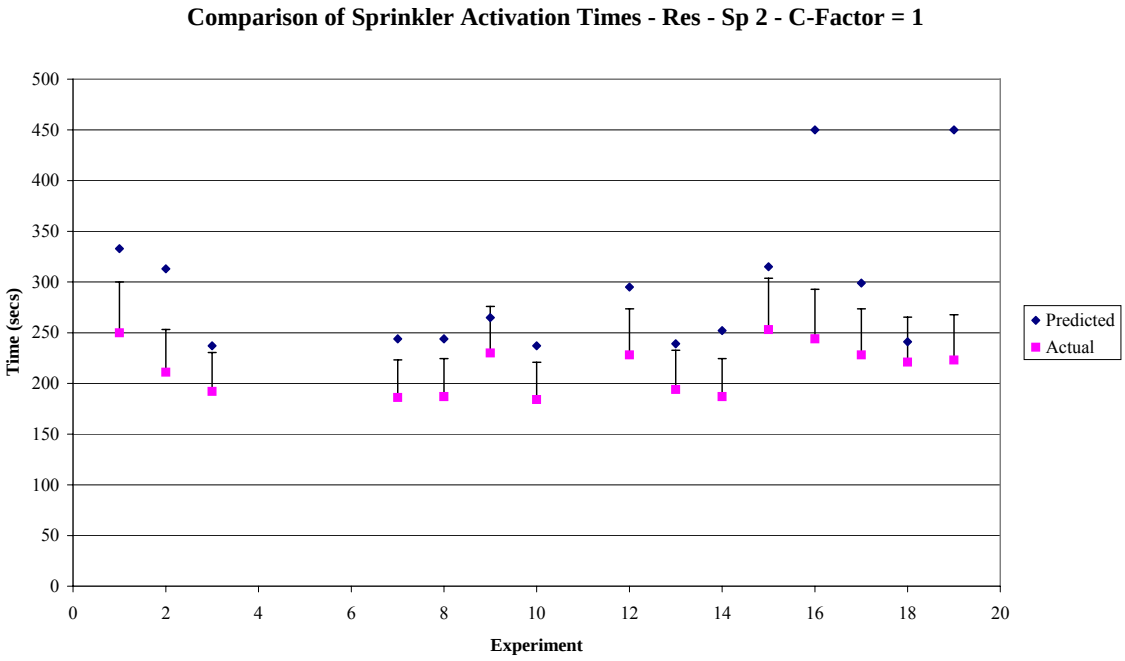

Figure 9.20 Comparison of sprinkler activation times, residential, sp 2 c = 1

Sprinkler Position	< 20 %	< 25 %	< 30 %
1	1/9	3/9	6/9
2	2/15	5/15	7/15
Combined (%)	12	33	54

Table 9-5 Sprinkler comparison residential, c = 1

Sprinkler Position	< 20 %	< 25 %	< 30 %
1	7/12	9/12	9/12
2	3/5	3/5	3/5
Combined (%)	59	71	71

Table 9-6 Sprinkler comparison standard response, c = 0.65

Sprinkler Position	< 20 %	< 25 %	< 30 %
1	2/12	6/12	7/12
2	2/5	3/5	3/5
Combined (%)	23	53	59

Table 9-7 Sprinkler comparison standard response, c = 1

Sprinkler Position	< 20 %	< 25 %	< 30 %
1	0/12	0/12	5/12
2	0/5	0/5	2/5
Combined (%)	0	0	41

Table 9-8 Sprinkler comparison standard response, c = 1.5

Sprinkler Position	< 20 %	< 25 %	< 30 %
1	0/12	0/12	1/12
2	0/5	0/5	1/5
Combined (%)	0	0	12

Table 9-9 Sprinkler comparison standard response, c = 2

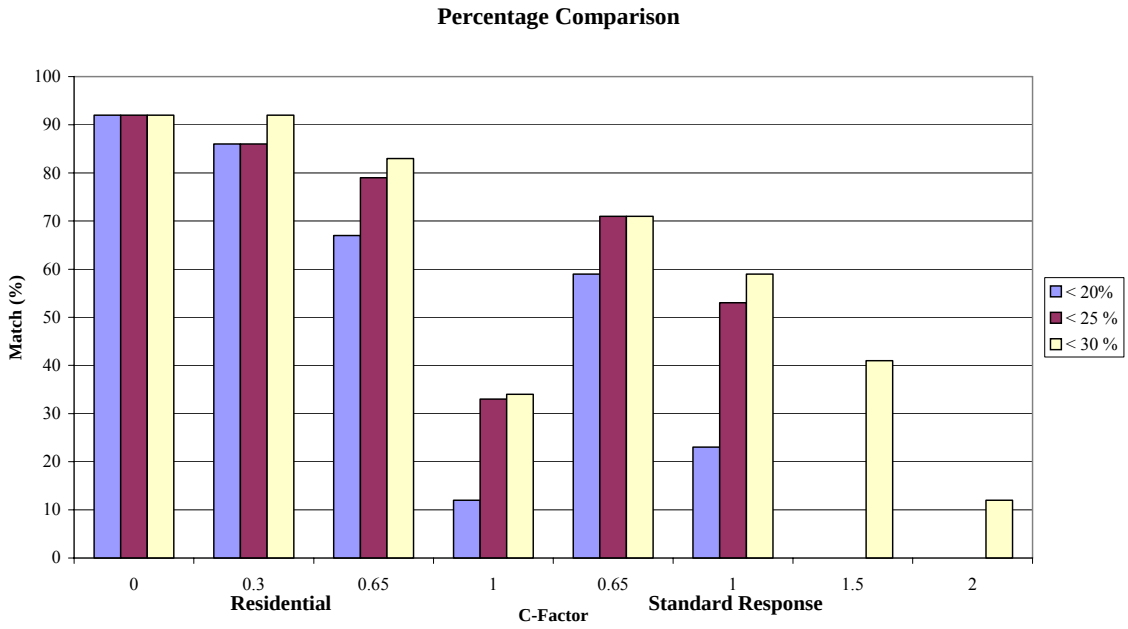

Figure 9.21 Percentage comparison of c-factors

Figure 9.21 summaries the information presented in the sprinkler comparison Table 9-2 - Table 9-9. It is shown that the comparison is generally more favourable for the residential heads than for the standard response heads. Activation times predicted using c-factors of 0 and 0.3 are extremely comparable with match percentage in excess of 85 % for all comparisons (difference < 20 – 30 %). It should be noted that the predicted activation times were generally in excess of the actual activation times, except for a fraction of the results that involved residential heads with a c-factor of 0 and 0.3. For the recommended C-factor of 0.65 the comparison was reasonable, 83 % of the predictions were within 30 % of the actual times. For a c-factor of 1, the comparison was not good, no more than 34 % of the predictions were within 30 % of the actual times.

For standard response heads a c-factor of 0.65 gives the closest comparison between actual and predicted activation times. 71 % of the predictions were within 30 % of the actual activations. All predicted activations were in excess of the actual activations. The comparisons for a c-factor of 1 are similar but looser. It is interesting to note that for c-factors of 1.5 and 2, there were no activations that were within 25 % of the actual activations.

It is clear from the above analysis that c-factors significantly effect the predicted sprinkler activation times. The difference can be up to 50 % of the actual activation time. This factor needs to be considered when FDS is used to predict critical life safety time lines based on sprinkler activation times.

Generally the predictions were conservative, except for some results for residential heads with a c-factor of 0.3 or less. If a prediction is conservative, this is likely to lead to a larger factor of safety for a subsequent fire safety design. On the other hand if the predicted activation times are shorter, there could be a reduction in the factor of safety for a particular design.

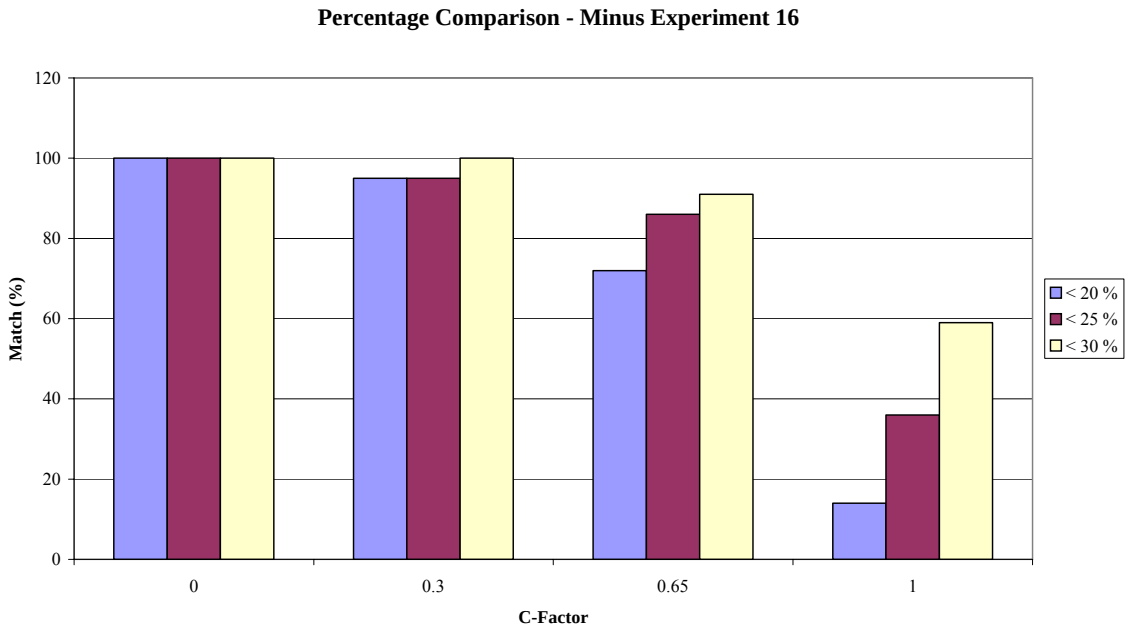

Figure 9.22 Percentage comparison minus experiment 16

Figure 9.22 replicates Figure 9.21 for residential heads omitting data for experiment 16. As previously discussed there is a possibility that data for experiment 16 is faulty.

9.3. Further Analysis

This section provides further analysis for sprinkler activation predictions given for simulations using a c-factor of 0.65. The supplier of the sprinkler head recommended

that a c-factor of 0.65, but could not guarantee the value. The results (c-factor = 0.65) from the simulations were split into groups based on sprinkler type and fire position.

9.3.1. Center Fire Activations

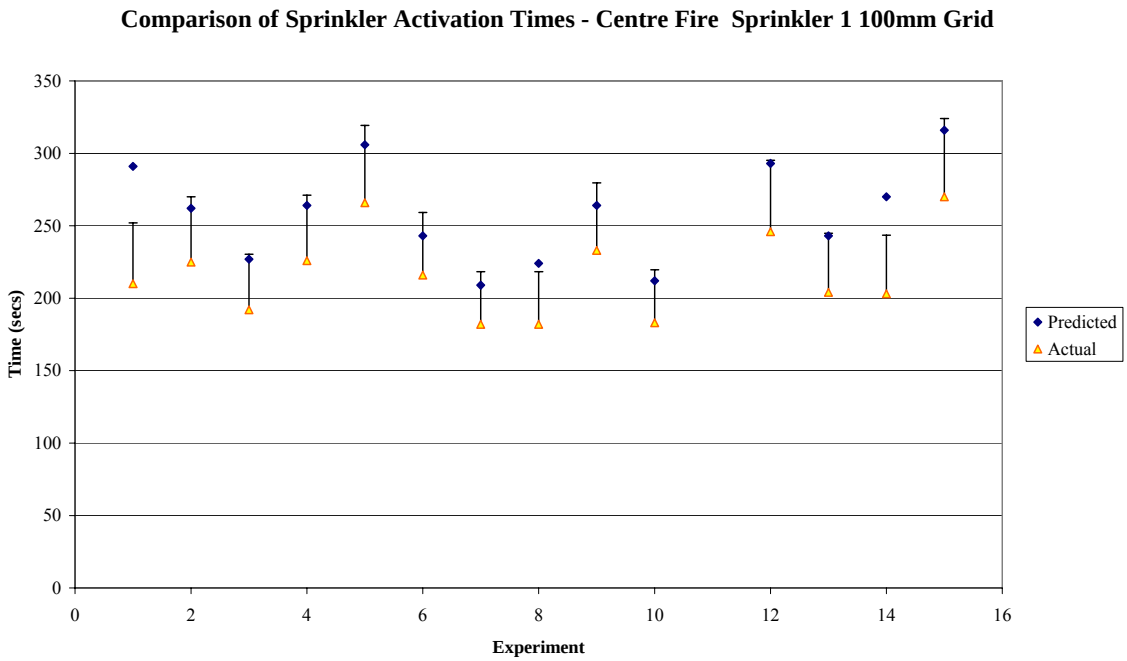

Figure 9.23 Comparison of sprinkler activation times center fire sp 1

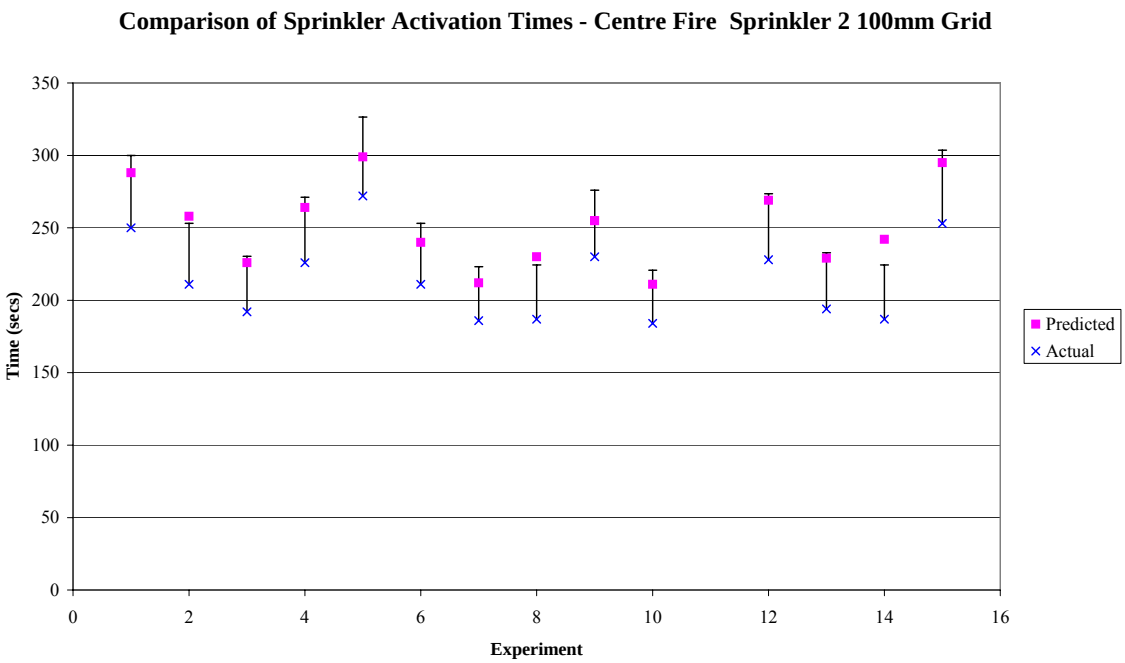

Figure 9.24 Comparison of sprinkler activation times center fire sp 2

Figure 9.23 and Figure 9.24 illustrate the comparison of activation times for experiments with centrally placed fires. The sprinkler heads involved are either residential or standard response. The error bars represent 20 %. In 82 % of the cases, the predicted activation time are within 20 % of the actual activation time, and 96 % of the cases are within 30 % of the actual. 27 of the 28 predicted activations are comparable with the actual activation times.

9.3.2. Corner Fire Activations

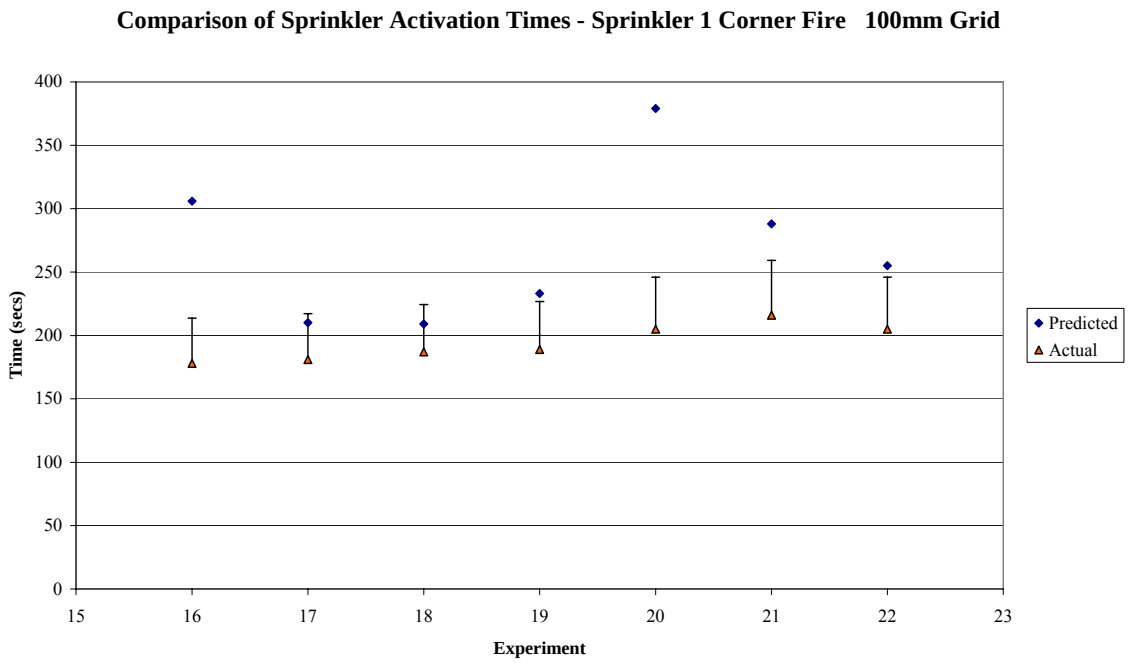

Figure 9.25 Comparison of sprinkler activation times corner fire sp 1

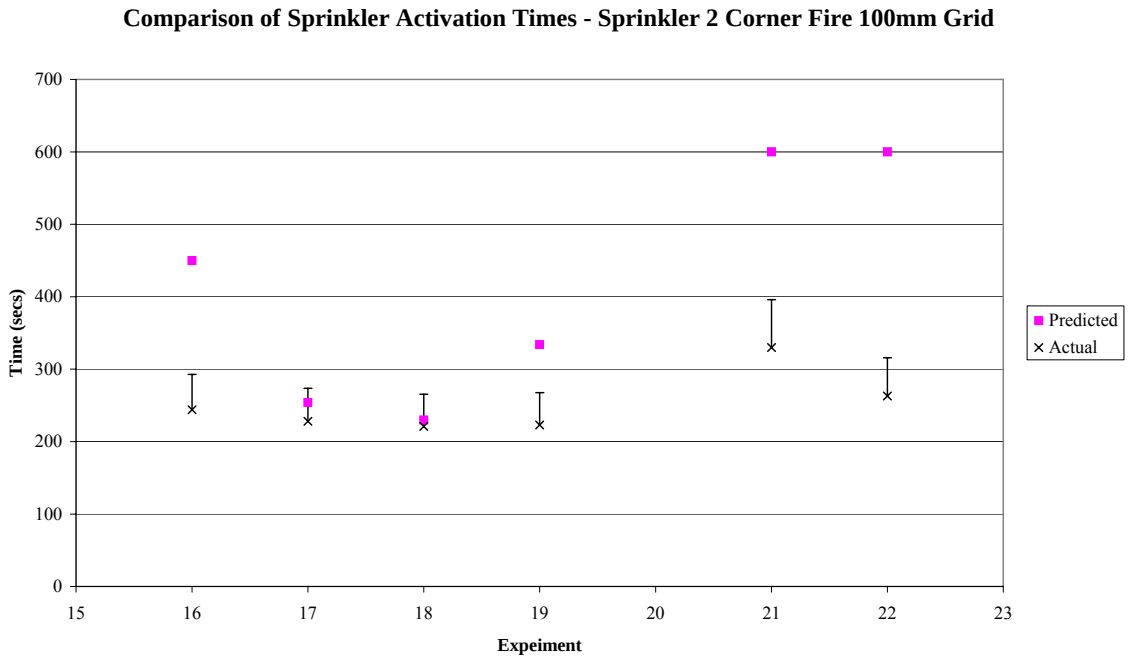

Figure 9.26 Comparison of sprinkler activation times center fire sp 2

Figure 9.25 and Figure 9.26 illustrates the comparison of activation times for experiments with the fire placed in the corner of the compartment. The sprinkler

heads involved are either residential or standard response. The error bars represent 20 %. In 39 % of the cases, the predicted activation time were within 20 % of the actual activation time, and 46 % of the cases were within 30 % of the actual. 6 of the 13 predicted activations were comparable with the actual activation times.

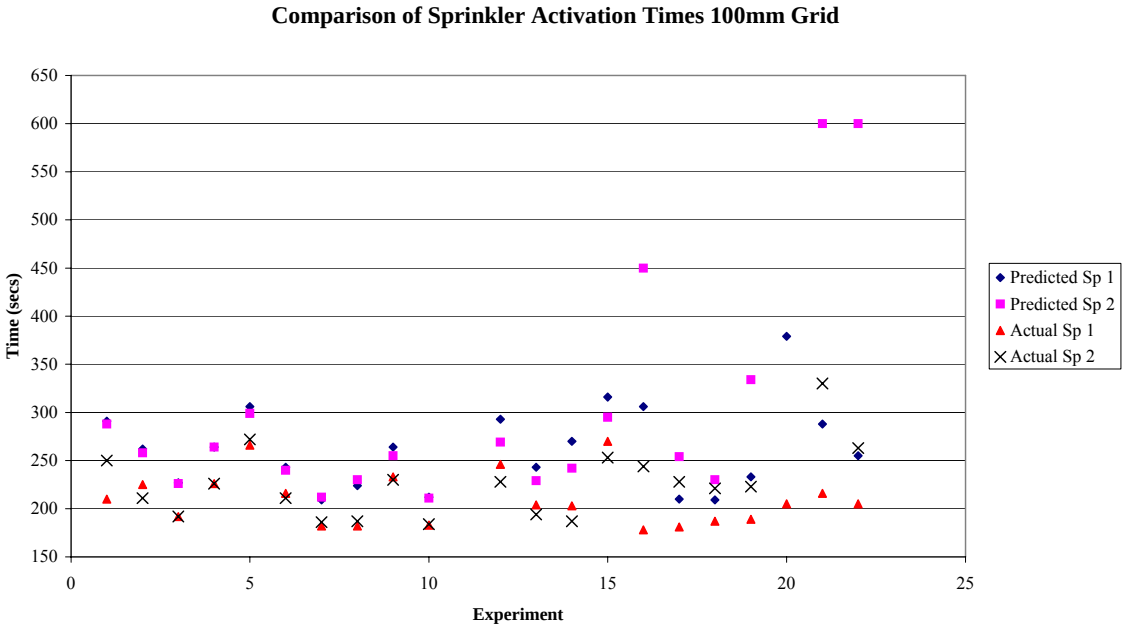

Figure 9.27 Comparison of sprinkler activation times

Figure 9.27 illustrates that the predicted and actual activation times are reasonably comparable for experiments 1 – 15. For experiments 16 – 22 the predicted activation times for sprinkler 2 deviate from the actual for the standard response sprinklers. This is especially true for the 93^{o}C standard response head.

9.3.3. Adjusted Values

As explained, the actual HRR curves for the experimental fires did not contain data for the complete burn of the chairs. In most cases the HRR curves calculated from the mass loss data did not contain a decay period. For the simulations the HRR curve was programmed to grow then remain at the HRR value of the last data entry until the simulation finished. This produced the situations were the HRR curve reached a steady state phase.

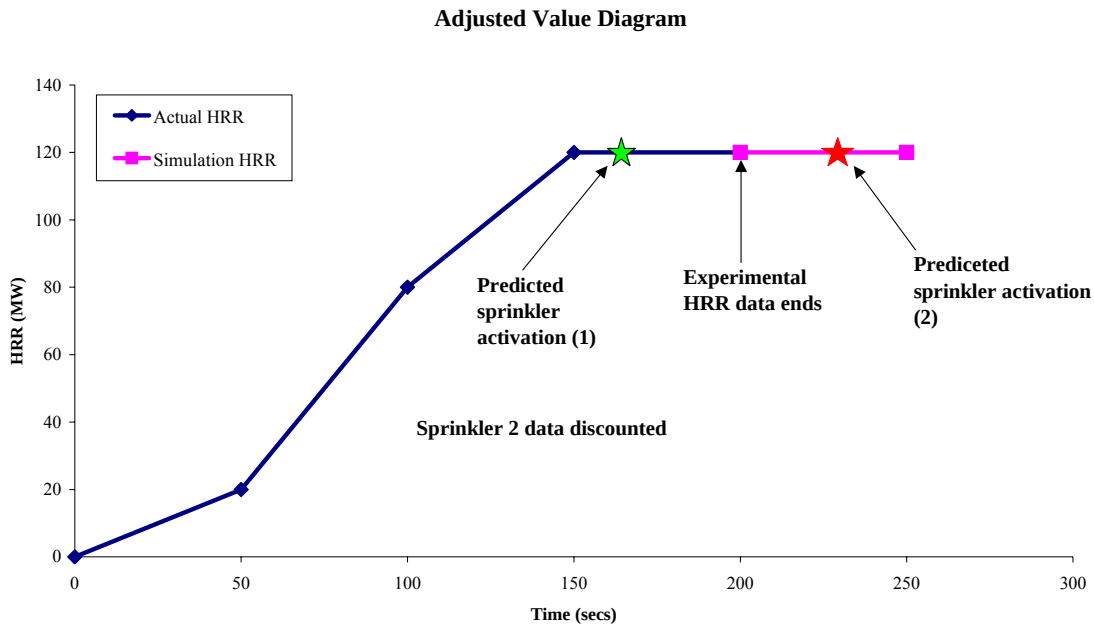

Figure 9.28 Adjusted value diagram

In assuming that the design fire used became steady state following the growth period, the sprinkler activation times would become skewed. To reduce the uncertainty, the experimental data was filtered. The filtering removed all predicted data from the point forward at which the fire was extinguished. Therefore if the predicted sprinkler activation occurred after the actual fire was extinguished then the data set was removed. Figure 9.28 illustrates the filtering method. It could be argued that this gives a truer validation of FDS as the actual and prescribed fires are of the same form.

Experiment	Percentage Difference Sprinkler 1	Percentage Difference Sprinkler 2
1	38.6	15.2
2	16.4	22.27
3	18.2	17.71
4	16.8	16.8
6	12.5	13.74
7	14.8	13.98
9	13.3	10.87
10	15.8	14.67
12	19.1	17.98
13	19.1	18.04
14	-	29.41
15	17	16.6
17	16	-
18	11.8	4.07
19	23.3	49.78
21	33.3	-
22	24.4	-

Table 9-10 Comparison of adjusted activation times

- denotes that the predicted activation time was outside the actual HRR data

The adjusted data is comparable with the unadjusted data. 80 % of the predicted activation times are within 20 % of the actual activation times. 87 % of the predicted results are within 25 % of the actual and 90 % are within 30 %.

9.4. Temperature at Sprinkler Activation

This section reports on the actual and predicted temperatures measured by the TC positioned adjacent to the sprinklers. The temperature data for the actual experiments is limited due to technical problems encountered with the temperature measurement and recording equipment. However there is sufficient data available to identify any pattern with a reasonable degree of certainty.

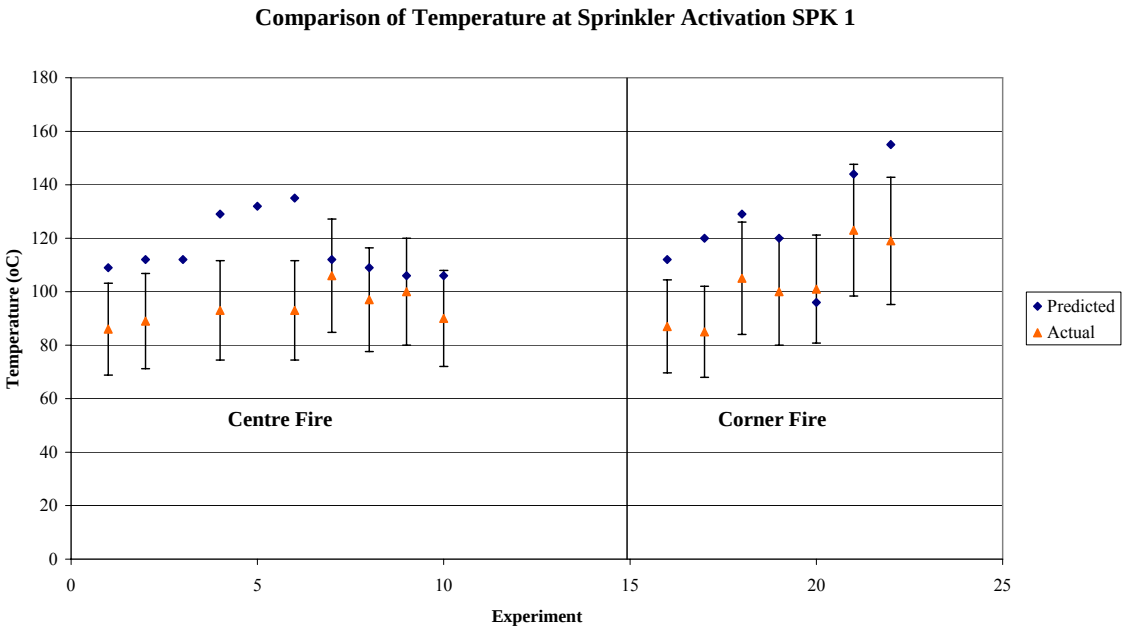

Figure 9.29 Comparison of temperatures at sprinkler activation sp 1

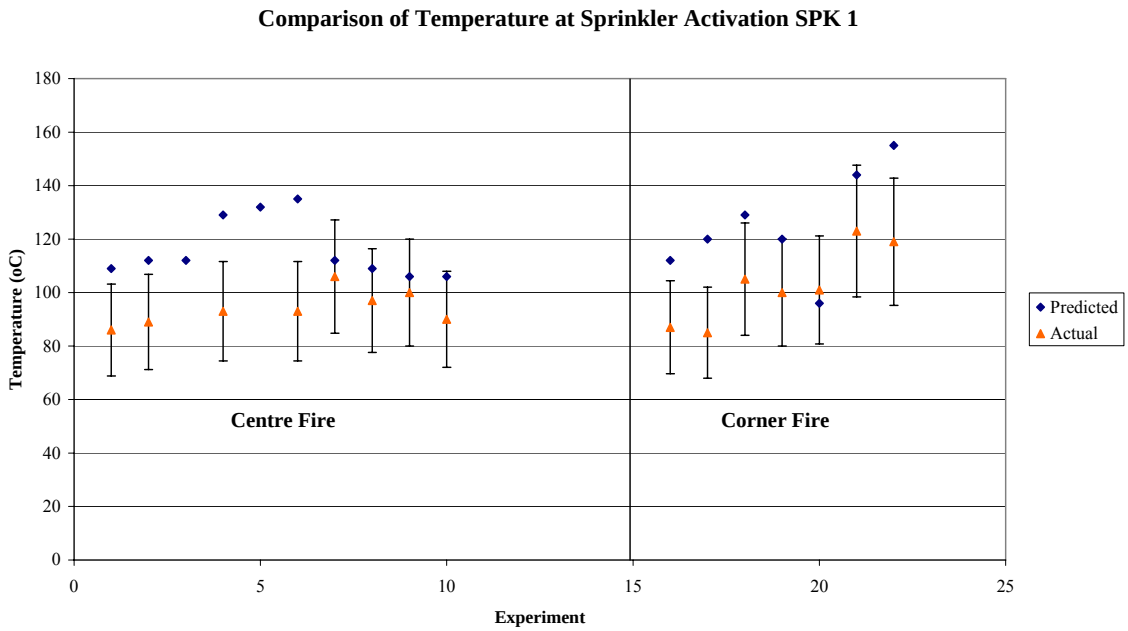

Figure 9.30 Comparison of temperatures at sprinkler activation sp 2

Figure 9.29 and Figure 9.30 illustrates the comparison between the temperatures measured by a TC positioned adjacently to sprinkler head for the actual experiments and the corresponding predicted temperatures. Generally the predicted temperatures are higher than the actual at the time of sprinkler activation with 58 % being within 20 % of the predicted temperatures.

The sprinkler activation model used by FDS (equation 15) has the following input variables, gas temperature and velocity. If the predicted activation temperature is higher than the actual and the TC temperature gradients histories of the predicted and actual are similar, then the velocity component of the sprinkler activation model must be different, assuming that the sprinkler activation model used is accurate. It may be possible that FDS predictions for velocity are either under or over calculated.

9.5. HRR Comparison

This section compares the HRR at the time of sprinkler activation for the actual and predicted data.

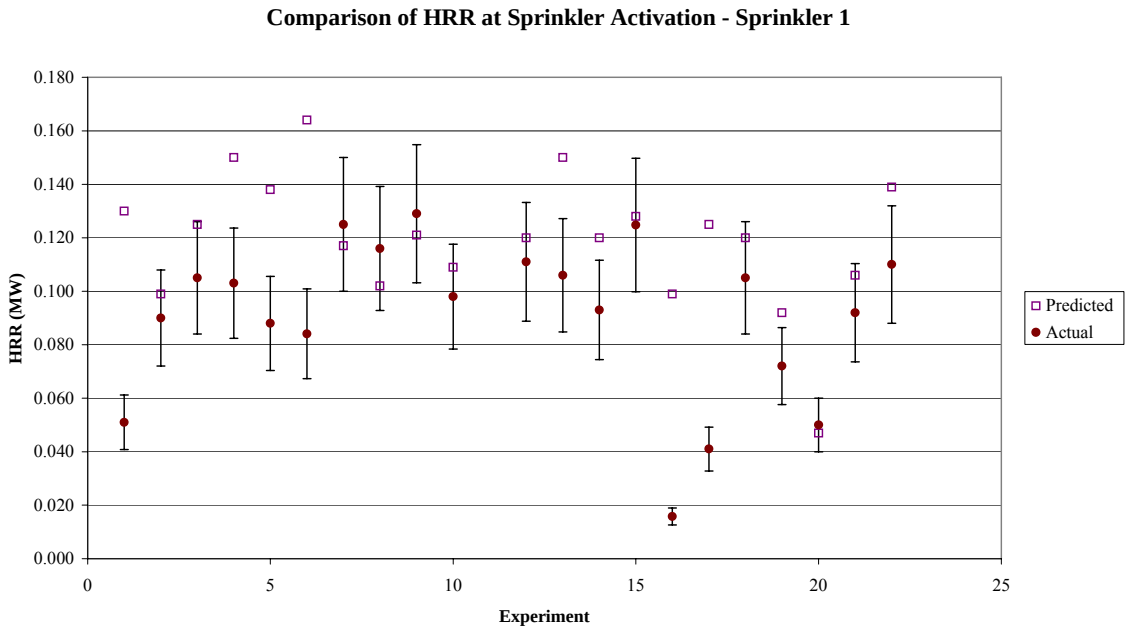

Figure 9.31 Comparison of HRR at sprinkler activation – sprinkler 1

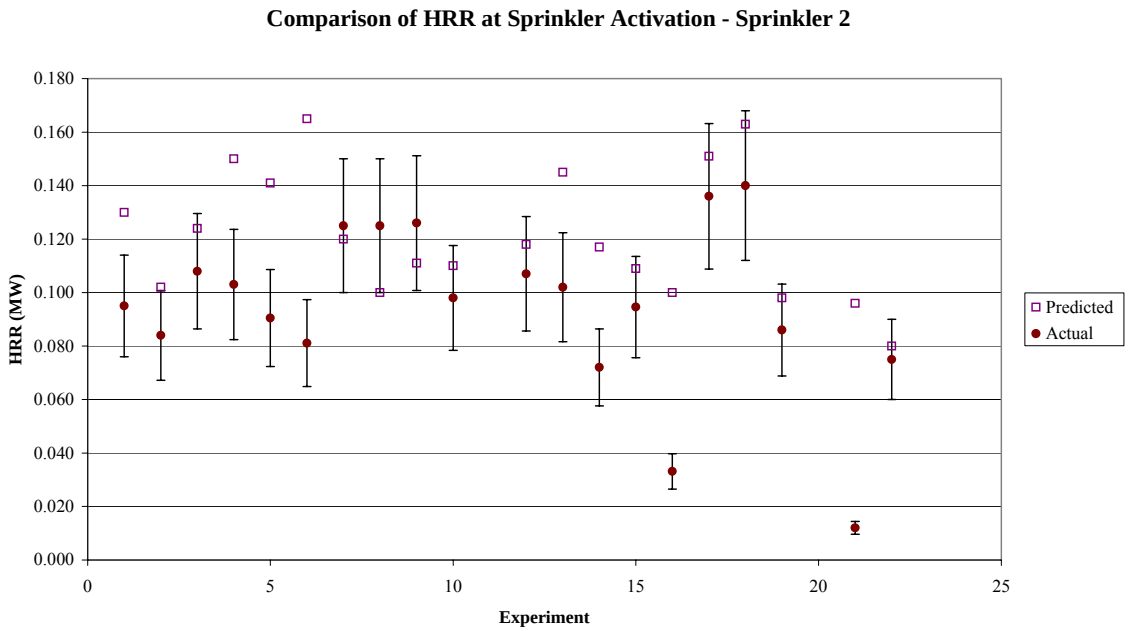

Figure 9.32 Comparison of HRR at sprinkler activation – sprinkler 2

Figure 9.31 shows the comparison of HRR for sprinkler 1. For sprinkler location 1 (non door end) the predicted HRR are within 20 % of the actual HRR at the time of sprinkler activation for 52 % of the experiments. The predicted HRR is generally greater than the actual with only 19 % of the predicted being less than the actual. For sprinkler location 2 (Figure 9.32) 60 % of the predictions are within 20 % of the actual. About 15 % of the predictions are less than the actual HRR.

A possible reason for HRR being higher at the time of activation (predicted), might be representative of the longer sprinkler activation times. That is, the simulation has progressed along the HRR curve, and since the HRR is growing the corresponding HRR at activation is greater.

9.6. Velocity Profile

Unfortunately no velocity profiles were measured during the experiments. As gas velocity is used to predict sprinkler activation times, it would have been useful to have made a comparison between the actual and predicted velocities. Through it is not possible to make a comparison with actual velocities it is possible to make a comparison of velocities for simulations using different grid sizes.

Figure 9.33 and Figure 9.34 compare the predicted velocity histories at the sprinkler heads for experiment 6 for grid sizes of 75, 100 and 150 mm. The sensitivity analysis has shown that there is little difference in temperature predictions (sp 1 and 2) for 75 and 100 mm grid sizes. However the velocity profiles for those simulations differ significantly in comparison to the temperature differences. This could explain the differences in the predicted sprinkler activation times between the 75 and 100 mm simulations.

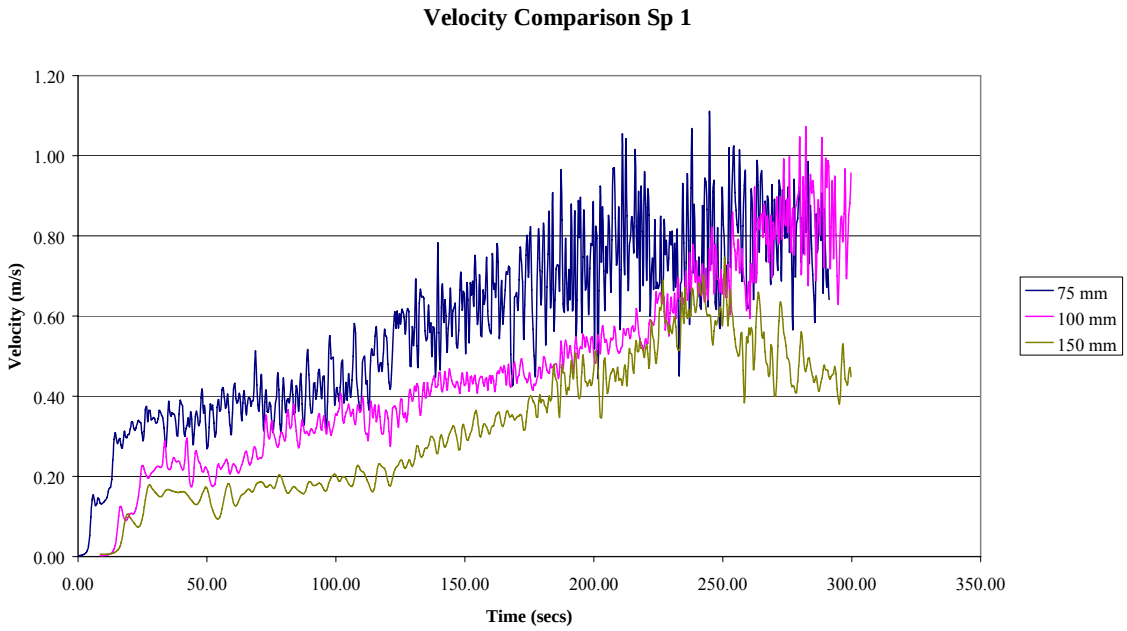

Figure 9.33 Velocity comparison sp 1

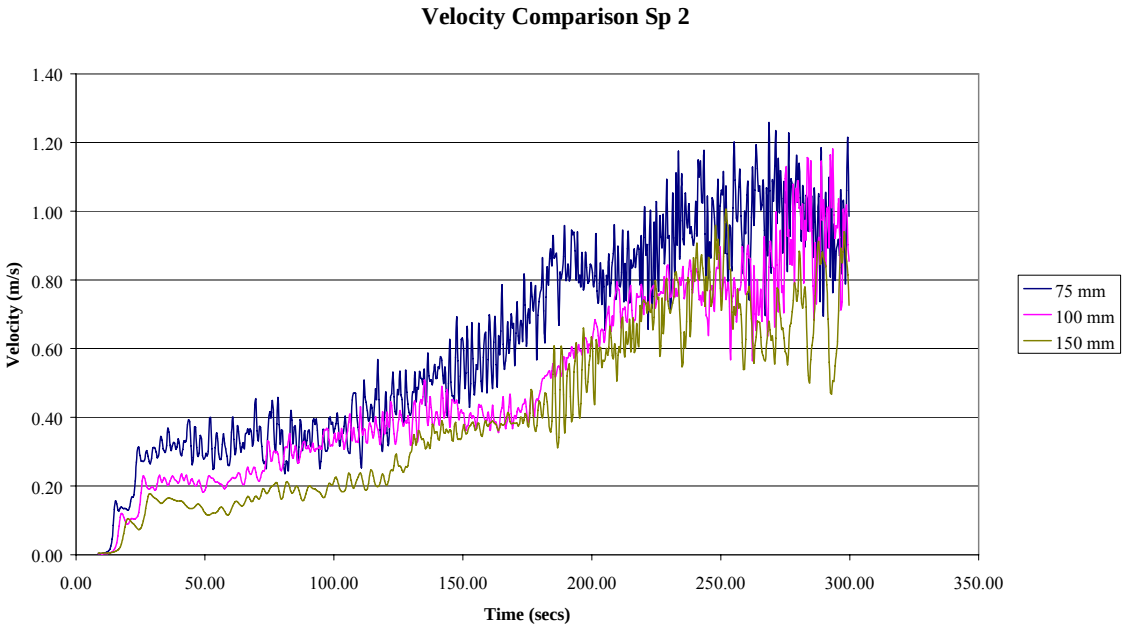

Figure 9.34 Velocity comparison sp 2

9.7. Comparison Summary

This section summaries the findings of the comparisons made between the actual and predicted data sets.

- For TC positions 1 and 2 FDS slightly over predicts the rate in raise of temperatures and the maximum temperatures. The predicted temperatures are generally within 20 % of the measured temperatures. For TC 1 and 2, the thermal lag associated with the bare wire TC's may account for some of the differences between the temperatures.
- The predicted and actual temperatures (TC 3 – 8) differ significantly. There is a significant lag between the predicted and actual temperatures. The actual TC temperatures run parallel to the predicted TC temperatures. A possible reason for this, is that the sheathed TC's have a significant thermal response due to the thermal mass of the covering metal.
- Assigning a RTI of 30 to heat detectors gave favorable temperature predictions to the actual. These predictions were within 20 % of the measured temperatures.
- Generally predicted sprinkler activation times were longer than actual sprinkler activation times.
- For experiments where the fire was positioned in the center of the room, predicted and actual sprinkler activation times were comparable.
- For the experiments where the fire was positioned in the corner of the room, predicted and actual sprinkler activation times were not favorable for sprinkler 2 (door end).
- The c-factor value has a significant effect on the predicted sprinkler activation times, lower c-factors result in better comparisons between the actual and predicted.
- A c-factor of 0.65 gives reasonable comparisons for residential heads.
- A c-factor of 0 – 0.3 gives excellent comparisons for the residential heads.
- Generally the HRR at the time of sprinkler activation was higher for the predicted than the actual

- TC 1 and 2 gave a higher predicted temperature than actual temperature at the time of sprinkler activation. A percentage of this may be attributed to thermal lag.

By using a c-factor that is less than the given c-factor better comparisons were given. The supplier made it clear that there is a great deal of uncertainty with this value, this may of effected the closeness of the comparisons. Otherwise it may be prudent to use lower c-factors to offset differences between the actual and predicted sprinkler activation times. Caution must be used if this approach is to be applied as the data has shown that predicted activation times for lower c-factor values can be shorter than the actual activation times.

If it is assumed that the sprinkler activation model is reasonably accurate, and that the sprinkler head technical data is correct and agree that the predicted TC's temperatures are relatively close to the actual TC temperatures (modifying for thermal lag). It could be argued that the predicted velocity profiles are different for the fire and environmental conditions portrayed in this research. The reason for putting this argument forward is that the sprinkler model used in FDS has three variables. And if it is assumed that the sprinkler temperature is a product of the gas velocity and temperature, then just two variables. If it is assumed that the gas temperatures are reasonably close, if not higher which should be favorable to a quicker activation, then the velocity profile history must be different. Unfortunately due to limitations on equipment no velocity profiles were taken during the actual experiments. This is an area for further study.

For a 100 mm grid size FDS over predicted the activation times for most of the simulations. It would interesting to investigate (over several simulation) the effect that reducing the grid size to 50 mm would have on the sprinkler activation times. This is also an area for further research.

10 Summary

10.1. Experimental Work

- Gas activation temperatures at the time of sprinkler activation are highest for 93^{o}C standard response heads.
- More aggressive HRR curves resulted in quicker sprinkler activations.
- Activation times are dependent on the nominal temperature rating of sprinkler heads.
- The difference in activation times for the residential and 68^{o}C standard response heads was less than 10 %.
- Fire position made a difference to compartment temperature profile.
- The door configuration did not effect activation times.

10.2. FDS Simulations

- 100 mm grid size was used for the simulations, this was based on the sensitivity analysis, which concluded that 150 mm grid under predicted both temperature and sprinkler activation times. 50 mm grid size over predicted temperatures as well as being time intensive.
- Fire was modeled as a HRR using the ramp function.
- Run times ranged from 8 – 12 hours.
- Various c-factor values were used.
- Heat detectors and TC's were used to measure temperatures.
- For a grid size of 50 mm, the simulation became unstable and crashed when using the restart function.

10.3. FDS Results

- The c-factor value has a significant influence on sprinkler activation times, with up to a 50 % difference between activation times for the smallest and highest value.
- Not all sprinklers were predicted to activated – 93^{o}C standard response sprinklers in location 2 (door end) failed to activate.
- FDS predicted that residential sprinklers would activate before standard response for a given fire.
- FDS predicted that the sprinkler closer to the fire would activate before the sprinkler further away from the fire, for heads of the same kind.
- The door position did not significantly effect sprinkler activation times.
- The door position had effect on the temperature measurements for the wall TC's.

10.4. Comparison

- For TC positions 1 and 2 FDS slightly over predicts the rate in raise of temperatures and maximum temperatures. The predicted temperatures are generally within 20 % of the measured temperatures. For TC 1 and 2 , the thermal lag associated with bare wire TC's may account for some of the differences between the temperatures.
- The predicted and actual temperatures (TC 3 – 8) differ significantly. However the actual TC temperatures run parallel to the predicted TC temperatures. A possible reason, is that the sheathed TC's have a significant thermal responsiveness due to the thermal mass of the covering metal.
- Predicted heat detector temperatures were within 20 % of the actual TC temperatures.
- Predicted sprinkler activation times were generally longer than actual sprinkler activation times.
- For experiments where the fire was positioned in the center of the room, predicted and actual sprinkler activation times were comparable if a c-factor of 0.65 or less was used.

- For the experiments where the fire was positioned in the corner of the room, predicted and actual sprinkler activation times were not favorable.
- Standard Response 93^{o}C gave the worst sprinkler activation comparisons.
- Generally the HRR at the time of sprinkler activation was higher for the predicted than the actual.
- TC 1 and 2 gave a higher predicted temperature than actual temperature at the time of sprinkler activation. A percentage of this may be due to the difference between the physical thermocouple and the virtual thermocouple – thermal lag.
- The selection of the c-factor value has a significant effect on the closeness of the comparison.

11 Conclusion

FDS predicted sprinkler activation times for residential and 68^{o}C standard response heads reasonably well for centrally placed fires for simulations using a c-factor of 0.65. For 96 % of the simulations, the predicted activations were within 30 % of the actual activations.

For the corner fire, the comparison is not so encouraging, 46 % of the predicted activations were within 30 % of the actual activations. For sprinkler location 2 (corner fire), 33 % of predicted activations were within 30 % of the actual activation times. For sprinkler location 1, 71 % of predicted activation times were within 30 % of actual activation times. The comparison improves if experiment 16 is omitted. If this is done, 83 % of the predicted activation times are within 30% of the actual, for sprinkler 1 and 40 % for sprinkler 2.

If it is assumed that the sprinkler activation model is reasonably accurate, and that the used sprinkler technical data is correct, and that the predicted temperatures are relatively (within 20 %) close to the actual. It could be argued that the velocity profiles in FDS deviated from the experiment, especially for sprinkler 2 when a corner fire is simulated. It is possible that as distance increases from the fire source, the gas velocity predicted by FDS decreases disproportionally (slows down to much) in comparison with the actual gas velocity.

The reason for putting this argument forward is that the sprinkler model used in FDS has three variables. If it is assumed that the sprinkler temperature is a product of the gas velocity and temperature, then just two variables. If it is assumed that the gas temperatures are reasonably close, if not higher which should be favorable to a quicker activation, then the velocity profile history must be different for the prediction.

Unfortunately due to limitations on equipment no velocity profiles were taken during the actual experiments. This is an area for further study.

Choosing the correct c-factor is essential. It has been shown that c-factor values can result in up to 50 % variance in predicting sprinkler activation times. If the sprinkler activation time is critical for the success of a fire safety strategy, then great care has to go into selecting the appropriate c-factor.

12 References

1. Buchanan, A., Fire Engineering Design Guide, Center for Advanced Engineering, New Zealand 2001.
2. Karlsson, B. and Quintiere, J., Enclosure Fire Dynamics, CRC Press, Boca Raton, Florida, 2000.
3. McGrattan, K., Baum, H., Rehm, R., Hamins, A., Forney, G., Hostikka, S., Fire Dynamics Simulator (Version 3) – Technical Reference Guide, NISTIR 6783, NIST, Gaithersburg, Maryland, USA, 2002.
4. Wade., C, BRANZFIRE Software Version 2003.1, Building Research Association of New Zealand Incorporated, Wellington, 2003.
5. CFAST Software, NIST, Building and Fire Research Laboratory Gaithersburg, Maryland 20899.
6. Petterson, N., Assessing the Feasibility of Reducing the Grid Resolution in FDS Field Modeling, Fire Engineering Research Report, University of Canterbury, New Zealand, 2002.
7. Mawhinney, N., Galea, E.R., Hoffman, N. and Patel, M.K., A critical Comparison of a Phonetics Based Fire Field Model with Experimental Compartment Fire Data, Journal of Fire Protection Engineering, 6, 137 –152, 1994.
8. McGrattan, K., Forney, G., Hostikka, S., Kuldeep, P., Fire Dynamics Simulator (Version 3) – User's Guide, NISTIR 6784, NIST, Gaithersburg, Maryland, USA, 2002.
9. Nelson, H., Phlogiston to Computational Fluid Dynamics, Society of Fire Protection Engineering Magazine, Winter 2002, pp 9 – 17.
10. Bilger, R., Computational Field Model in Fire Research and Engineering, Procedures Forth Internal Symposium, Fire Safety Science, pp 95 – 110, June 1994.
11. Sutula, J., Fire Dynamic Simulator in Fire Protection Engineering Consulting, Society of Fire Protection Engineering Magazine, Spring 2002, pp 33 – 44.
12. Bounagui, A., Benichou, N., Literature Review on the Modeling of Fire Growth and Smoke Movement, National Research Council, Canada, 2003.

13. Fire Safety Engineering Group, School of Computing and Mathematical Science, University of Greenwich, www.fseg.gre.ac.uk
14. Cox, P., 'Basic Considerations', Combustion Fundamentals of Fire, Ed.G.Cox, Academic Press, London, 1995.
15. Steckler, K., Quintiere, G., Rinkinen, J., Flow Induced by Fire in a Compartment. NBSIR 82 –2520, National Bureau of Standards, Washington, 1982.
16. Kerrison, L., Mawhinney, N., Galea, E.R., Hoffman, N., Patel, K., A Comparison of a FLOW 3D Based Fire Field Model with Experimental Room Fire Data, Fire Safety Journal, 23, 387-411, 1994.
17. Nielsen, C., An Analysis of Pre-Flashover Fire Experiments with Field Modeling Comparisons, Fire Engineering Report, University of Canterbury , New Zealand, 2000.
18. ISO 9705 International Standard, "Fire Tests – Full Scale Room Test for Surface Products" First Edition Ref Number ISO/TC92/WG7/NI24, 1993-05-15.
19. Friday, P., Mowrer, F., Comparison of FDS Model Predictions with FM/SNL Fire Test Data, NIST, Gaithersburg, USA, 2001.
20. Olenick, S., Klassen, M., Roby, R., Validation Study of FDS for a High-Rack Storage Fire Involving Pool Chemicals, Society of Fire Protection Engineers Final Proceedings 3rd Technical Symposium on Computer Applications in Fire Protection Engineering, pp53-63, 2001.
21. Wood, J., Tubbs, J., Comparing Fire Dynamics Simulator with Compartment Fire Test Data, Society of Fire Protection Engineers Final Proceedings 3rd Technical Symposium on Computer Applications in Fire Protection Engineering, pp77-88, 2001.
22. Vettori, R., NISTIR 6253, Effect of an Obstructed Ceiling on the Activation Time of a Residential Sprinkler, National Institute of Standards and Technology, Gaithersburg, MD, November 1998.
23. UL1626, Standard for Safety for Residential Sprinklers for Fire-Protection Service.
24. Electronic Temperature Instruments Ltd, United Kingdom
25. Pico Technology Limited, The Mills House, Cambridge St, St Neots, Cambridgeshire, United Kingdom.

26. Mettler Toledo, Spider Indicator, Technical Manual.
27. New Zealand Standards 4515 Fire Sprinkler Systems for Residential Occupancies, Standards New Zealand.
28. New Zealand Standards 4517 Fire Sprinkler Systems for Houses, Standards New Zealand.
29. New Zealand Standards 4541:2003 Automatic Fire Sprinkler Systems, Standards New Zealand.
30. Gem Sprinkler Product Catalogue, 1997, Gem Sprinkler Company, www.gemsprinkler.com.
31. NFPA 13D Standard for the installation of sprinkler systems in one and two family dwellings and manufactured homes, NFPA, 1 Batterymach Park, Quincy, Massachusetts, USA.
32. NFPA 13R Standard for the installation of sprinkler systems in residential occupancies up to and including four stories in height, NFPA, 1 Batterymach Park, Quincy, Massachusetts, USA.
33. NFPA 13 Standard for the installation of sprinkler systems, NFPA, 1 Batterymach Park, Quincy, Massachusetts, USA.
34. Technical Data Sheet for LFII Residential Pendent Sprinklers, www.tyco.com.
35. Technical Data Sheet for Standard Response, Standard Cover Pendent Sprinklers, www.tyco.com.
36. Puchovsky, M., Section 10.11 Automatic Sprinkler Systems, Fire Protection Handbook, NFPA, 19th Ed, 2003.
37. Flemming, R.., Chapter 4-3, Automatic Sprinkler Systems Calculations, The SFPE Handbook of Fire Protection Engineering,3rd, NFPA, Qunicy, Massachusetts, USA, 2002.
38. Nash, P., Young, R., Automatic Sprinkler Systems for Fire Protection 3rd Ed, Paramount Publishing Limited, England, 1991.
39. Approval Standard for Automatic Sprinklers for Fire Protection, Class Series 2000, Factory Mutual Global Technology, 2002.
40. Fleming, R., Principles of Automatic Sprinkler System Performance, Chapter 9, Section 10, Fire Protection Handbook, NFPA, 19th Ed, 2003.
41. Chin, K., Development of Bench-Scale of Sprinkler and Smoke Detector Activation/Response Time, Fire Engineering Research Report, University of Canterbury, New Zealand, 2002.

42. Heskestad, G., Hill, R., Quantification of Thermal Responsiveness of Automatic Sprinklers Including Conduction Effects, Fire Safety Journal, pp 113 –125, 1988.
43. Isman, K., Automatic Sprinkler, Chapter 10, Section 10, Fire Protection Handbook, NFPA, 19th Ed, 2003.
44. Babrauskas, V., Chapter 3-3, The Cone Calorimeter, The SFPE Handbook of Fire Protection Engineering,3rd, NFPA, Qunicy, Massachusetts, USA, 2002.
45. Hume, B., Water Mist Suppression in Conjunction with Displacement Ventilation, Fire Engineering Research Report, University of Canterbury, New Zealand 2003.
46. Patankar, S., Numerical Heat Transfer and Fluid Flow, Hemisphere Publishing, New York, USA, 1980.
47. Hinze, J., Turbulence, 2nd Ed, McGraw-Hill, New York.
48. Floyd, J., Baulm, H., McGratten, A mixture fraction combustion model for fire simulation using CFD, The International Conference on Engineered Fire Protection Design, pp279 – 290, 2001.
49. DiMarzo, M., The Effect of Minute Water Droplets on a Simulated Sprinkler Link Thermal Response, Technical Paper, University of Maryland.
50. Forney,G., McGratten, K.,User's Guide for Smokeview Version 3.1 – A Tool for Visualizing Fire Dynamics Simulation Data, NISTIR 6980, NIST, Gaithersburg, Maryland, USA.
51. www.fireforum.ac.ca, Fire Dynamics Simulator forum group, correspondence by Dave McGill.
52. www.Skutt.com, Skutt Ceramic Product, How To Evaluate Thermocouples.
53. Bolles W L, Measurement of Gas Temperatures by means of Thermocouples. Petroleum Refiner, Vol 27, No. 2, Feb 1948.
54. Holman, J., Experimental Methods for Engineers, McGraw-Hill, USA, 1978.

Appendices

Appendix A
Experimental Results

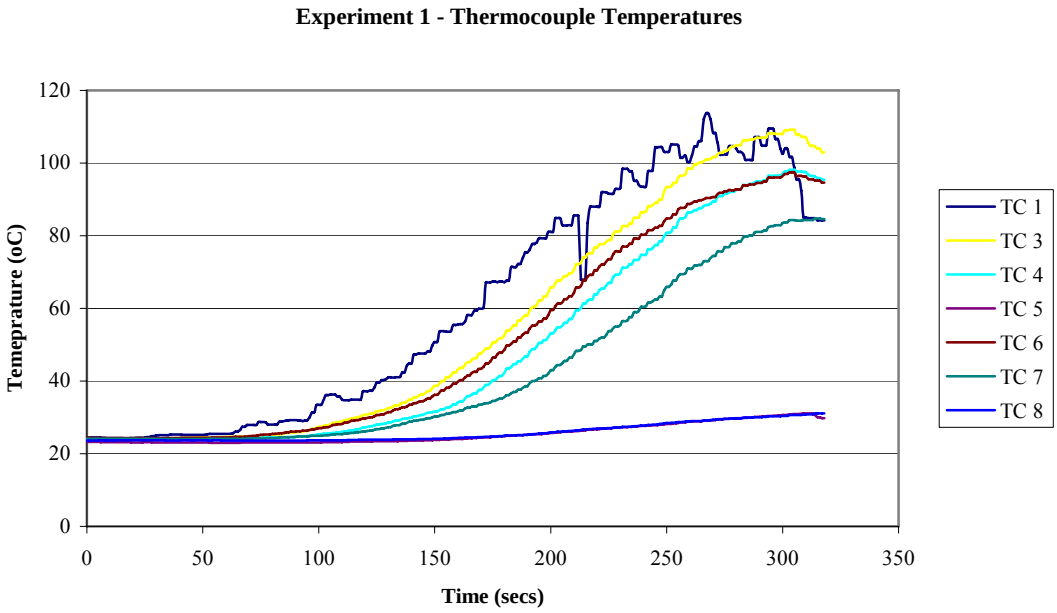
Experiment 1 - Thermocouple Temperatures
Temeprature (oC)
120
100
80
60
40
20
0
0
50
100
150
200
250
300
350
Time (secs)
TC 1
TC 3
TC 4
TC 5
TC 6
TC 7
TC 8

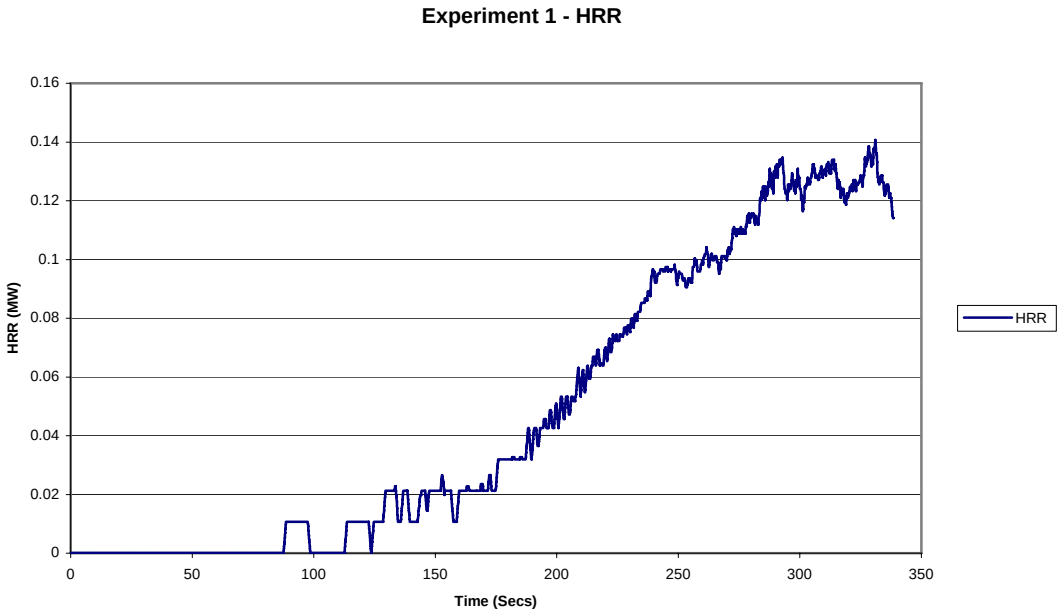
Experiment 1 - HRR
HRR (MW)
0.16
0.14
0.12
0.1
0.08
0.06
0.04
0.02
0
0
50
100
150
200
250
300
350
Time (Secs)
HRR

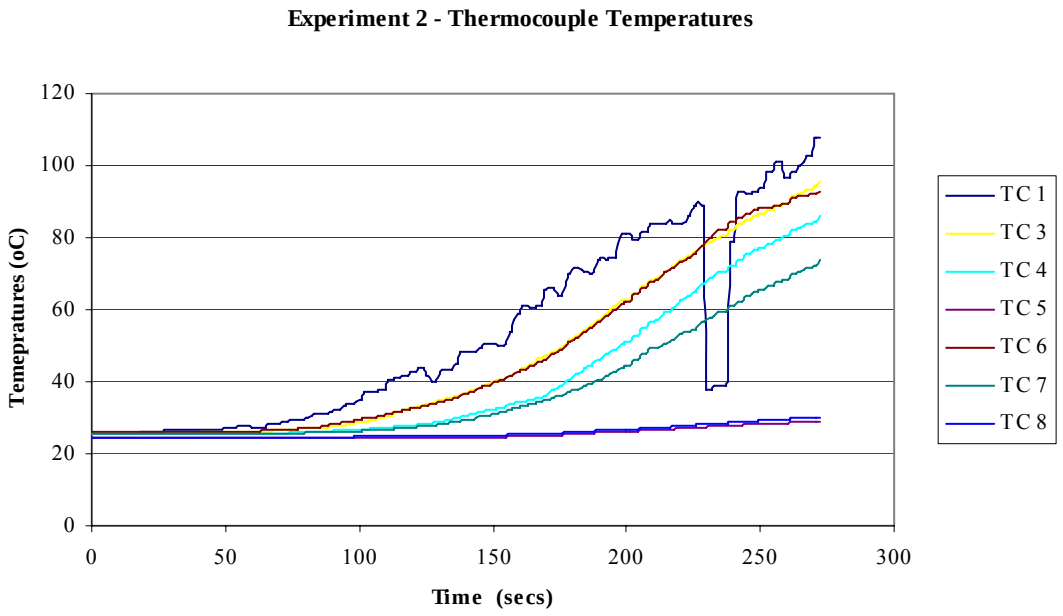
Experiment 2 - Thermocouple Temperatures
Temepratures (oC)
120
100
80
60
40
20
0
0
50
100
150
200
250
300
Time (secs)
TC 1
TC 3
TC 4
TC 5
TC 6
TC 7
TC 8

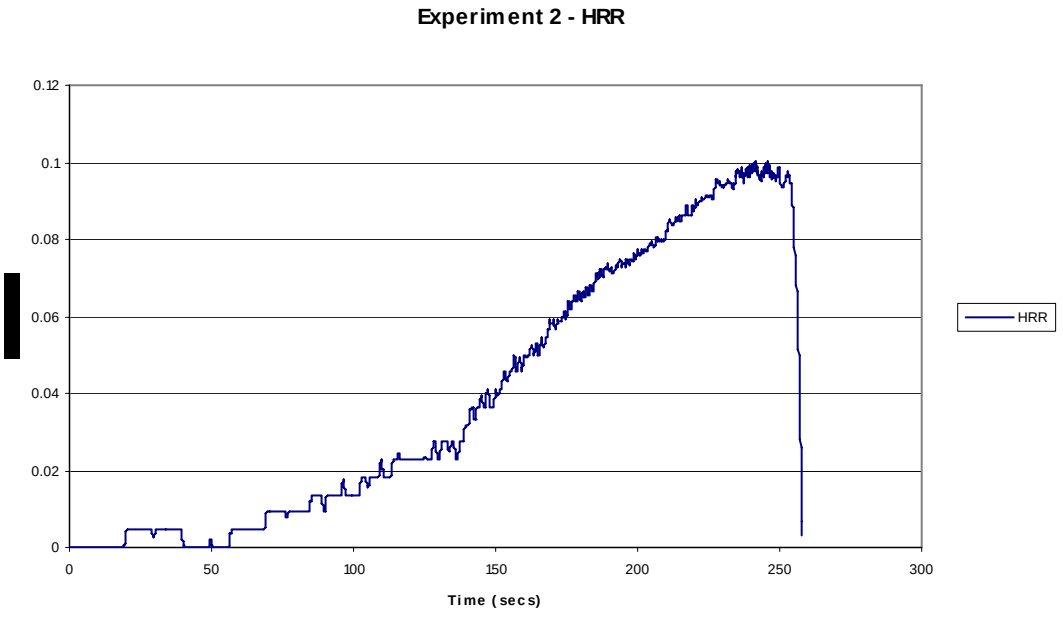
Experiment 2 - HRR
0.12
0.1
0.08
0.06
0.04
0.02
0
0
50
100
150
200
250
300
Time (secs)
HRR

Experiment 3 - Thermocouple Temperatures

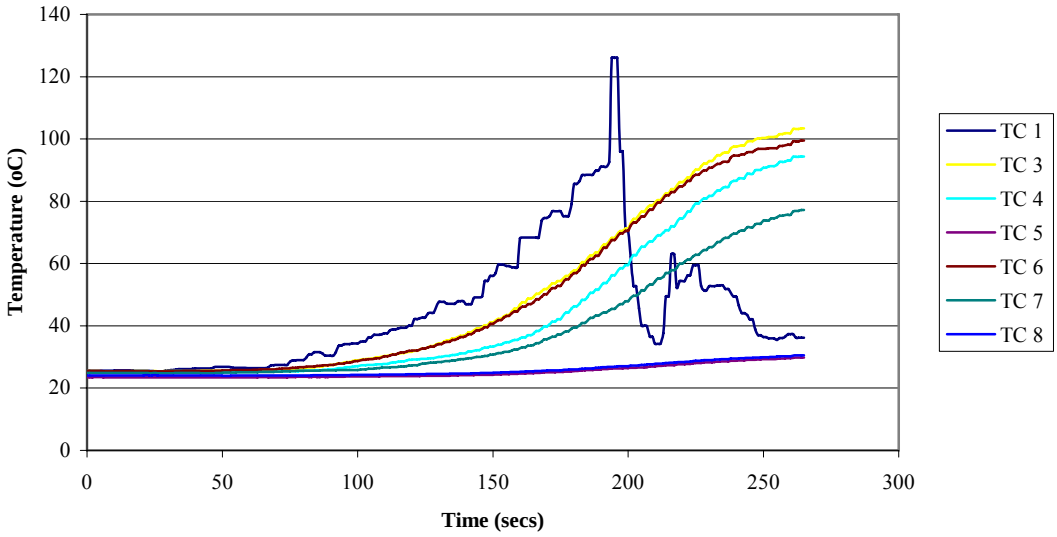

Experiment 3 - HRR

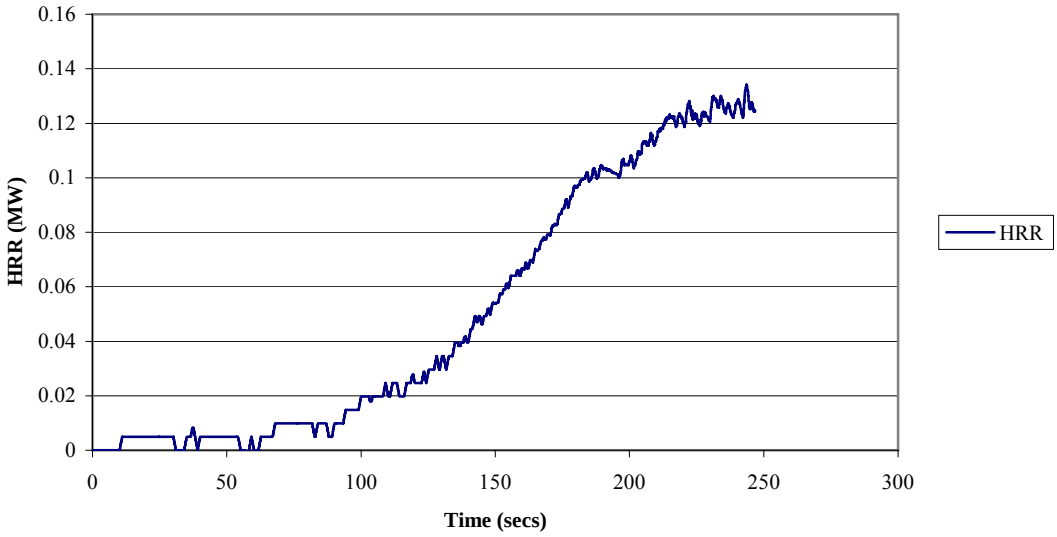

Experiment 4 : Thermocouple Temperatures

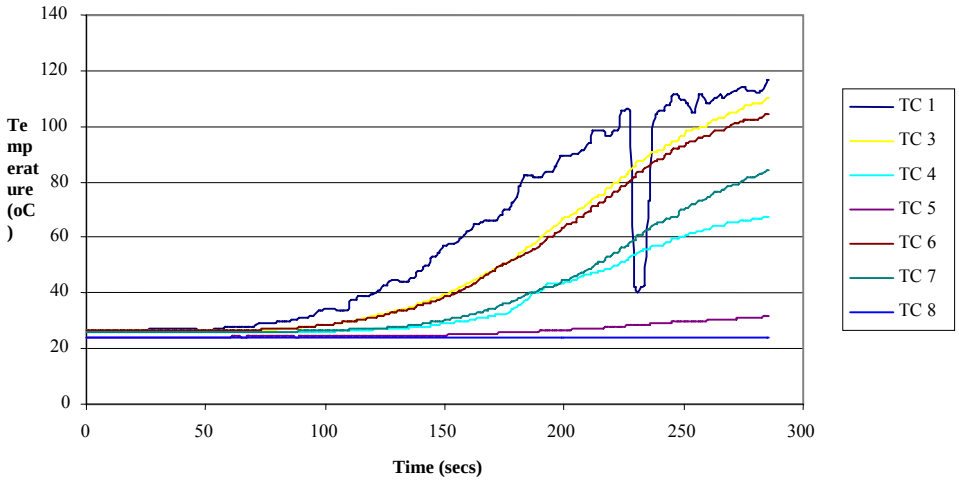

Experiment 4 - HRR

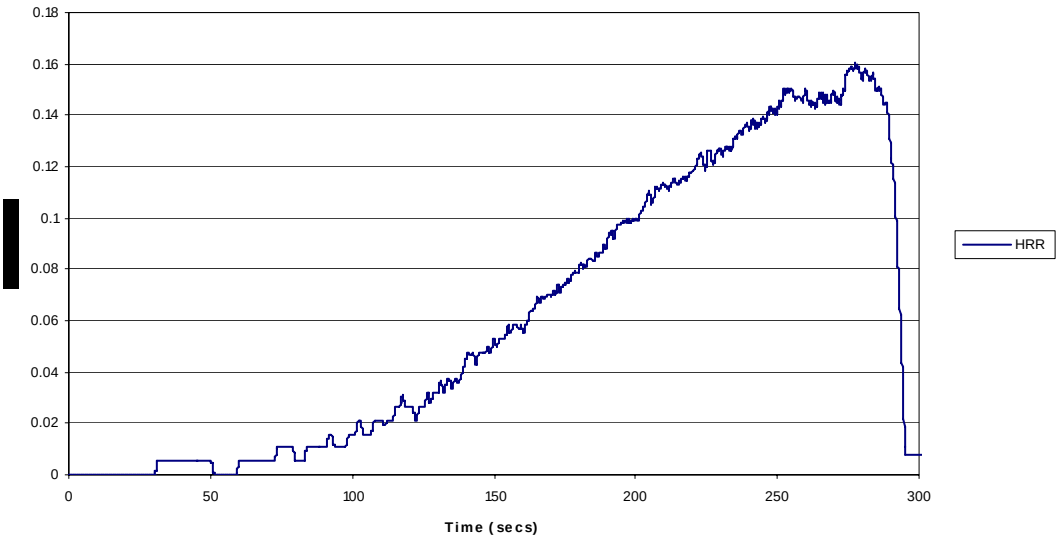

Experiment 5 - Thermocouple Temperatures

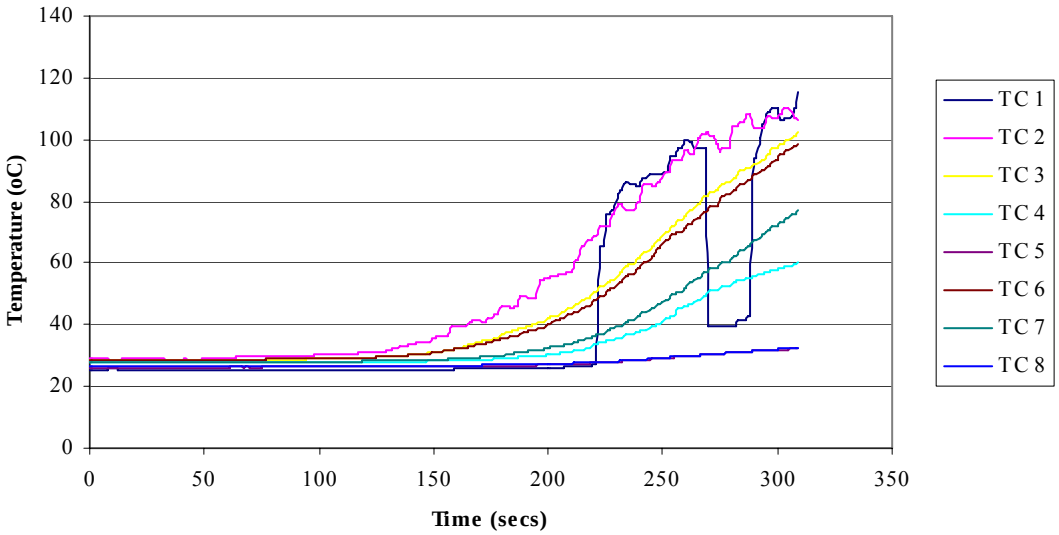

Experiment 5 - HRR

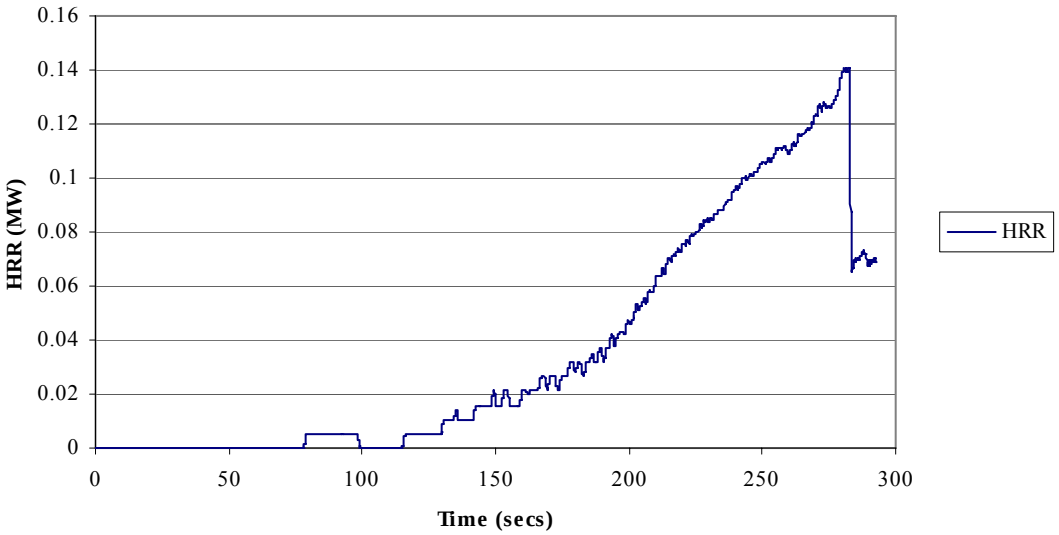

Experiment 6 - Thermocouple Temperatures

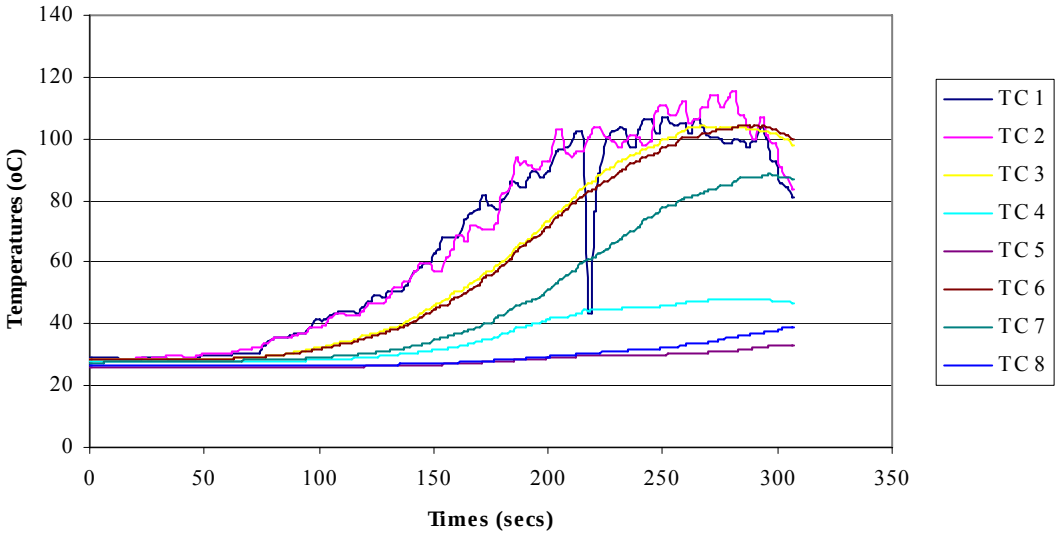

Experiment 6 - HRR

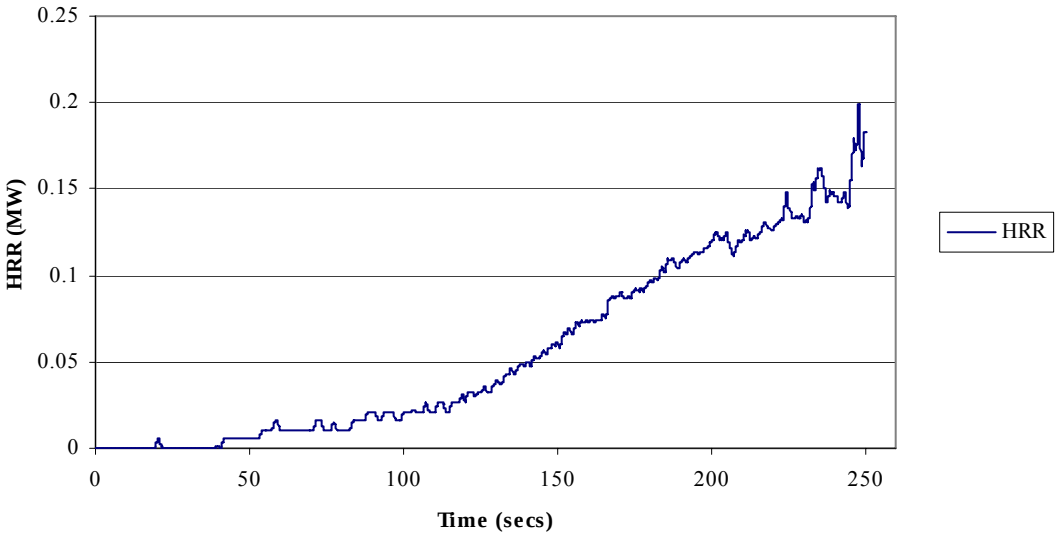

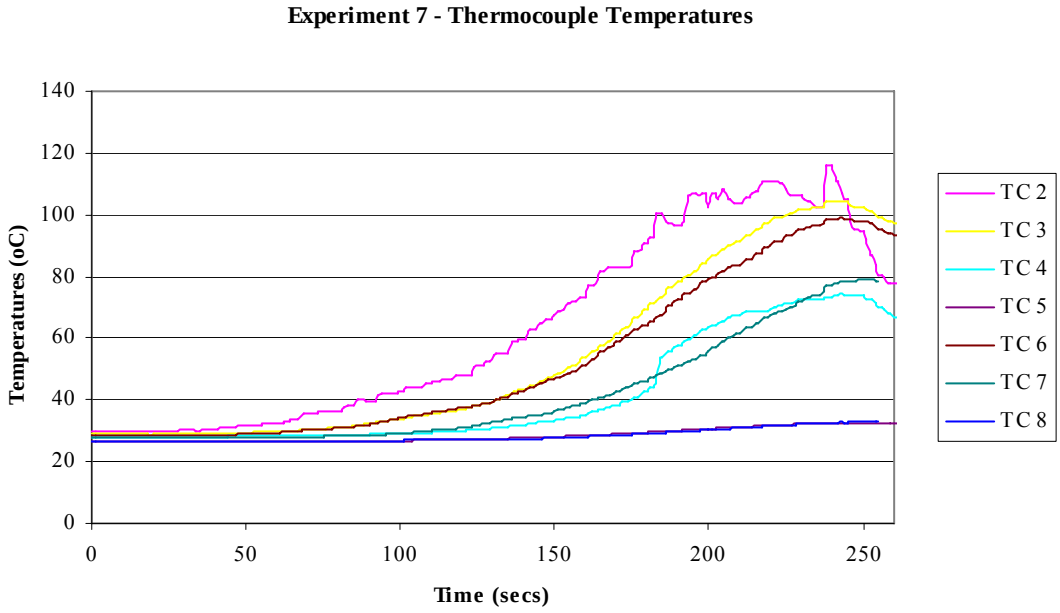
Experiment 7 - Thermocouple Temperatures
Temperatures (oC)
140
120
100
80
60
40
20
0
0
50
100
150
200
250
Time (secs)
TC 2
TC 3
TC 4
TC 5
TC 6
TC 7
TC 8

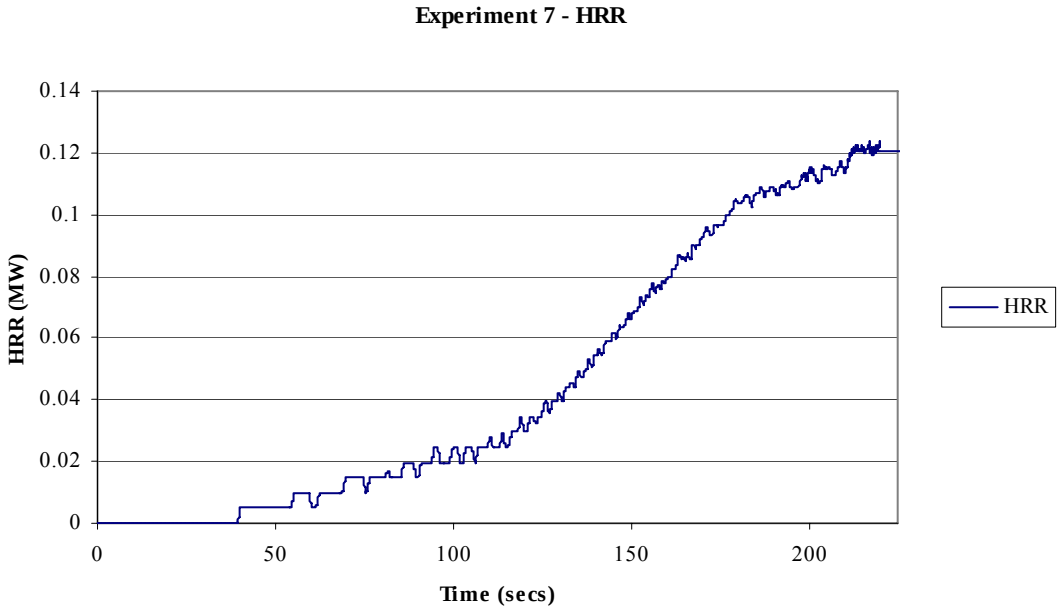
Experiment 7 - HRR
HRR (MW)
0.14
0.12
0.1
0.08
0.06
0.04
0.02
0
0
50
100
150
200
Time (secs)
HRR

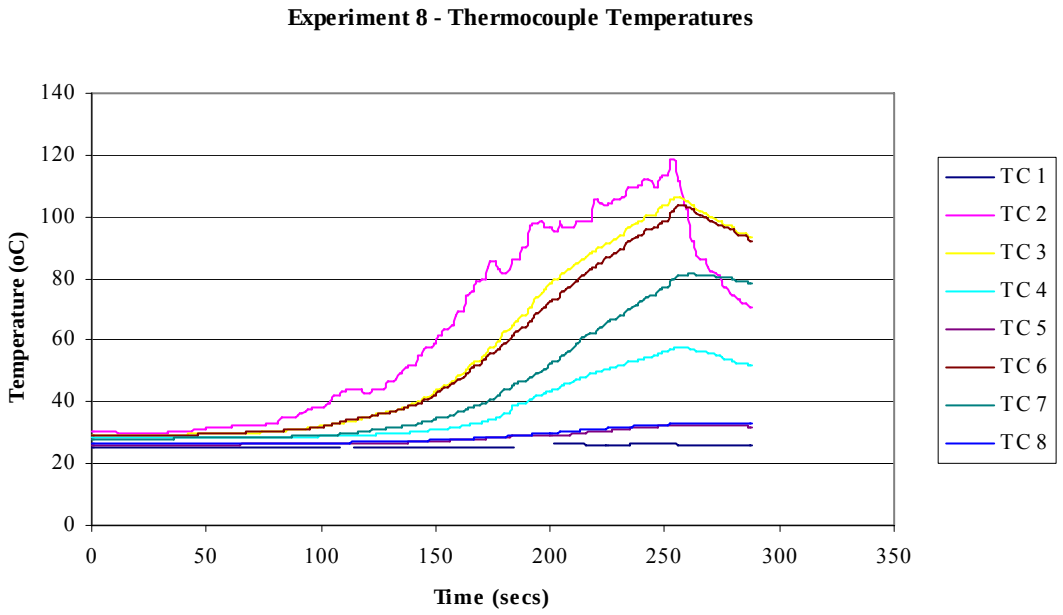
Experiment 8 - Thermocouple Temperatures
Temperature (oC)
140
120
100
80
60
40
20
0
0
50
100
150
200
250
300
350
Time (secs)
TC 1
TC 2
TC 3
TC 4
TC 5
TC 6
TC 7
TC 8

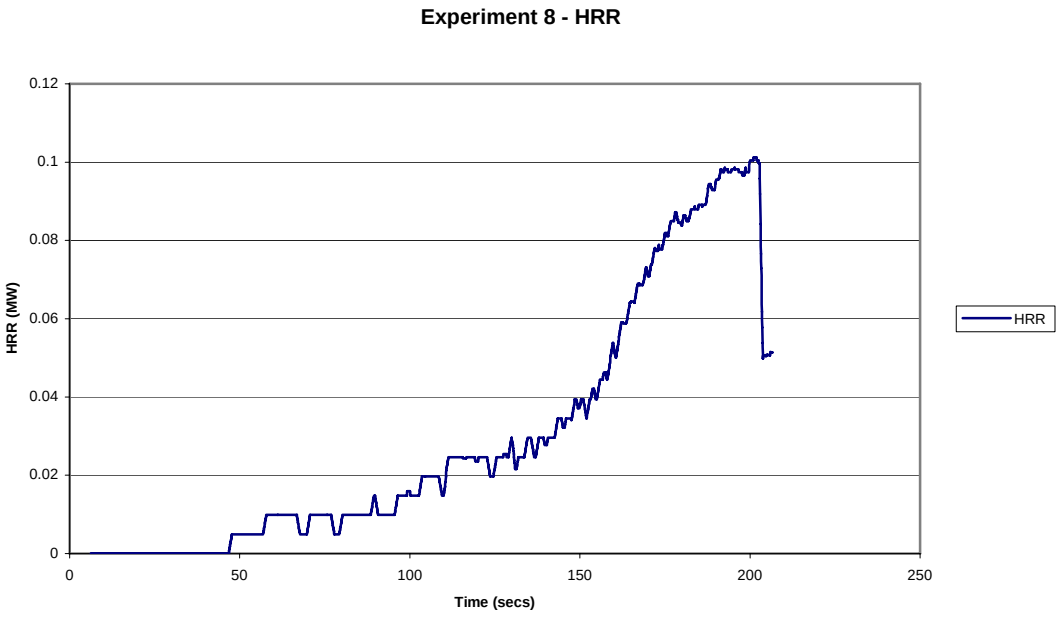
Experiment 8 - HRR
HRR (MW)
0.12
0.1
0.08
0.06
0.04
0.02
0
0
50
100
150
200
250
Time (secs)
HRR

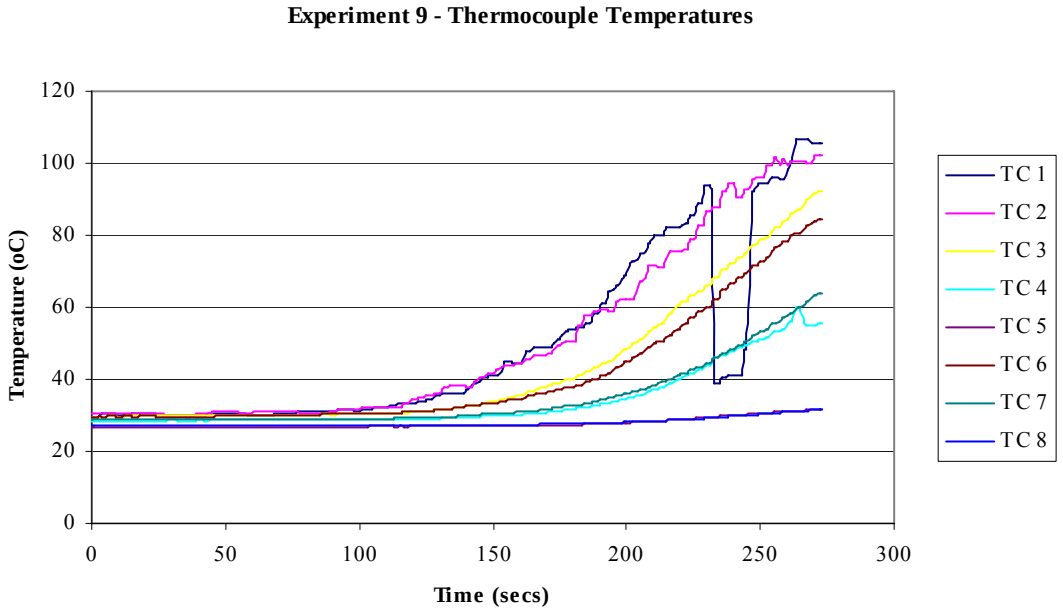
Experiment 9 - Thermocouple Temperatures
Temperature (oC)
120
100
80
60
40
20
0
0
50
100
150
200
250
300
Time (secs)
TC 1
TC 2
TC 3
TC 4
TC 5
TC 6
TC 7
TC 8

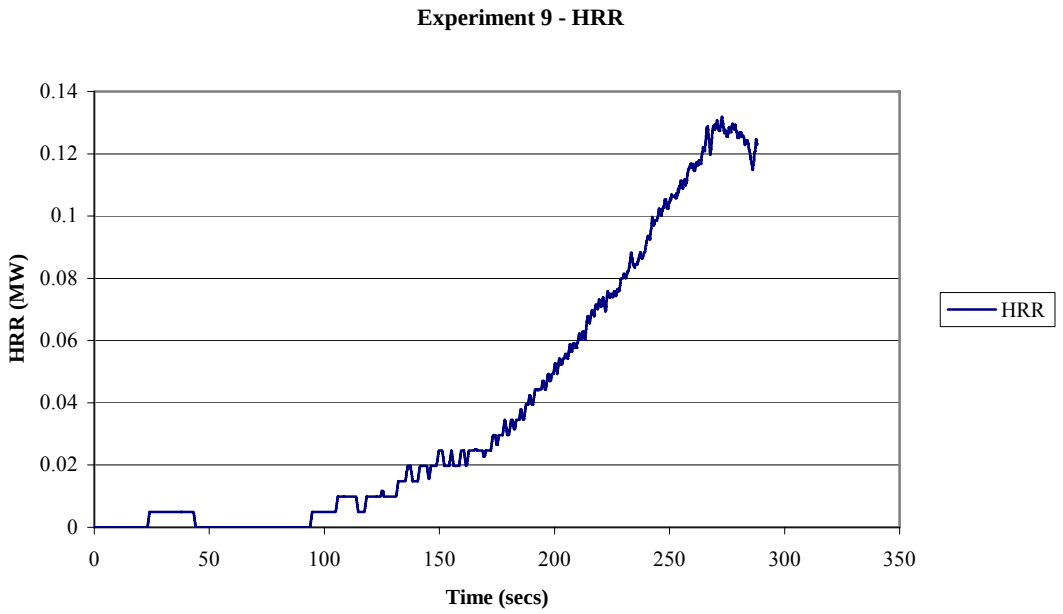
Experiment 9 - HRR
HRR (MW)
0.14
0.12
0.1
0.08
0.06
0.04
0.02
0
0
50
100
150
200
250
300
350
Time (secs)
HRR

Experiment 10 - Thermocouple Temperatures

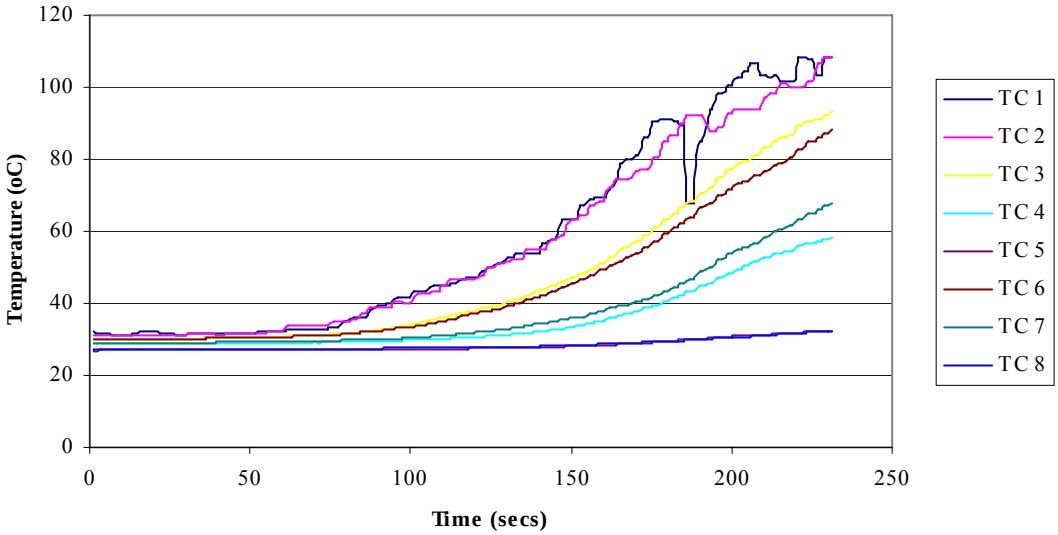

Experiment 10 - HRR

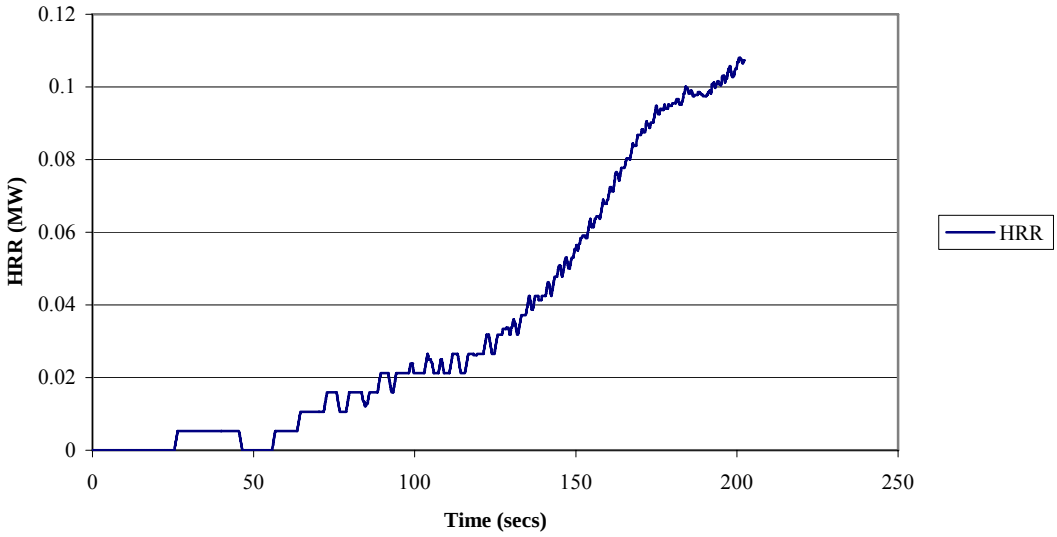

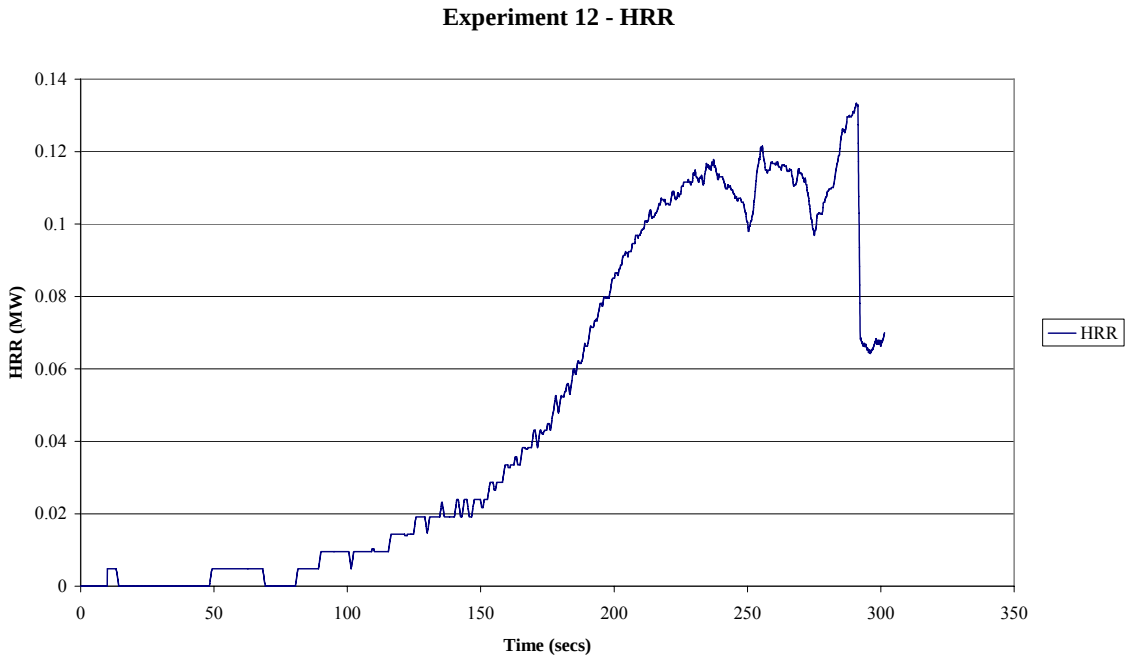
Experiment 12 - HRR
HRR (MW)
0.14
0.12
0.1
0.08
0.06
0.04
0.02
0
0
50
100
150
200
250
300
350
Time (secs)
HRR

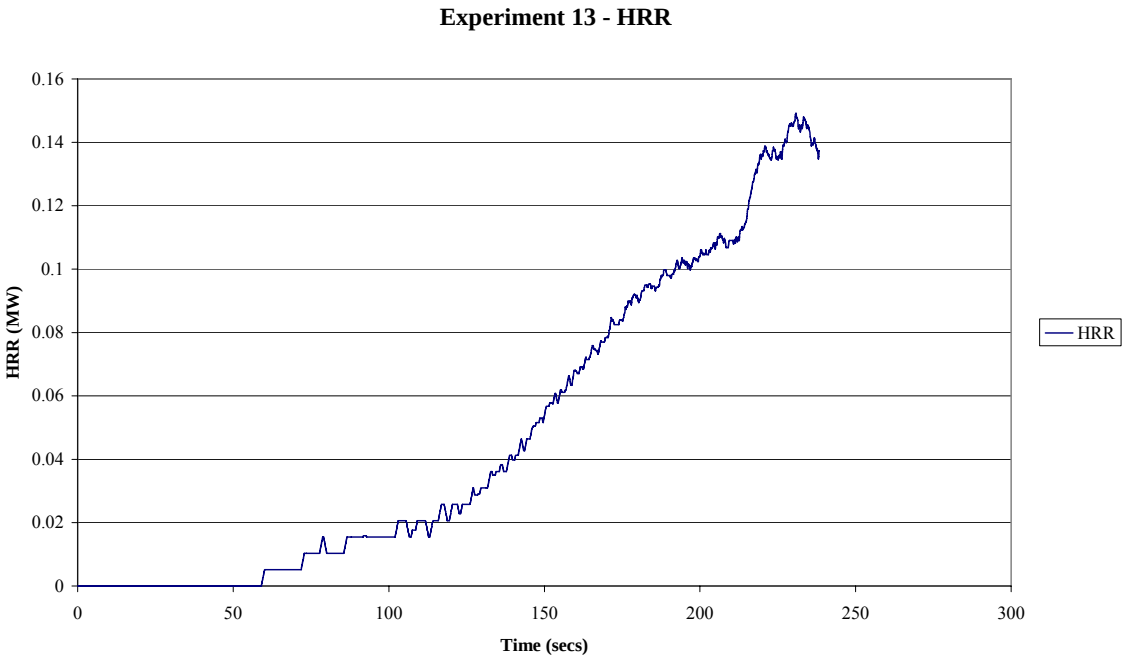
Experiment 13 - HRR
HRR (MW)
0.16
0.14
0.12
0.1
0.08
0.06
0.04
0.02
0
0
50
100
150
200
250
300
Time (secs)
HRR

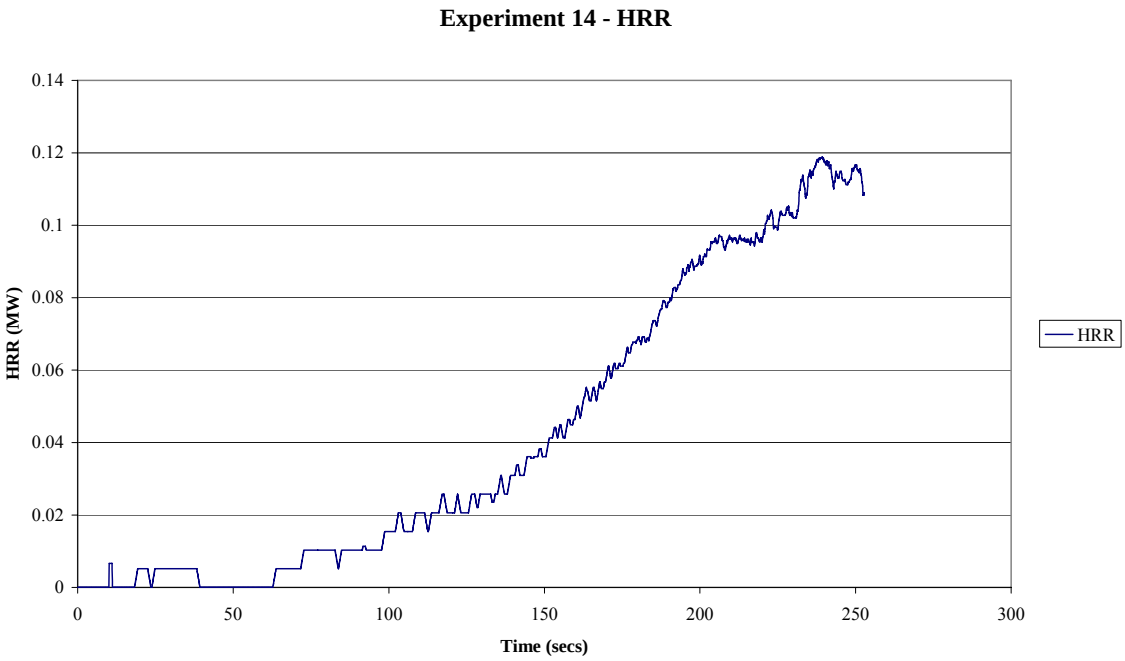
Experiment 14 - HRR
HRR (MW)
0.14
0.12
0.1
0.08
0.06
0.04
0.02
0
0
50
100
150
200
250
300
Time (secs)
HRR

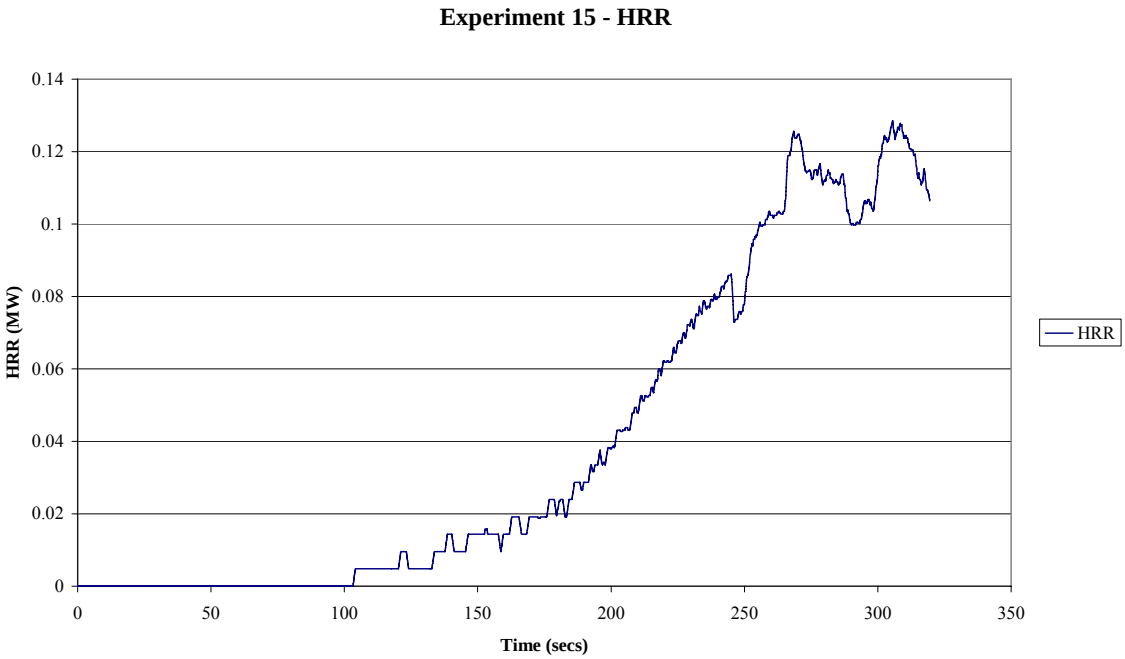
Experiment 15 - HRR
HRR (MW)
0.14
0.12
0.1
0.08
0.06
0.04
0.02
0
0
50
100
150
200
250
300
350
Time (secs)
HRR

Experiment 16 - Thermocouple Temperatures

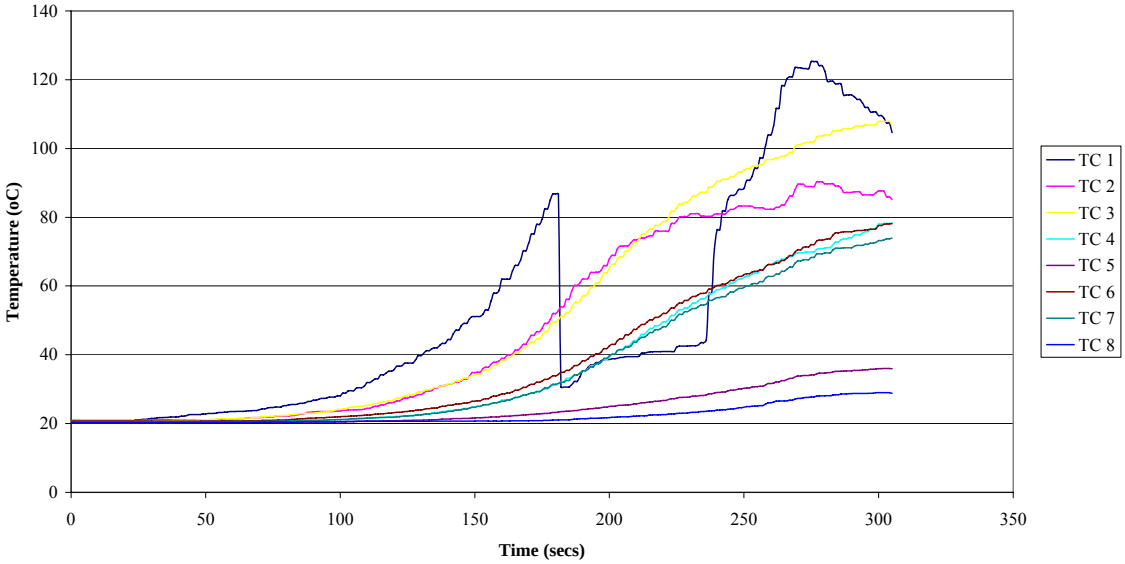

Experiment 16 - HRR

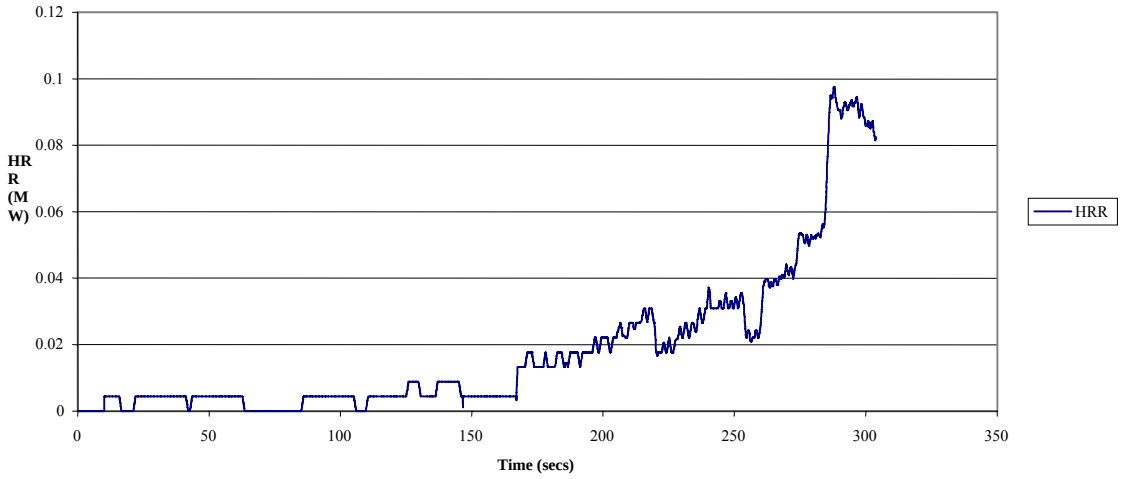

Experiment 17 - Thermocouple Temperatures

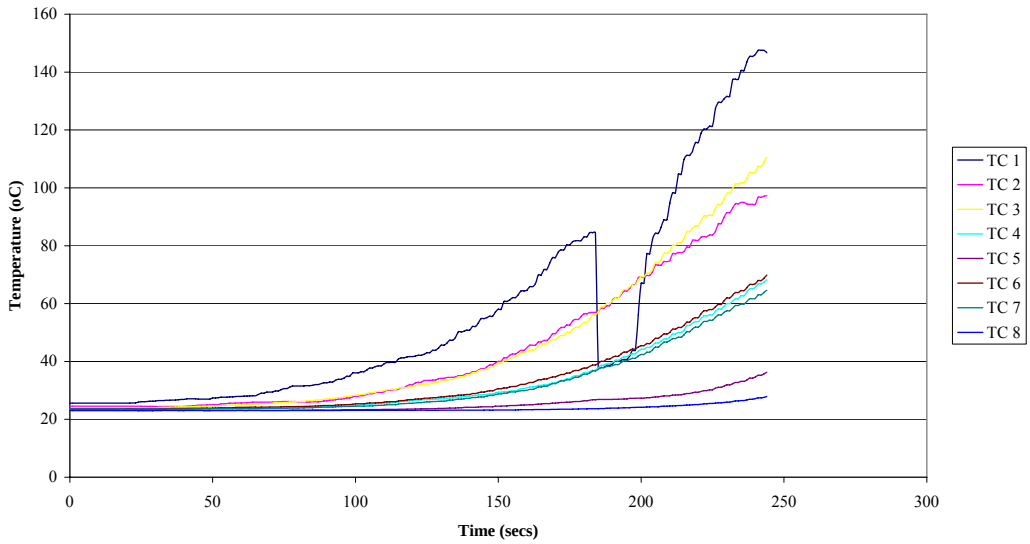

Experiment 17 - HRR

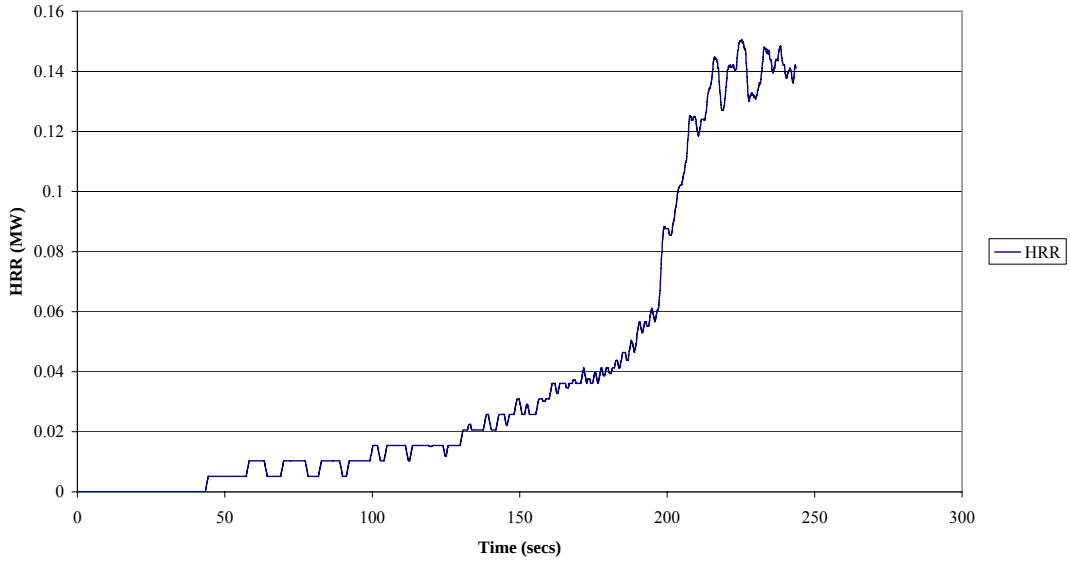

Experiment 18 - Thermocouple Temperatures

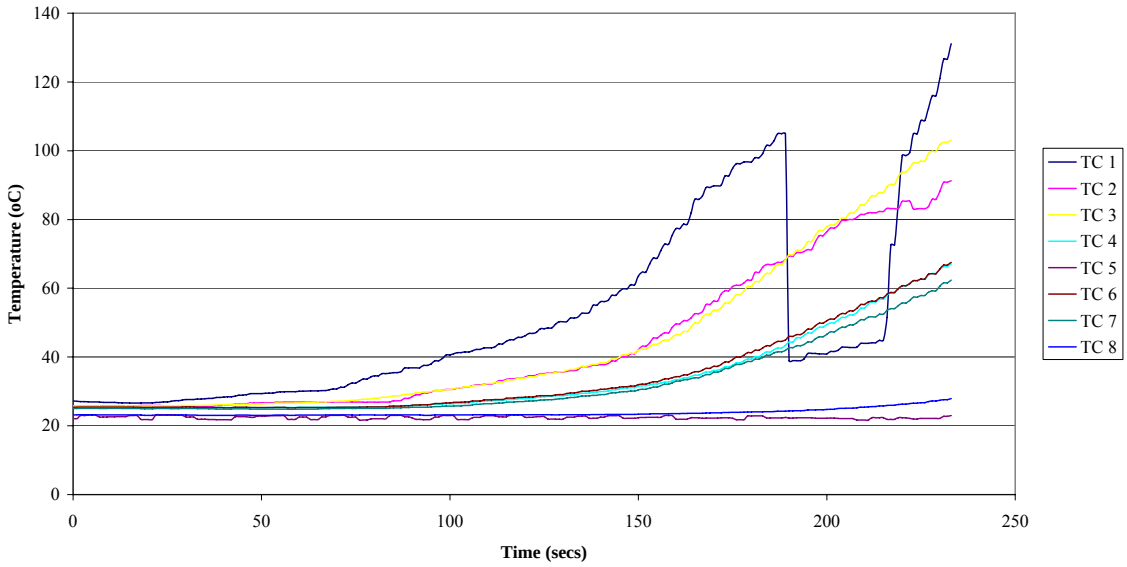

Experiment 18 - HRR

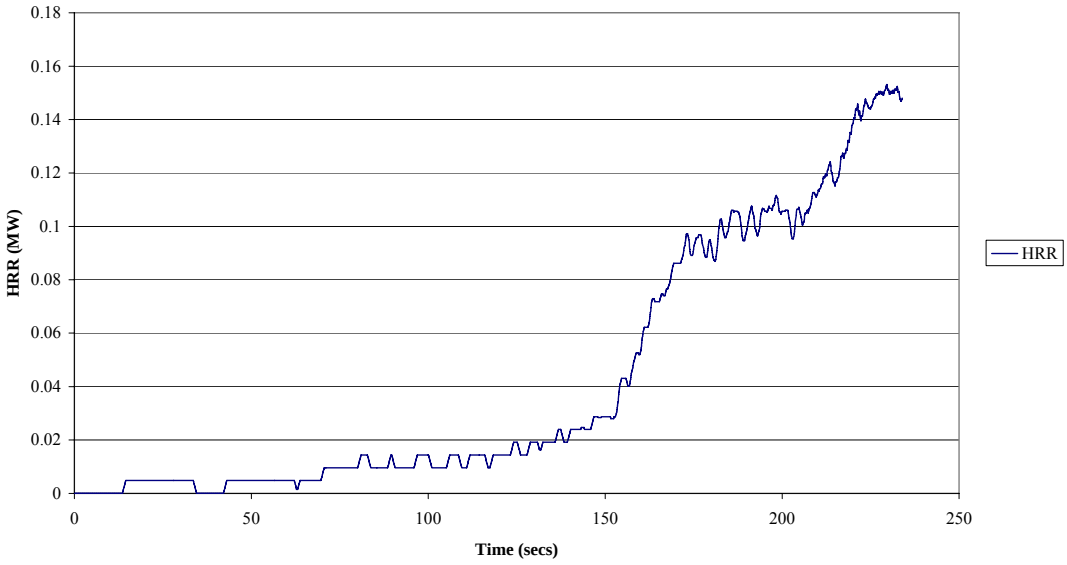

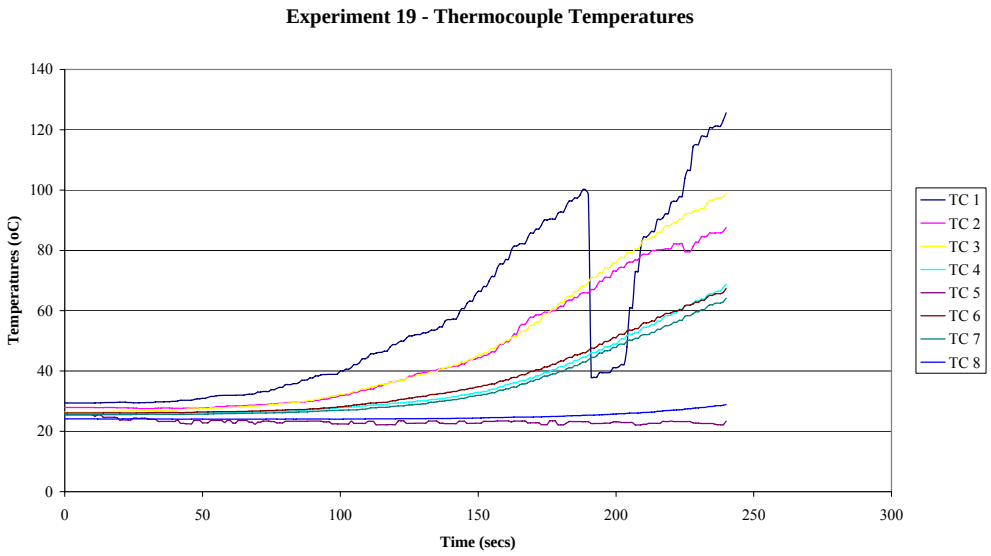
Experiment 19 - Thermocouple Temperatures
Temperatures (oC)
Time (secs)
0
20
40
60
80
100
120
140
0
50
100
150
200
250
300
TC 1
TC 2
TC 3
TC 4
TC 5
TC 6
TC 7
TC 8

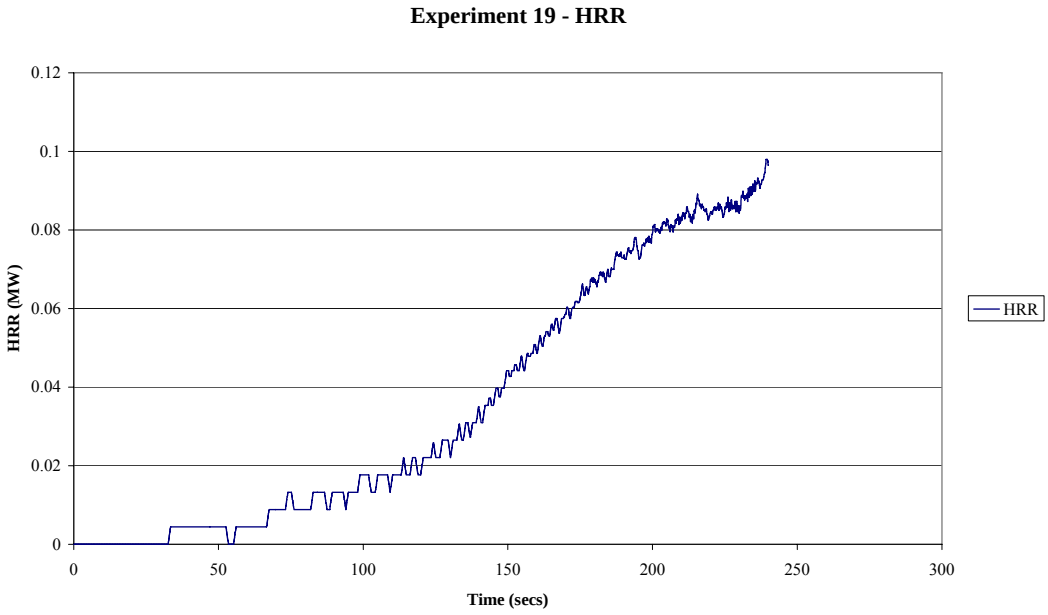
Experiment 19 - HRR
HRR (MW)
Time (secs)
0
0.02
0.04
0.06
0.08
0.1
0.12
0
50
100
150
200
250
300
HRR

Experiment 20 - Thermocouple Temperatures

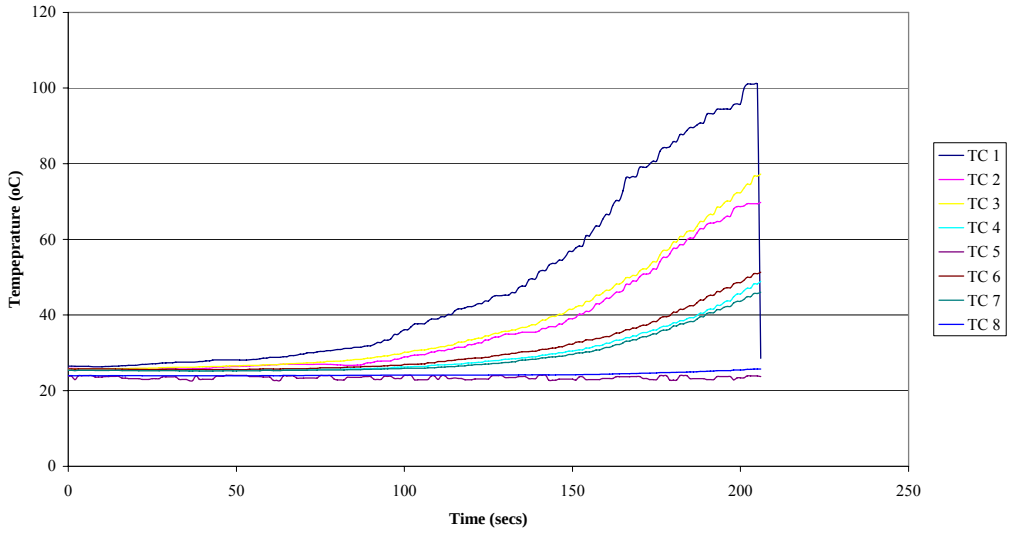

Experiment 20 - HRR

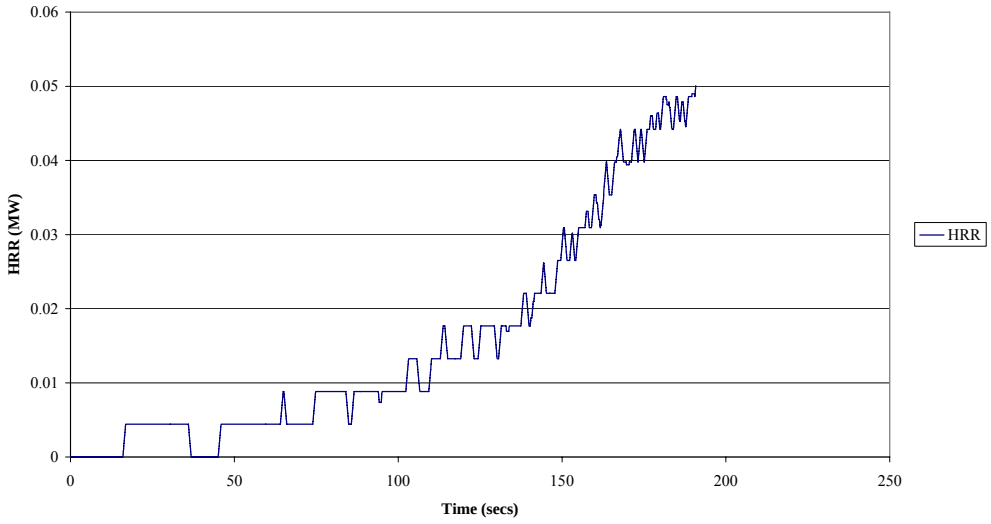

Experiment 21 - Thermocouple Temperatures

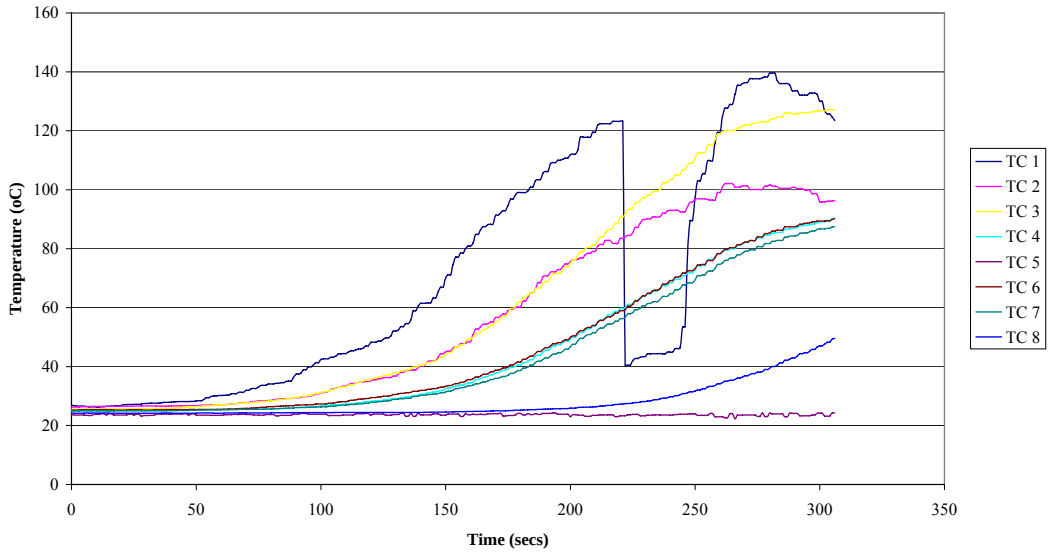

Experiment 21 - HRR

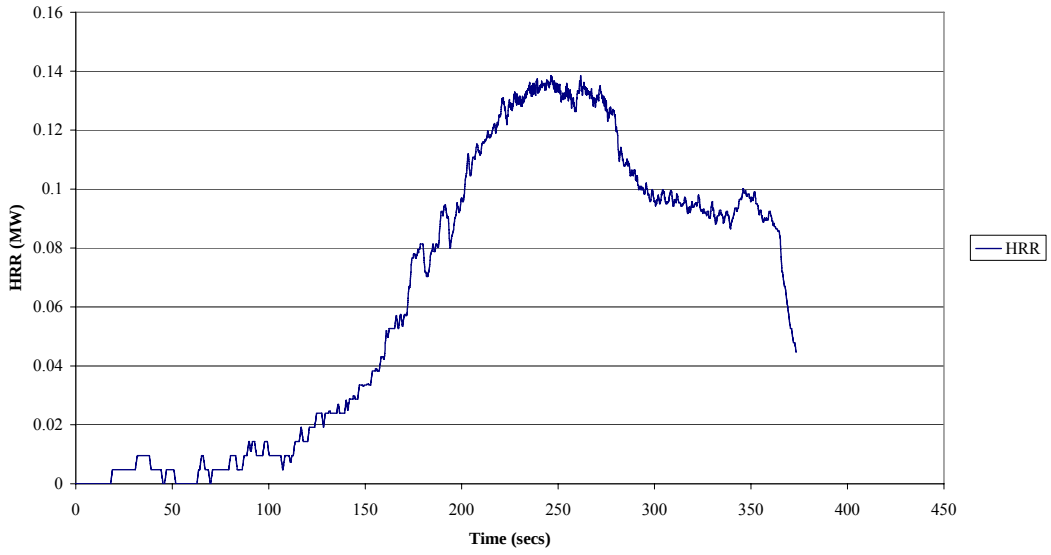

Experiment 22 - Thermocouple Temepratures

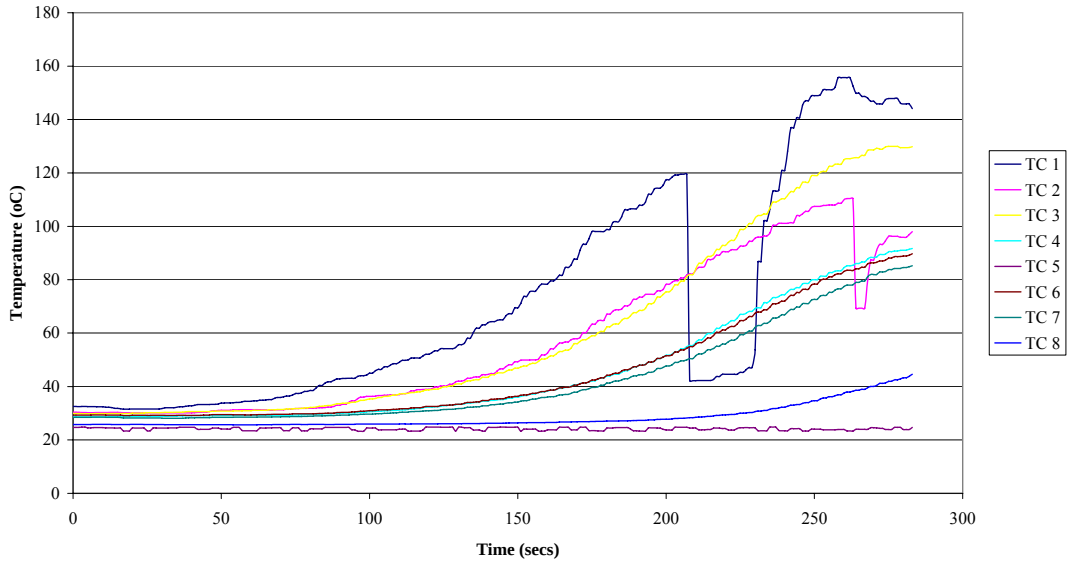

Experiment 22 - HRR

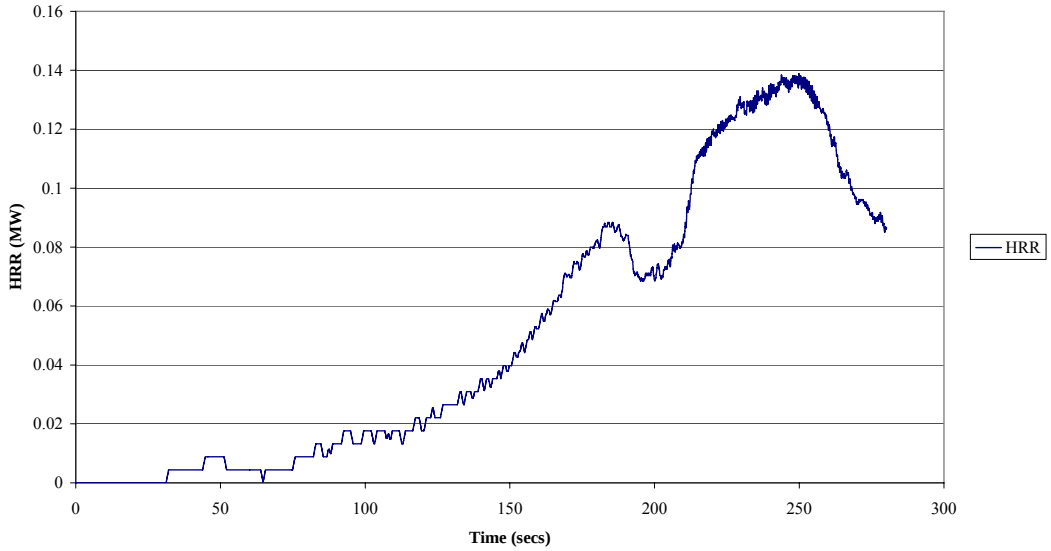

Appendix B

FDS Results

Experiment 1

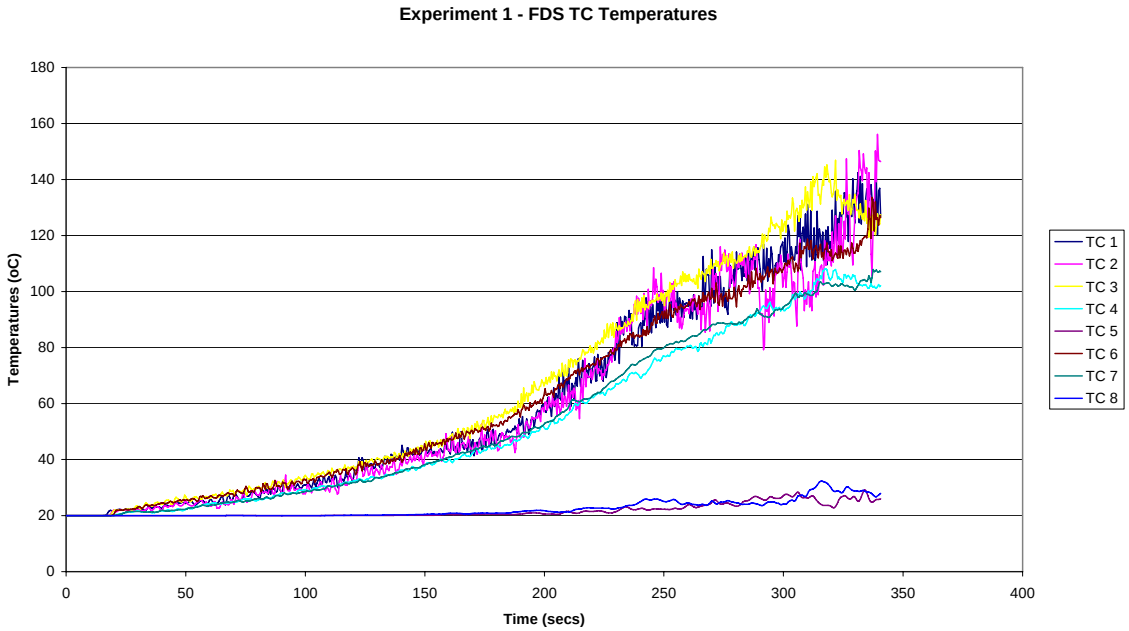

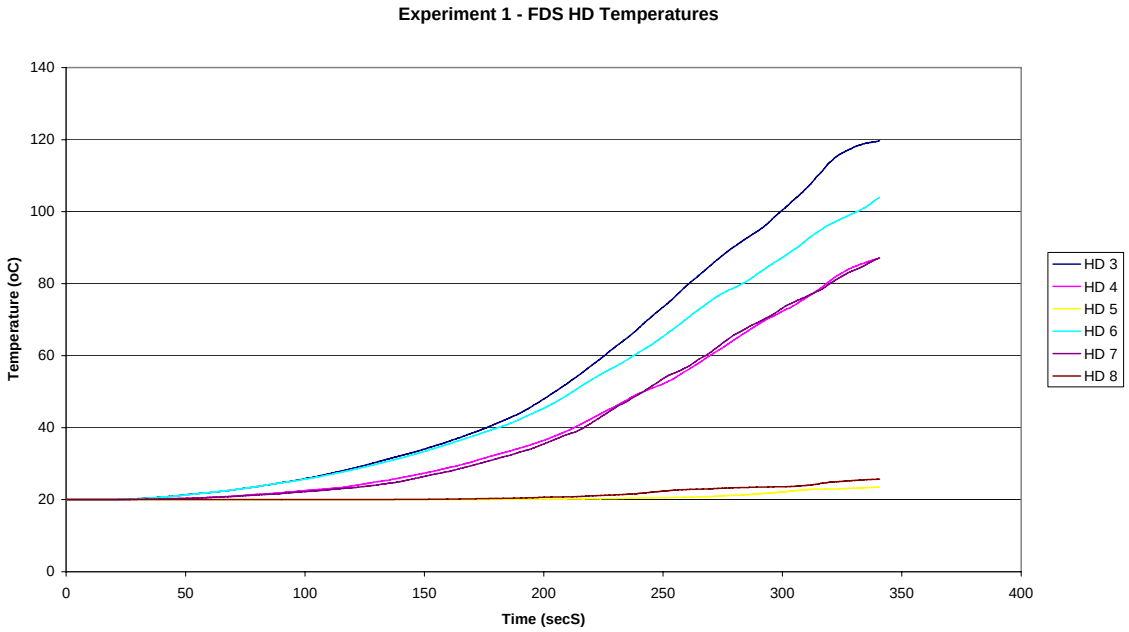

Experiment 1 - FDS HRR

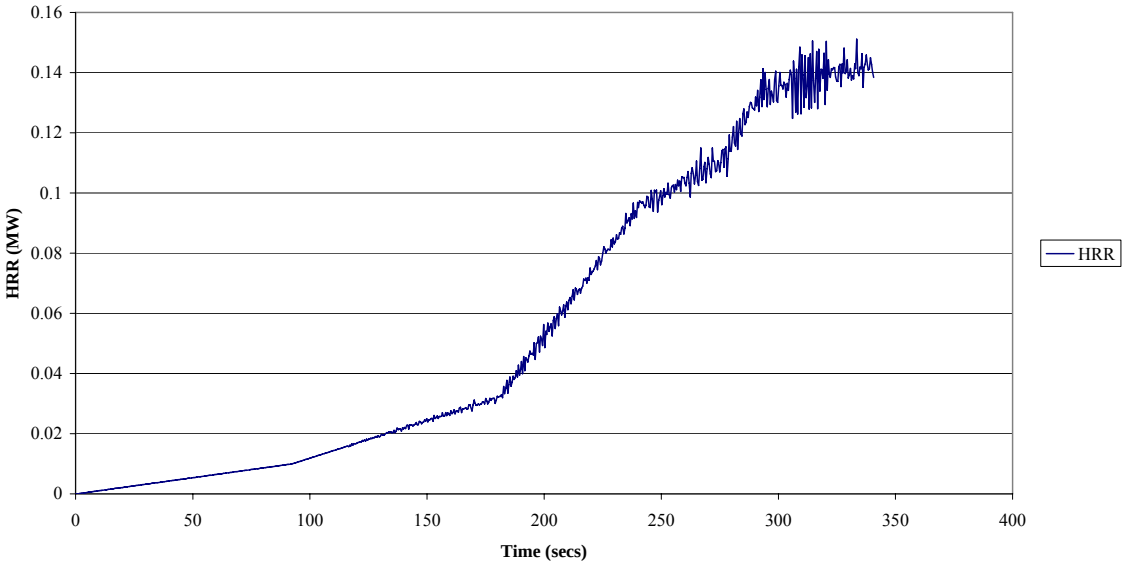

Experiment 1 - FDS Sprinkler Activation Times

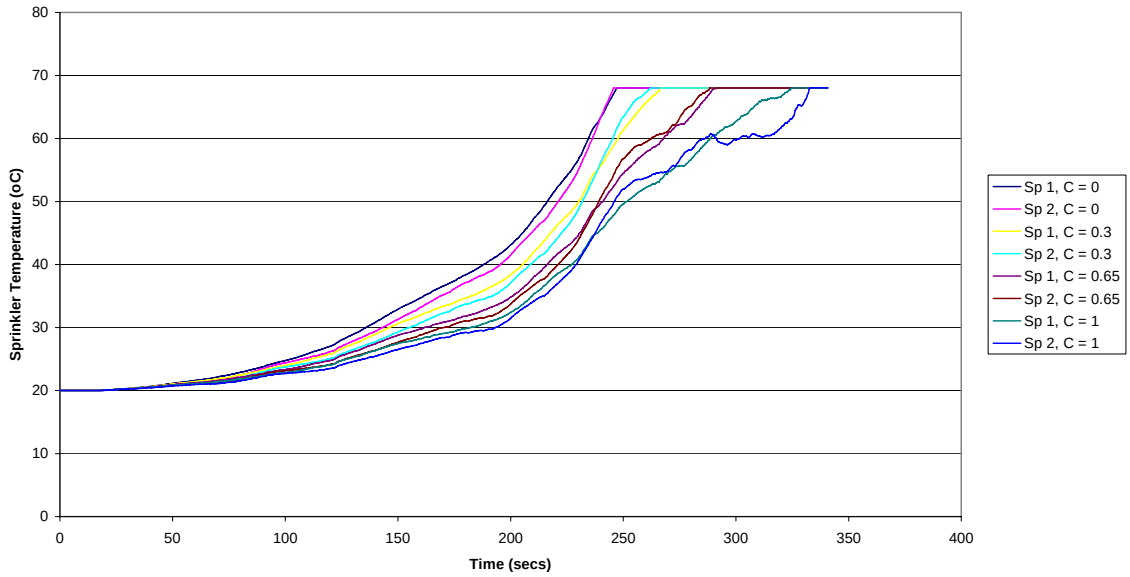

Experiment 2

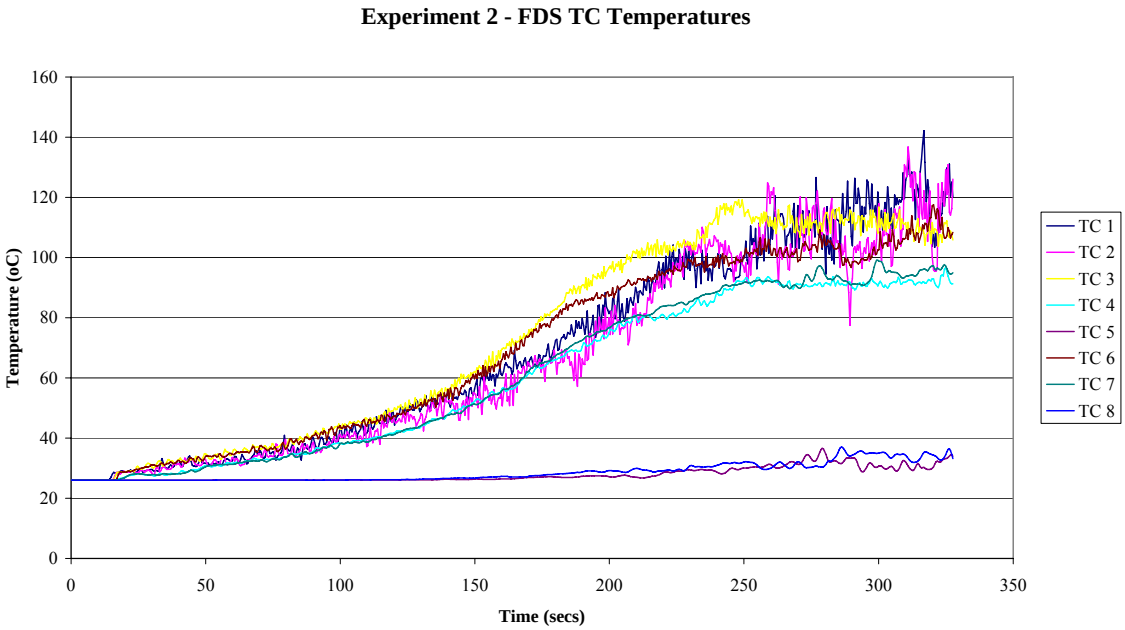

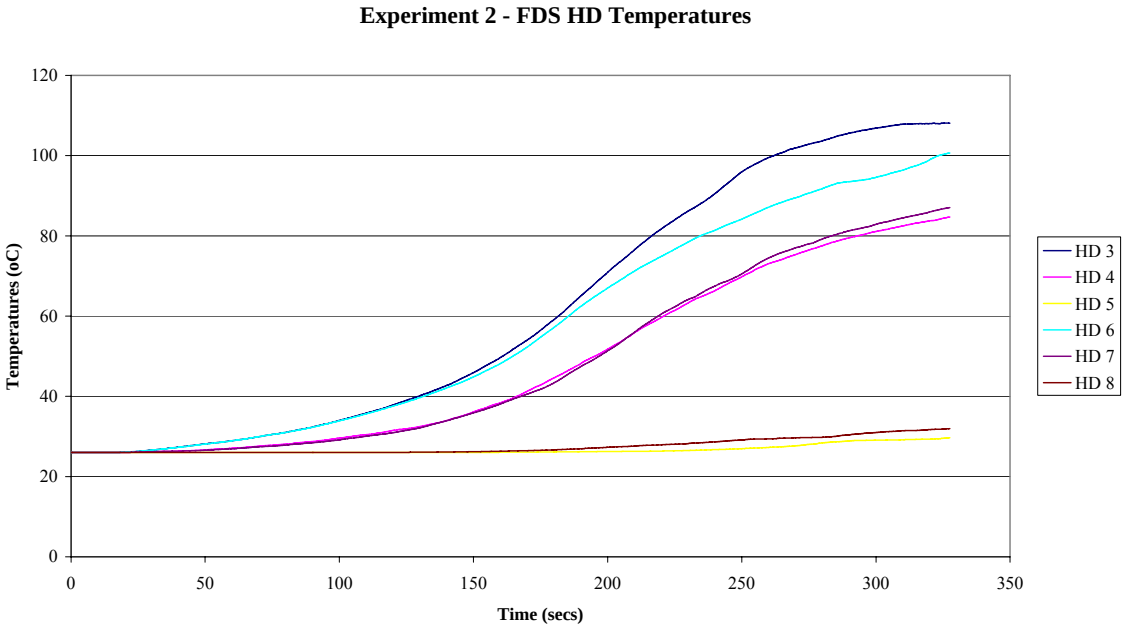

Experiment 2 - FDS HRR

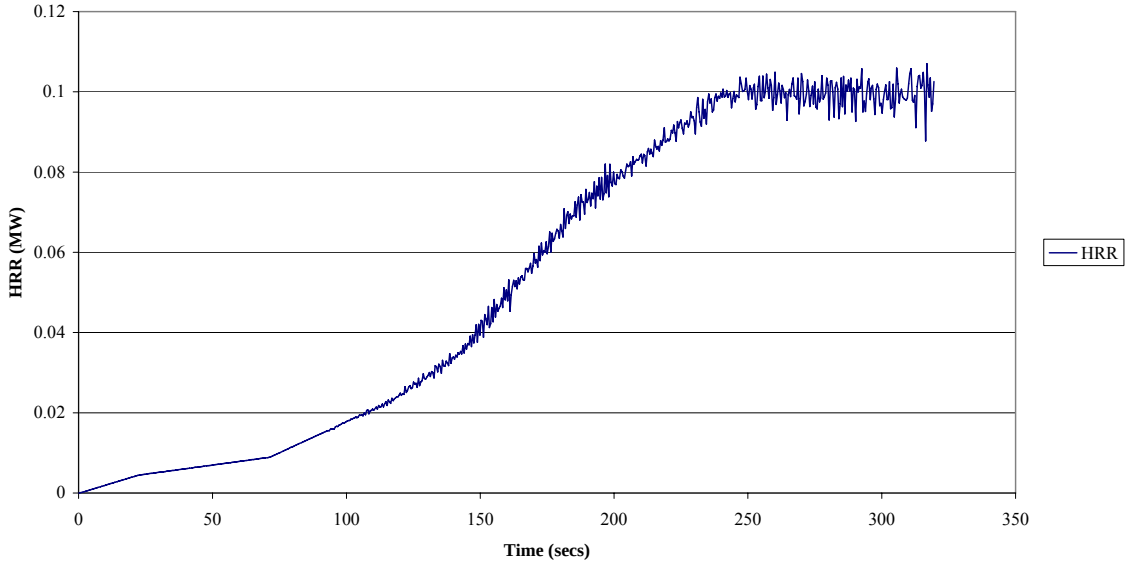

Experiment 2 - FDS Sprinkler Activation Times

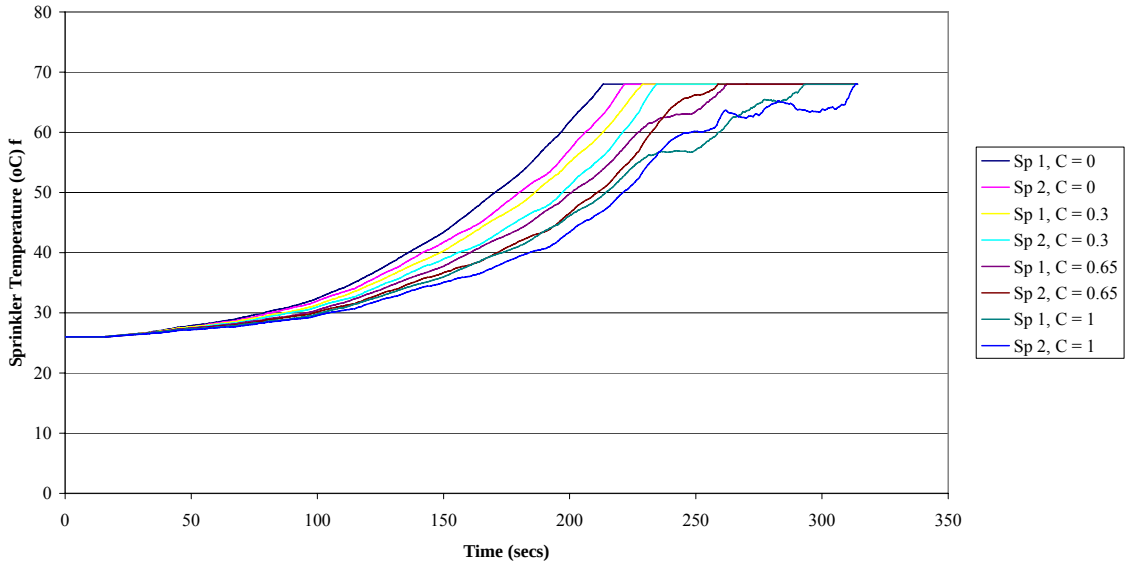

Experiment 3

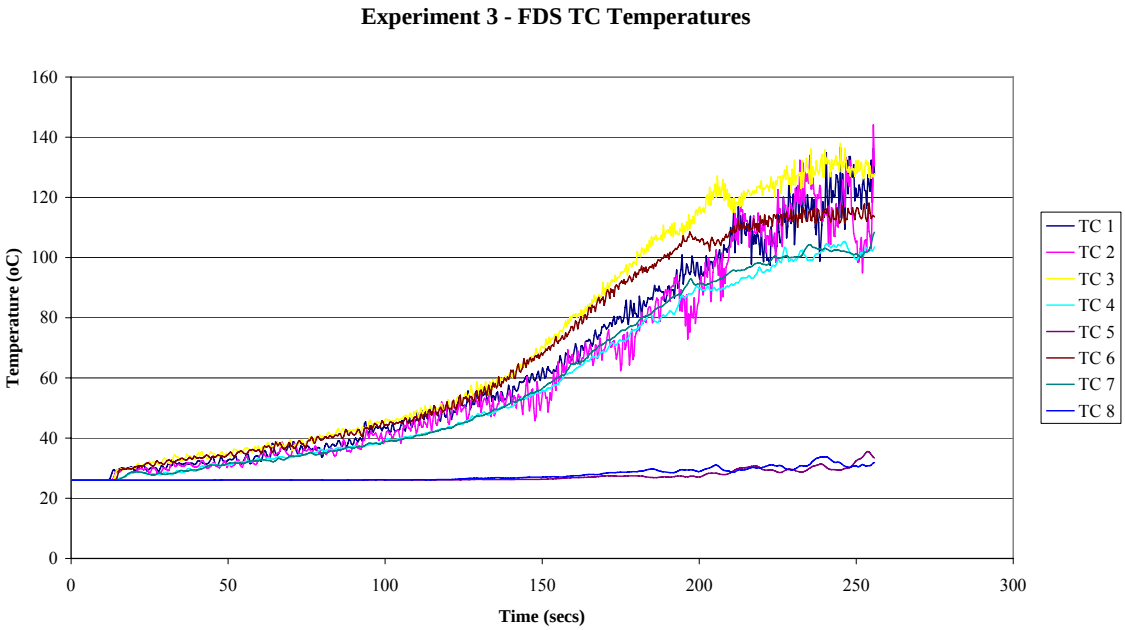

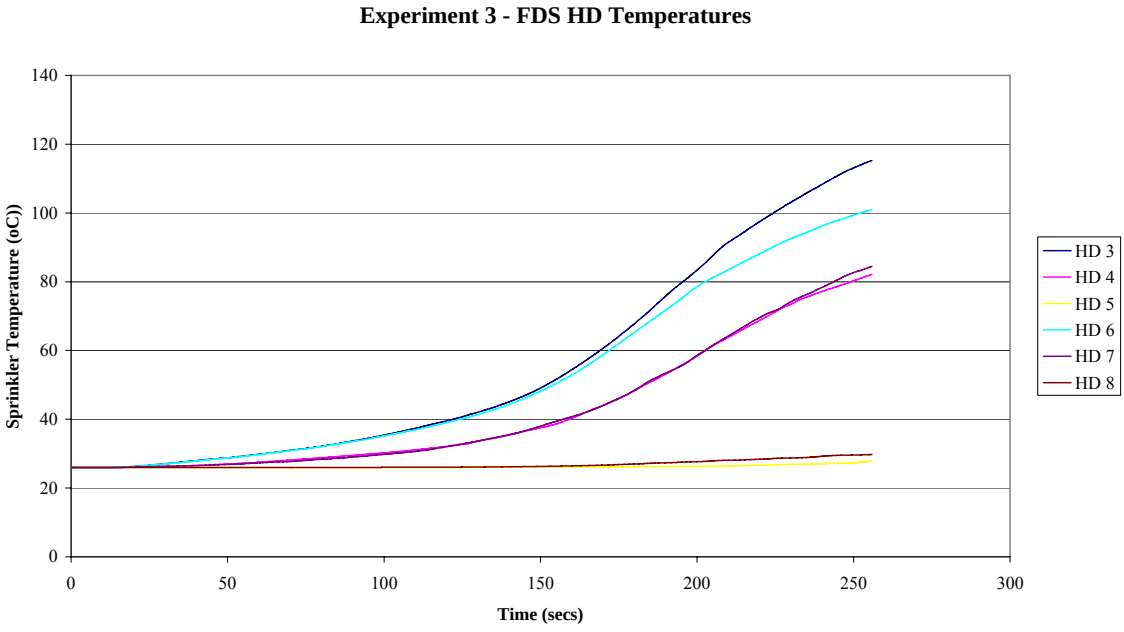

Experiment 3 - FDS HRR

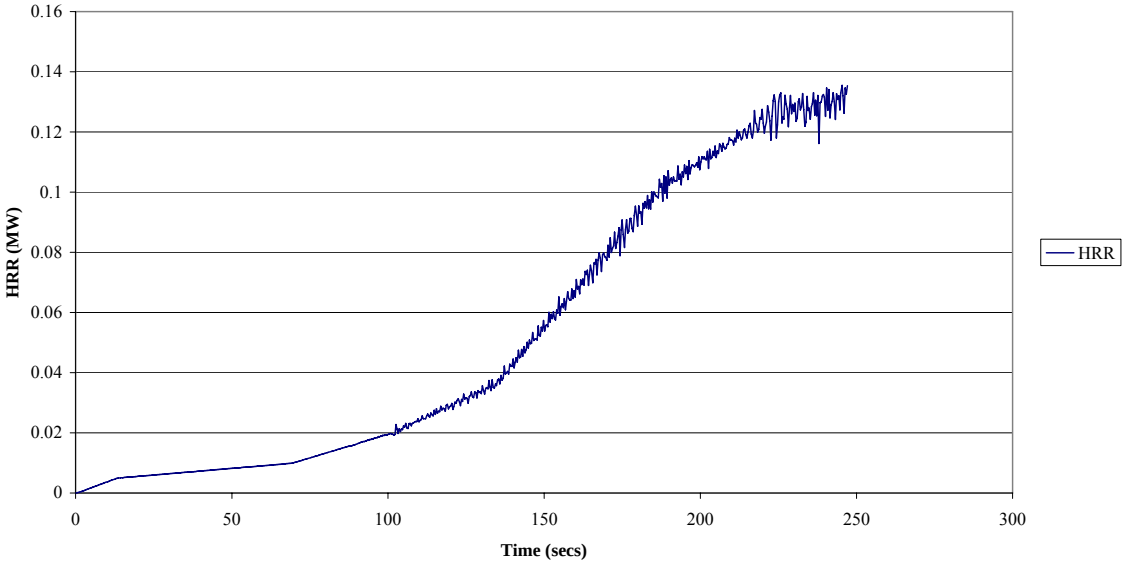

Experiment 3 - FDS Sprinkler Activation Times

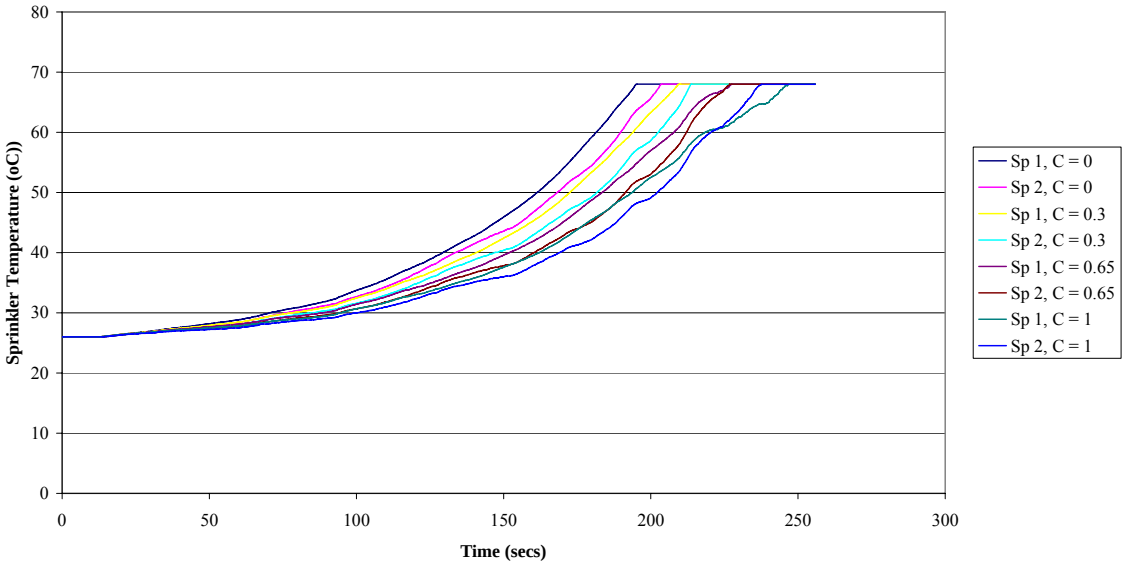

Experiment 4

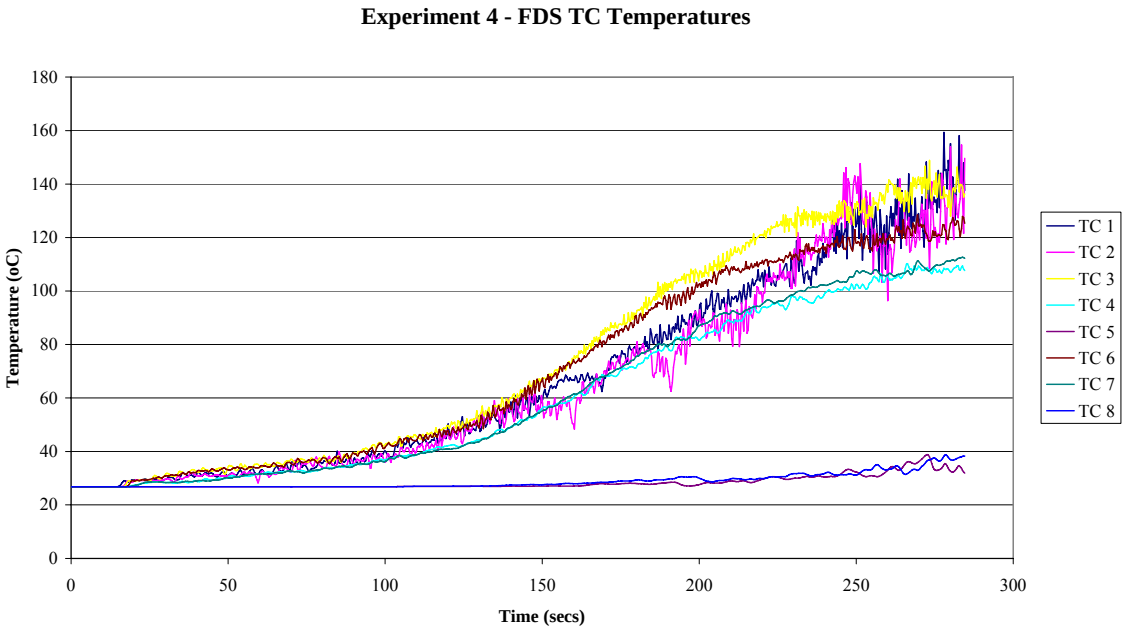

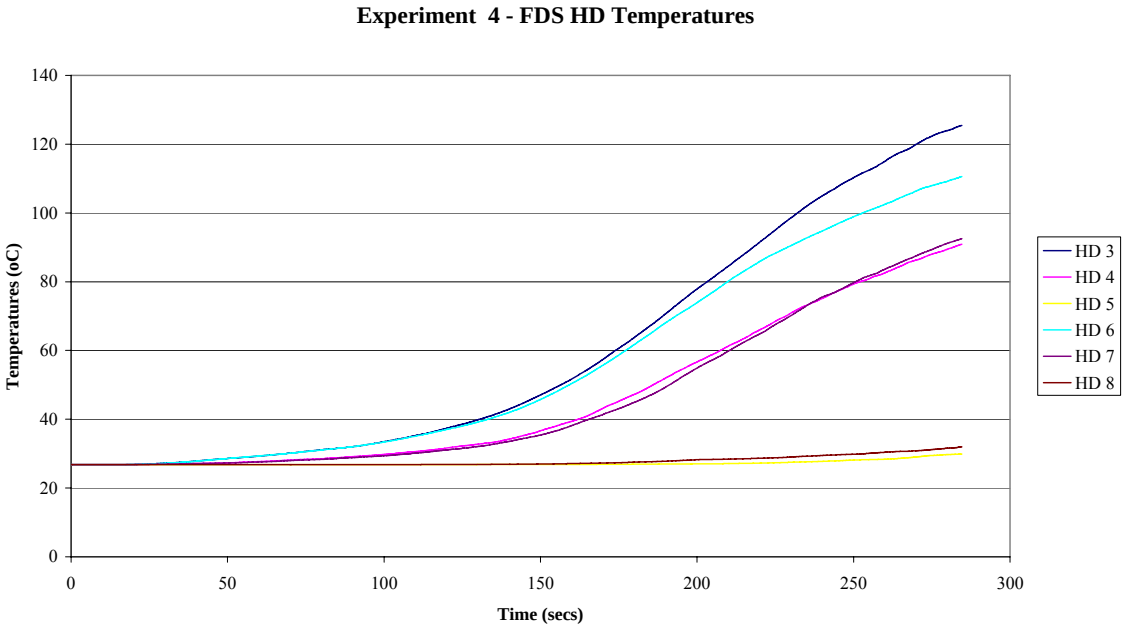

Experiment 4 - FDS HRR

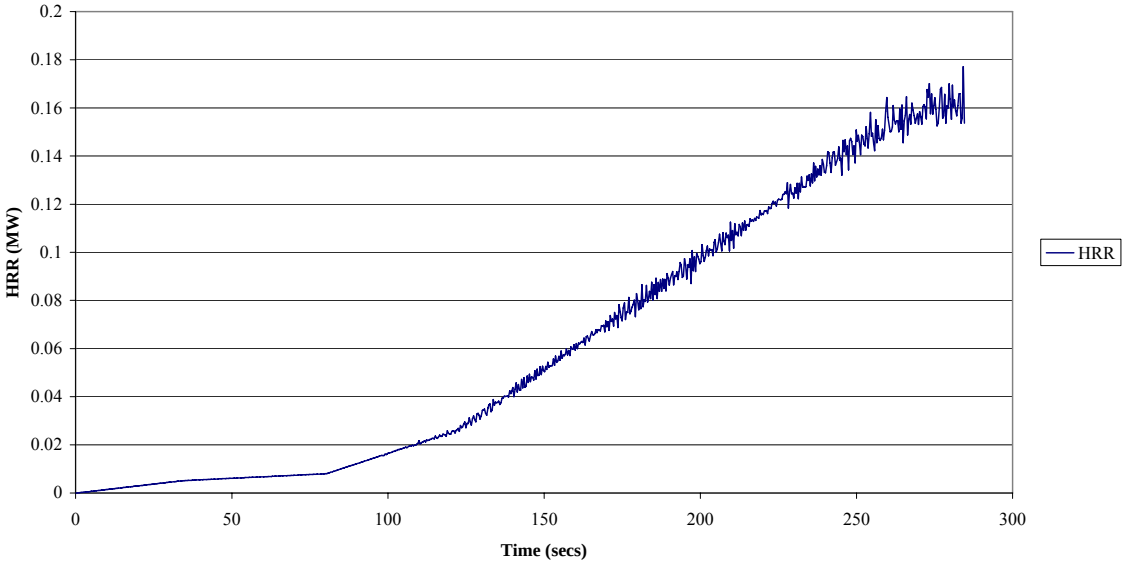

Experiment 4 - FDS Sprinkler Activation Times

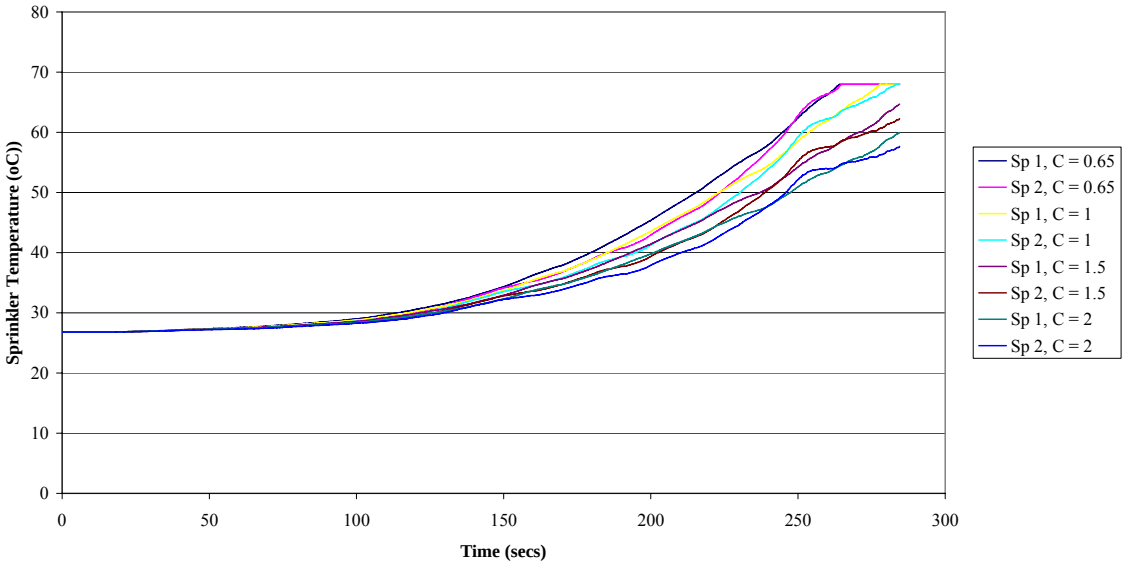

Experiment 5

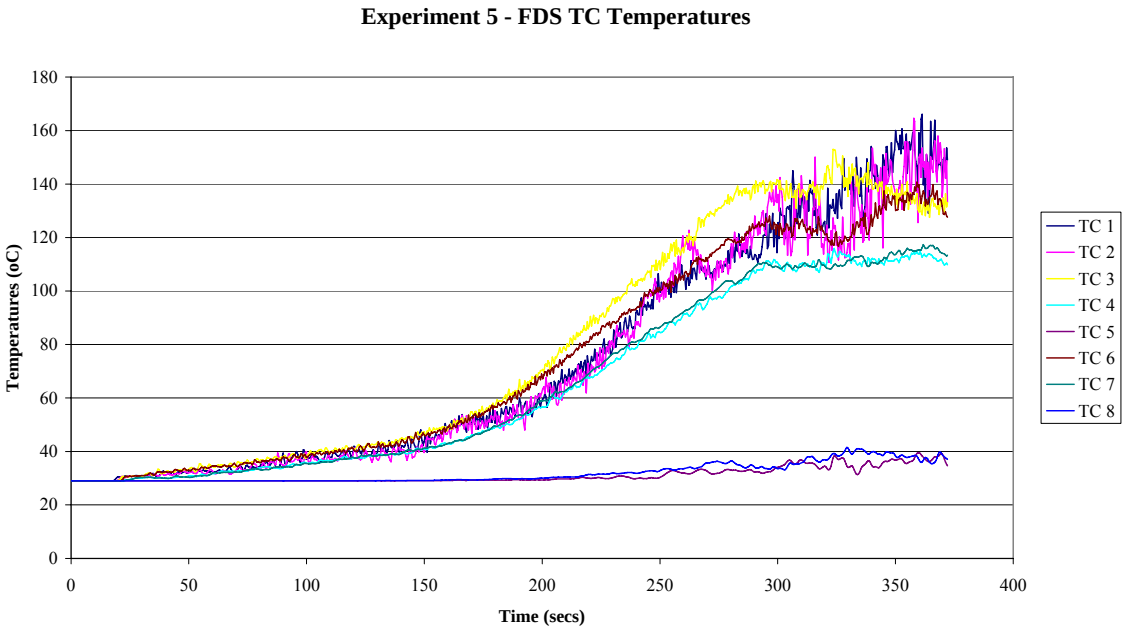

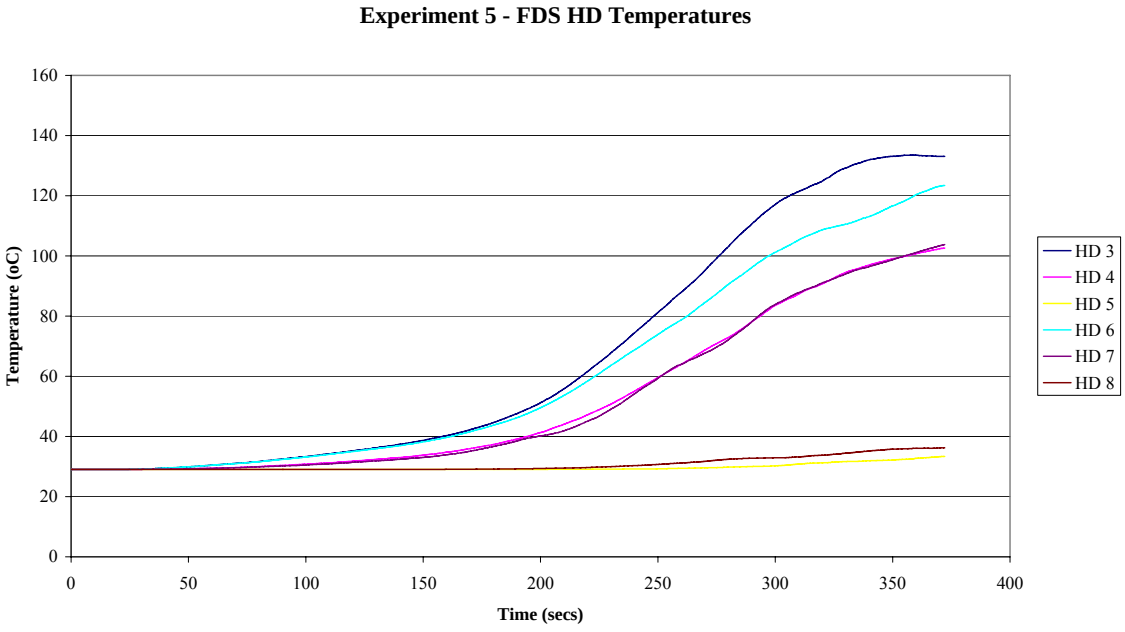

Experiment 5 - FDS HRR

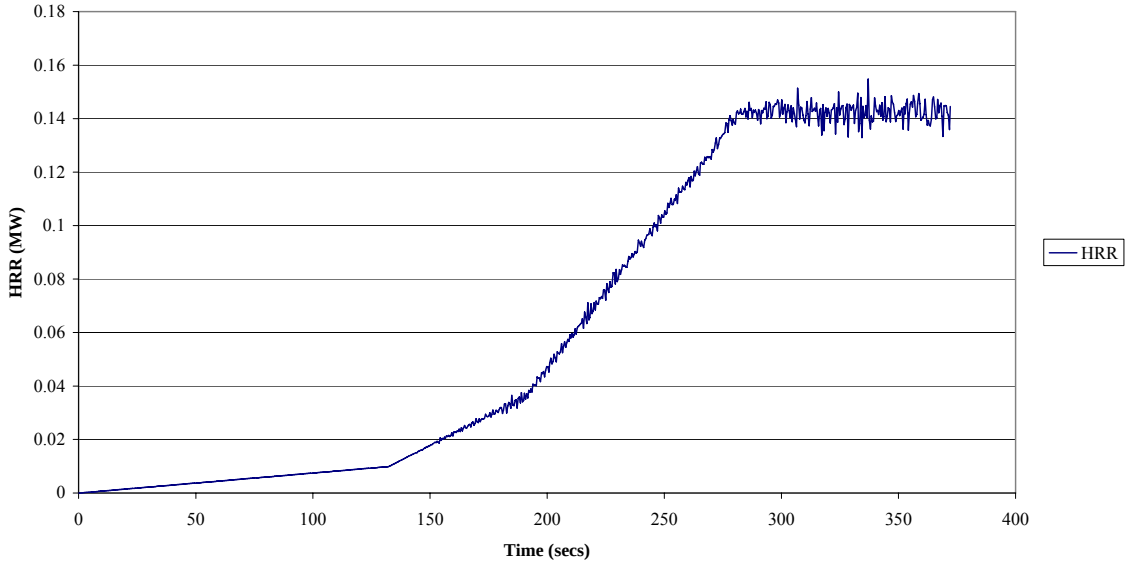

Experiment 5 - FDS Sprinkler Activation Times

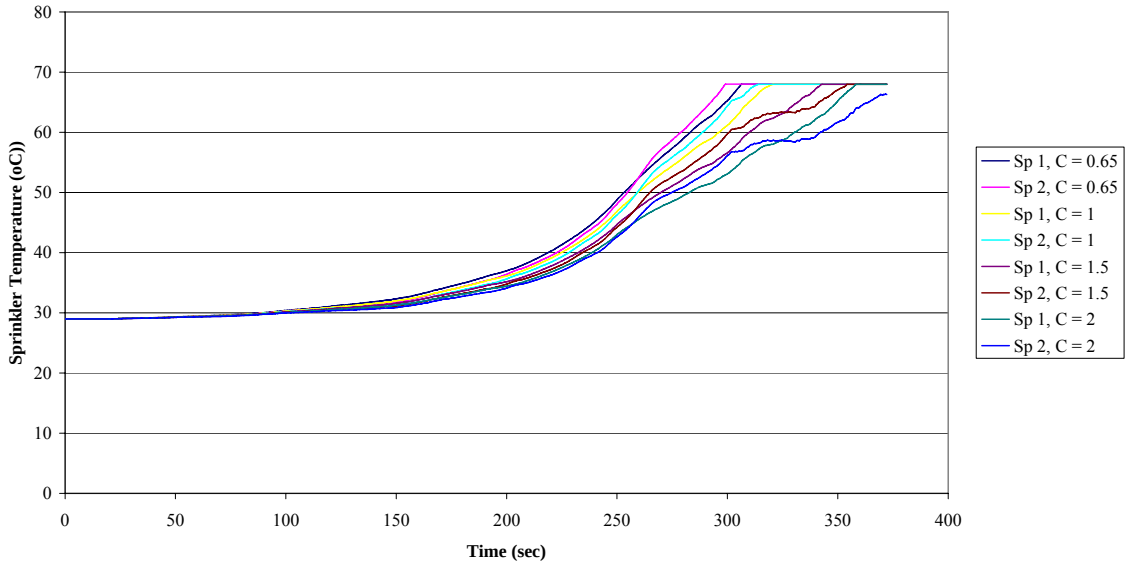

Experiment 6

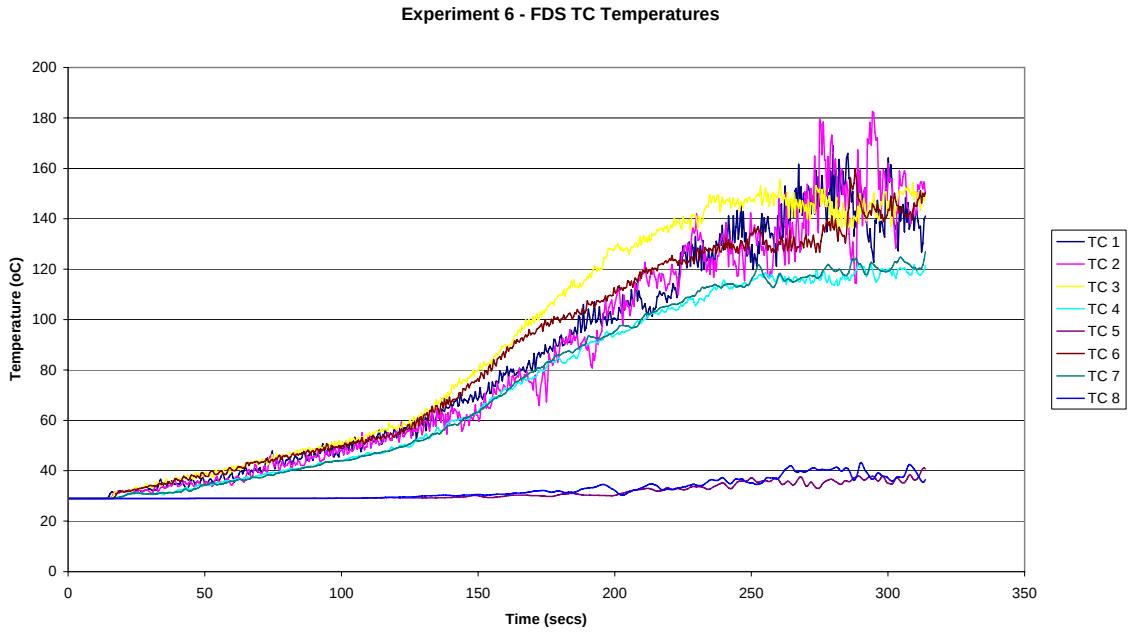

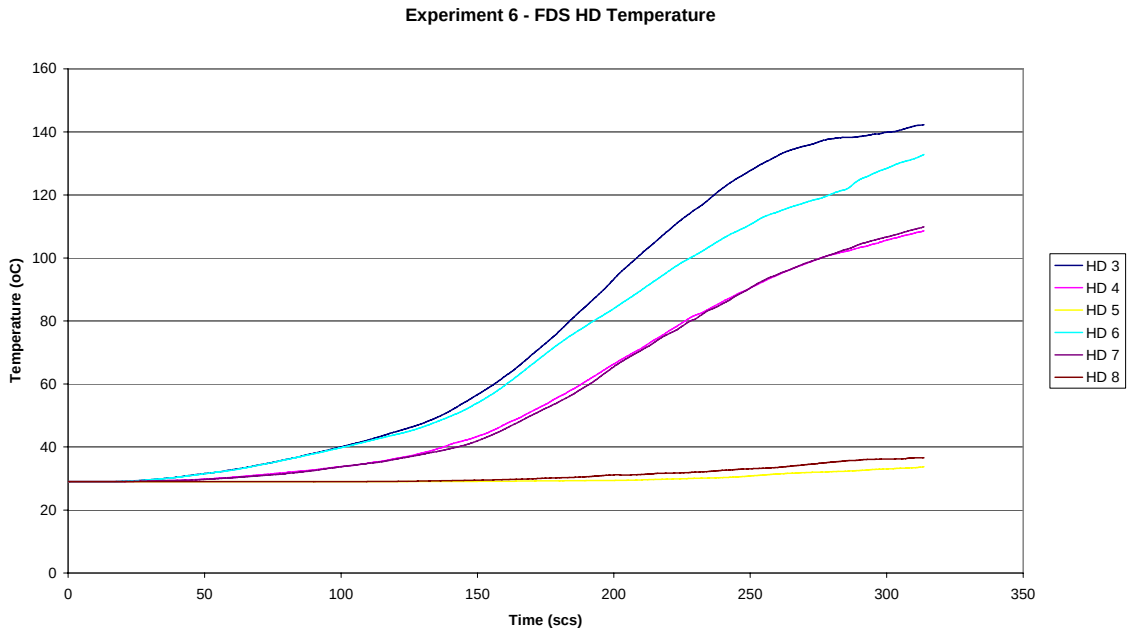

Experiment 6 - FDS HRR

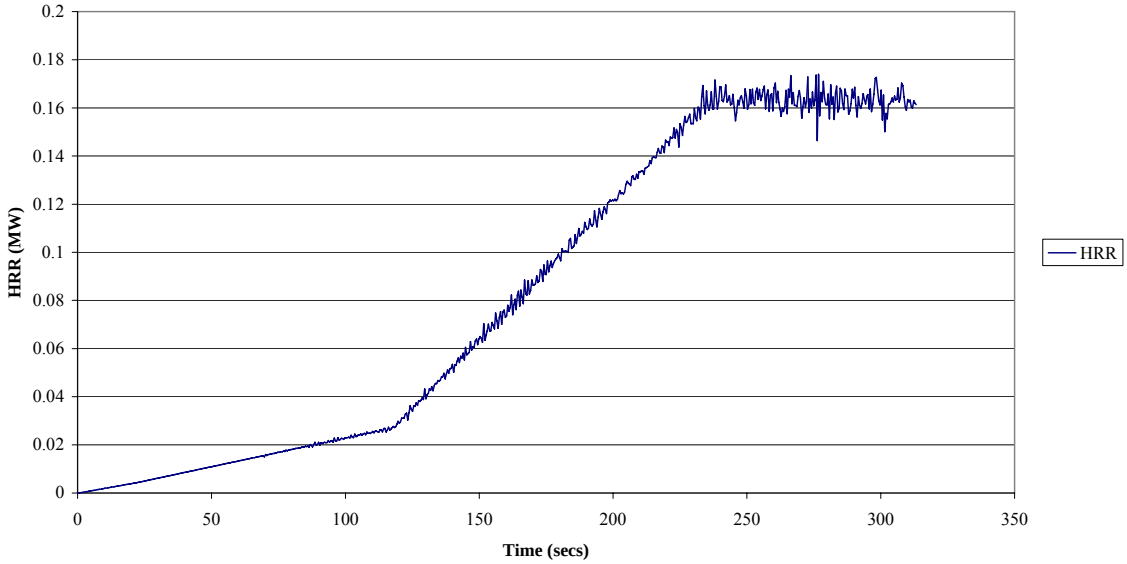

Experiment 6 - FDS Sprinkler Activation Times

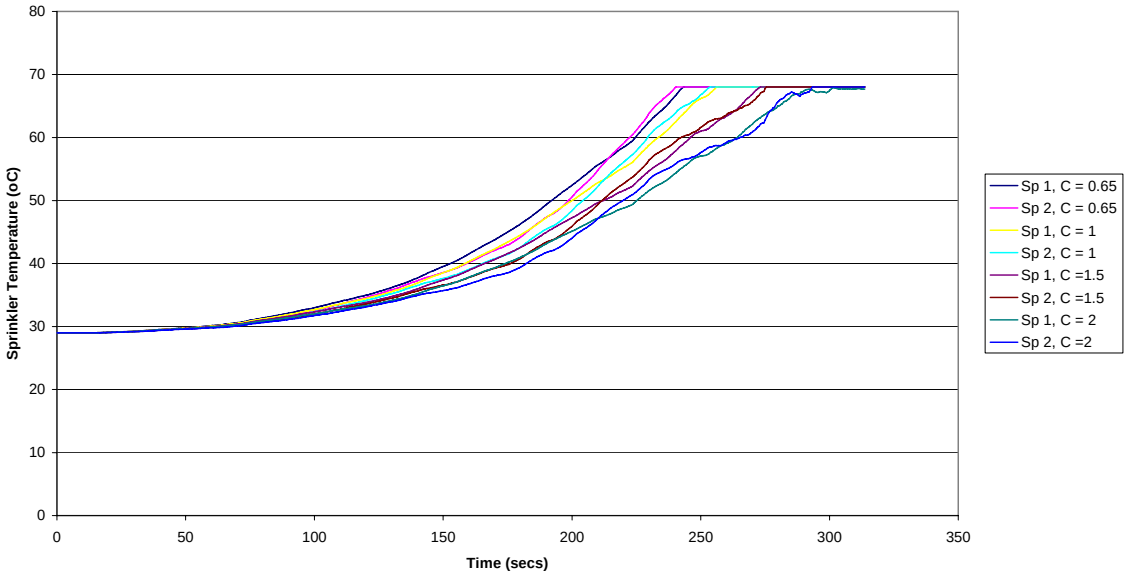

Experiment 7

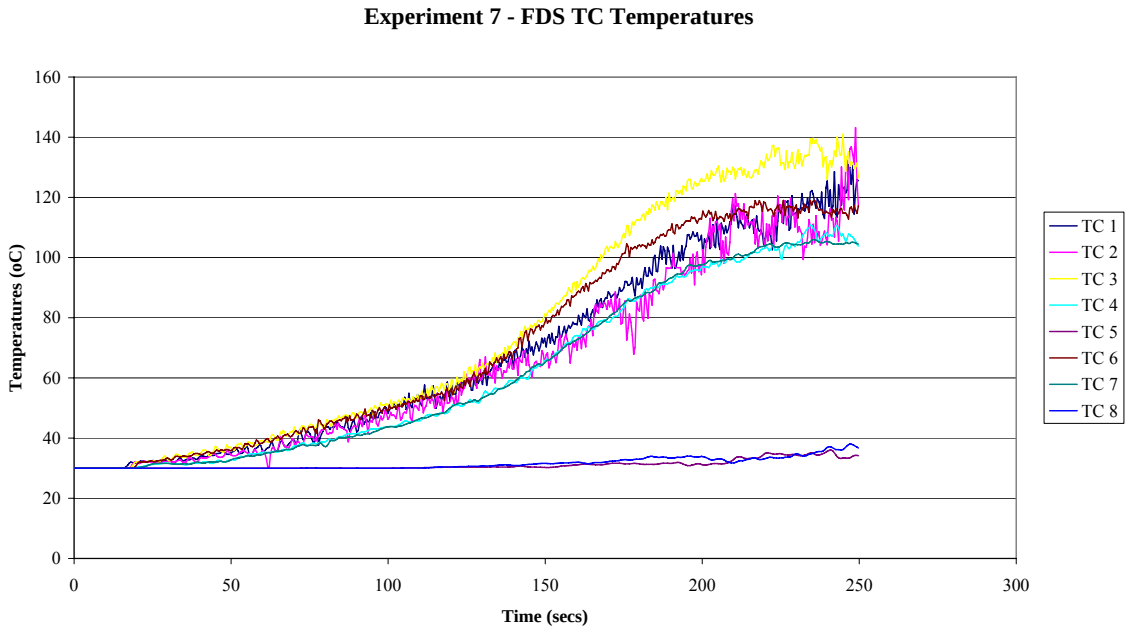

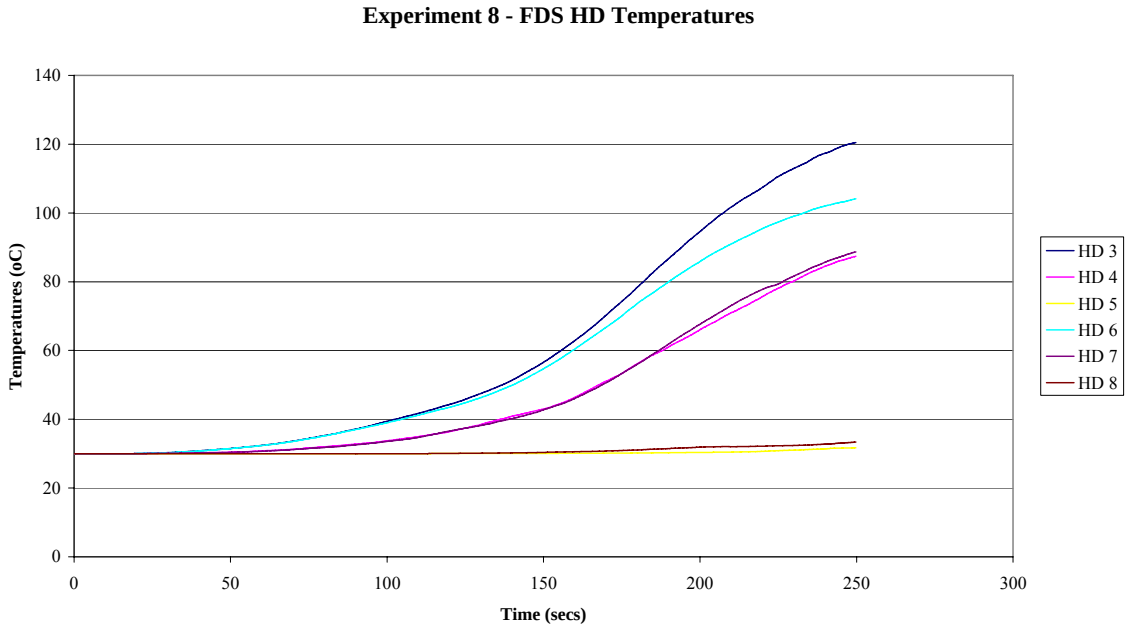

Experiment 7 - FDS HRR

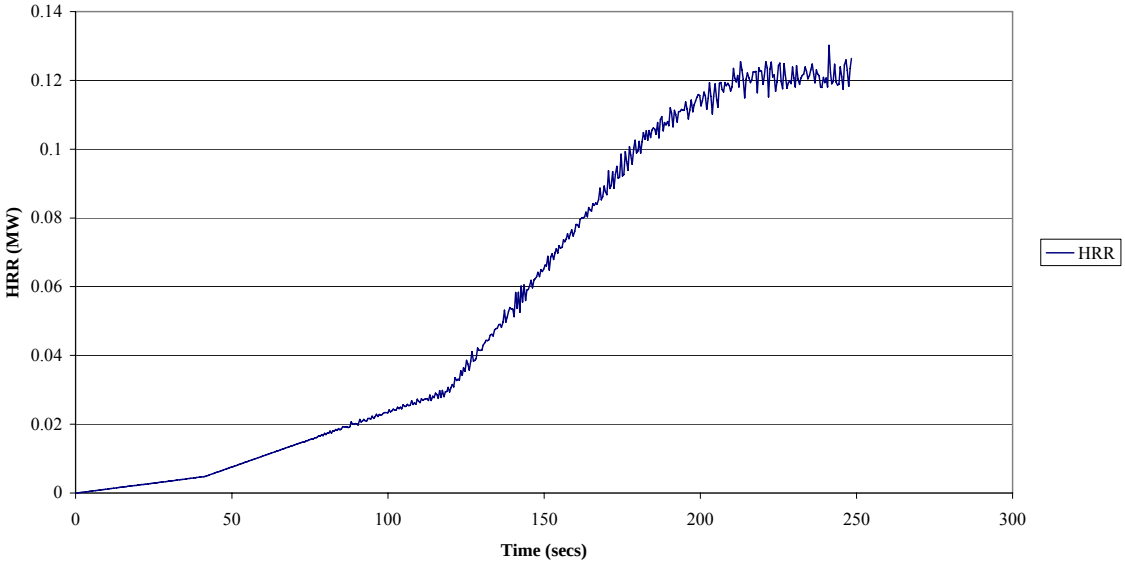

Experiment 7 - FDS Sprinkler Activation Times

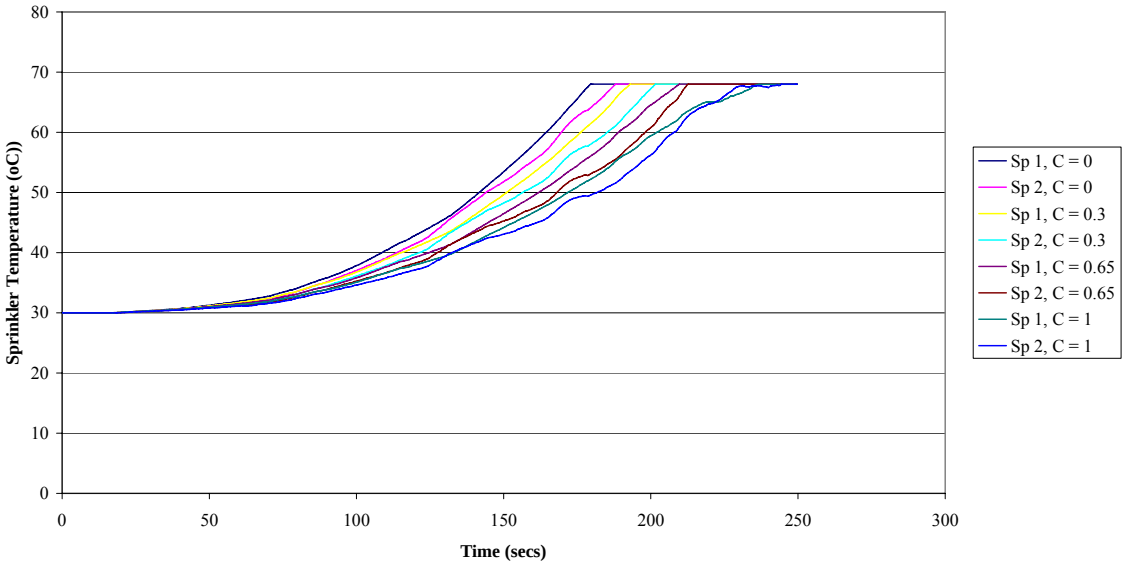

Experiment 8

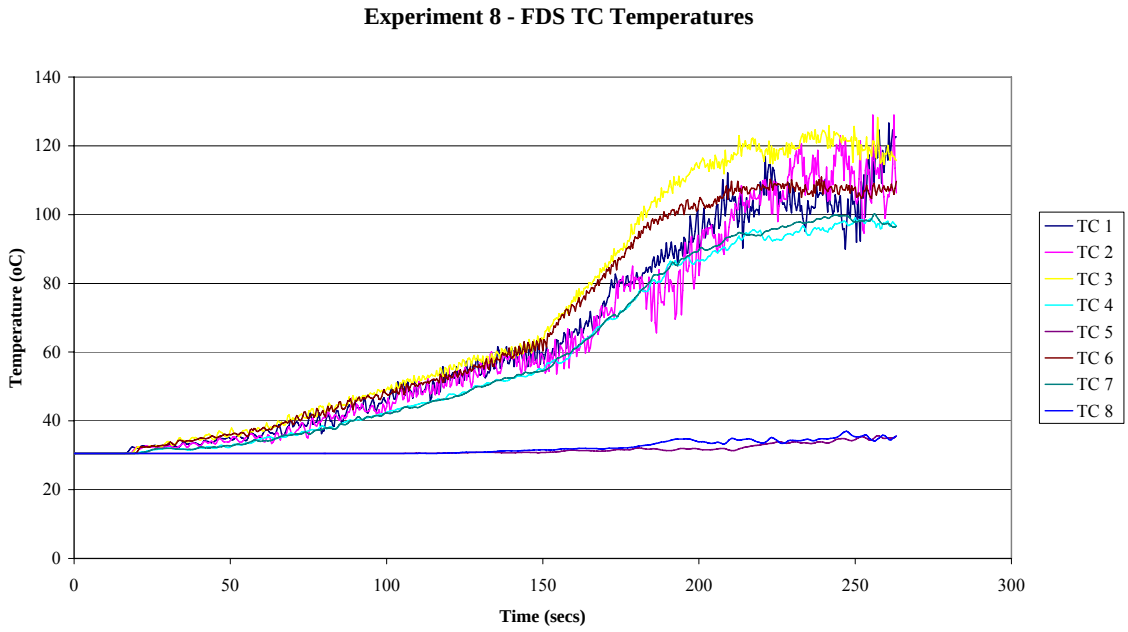

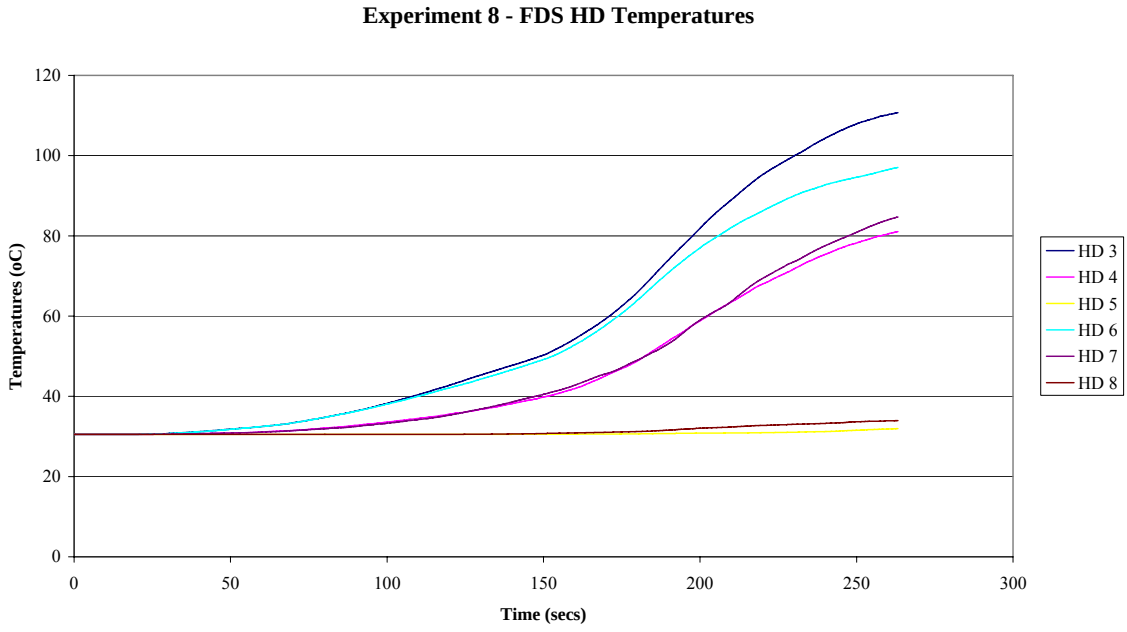

Experiment 8 - FDS HRR

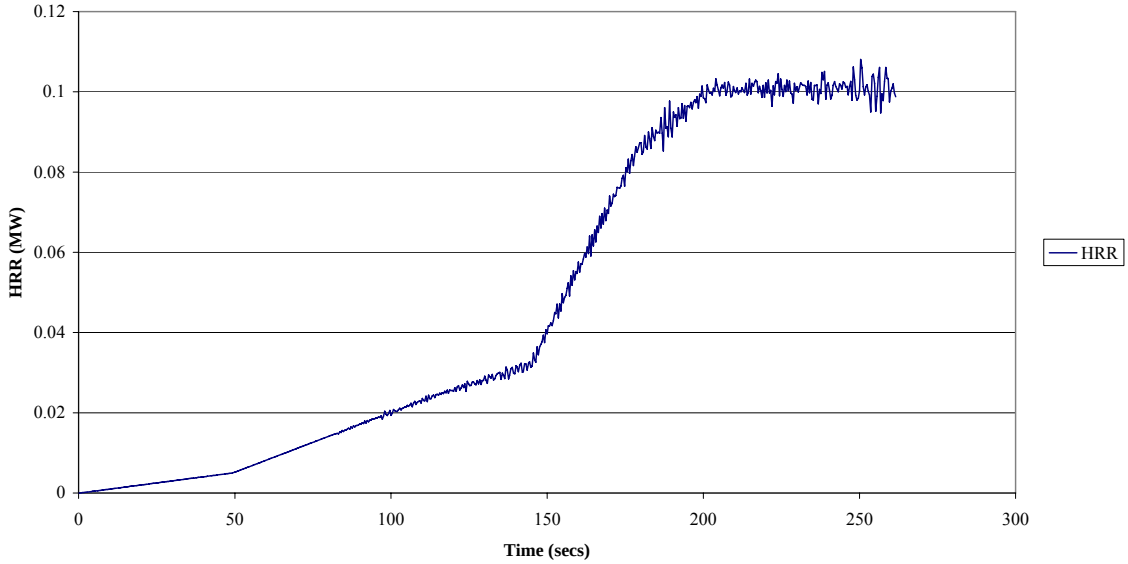

Experiment 8 - FDS Sprinkler Activation Times

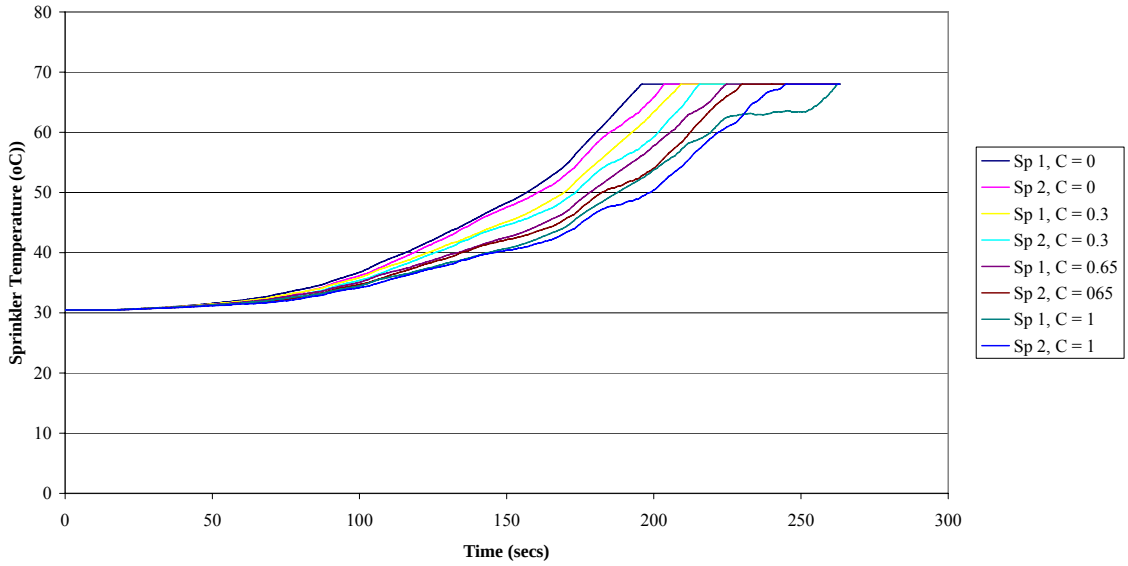

Experiment 9

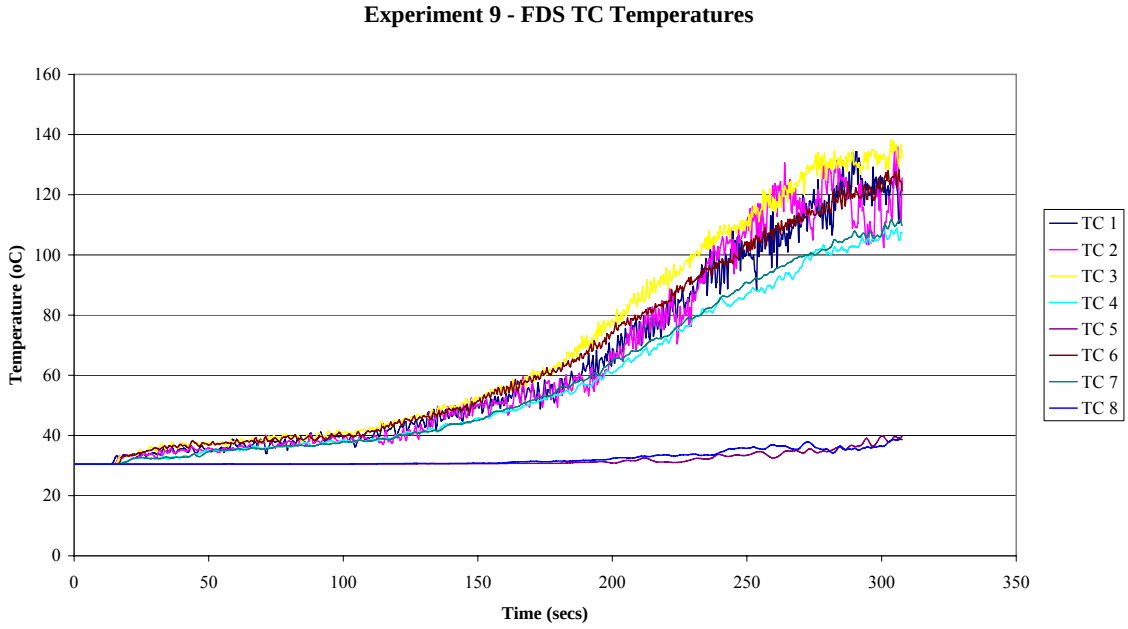

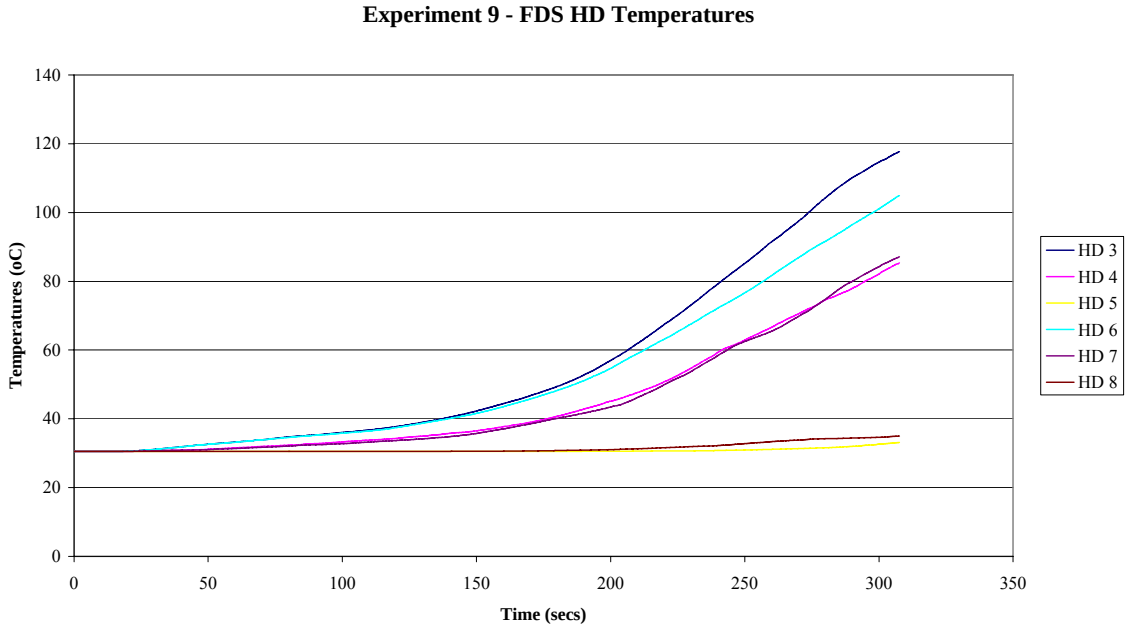

Experiment 9 - FDS HRR

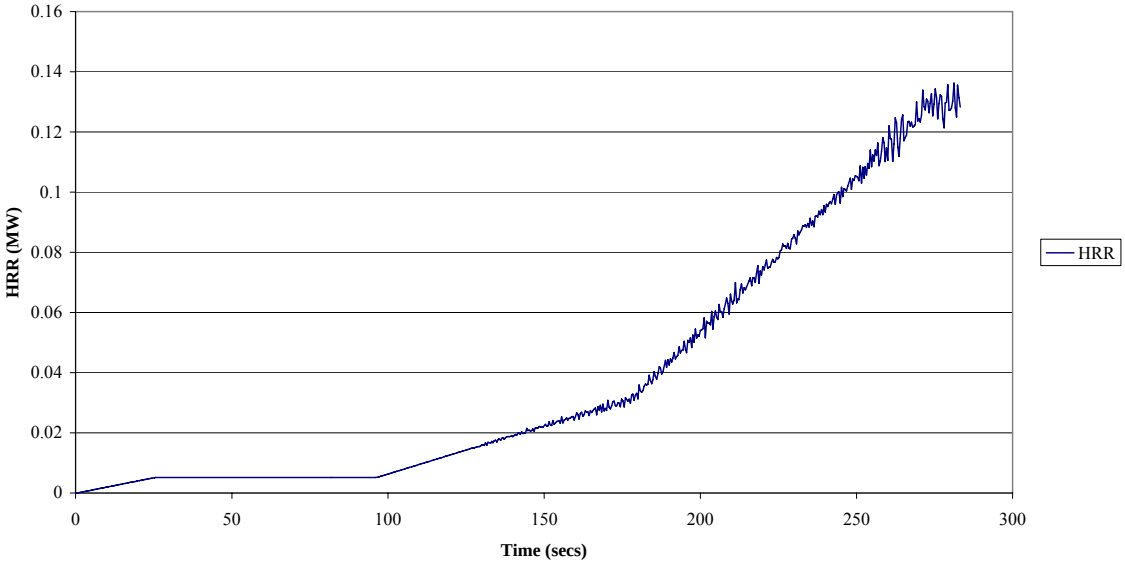

Experiment 9 - FDS Sprinkler Activation Times

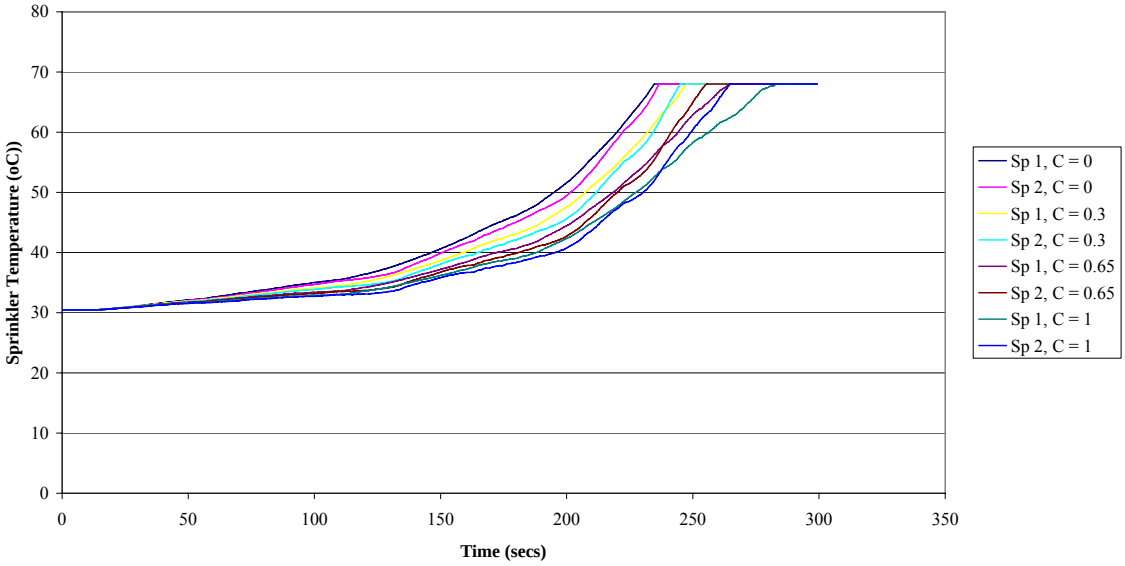

Experiment 10

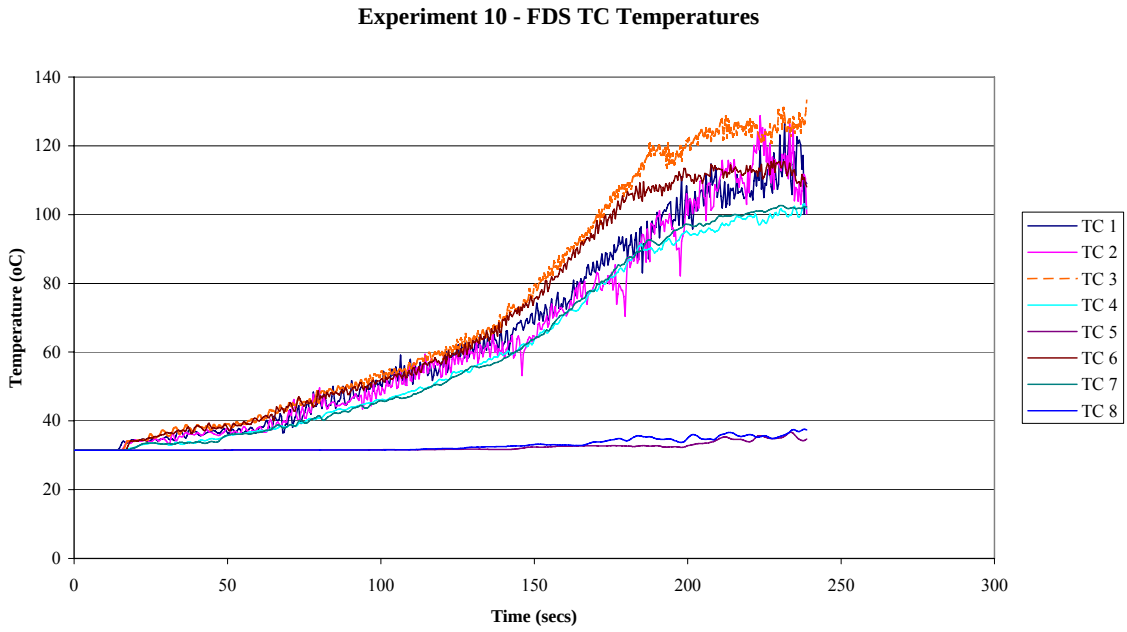

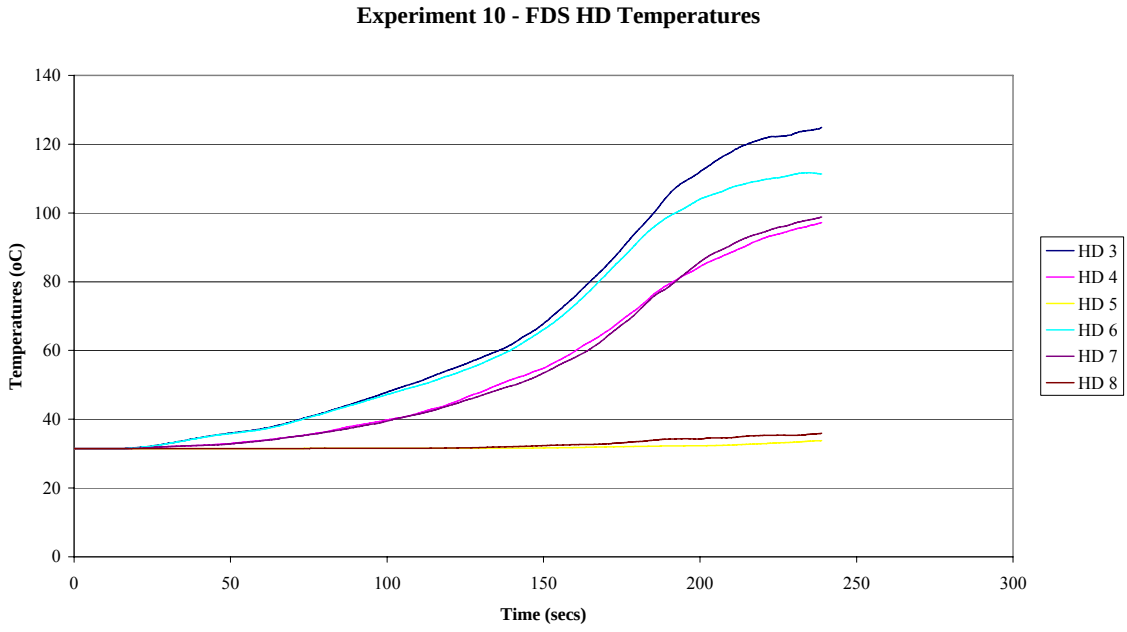

Experiment 10 - FDS HRR

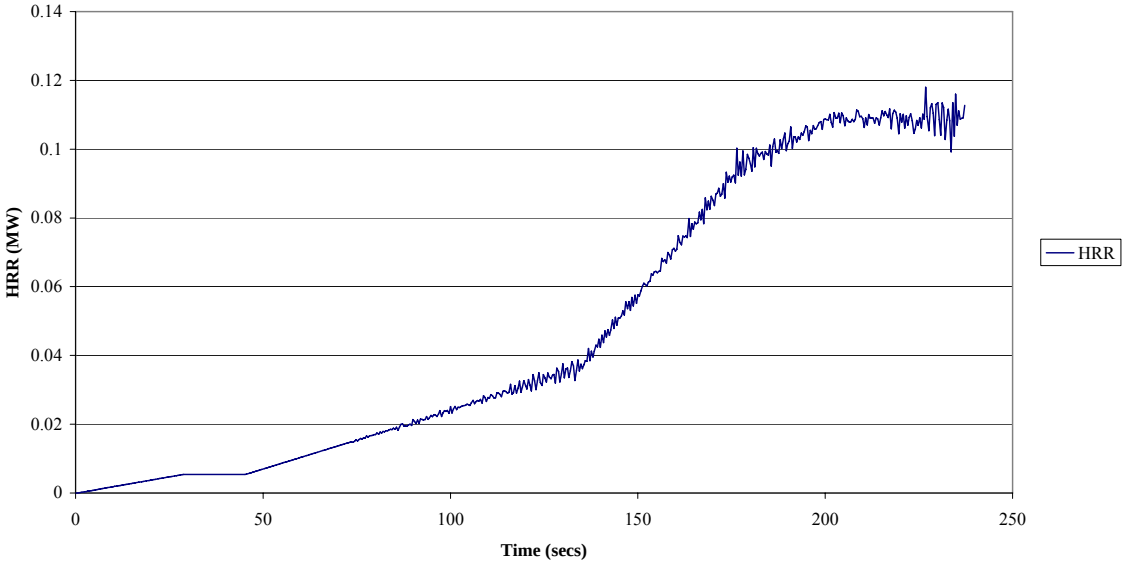

Experiment 10 - FDS Sprinkler Activation Times

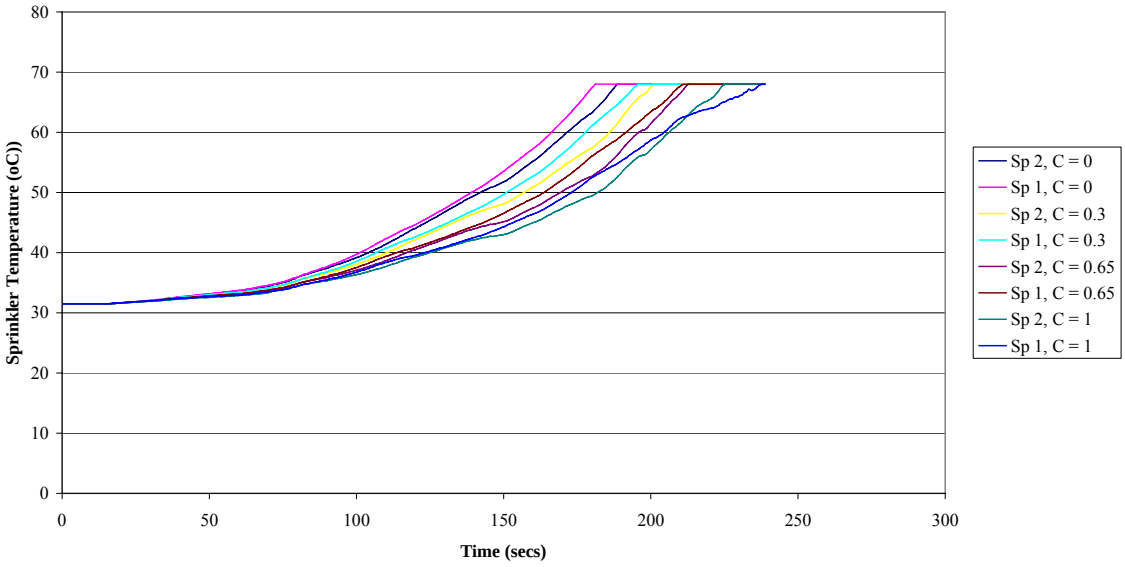

Experiment 12

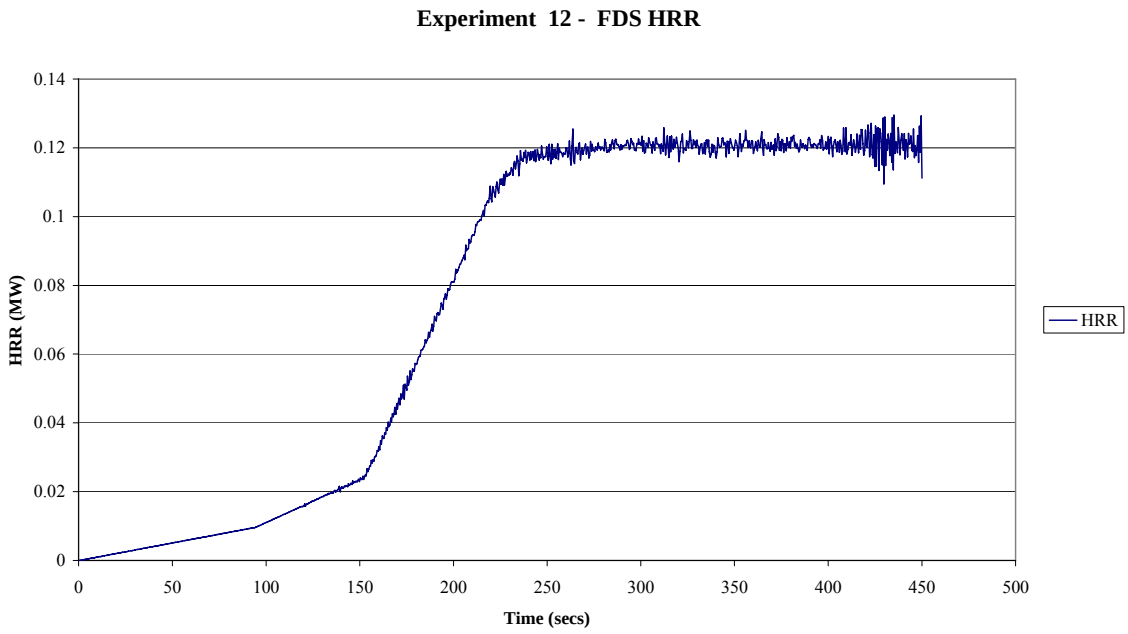

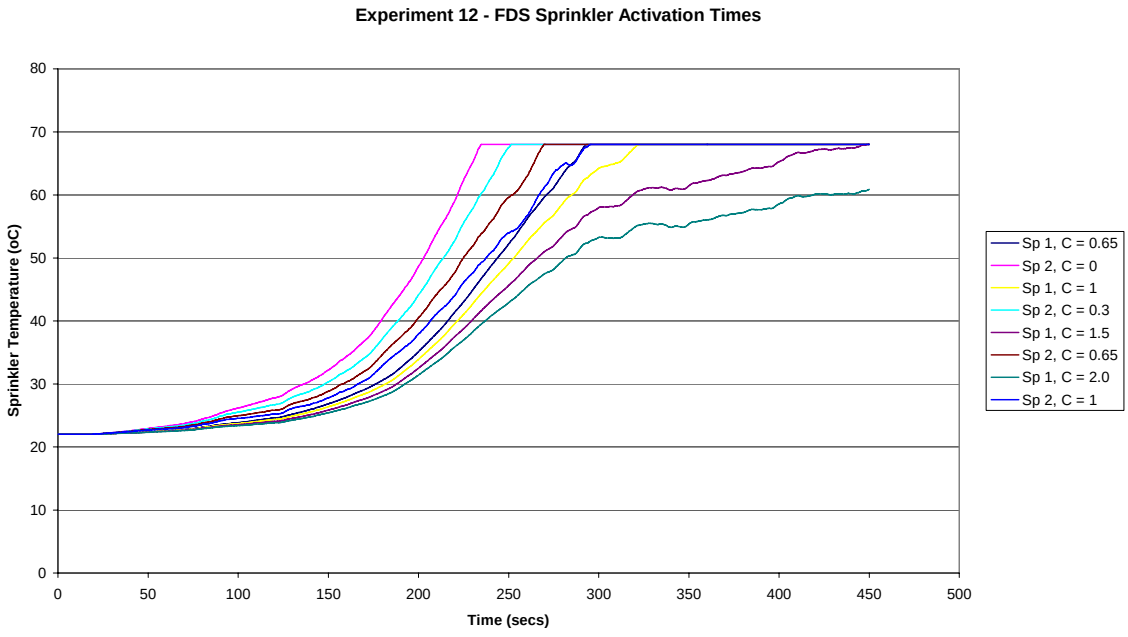

Experiment 13

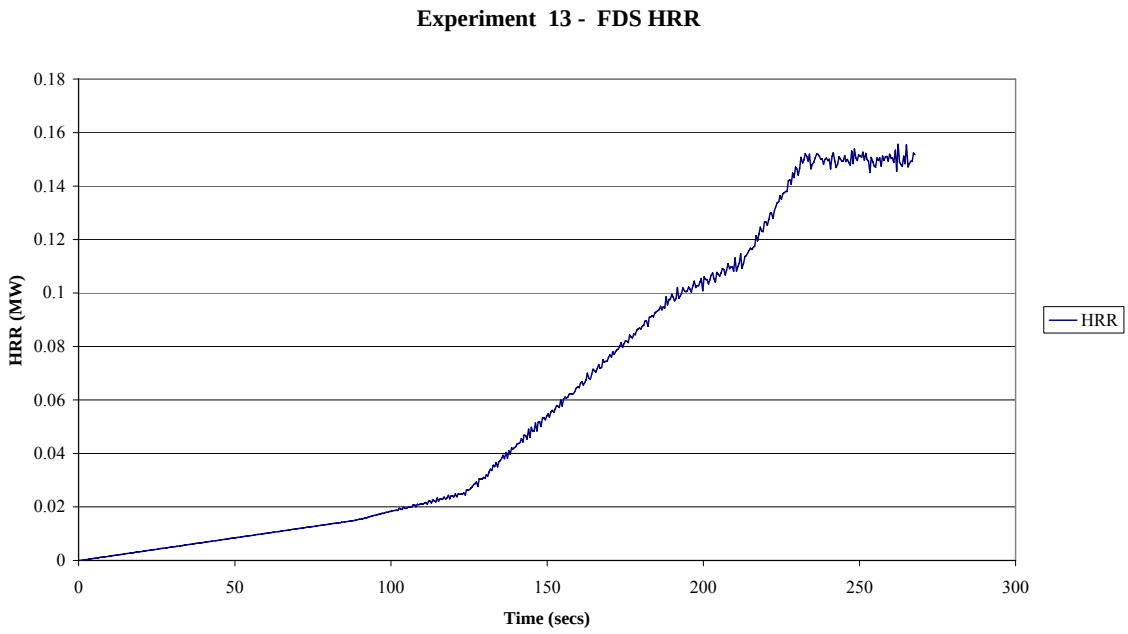

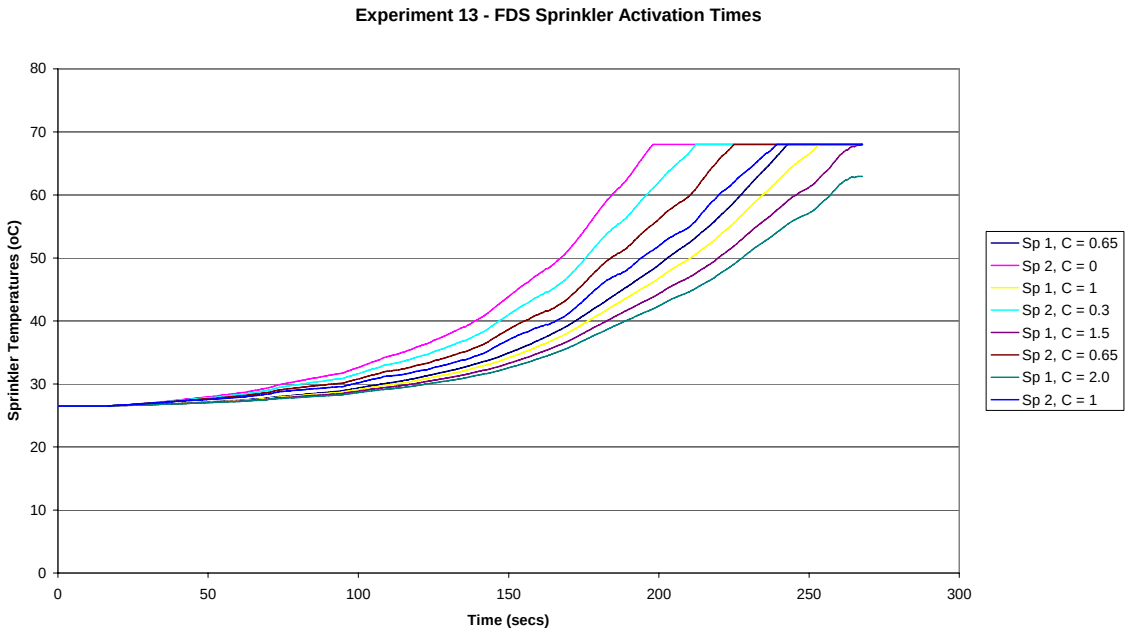

Experiment 14

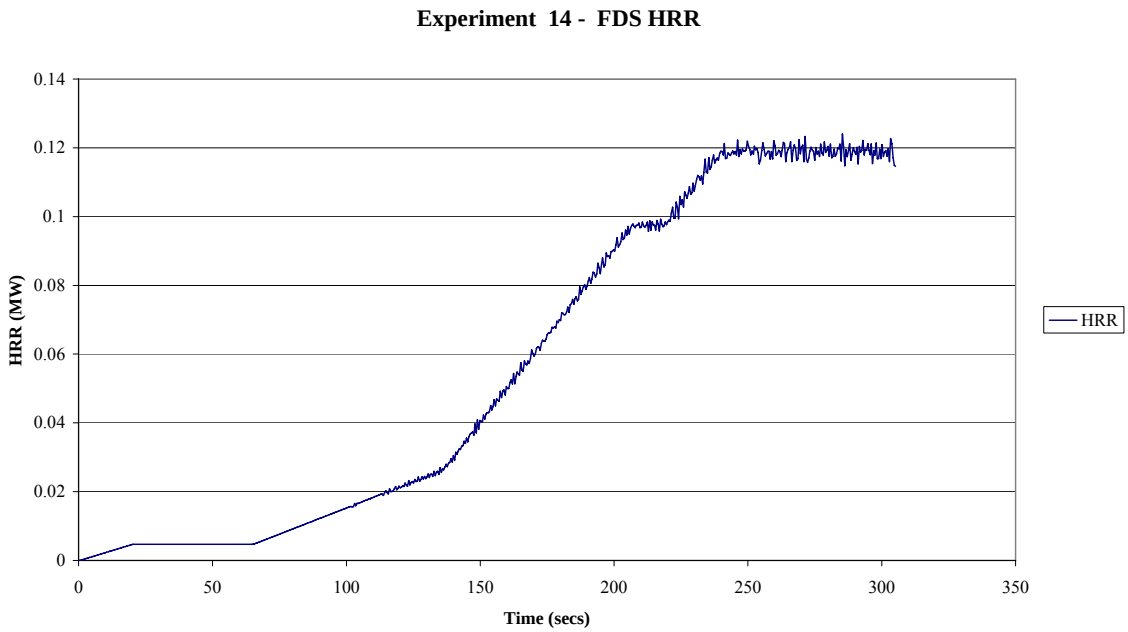

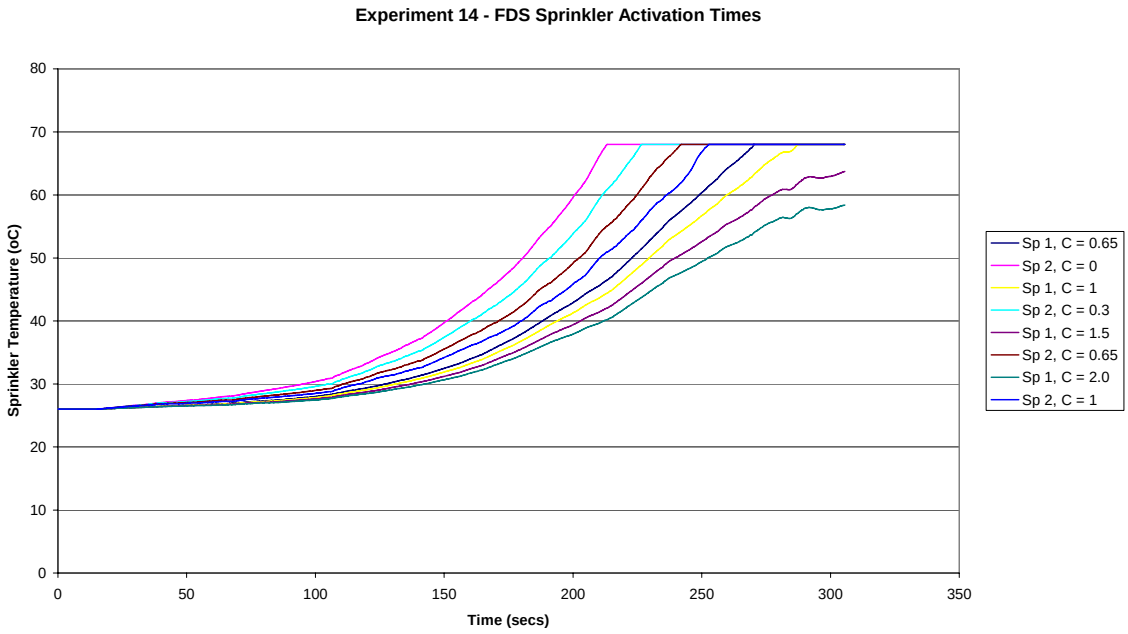

Experiment 15

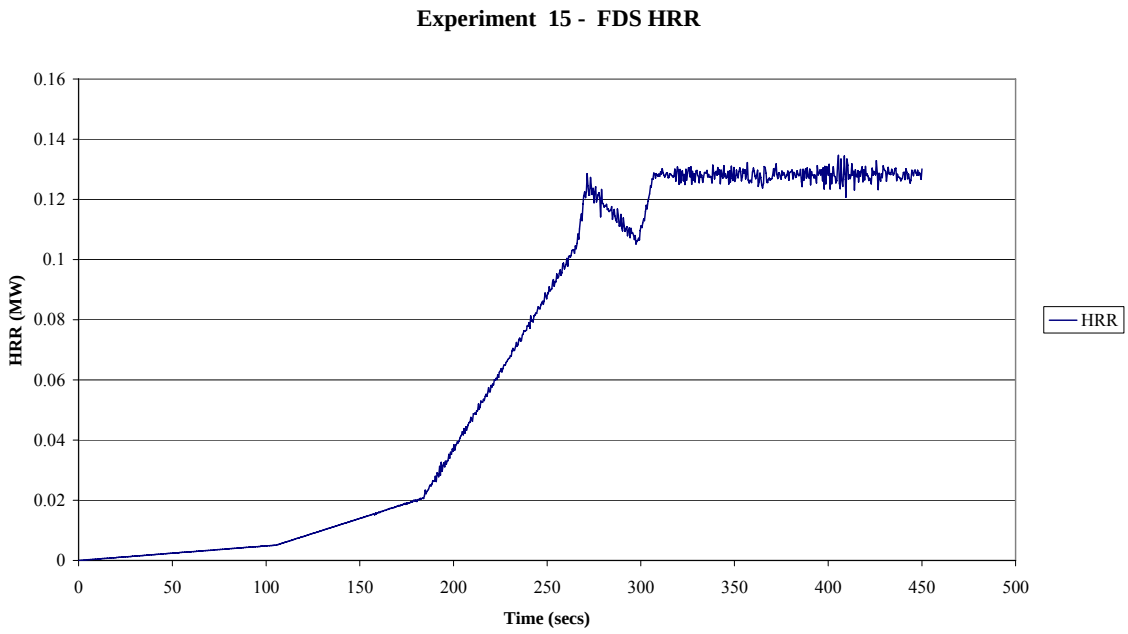

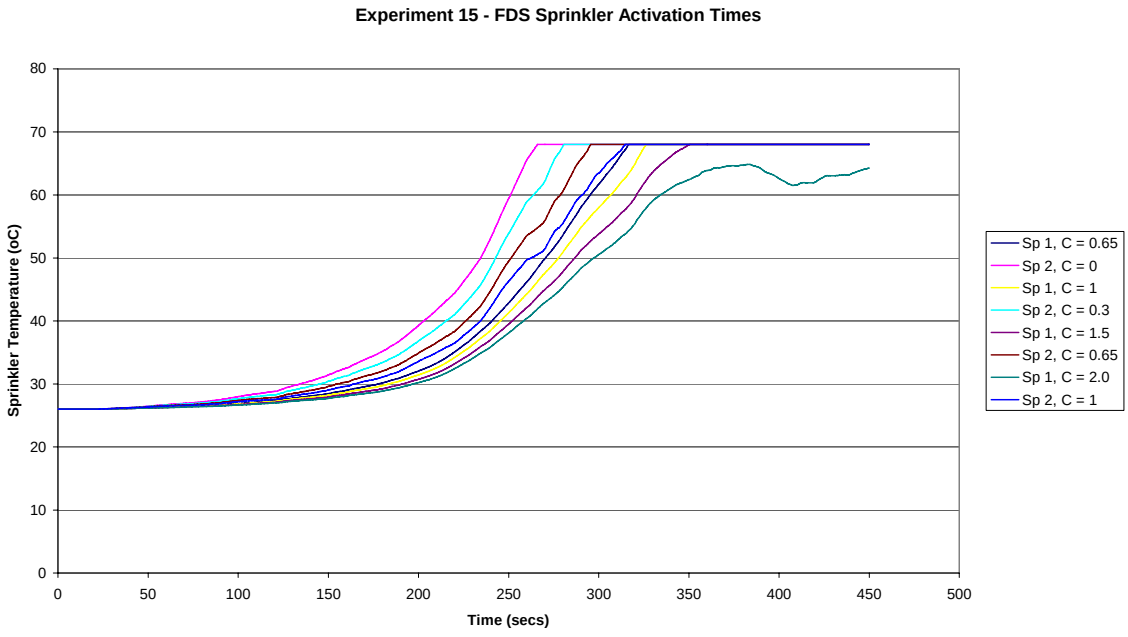

Experiment 16

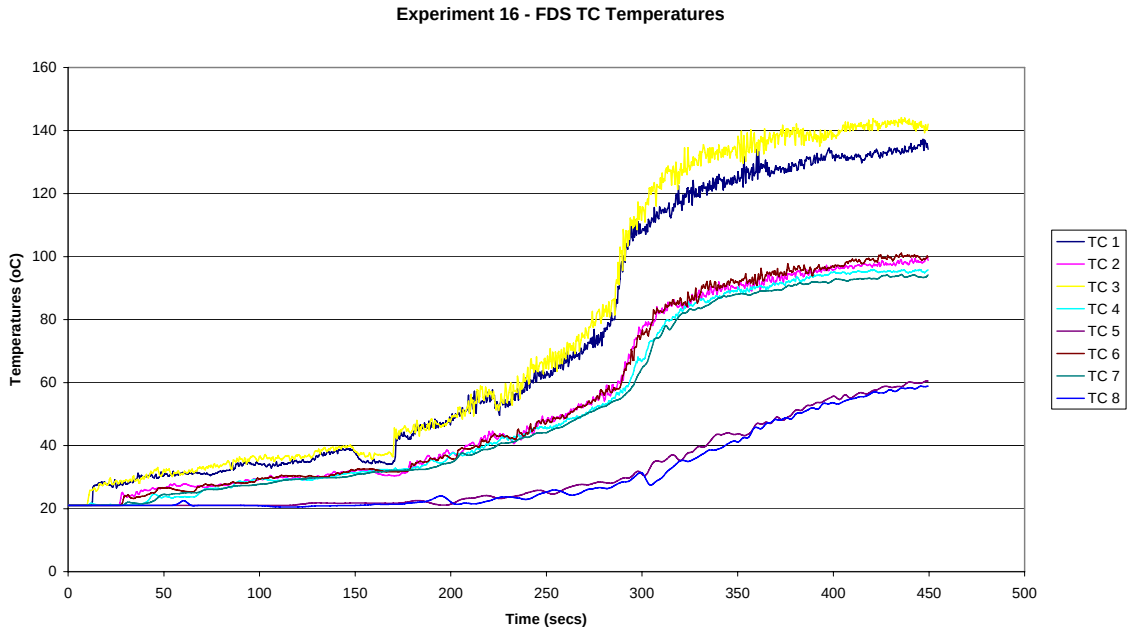

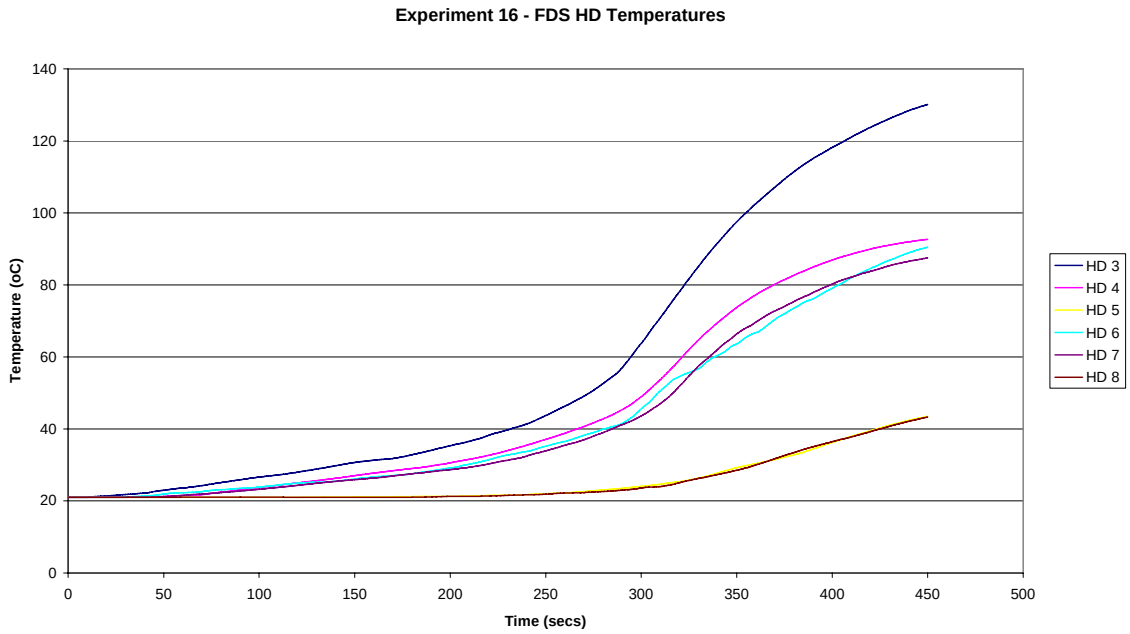

Experiment 16 - FDS HRR

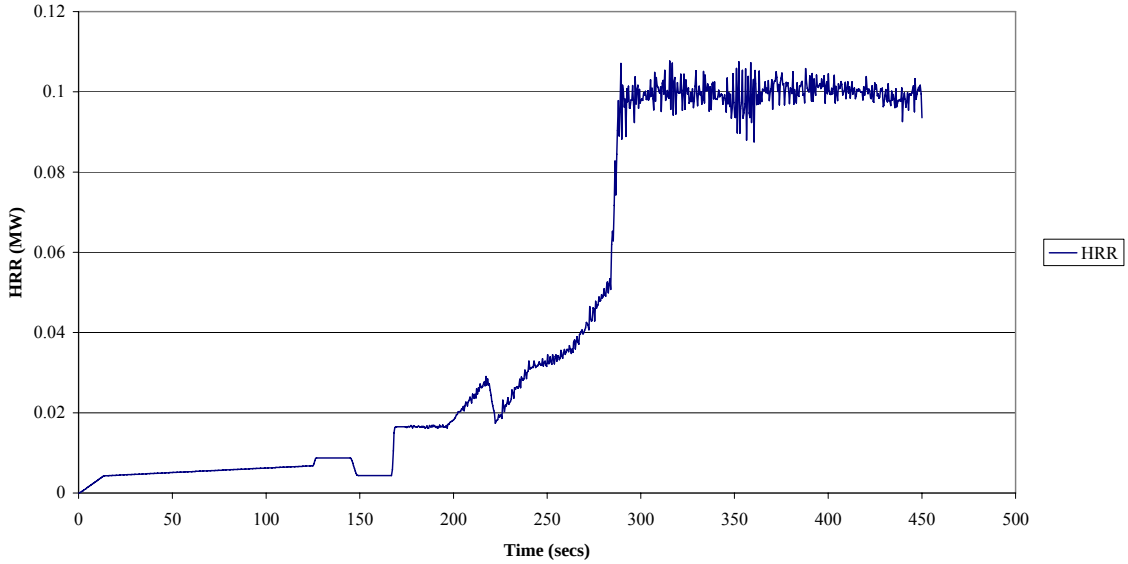

Experiment 16 - FDS Sprinkler Activation Times

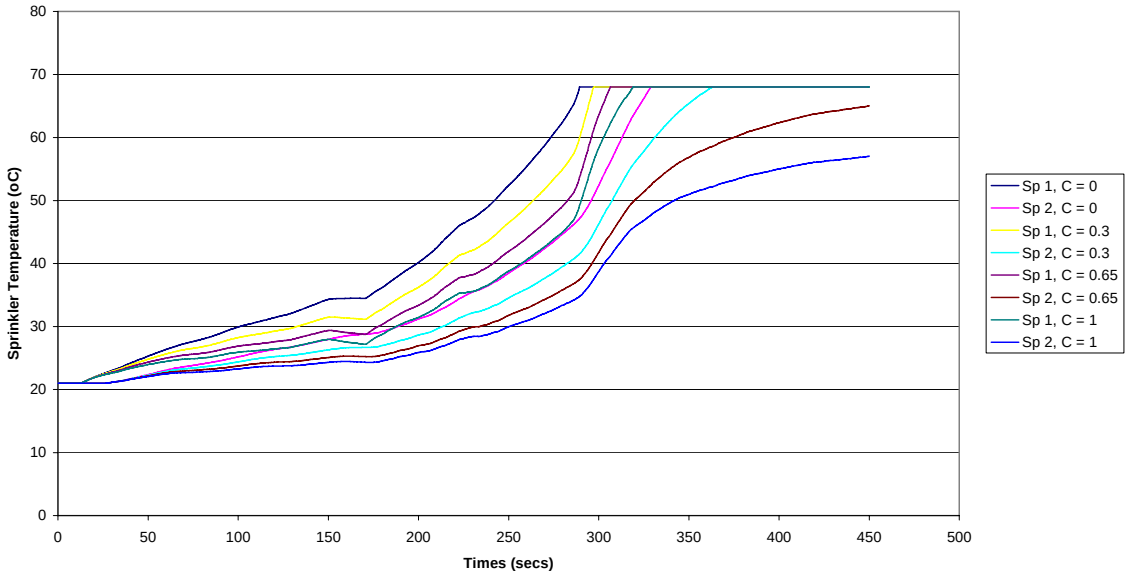

Experiment 17

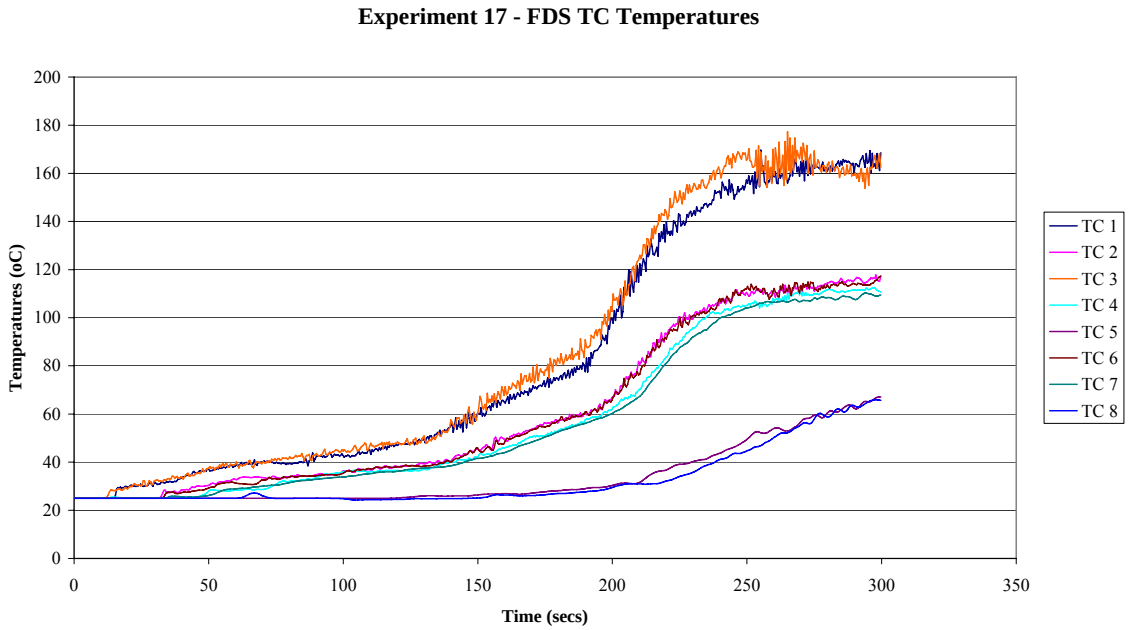

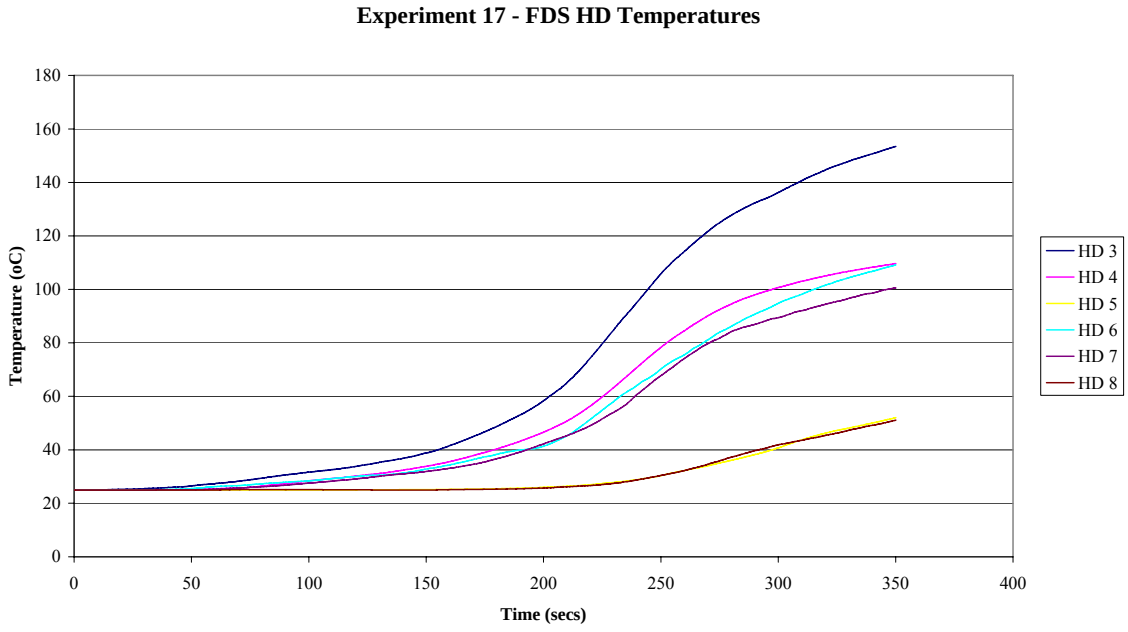

Experiment 17 - FDS HRR

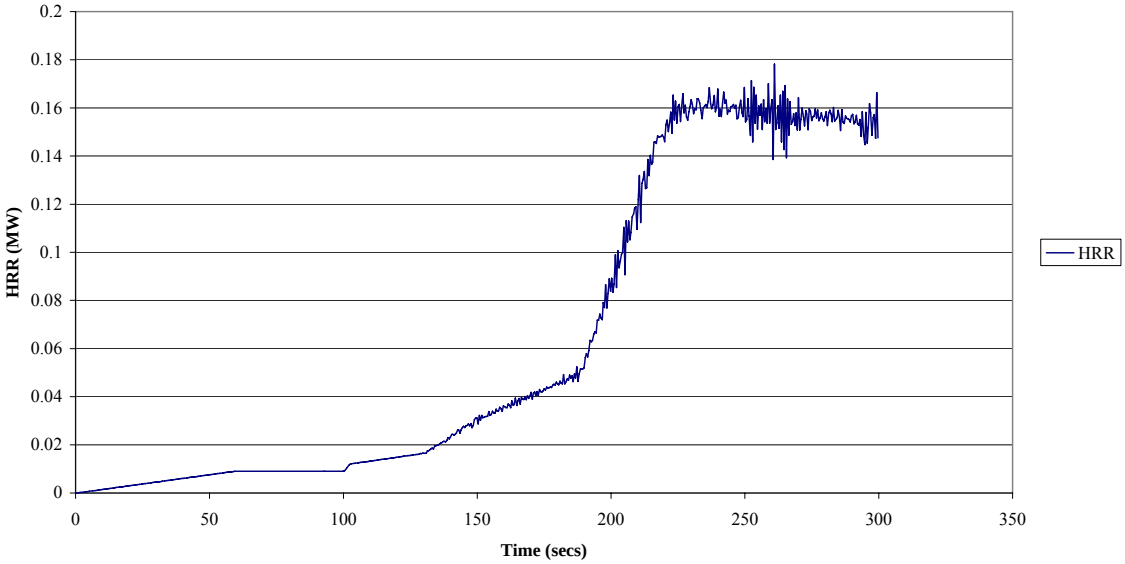

Experiment 17 - FDS Sprinkler Activation Times

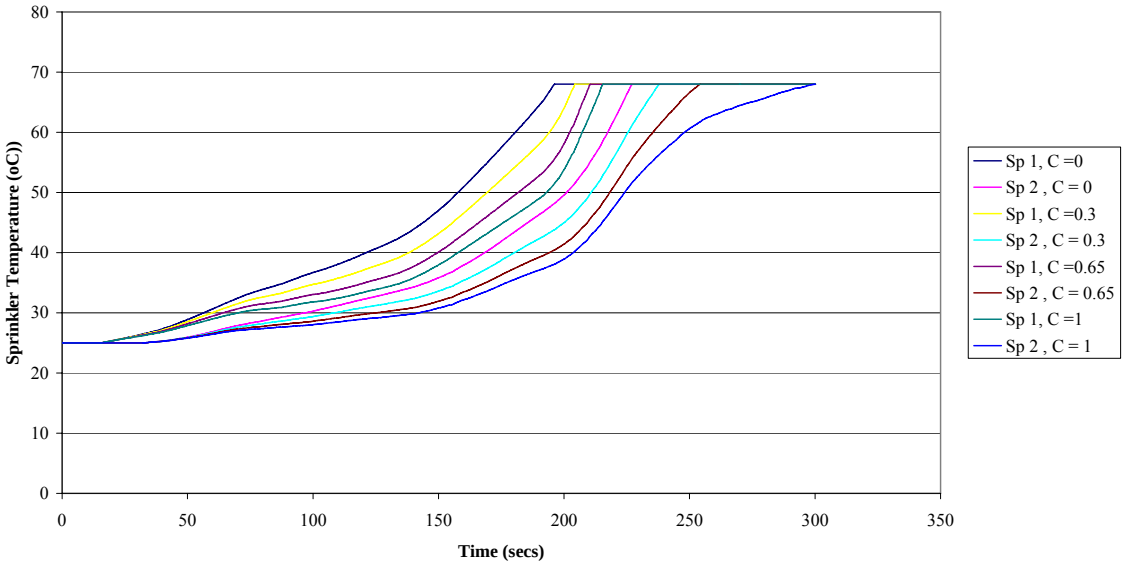

Experiment 18

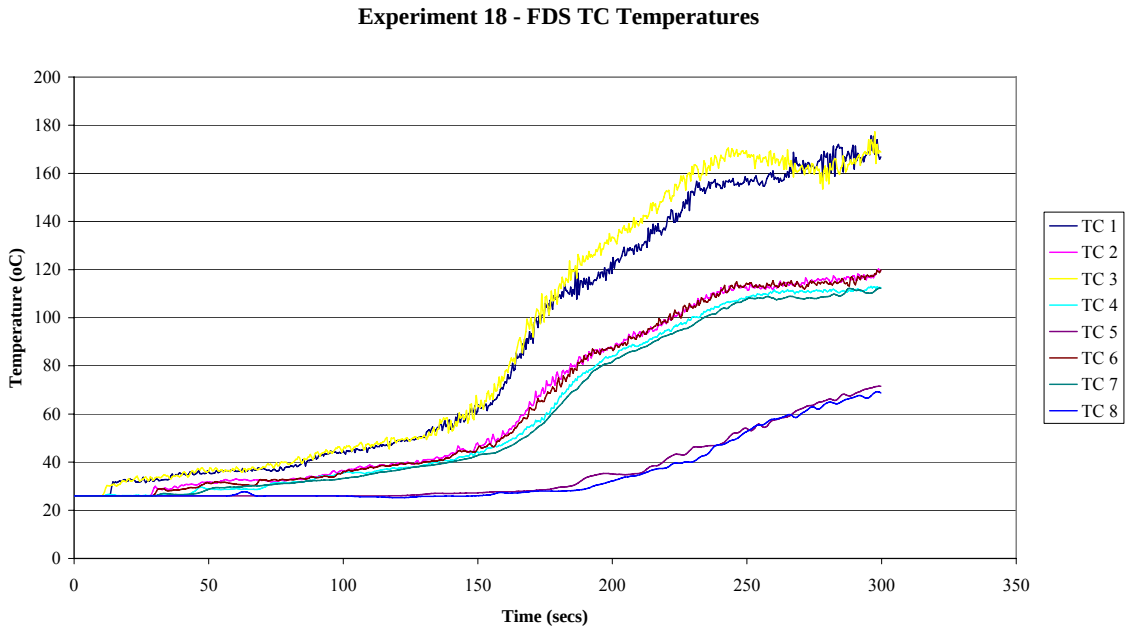

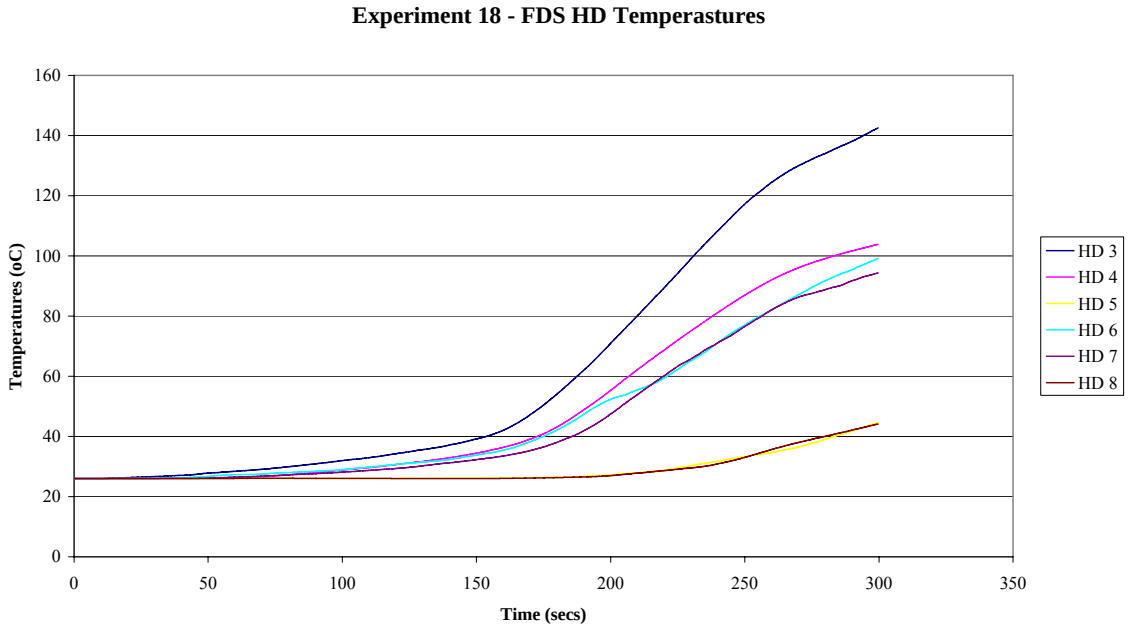

Experiment 18 - FDS HRR

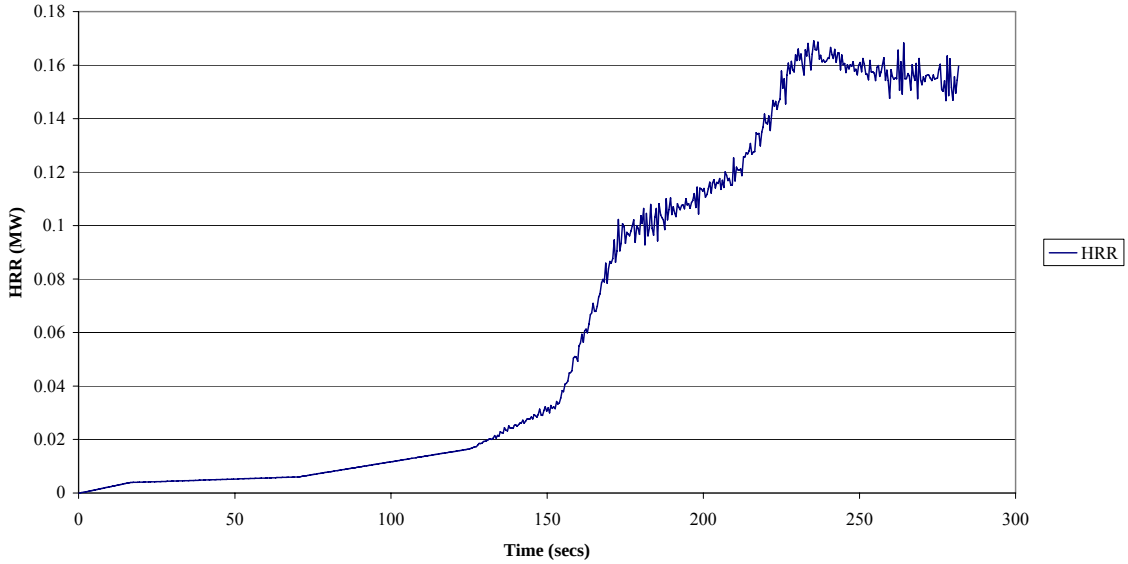

Experiment 18 - FDS Sprinkler Activation Time

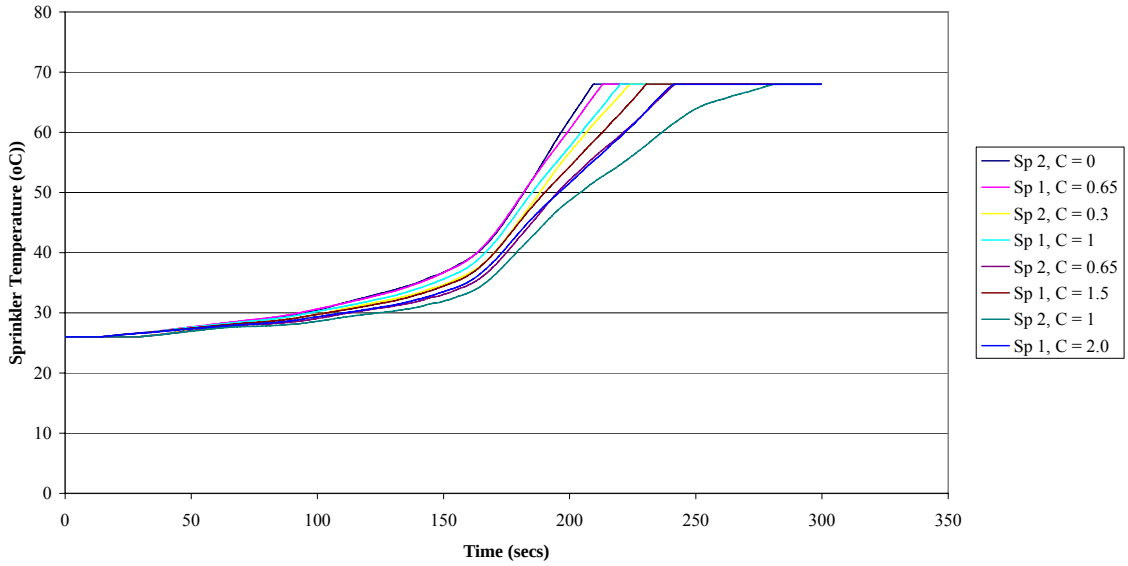

Experiment 19

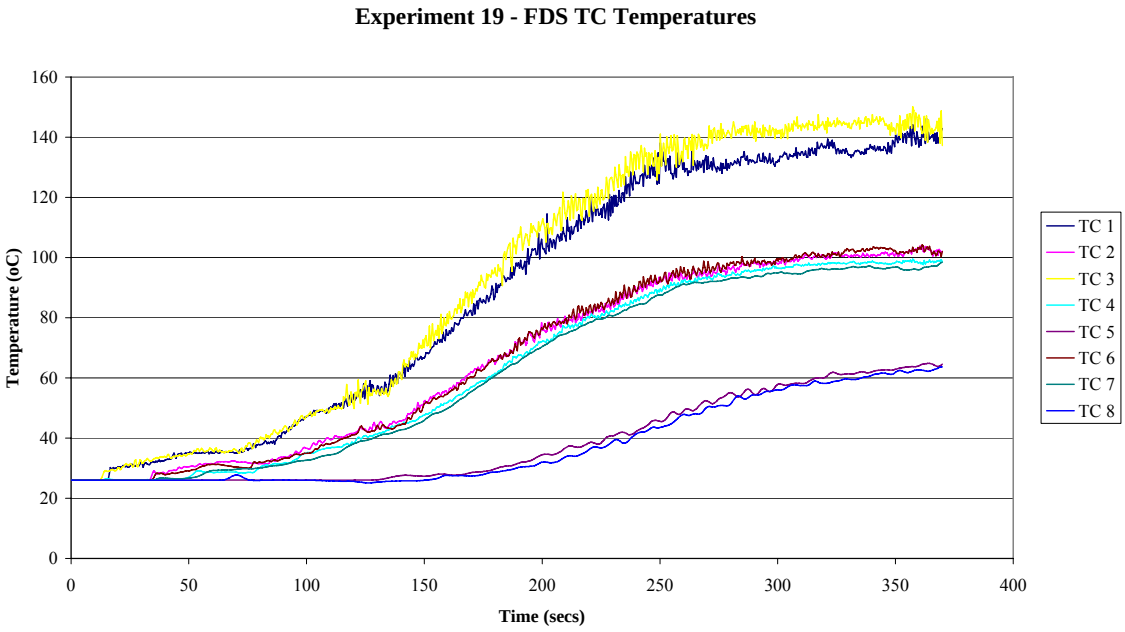

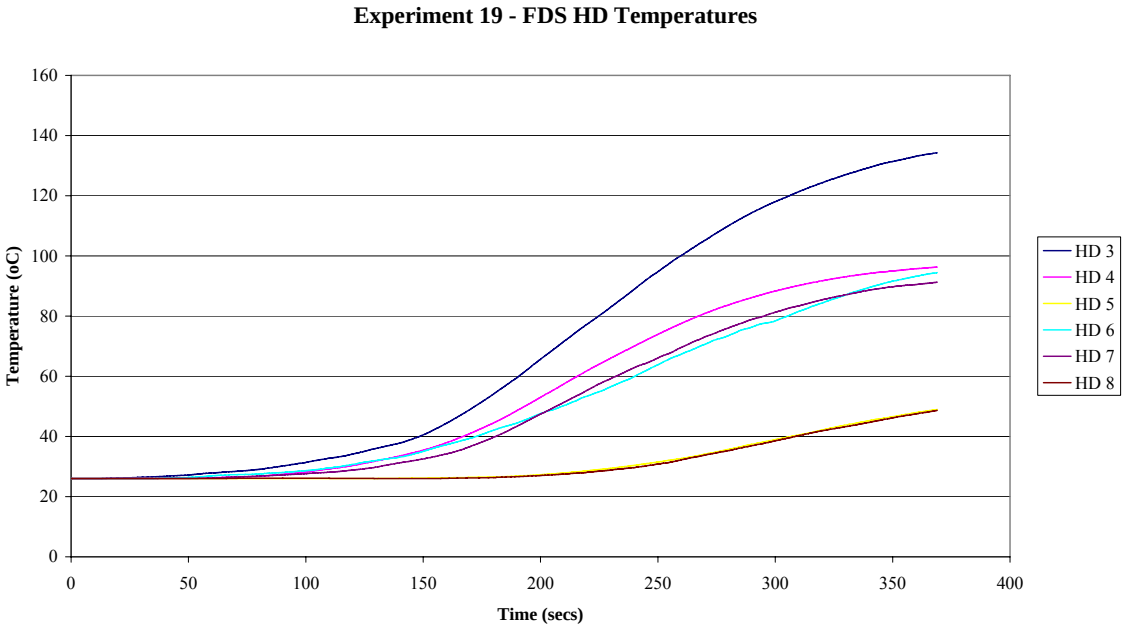

Experiment 19 - FDS HRR

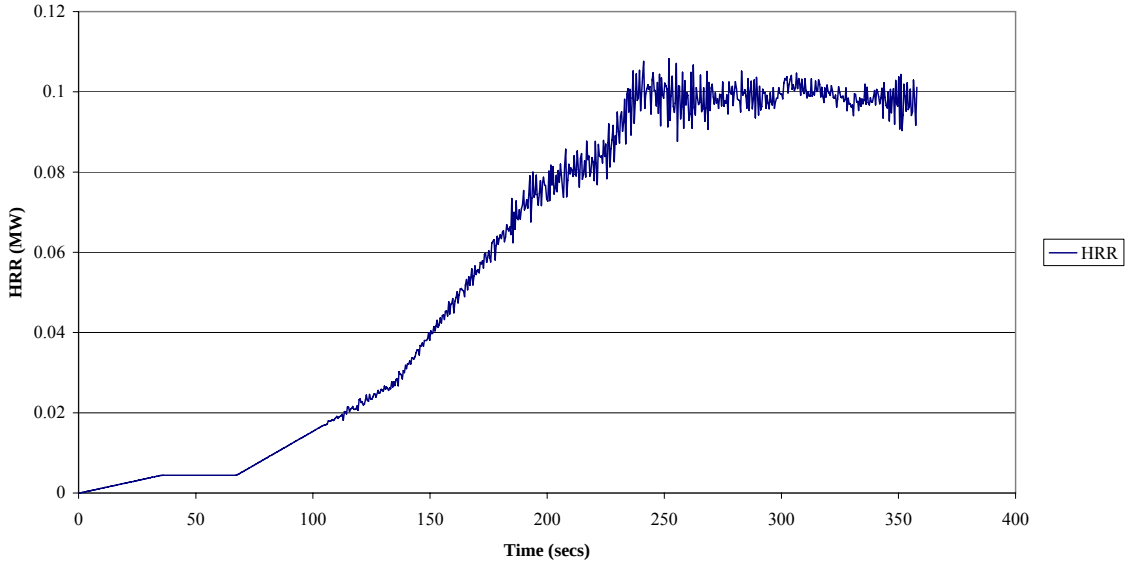

Experiment 19 - Sprinkler Activation Times

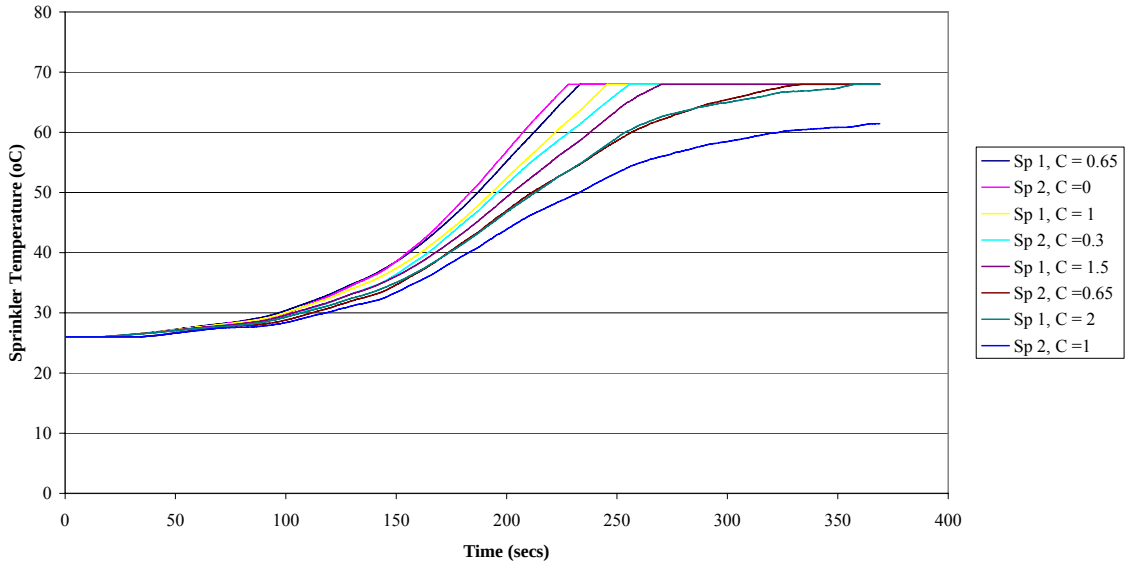

Experiment 20

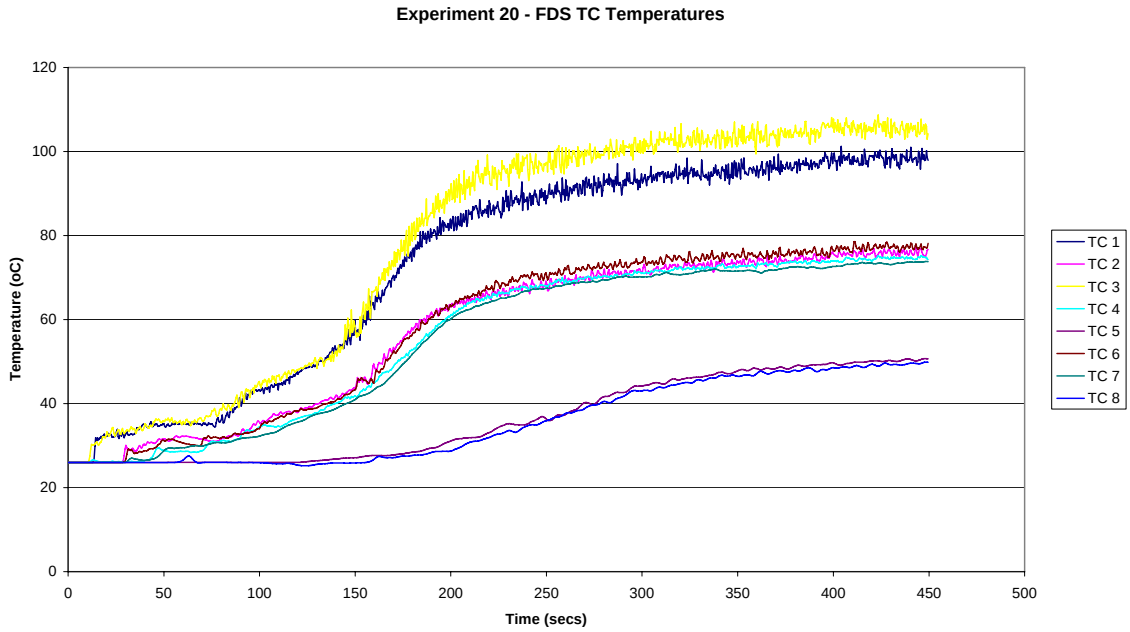

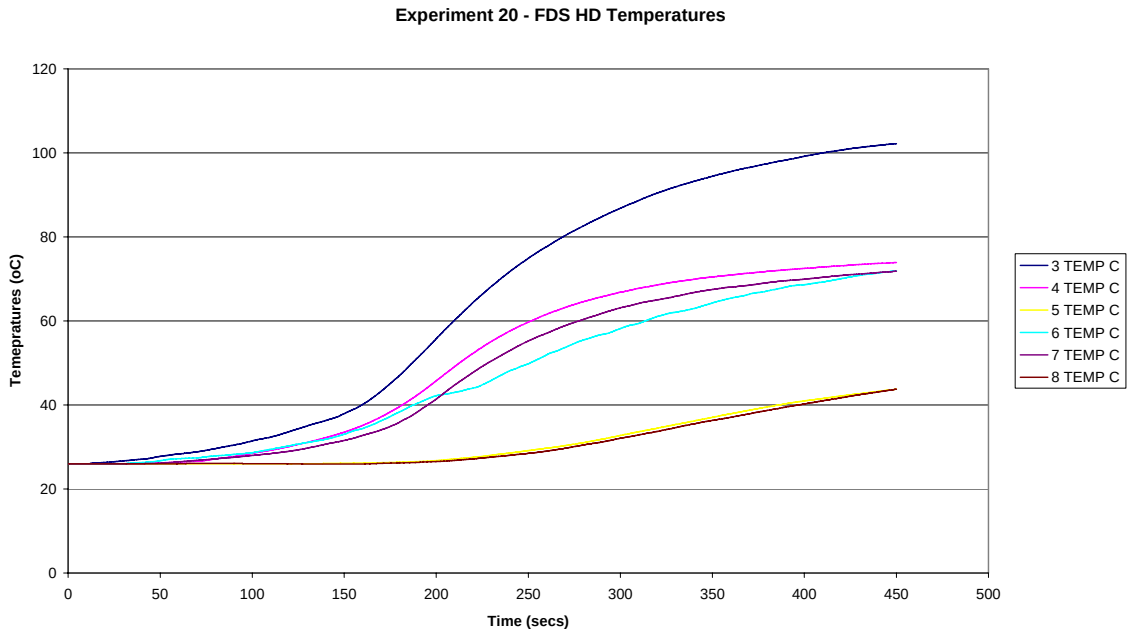

Experiment 20 - FDS HRR

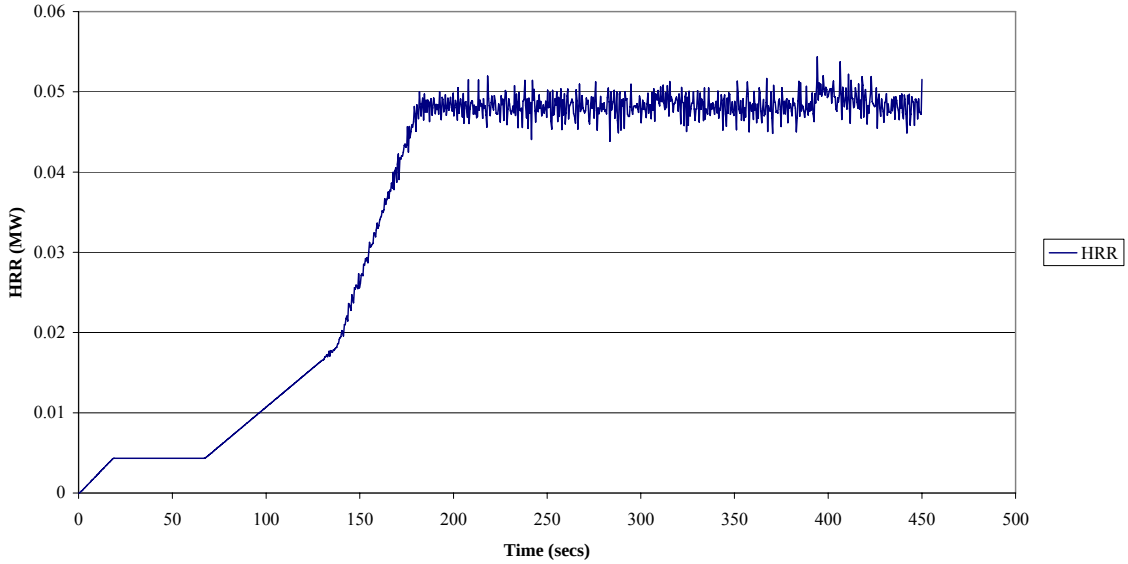

Experiment 20 - FDS Sprinkler Activation Times

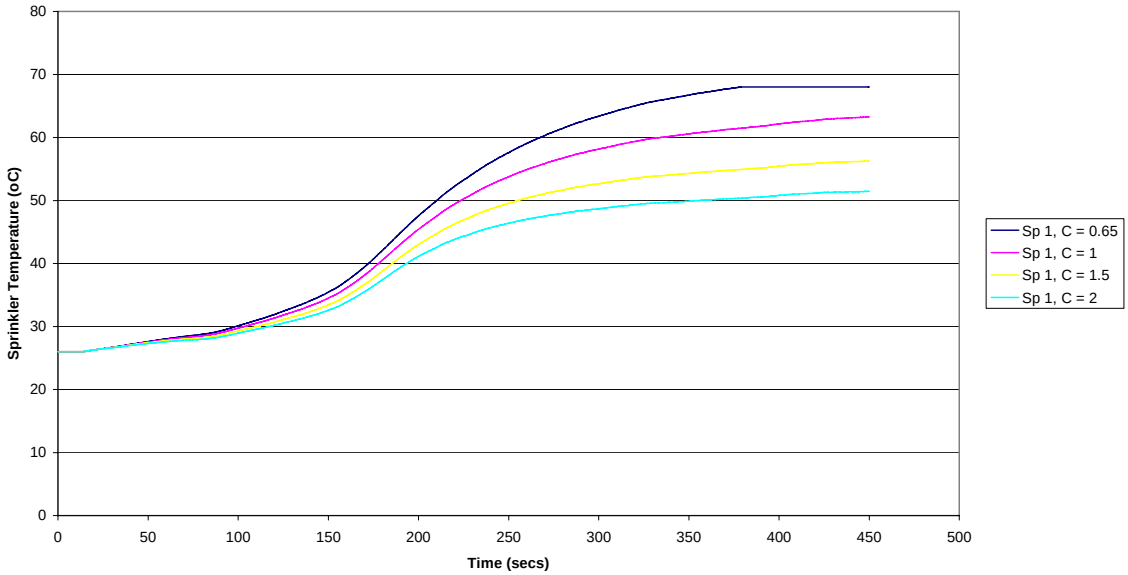

Experiment 21

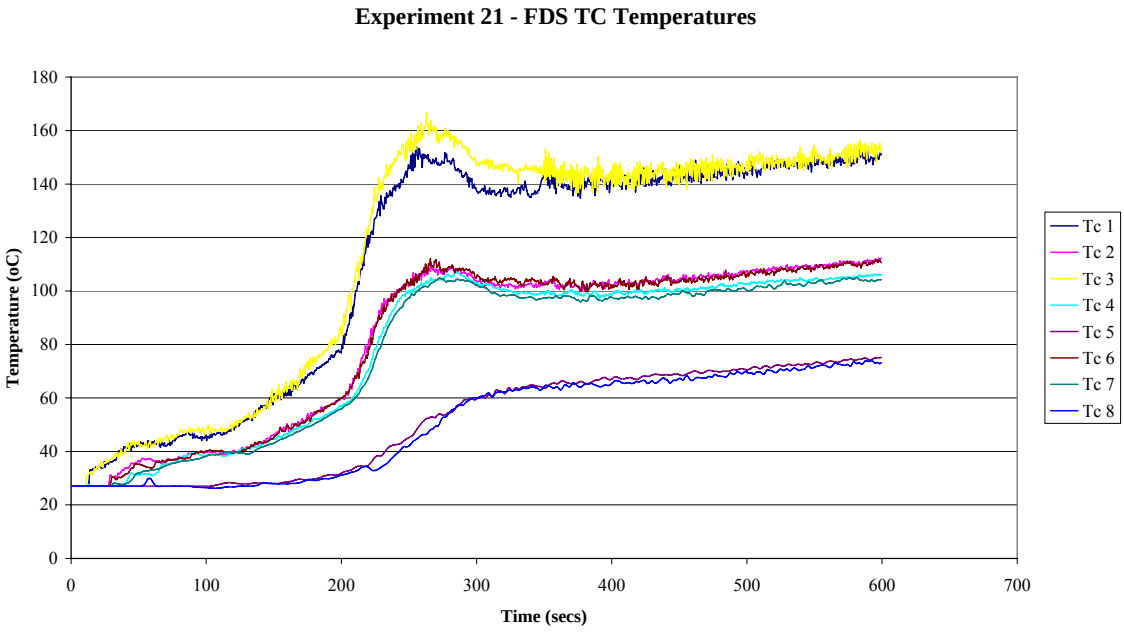

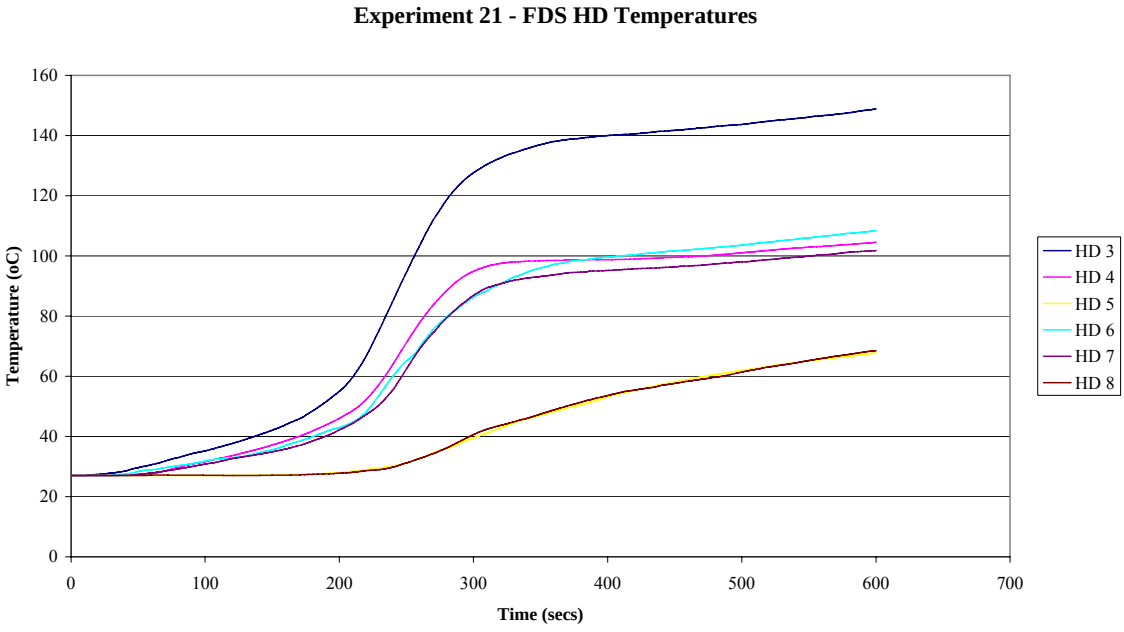

Experiment 21 - FDS HRR

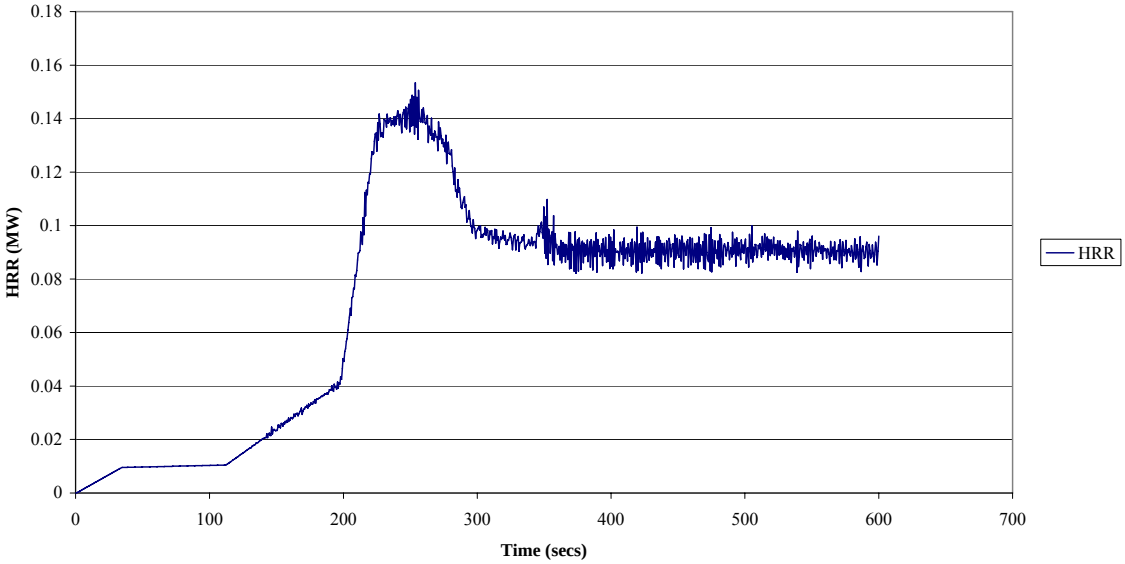

Experiment 20 - FDS Sprinkler Activation Times

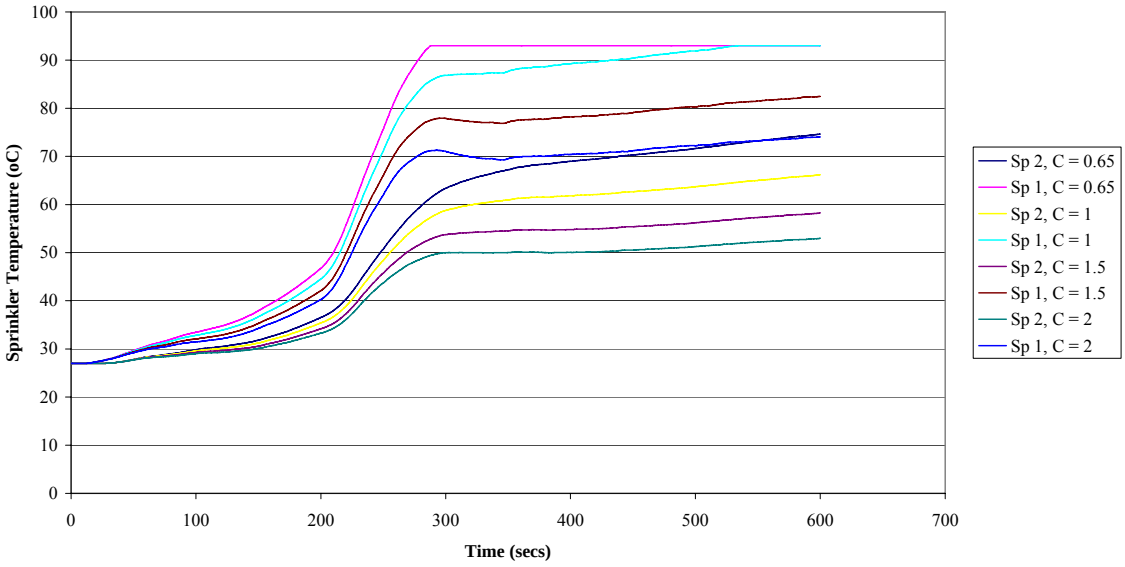

Experiment 22

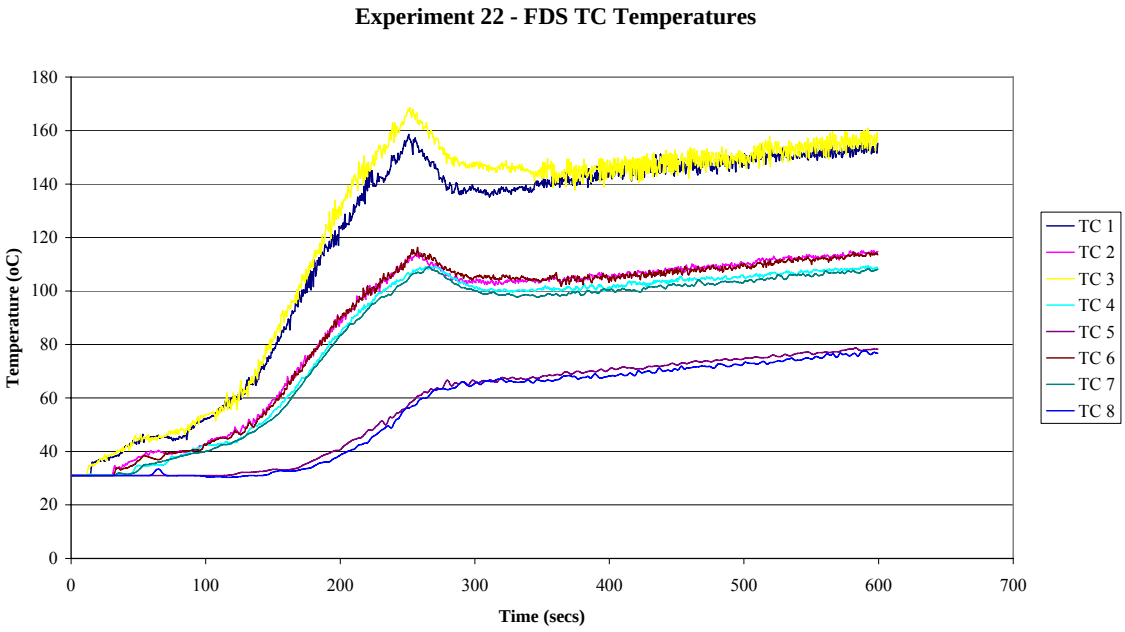

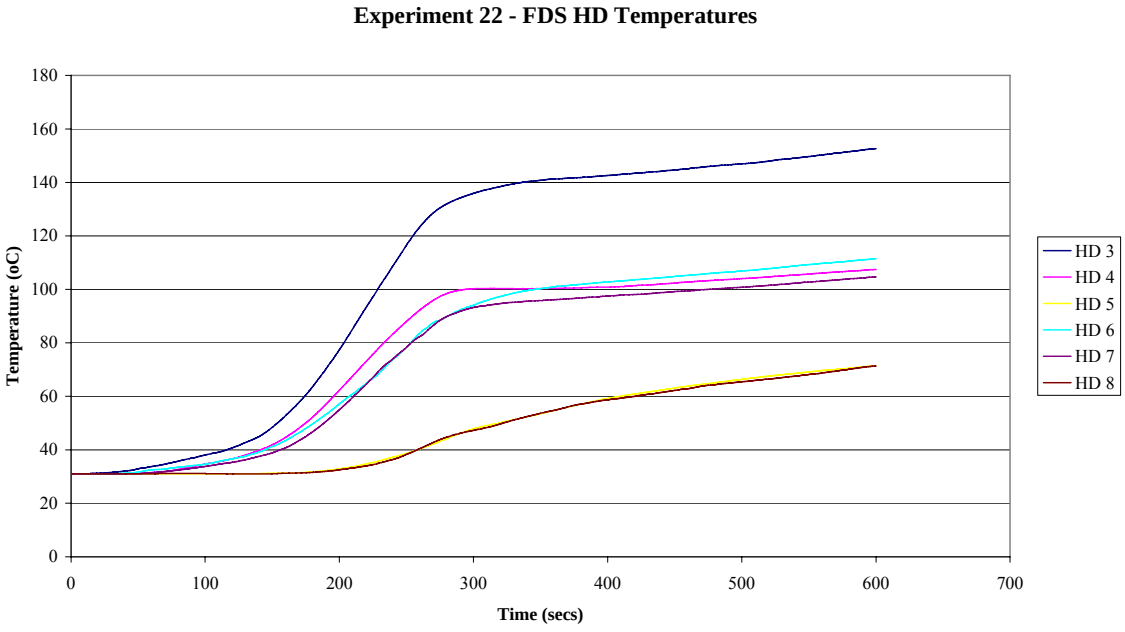

Experiment 22 - FDS HRR

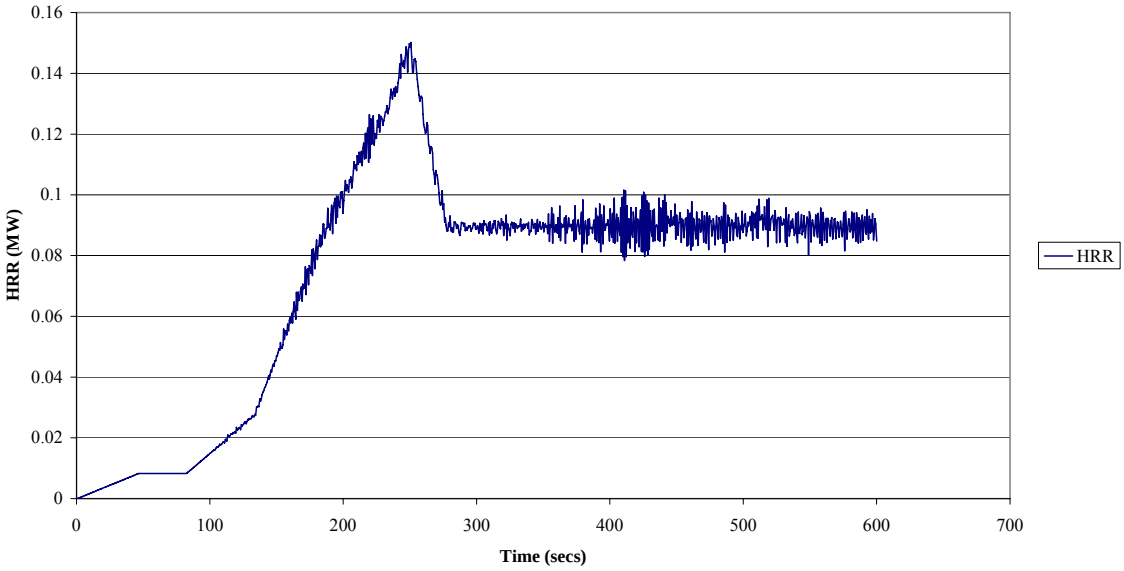

Experiment 22 - FDS Sprinkler Activation Times

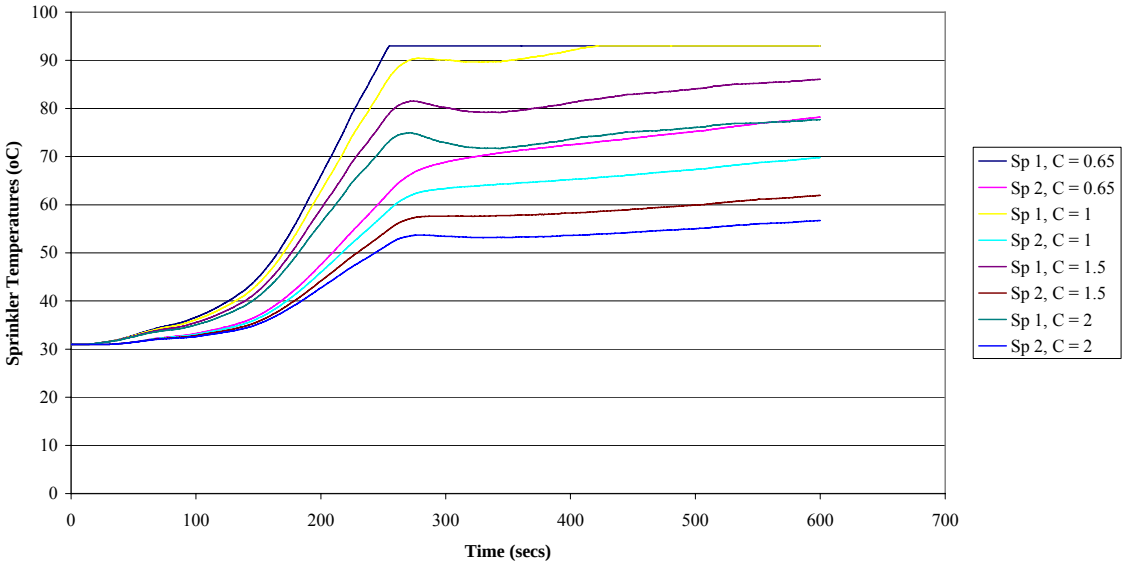

Predicted Sprinkler Activation Times

Residential Sprinkler Head								
c-factor	0		0.3		0.65		1	
Sprinkler	1	2	1	2	1	2	1	2
1	247	245	266	262	291	288	324	333
2	213	221	229	234	262	258	293	313
3	195	203	209	213	227	226	247	237
7	179	188	193	201	209	212	237	244
8	196	203	209	215	224	230	262	244
9	234	236	247	245	264	255	283	265
10	188	181	200	196	212	211	225	237
12		234		251		269		295
13		198		212		229		239
14		213		226		242		252
15		265		280		295		315
16	289	328	297	363	306	450	319	450
17	191	227	204	238	210	254	215	299
18		213		220		230		241
19		228		256		334		450

Standard Response Sprinkler Heads								
c-factor	0.65		1		1.5		2	
Sprinkler	1	2	1	2	1	2	1	2
4	264	264	277	283	284	284	284	284
5	306	299	320	314	343	354	358	372
6	243	240	256	253	273	275	313	293
12	293		332		448		450	
13	243		253		267		267	
14	270		287		305		305	
15	316		326		350		450+	
18	209		224		242		281	
19	233		245		270		357	
20	379		450		450		450	
21	288	600	535	600	600	600	600	
22	255	600	422	600	600	600	600	

Appendix C

Comparison

Experiment 1

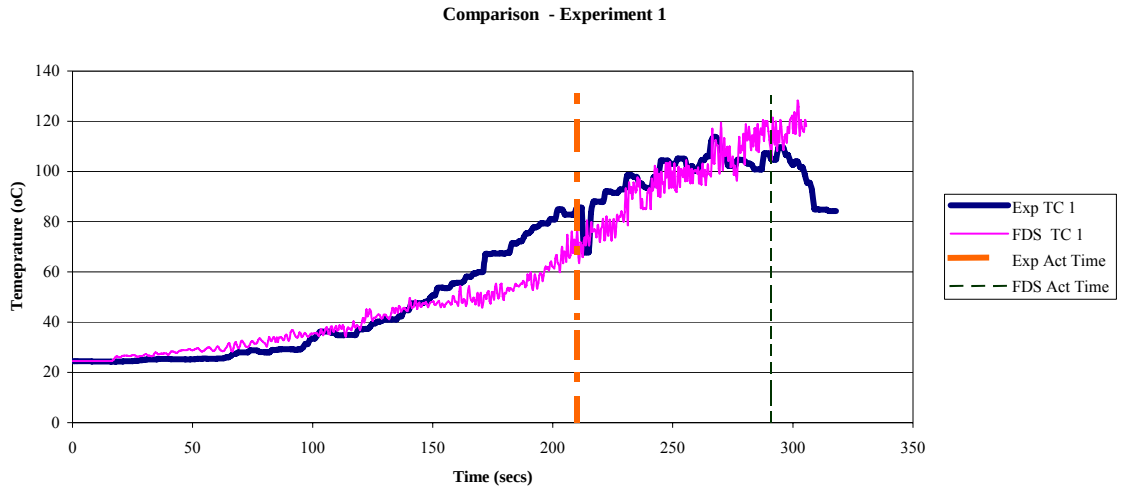

Experiment 2

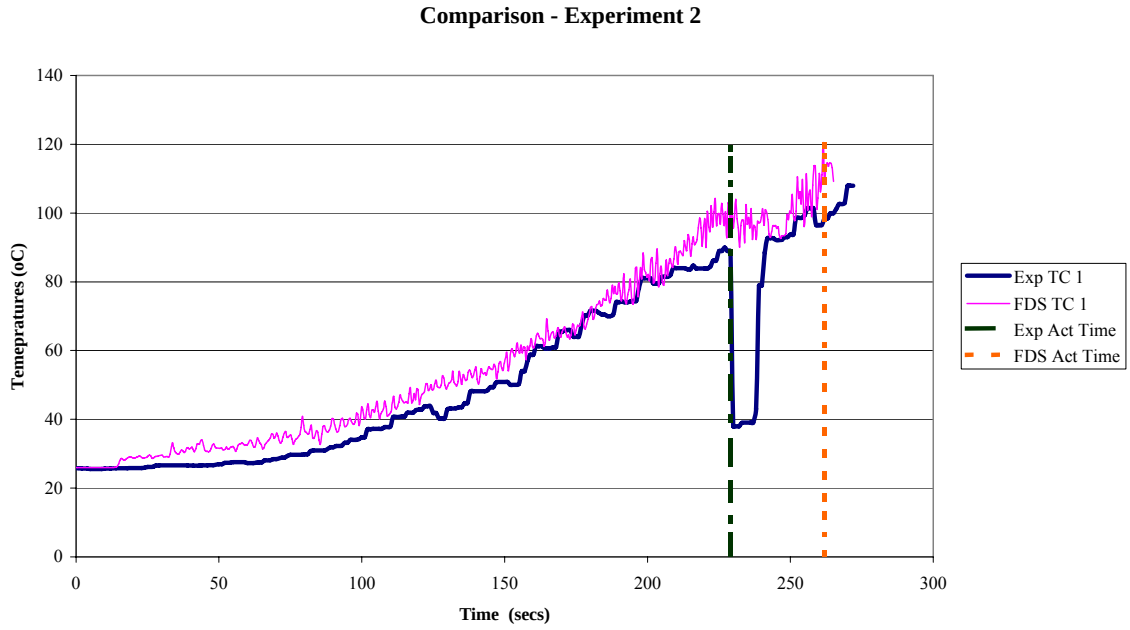

Experiment 3

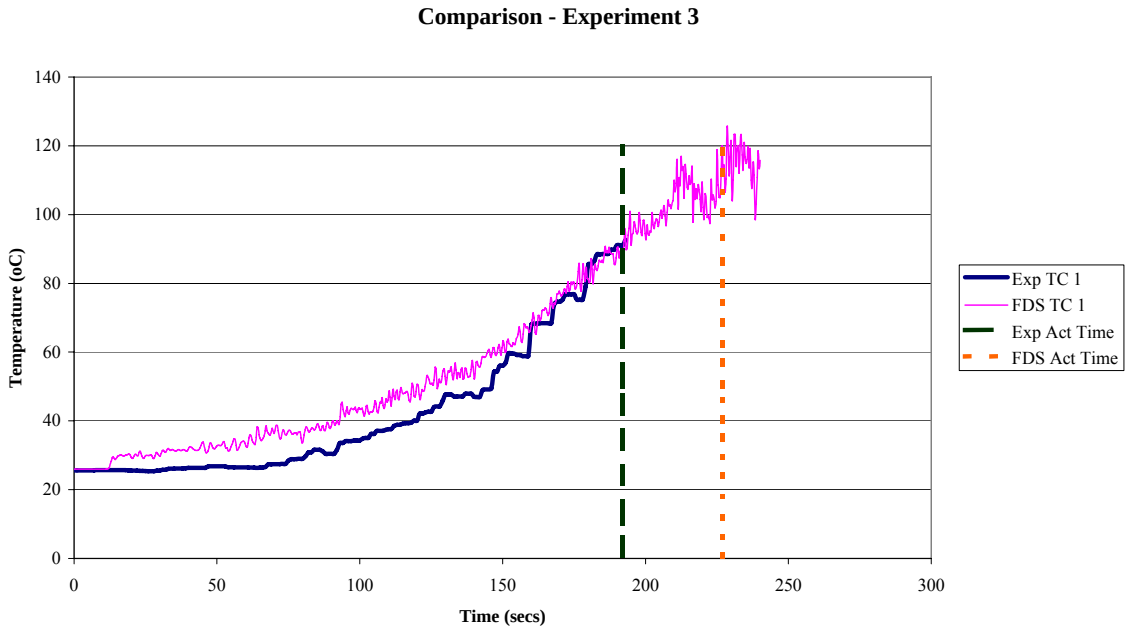

Experiment 4

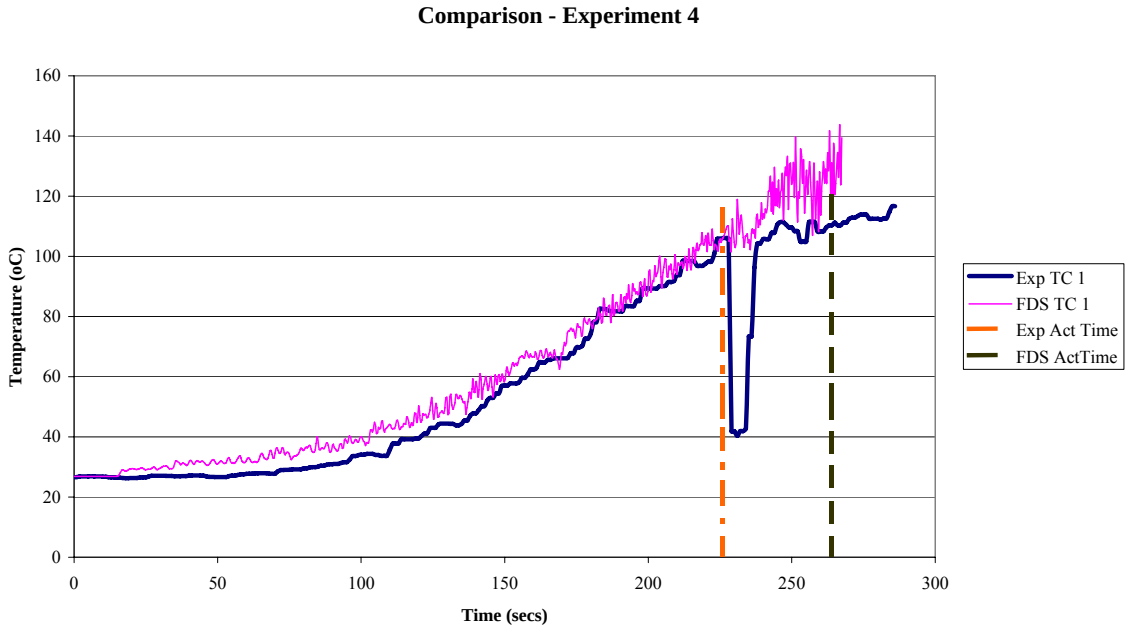

Experiment 5

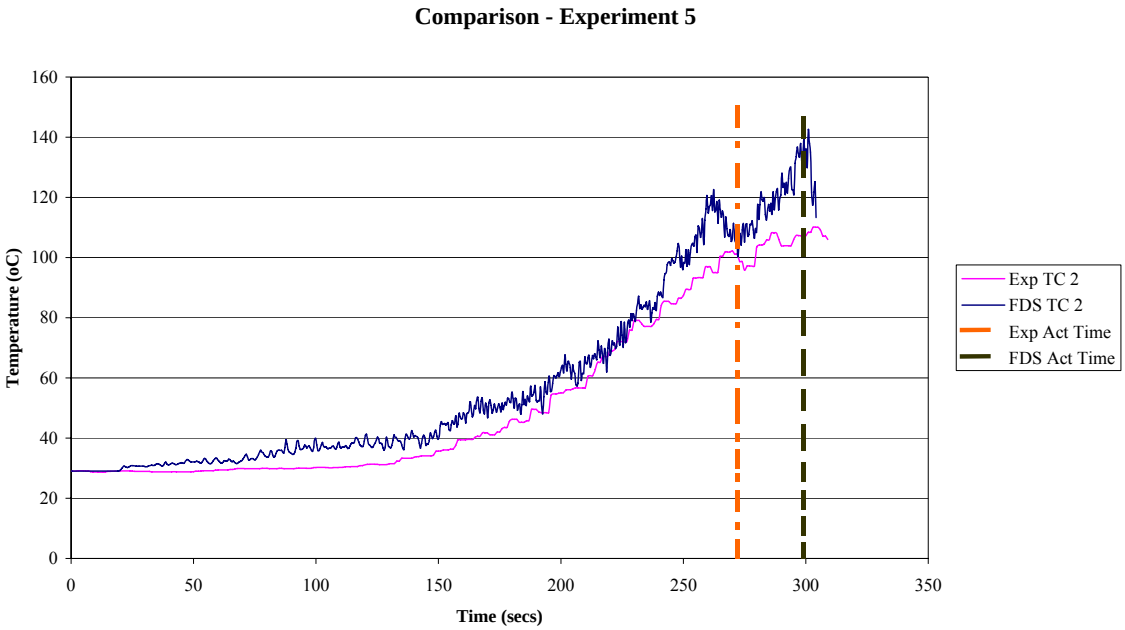

Experiment 6

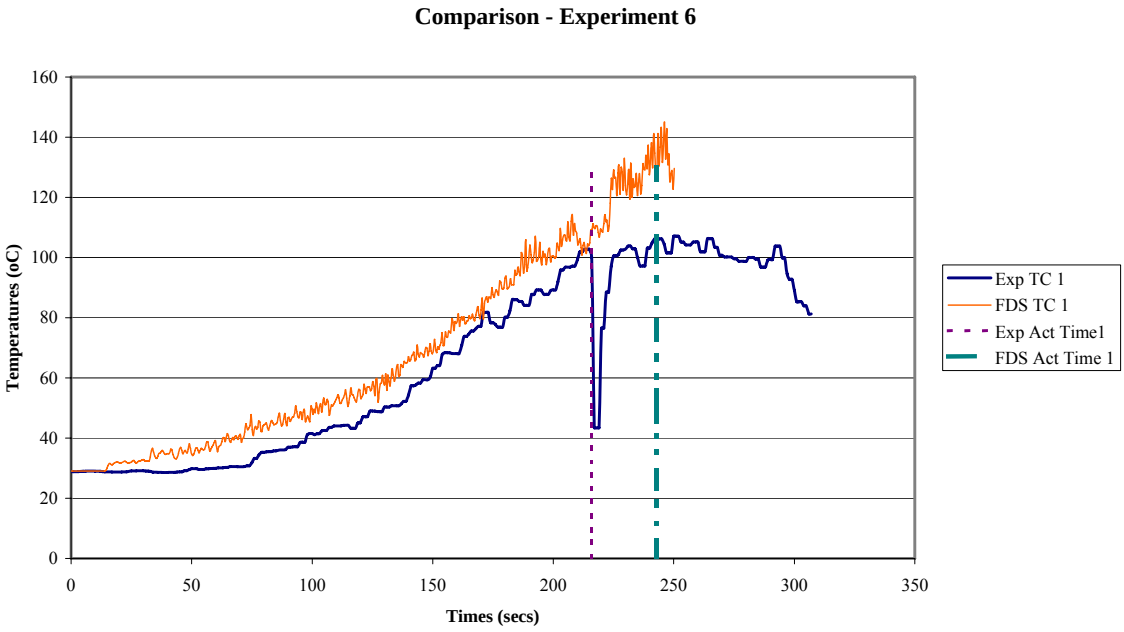

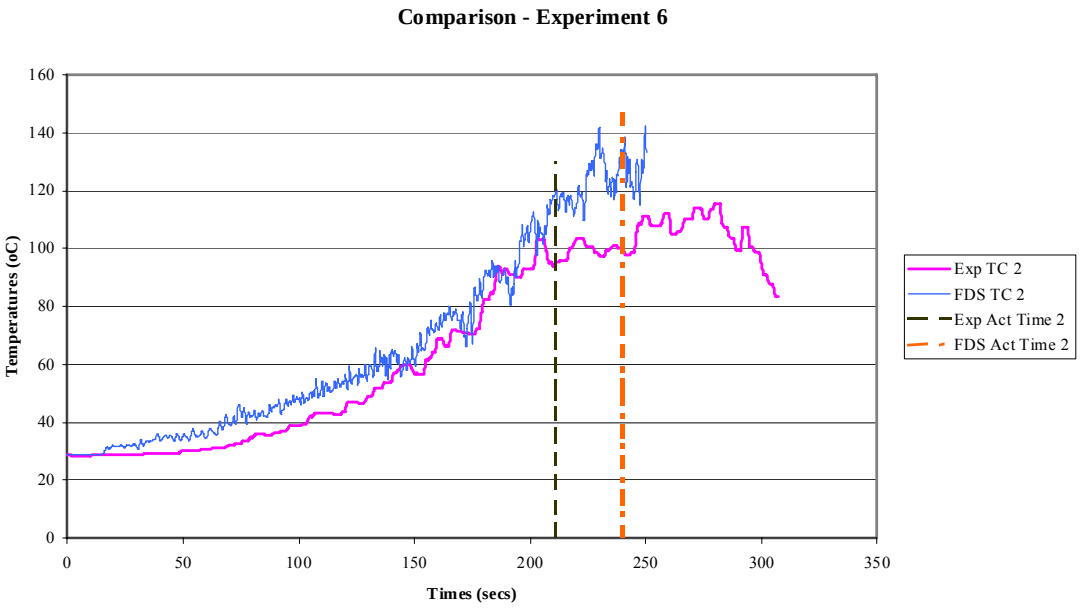

Experiment 7

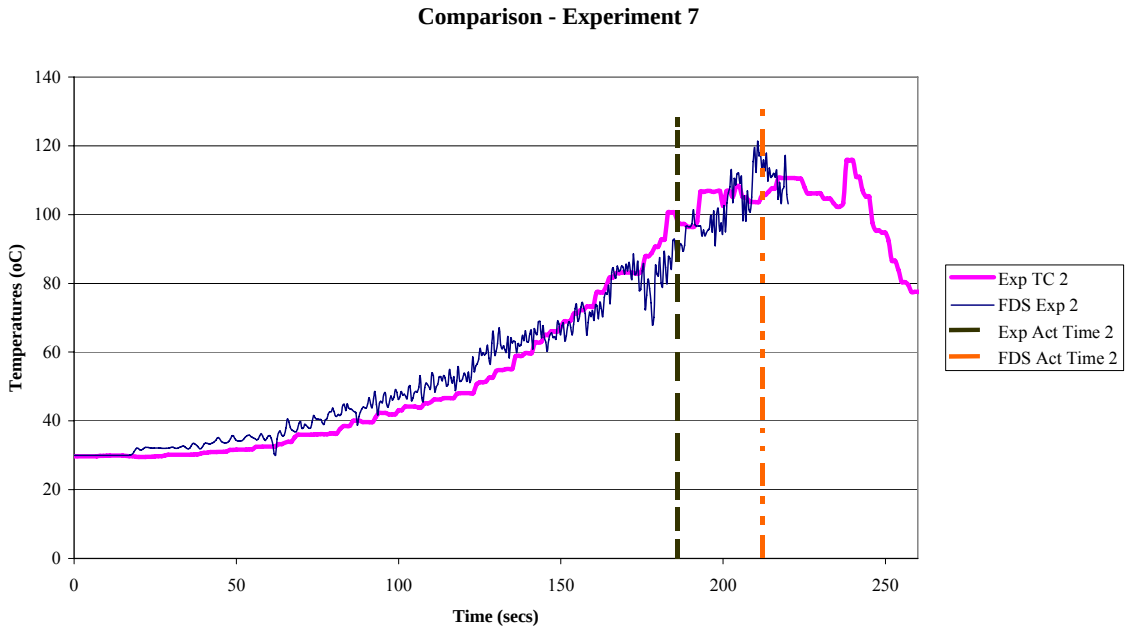

Experiment 8

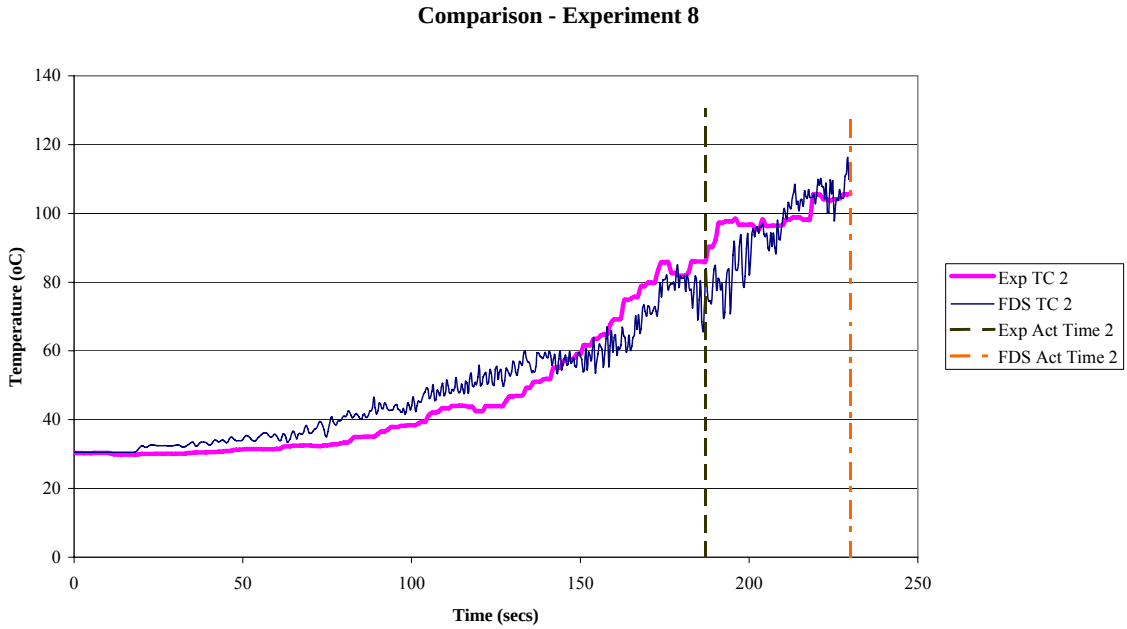

Experiment 9

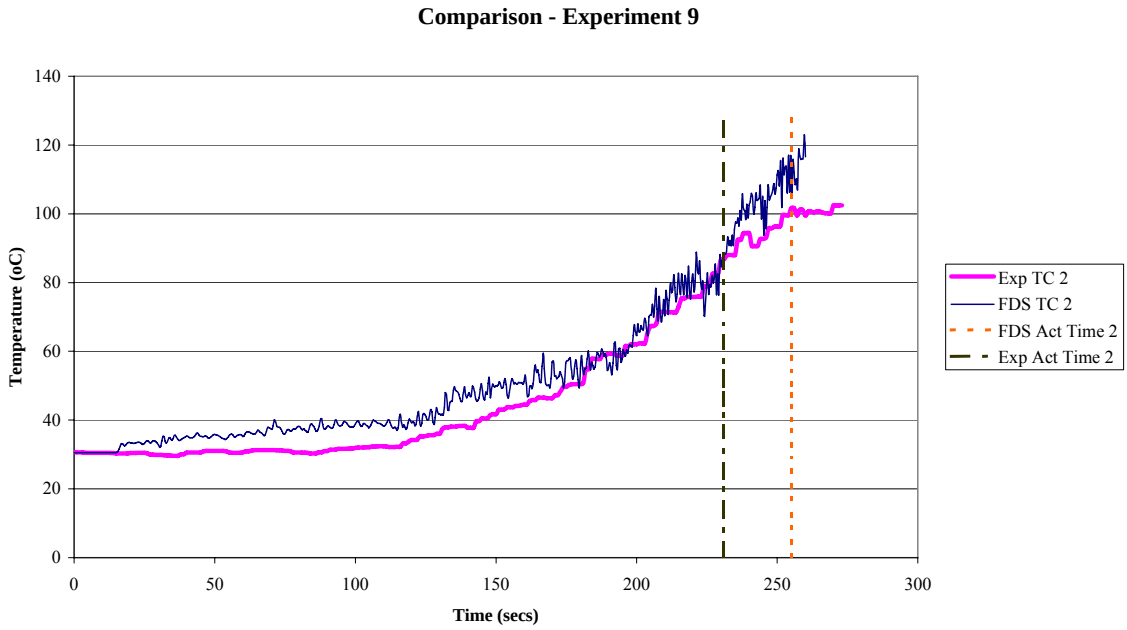

Experiment 10

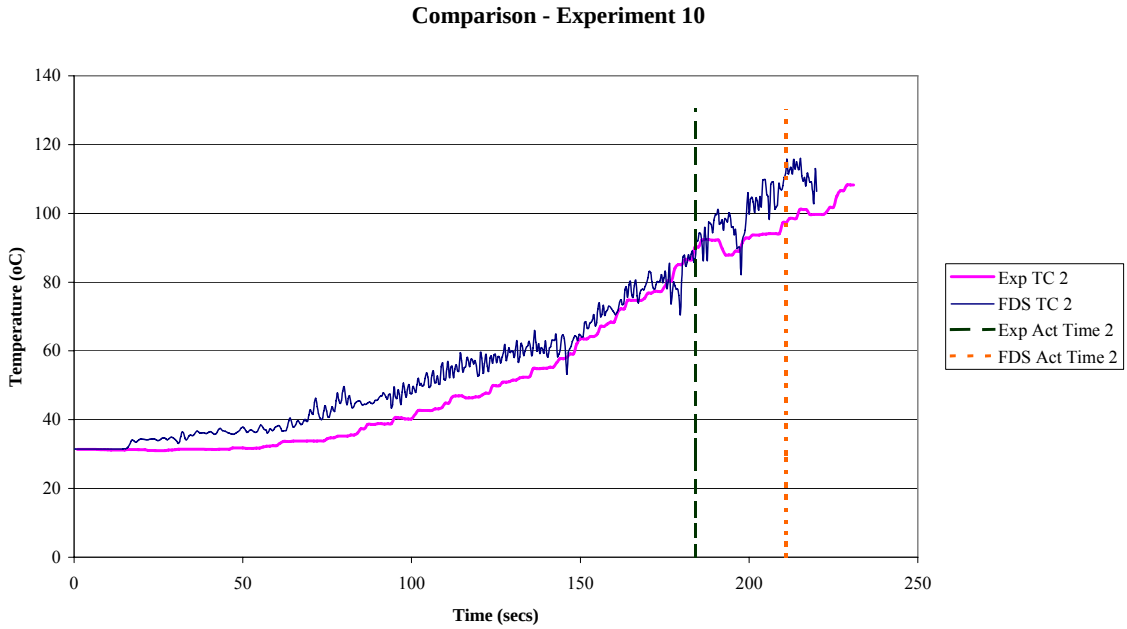

No Comparison Graphs for Experiments 11-16 due to no actual temperature data for those experiments.

Experiment 16

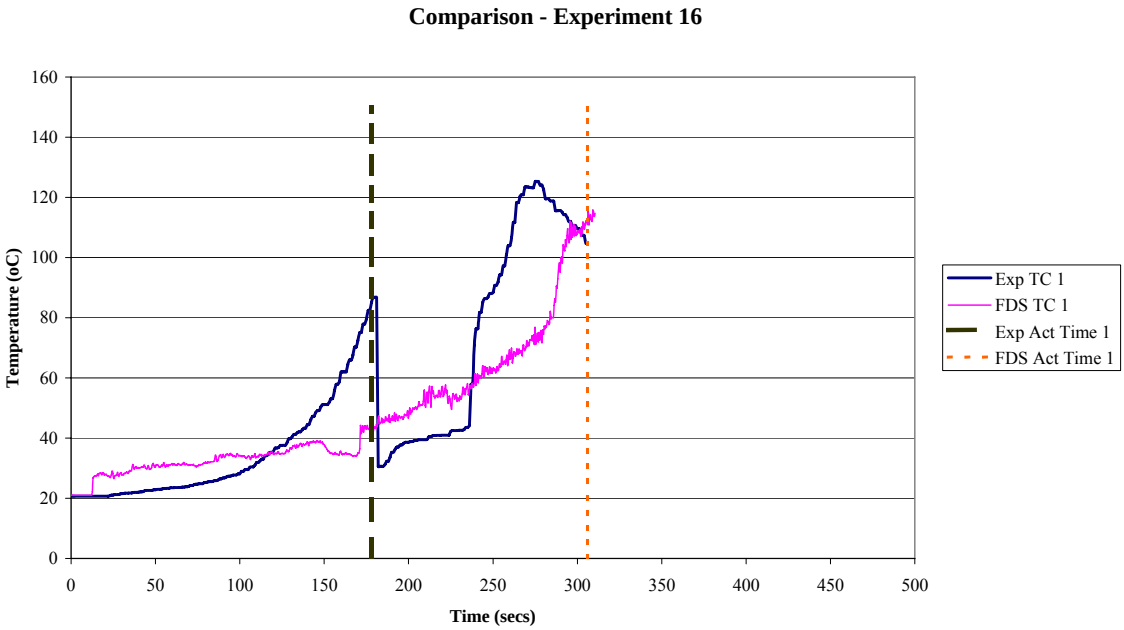

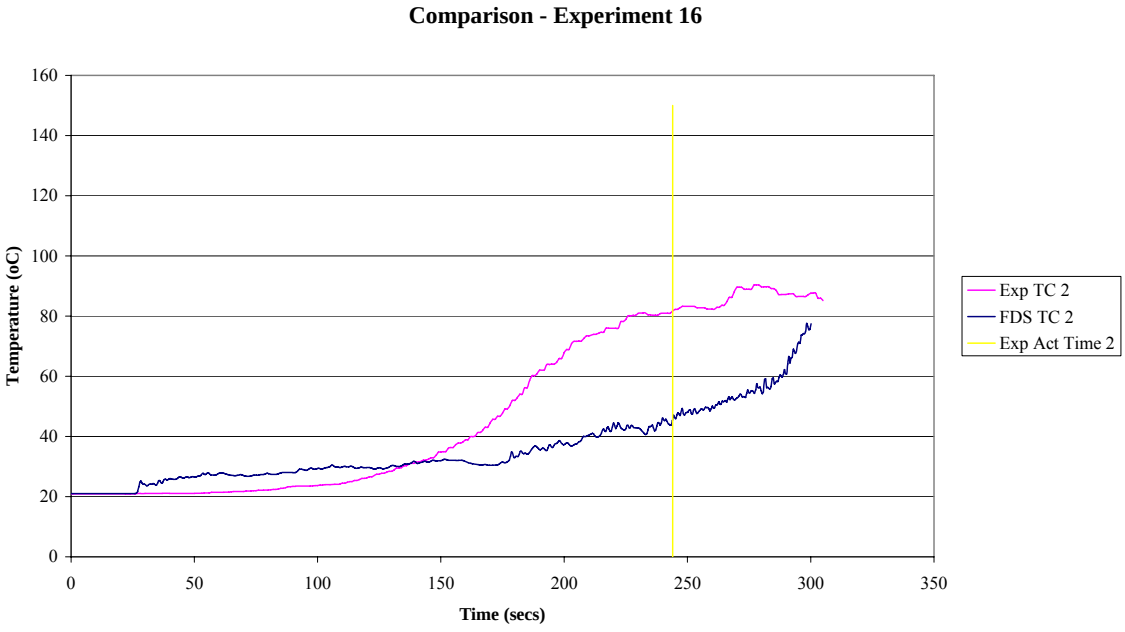

Experiment 17

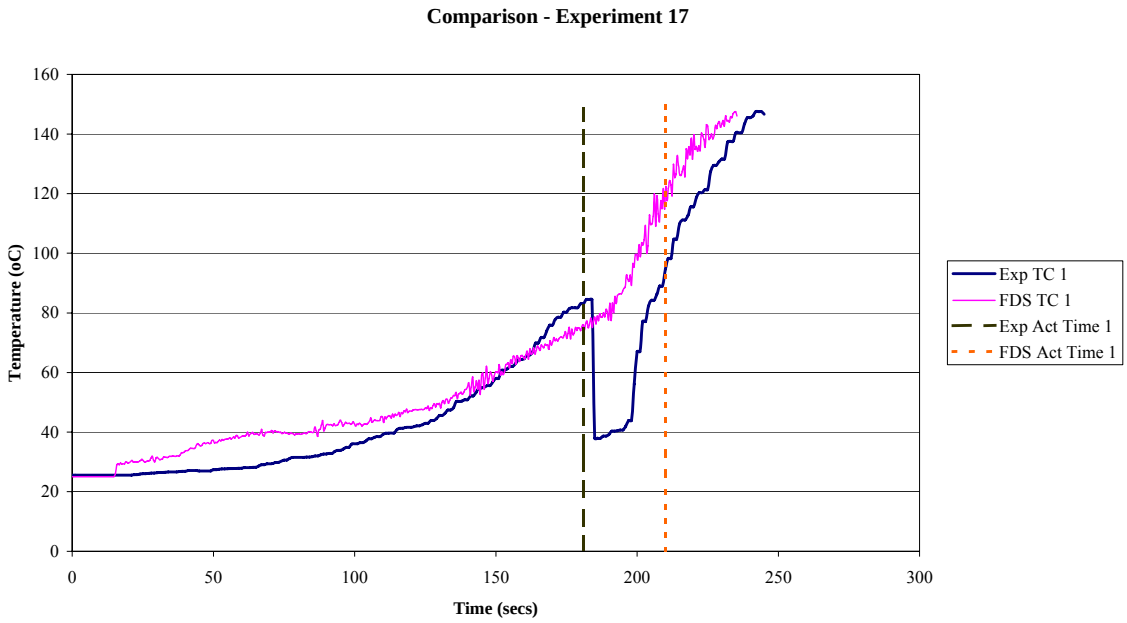

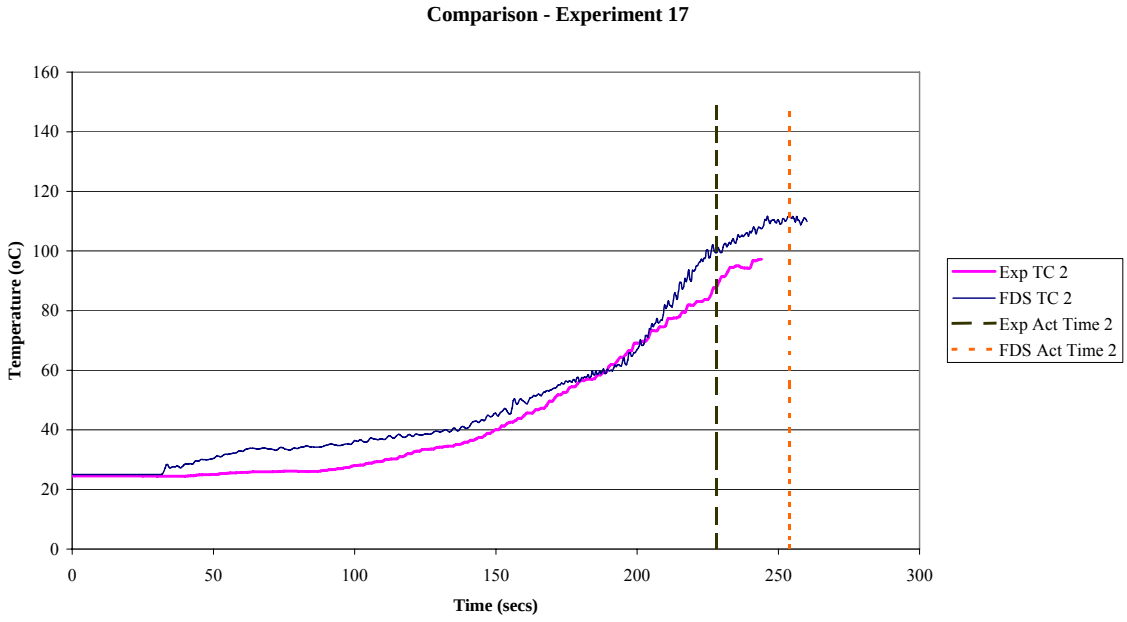

Experiment 18

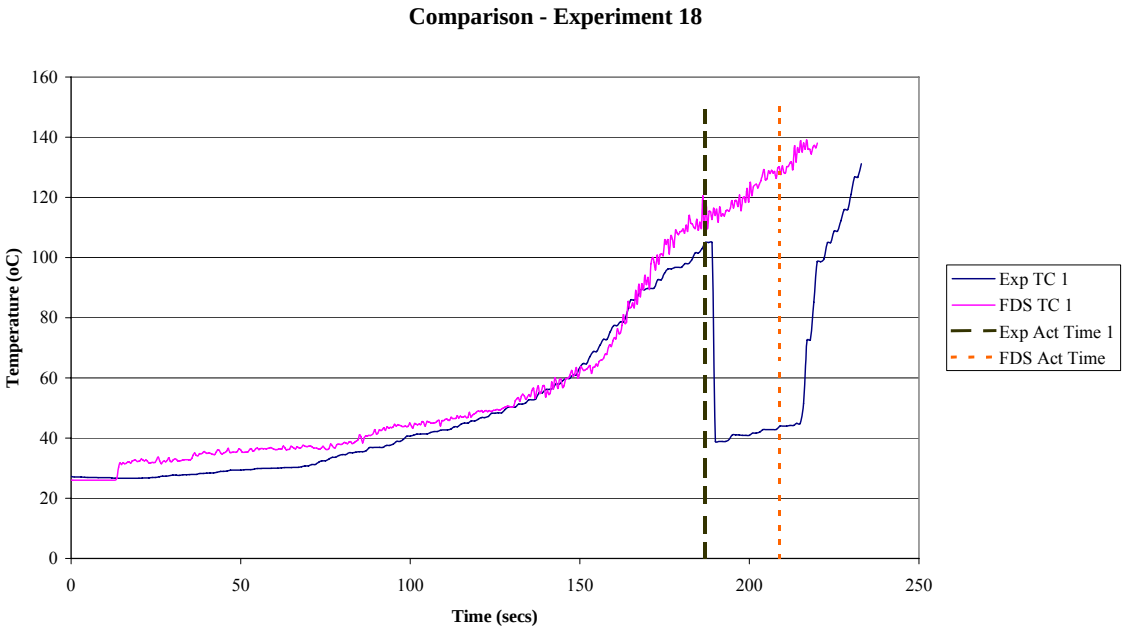

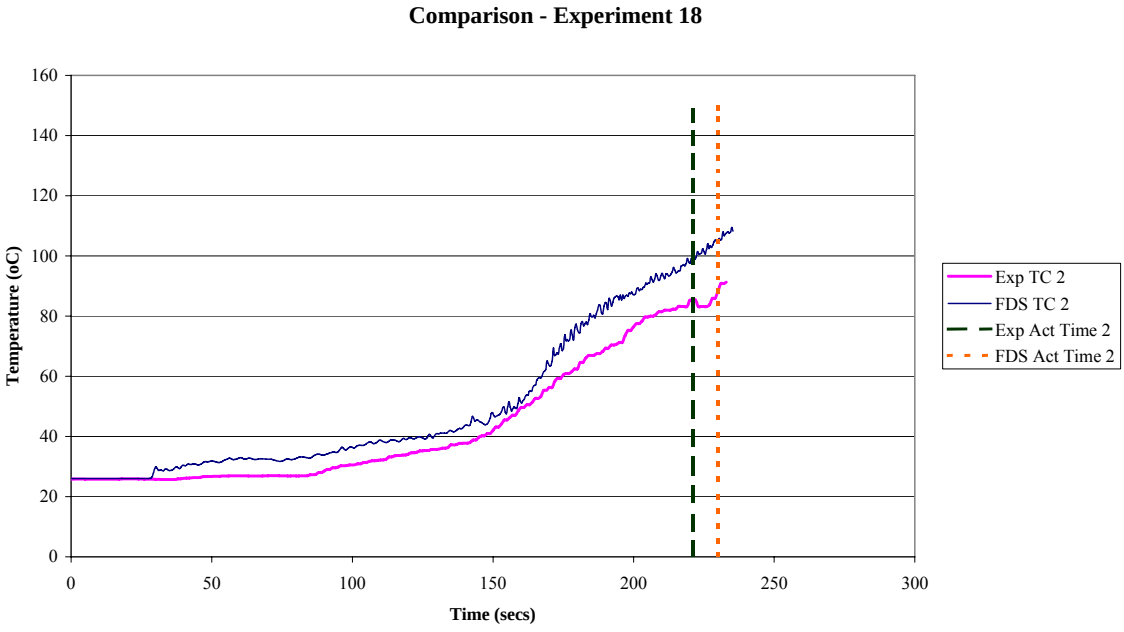

Experiment 19

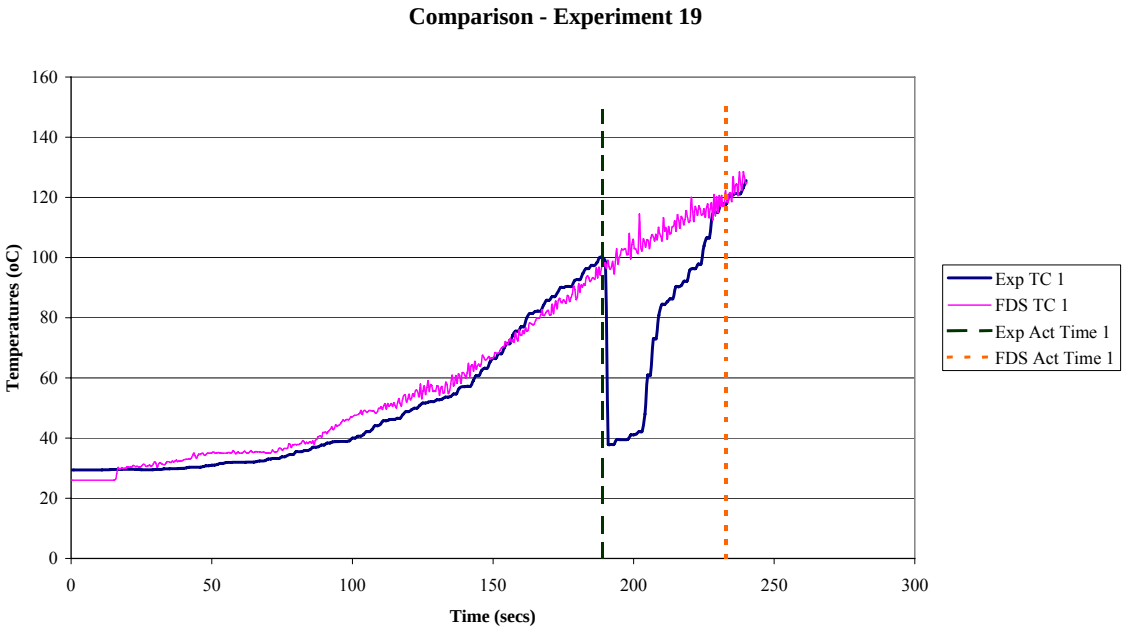

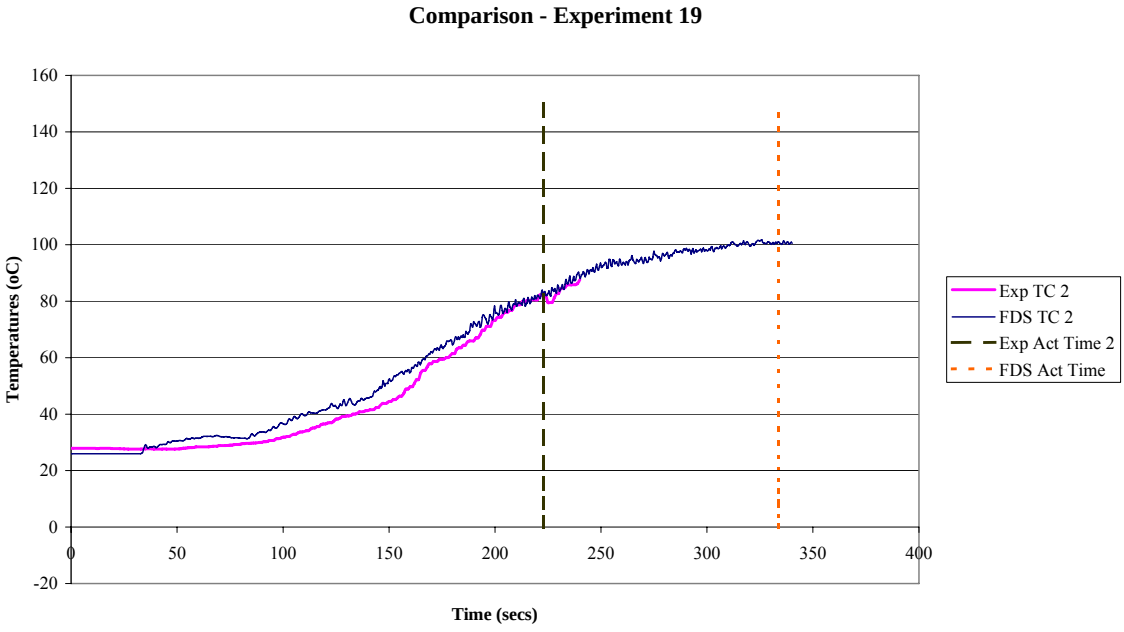

Experiment 20

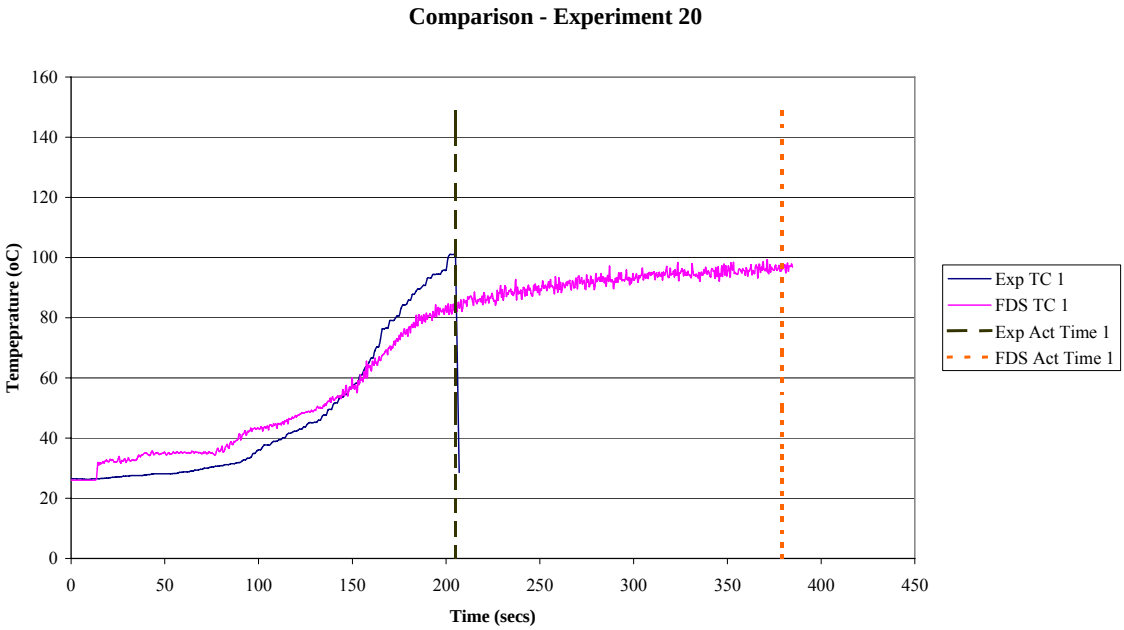

Experiment 21

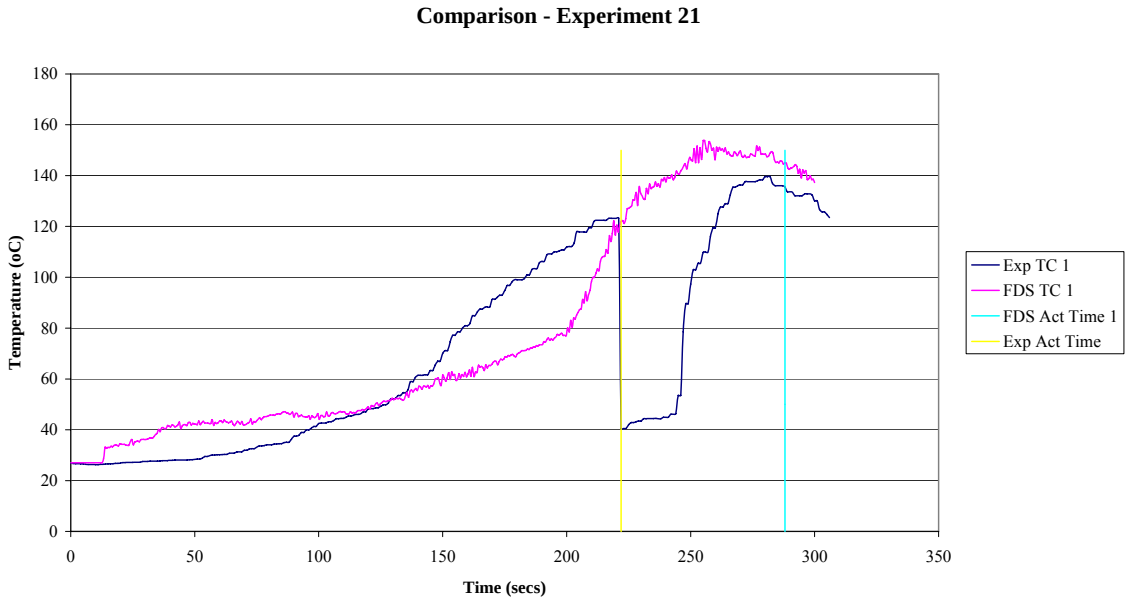

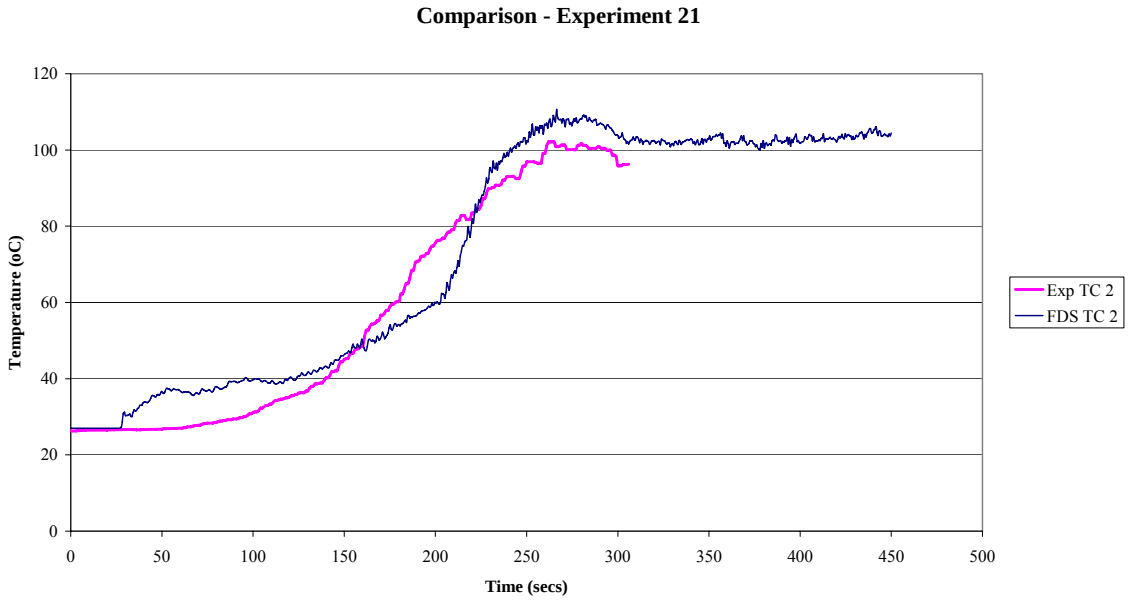

Experiment 22

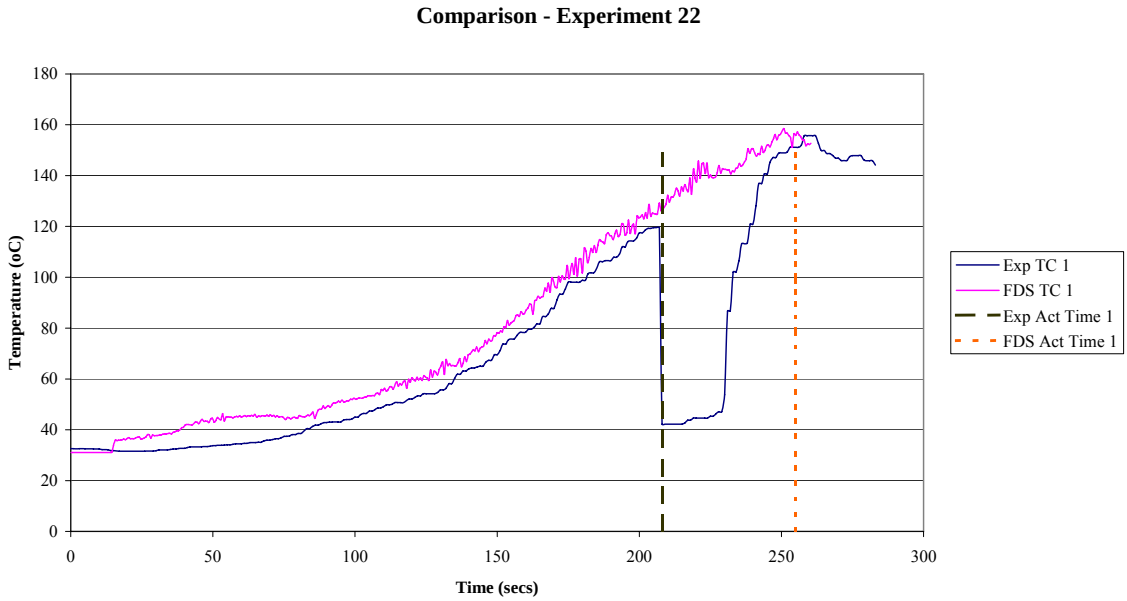

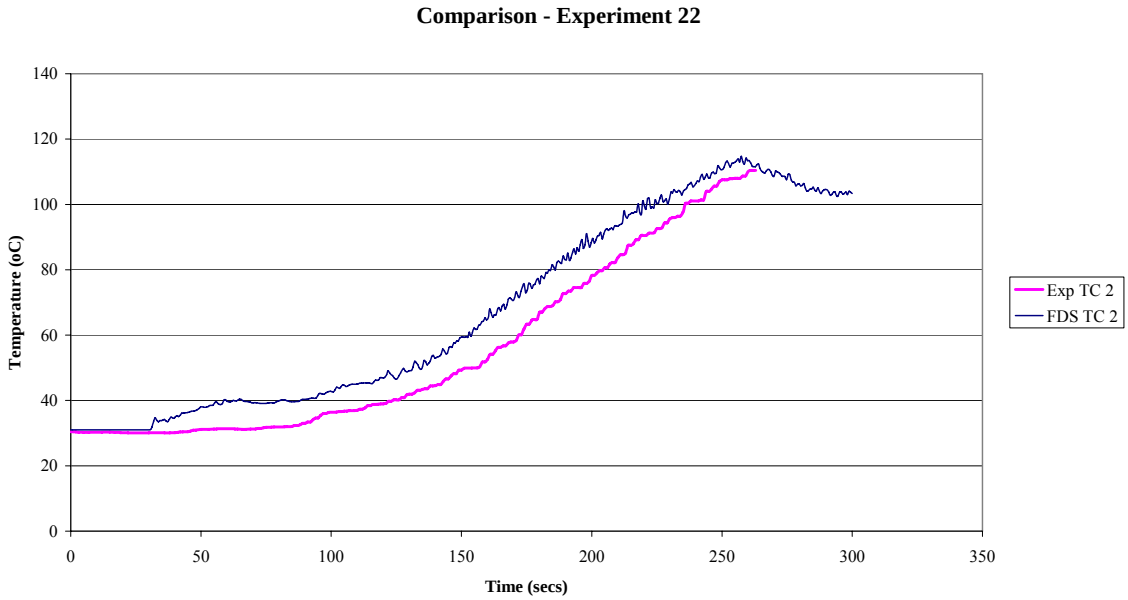

Appendix D

FDS Input File

```
&HEAD CHID=’EXPERIMENT 1’, TITLE=’INPUT FILE FOR EXP 1’/
&GRID IBAR=90,JBAR=45,KBAR=25/

&PDIM XBAR0=-0.8,XBAR=8.20,YBAR0=-0.30,YBAR=4.20,ZBAR=2.5/
&TIME TWFIN= 450. /

&SURF ID='FIRE',HRRPUA=3500,RAMP_Q='CHAIR FIRE' /
&VENT XB=3.9,4.3,1.9,2.0,0.65,0.65,SURF_ID='FIRE' /
&OBST XB=3.9,4.3,1.9,2.0,0.0,0.65,BLOCK_COLOR='GREEN',
SURF_ID='INERT'/ &
RAMP ID='CHAIR FIRE',T=0.0,F=0.0/

&RAMP ID='CHAIR FIRE',T=92.0,F=0.071/
&RAMP ID='CHAIR FIRE',T=180.0,F=0.228/
&RAMP ID='CHAIR FIRE',T=240.0,F=0.678/
&RAMP ID='CHAIR FIRE',T=276,F=0.786/
&RAMP ID='CHAIR FIRE',T=292,F=0.95/
&RAMP ID='CHAIR FIRE',T=331,F=1.0/

&MISC REACTION=’POLYURETHANE’,
DATABASE_DIRECTORY=’c:\nist….\database3\’/

&OBST XB=0.0, 8.2, 0.0, 0.1, 0.0, 2.4 BLOCK_COLOR='GRAY',
SURF_ID='GYPSUM BOARD' / WALL  RIGHT
&OBST XB=8.1, 8.2, 0.0, 4.2, 0.0, 2.4 BLOCK_COLOR='GRAY',
SURF_ID='GYPSUM BOARD' / WALL  BACK
&OBST XB=0.0, 8.2, 4.1, 4.2, 0.0, 2.4 BLOCK_COLOR='GRAY',
SURF_ID='GYPSUM BOARD' / WALL  LEFT
&OBST XB=0.0, 0.1, 0.0, 0.3, 0.0, 2.4 BLOCK_COLOR='GRAY',
SURF_ID='GYPSUM BOARD' /  DOOR BLOCK
&OBST XB=0.0, 0.1, 0.3, 1.1, 2.0, 2.4 BLOCK_COLOR='GRAY',
SURF_ID='GYPSUM BOARD' / DOOR SOFFIT
```

```
&OBST XB=0.0, 0.1, 1.0, 4.2, 0.0, 2.4 BLOCK_COLOR='GRAY',
SURF_ID='GYPSUM BOARD' / WALL FRONT
&OBST XB=0.0, 8.2, 0.0, 4.2, 2.4, 2.5 BLOCK_COLOR='GRAY',
SURF_ID='GYPSUM BOARD' / CEILING

&VENT CB='XBAR' ,SURF_ID='OPEN' /
&VENT CB='XBAR0',SURF_ID='OPEN' /
&VENT CB='YBAR' ,SURF_ID='OPEN' /
&VENT CB='YBAR0',SURF_ID='OPEN' /
&VENT CB='ZBAR' ,SURF_ID='OPEN'

&THCP XYZ=6.0,2.1,2.380,QUANTITY='TEMPERATURE',LABEL='1' /
&THCP XYZ=2.0,2.1,2.380,QUANTITY='TEMPERATURE',LABEL='2' /
&THCP XYZ=6.0,0.6,2.3,QUANTITY='TEMPERATURE',LABEL='3' /
&THCP XYZ=6.0,0.6,2.1,QUANTITY='TEMPERATURE',LABEL='4' /
&THCP XYZ=6.0,0.6,1.0,QUANTITY='TEMPERATURE',LABEL='5' /
&THCP XYZ=2.0,0.6,2.3,QUANTITY='TEMPERATURE',LABEL='6'/
&THCP XYZ=2.0,0.6,2.1,QUANTITY='TEMPERATURE',LABEL='7' /
&THCP XYZ=2.0,0.6,1.0,QUANTITY='TEMPERATURE',LABEL='8' /

&HEAT XYZ=6.0,0.6,2.3,RTI=30.,ACTIVATION_TEMPERATURE=160./
LOCATION 3
&HEAT XYZ=6.0,0.6,2.1,RTI=30.,ACTIVATION_TEMPERATURE=160./
LOCATION 4
&HEAT XYZ=6.0,0.6,1.0,RTI=30.,ACTIVATION_TEMPERATURE=160./
LOCATION 5
&HEAT XYZ=2.0,0.6,2.3,RTI=30.,ACTIVATION_TEMPERATURE=160./
LOCATION 6
&HEAT XYZ=2.0,0.6,2.1,RTI=30.,ACTIVATION_TEMPERATURE=160./
LOCATION 7
&HEAT XYZ=2.0,0.6,1.0,RTI=30.,ACTIVATION_TEMPERATURE=160./
LOCATION 8
```

```
&SPRK XYZ=2.10000  2.1000  2.380, MAKE='K-25' / sprinkler 1 c=0
&SPRK XYZ=6.10000  2.1000  2.380, MAKE='K-25' / sprinkler 2
&SPRK XYZ=2.10000  2.1000  2.380, MAKE='K-26' / sprinkler 1 c=0.3
&SPRK XYZ=6.10000  2.1000  2.380, MAKE='K-26' / sprinkler 2
&SPRK XYZ=2.10000  2.1000  2.380, MAKE='K-27' / sprinkler 1 c=0.65
&SPRK XYZ=6.10000  2.1000  2.380, MAKE='K-27' / sprinkler 2
&SPRK XYZ=2.10000  2.1000  2.380, MAKE='K-28' / sprinkler 1 c=1
&SPRK XYZ=6.10000  2.1000  2.380, MAKE='K-28' / sprinkler 2

&SLCF PBX=4.1 QUANTITY='TEMPERATURE'/
&SLCF PBY=0.4 QUANTITY='TEMPERATURE'/
&SLCF PBY=1.9 QUANTITY='TEMPERATURE'/
&SLCF PBX=0.1 QUANTITY='TEMPERATURE',VECTOR=.TRUE. /
&SLCF PBX=2.1 QUANTITY='TEMPERATURE',VECTOR=.TRUE. /
```

Below is an example of a sprinkler data file for a residential sprinkler head with a RTI of 36 and a C-factor of 0.3.

```
MANUFACTURER
TYCO
MODEL
RESIDENTIAL
OPERA0001
K-FACTOR
0.0
RTI
36.
C-FACTOR
0.30
OFFSET_DISTANCE
0.20
ACTIVATION_TEMPERATURE
68.
SIZE_DISTRIBUTION
```

```
1
1300.,2.43,0.58
VELOCITY
1
30. 90. 10.0

&SLCF PBX=4.1 QUANTITY='TEMPERATURE'/
&SLCF PBY=0.4 QUANTITY='TEMPERATURE'/
&SLCF PBY=1.9 QUANTITY='TEMPERATURE'/
&SLCF PBX=0.1 QUANTITY='TEMPERATURE',VECTOR=.TRUE. /
&SLCF PBX=2.1 QUANTITY='TEMPERATURE',VECTOR=.TRUE. /
```

Appendix E
Glossary of Terms

Glossary of Terms

Acronyms

ASET	Available Safe Egress Time
CFD	Computational Fluid Dynamics
FDS	Fire Dynamics Simulator
FDS 3	Fire Dynamics Simulator3
HD	Heat Detector
HoC	Heat of Combustion
HRR	Heat Release Rate
ISO	International Standards Organisation
LES	Large Eddy Simulation
MISC	Miscellaneous
MLR	Mass Loss Rate
NFPA	National Fire Protection Association
RTI	Response Time Index
SFPE	Society for Fire Protection Engineers
SS	Standard Response Standard Spray
TC	Thermocouple
UL	United Laboratories

Nomenclature

A	area of the body exposed to gas flow
c	specific heat of the body
c	conductivity factor
C	empirically derived constant
C_p	constant pressure specific heat
D	diffusion coefficient, fire diameter
D*	characteristic fire diameter
H_o	HRR per unit mass of oxygen consumed
f	external force vector (sprinkler droplet drag)
g	acceleration of gravity
h	enthalpy; heat transfer coefficient
h_c	convective heat transfer co-efficient
h_i	enthalpy of ith species
I	radiation intensity
I_b	radiation blackbody intensity
K	thermal conductivity, turbulent kinetic energy
L	flame height
m	mass of body
M_i	molecular weight of ith gas species
m_o'''	oxygen consumption rate
p	pressure
q_r	radiative heat flux vector
q'''	heat release rate per unit volume
Q*	dimensionless HRR
$\dot{Q}$	total heat release rate
$\dot{Q}_c$	convective heat release rate
T	temperature
t	time
u	velocity
u (u, v, w)	velocity vector

W_i'''	production rate of ith species per unit volume
Y_F	mass fraction of fuel in the fuel stream
Y_i	mass fraction of ith species
Y_O	mass fraction of oxygen
Y_o^{inf}	mass fraction of oxygen in ambient
z	height above fire base
Z	mixture fraction
Z_f	mixture fraction at flame surface
$Z_{f,eff}$	effective flame mixture fraction
τ	tau
RTI_v	virtual RTI
ρ	density
δx	nominal grid size
ε	viscous dissipation energy
κ	absorption coefficient
μ	dynamic viscosity
ρ	density
σ	Stefan-Boltzmann constant
τ	viscous stress tensor
ν_i	stoichiometric coefficient
χ_r	local radiative loss fraction